IAEA TECDOC SERIES

IAEA-TECDOC-1949

IAEA-TECDOC-1949

Phenomenology, Simulation and Modelling of Accidents in Spent Fuel Pools

Proceedings of a Technical Meeting

IAEA
International Atomic Energy Agency

PHENOMENOLOGY, SIMULATION AND MODELLING OF ACCIDENTS IN SPENT FUEL POOLS

The following States are Members of the International Atomic Energy Agency:

AFGHANISTAN
ALBANIA
ALGERIA
ANGOLA
ANTIGUA AND BARBUDA
ARGENTINA
ARMENIA
AUSTRALIA
AUSTRIA
AZERBAIJAN
BAHAMAS
BAHRAIN
BANGLADESH
BARBADOS
BELARUS
BELGIUM
BELIZE
BENIN
BOLIVIA, PLURINATIONAL STATE OF
BOSNIA AND HERZEGOVINA
BOTSWANA
BRAZIL
BRUNEI DARUSSALAM
BULGARIA
BURKINA FASO
BURUNDI
CAMBODIA
CAMEROON
CANADA
CENTRAL AFRICAN REPUBLIC
CHAD
CHILE
CHINA
COLOMBIA
COMOROS
CONGO
COSTA RICA
CÔTE D'IVOIRE
CROATIA
CUBA
CYPRUS
CZECH REPUBLIC
DEMOCRATIC REPUBLIC OF THE CONGO
DENMARK
DJIBOUTI
DOMINICA
DOMINICAN REPUBLIC
ECUADOR
EGYPT
EL SALVADOR
ERITREA
ESTONIA
ESWATINI
ETHIOPIA
FIJI
FINLAND
FRANCE
GABON
GEORGIA
GERMANY
GHANA
GREECE
GRENADA
GUATEMALA
GUYANA
HAITI
HOLY SEE
HONDURAS
HUNGARY
ICELAND
INDIA
INDONESIA
IRAN, ISLAMIC REPUBLIC OF
IRAQ
IRELAND
ISRAEL
ITALY
JAMAICA
JAPAN
JORDAN
KAZAKHSTAN
KENYA
KOREA, REPUBLIC OF
KUWAIT
KYRGYZSTAN
LAO PEOPLE'S DEMOCRATIC REPUBLIC
LATVIA
LEBANON
LESOTHO
LIBERIA
LIBYA
LIECHTENSTEIN
LITHUANIA
LUXEMBOURG
MADAGASCAR
MALAWI
MALAYSIA
MALI
MALTA
MARSHALL ISLANDS
MAURITANIA
MAURITIUS
MEXICO
MONACO
MONGOLIA
MONTENEGRO
MOROCCO
MOZAMBIQUE
MYANMAR
NAMIBIA
NEPAL
NETHERLANDS
NEW ZEALAND
NICARAGUA
NIGER
NIGERIA
NORTH MACEDONIA
NORWAY
OMAN
PAKISTAN
PALAU
PANAMA
PAPUA NEW GUINEA
PARAGUAY
PERU
PHILIPPINES
POLAND
PORTUGAL
QATAR
REPUBLIC OF MOLDOVA
ROMANIA
RUSSIAN FEDERATION
RWANDA
SAINT LUCIA
SAINT VINCENT AND THE GRENADINES
SAN MARINO
SAUDI ARABIA
SENEGAL
SERBIA
SEYCHELLES
SIERRA LEONE
SINGAPORE
SLOVAKIA
SLOVENIA
SOUTH AFRICA
SPAIN
SRI LANKA
SUDAN
SWEDEN
SWITZERLAND
SYRIAN ARAB REPUBLIC
TAJIKISTAN
THAILAND
TOGO
TRINIDAD AND TOBAGO
TUNISIA
TURKEY
TURKMENISTAN
UGANDA
UKRAINE
UNITED ARAB EMIRATES
UNITED KINGDOM OF GREAT BRITAIN AND NORTHERN IRELAND
UNITED REPUBLIC OF TANZANIA
UNITED STATES OF AMERICA
URUGUAY
UZBEKISTAN
VANUATU
VENEZUELA, BOLIVARIAN REPUBLIC OF
VIET NAM
YEMEN
ZAMBIA
ZIMBABWE

The Agency's Statute was approved on 23 October 1956 by the Conference on the Statute of the IAEA held at United Nations Headquarters, New York; it entered into force on 29 July 1957. The Headquarters of the Agency are situated in Vienna. Its principal objective is "to accelerate and enlarge the contribution of atomic energy to peace, health and prosperity throughout the world".

IAEA-TECDOC-1949

PHENOMENOLOGY, SIMULATION AND MODELLING OF ACCIDENTS IN SPENT FUEL POOLS

PROCEEDINGS OF A TECHNICAL MEETING

INTERNATIONAL ATOMIC ENERGY AGENCY
VIENNA, 2021

For further information on this publication, please contact:

Nuclear Power Technology Development Section
International Atomic Energy Agency
Vienna International Centre
PO Box 100
1400 Vienna, Austria
Email: Official.Mail@iaea.org

Printed by the IAEA in Austria
April 2021

IAEA Library Cataloguing in Publication Data

Names: International Atomic Energy Agency.
Title: Phenomenology, simulation and modelling of accidents in spent fuel pools / International Atomic Energy Agency.
Description: Vienna : International Atomic Energy Agency, 2021. | Series: IAEA TECDOC series, ISSN 1011–4289 ; no. 1949 | Includes bibliographical references.
Identifiers: IAEAL 21-01389 | ISBN 978-92-0-104121-0 (paperback : alk. paper) |
ISBN 978-92-0-104021-3 (pdf)
Subjects: LCSH: Reactor fuel reprocessing — Accidents. | Nuclear facilities — Accidents. | Nuclear reactor accidents. | Spent reactor fuels.

FOREWORD

The IAEA International Experts' Meeting on Strengthening Research and Development Effectiveness in the Light of the Accident at the Fukushima Daiichi Nuclear Power Plant, held in Vienna in 2015, prepared a list of recommendations for research and development activities to be promoted by the IAEA. This comprehensive list represents a compilation of the experts' views on the needs for further R&D activities and international cooperative efforts. It was further refined at the Training Meeting on Post-Fukushima Research and Development Strategies and Priorities held in December 2015. To address the most important priorities identified during these two events, the IAEA organized a series of three technical meetings in 2017–2019.

In October 2017, the IAEA held a Technical Meeting on the Status and Evaluation of Severe Accident Simulation Codes for Water Cooled Reactors. The meeting was focused on the status of the state of the art severe accident codes and identified near term needs for further improvement and development; the technical document resulting from this meeting was issued in 2019.

Synthesis of the results obtained in the frame of experimental and analytical research on the behaviour of hydrogen and other combustible gas and discussion of the potential impact on hydrogen management and risk assessment were the main topics of the Technical Meeting on Hydrogen Management in Severe Accidents held at the IAEA in September 2018.

To review and discuss the analysis, simulation and modelling of severe accident progression in spent fuel pools, the IAEA organized the Technical Meeting on the Phenomenology, Simulation and Modelling of Accidents in Spent Fuel Pools in Vienna on 2–5 September 2019. This meeting included presentations on numerical models and codes used for the assessment and modelling of severe accidents in spent fuel pools and support of experimental data to simulation and modelling. A total of 34 participants from 23 Member States attended the meeting. This publication is the proceedings of the technical meeting and includes summaries of discussion, conclusions and recommendations made at the meeting as well as the papers presented.

The IAEA gratefully acknowledges the contributions of the meeting participants, in particular B. Jäckel (Switzerland) for preparing the summary of meeting discussions and recommendations. The IAEA officers responsible for this publication were A. Miassoedov of the Division of Nuclear Power and L. McManniman of the Division of Nuclear Fuel Cycle and Waste Technology.

CONTENTS

1. INTRODUCTION

This publication summarizes the results of the Technical Meeting on the Phenomenology, Simulation and Modelling of Accidents in Spent Fuel Pools which was held by the IAEA in Vienna on 2–5 September 2019.

The objectives of the meeting were to:

- Exchange information on the codes dedicated to SFP severe accident analysis, their capabilities, and validation status;
- Discuss the current knowledge gaps and therefore the prospects for future research and development (R&D) dedicated to SFP accident analysis;
- Discuss and review possible accident preventive or mitigative measures.

The emphasis was on achieving a better understanding of drivers for improvement and further development of codes with capabilities to address risks associated with accidents in SFPs, failure of the spent fuel, and the subsequent release of fission products.

A total of 34 participants from 23 Member States attended the meeting. The meeting included presentation of the submitted papers as well as discussion sessions to enable participants to contribute to the summary and highlights of the event, and to make recommendations to the IAEA on future activities in this area.

1.1. BACKGROUND

To address the most important priorities identified in the IAEA International Experts' Meeting on Strengthening Research and Development Effectiveness in the Light of the Accident at the Fukushima Daiichi Nuclear Power Plant, held in Vienna in 2015, the IAEA organised a series of three technical meetings to be held in 2017–2019.

The status of the state-of-the-art severe accident analysis codes and near-term needs for their further improvement and development was discussed in the Technical Meeting on the Status and Evaluation of Severe Accident Simulation Codes for Water Cooled Reactors held at IAEA in October 2017 [1].

Synthesis of the results obtained in the frame of experimental and analytical research on hydrogen/combustible gas behaviour and discussion of their potential impact on hydrogen management and risk assessment were the main topics of the Technical Meeting on Hydrogen Management in Severe Accidents held at IAEA in September 2018. The knowledge gaps identified during the meeting were discussed with respect to the current status of the available knowledge and ongoing efforts to close the remaining open issues.

To review and discuss analysis, simulation, and modelling of severe accident progression in spent fuel pools (SFPs), the IAEA organized the Technical Meeting on the Phenomenology, Simulation and Modelling of Accidents in Spent Fuel Pools in Vienna on 2–5 September 2019.

Current knowledge of the severe accident progression in SFPs is based on experimental data and computer simulations which have significant gaps in their ability to provide full understanding of the accident progression. Computer codes used to estimate the effects of a loss of coolant accident (LOCA) conditions in SFPs were specifically developed for the analysis of the reactor core in LOCA scenarios. Severe accident analysis tools based on computational modelling of the conditions that lead to such accidents and the accident propagations in SFPs of water cooled reactors account for partially uncovered fuel assemblies, hydrogen production, and high-temperature oxidation kinetics and burst behaviour of cladding in mixed air–steam conditions. Currently, the accident analysis tools used to analyse the cooling accidents in SFPs of light water reactors include computer codes for nuclear criticality safety, thermal-hydraulics, fuel rod behaviour, and severe accidents. Significant gaps and uncertainties exist in these codes when applied to the specific conditions of SFP accidents. In addition, a comprehensive severe accident code system for SFP accident analysis does not exist, because of the significantly different conditions and fuel arrangements in reactor cores compared to those in SFPs.

1.2. OBJECTIVE

The overall purpose of the Technical Meeting was to capture the state-of-the-art knowledge on the phenomenology of severe accidents in SFPs and on the codes which are being applied to analyse severe accident propagation in SFPs. The meeting also served as a forum for Member States to exchange knowledge on current and new code development and methodologies, to identify the gaps for future improvements, and gather information for collaboration on all these aspects.

1.3. SCOPE

This publication presents the papers submitted by the meeting participants and presented during the Technical Meeting on the Phenomenology, Simulation and Modelling of Accidents in Spent Fuel Pools, held in Vienna on 2–5 September 2019 and a summary of the discussions and recommendations from the Technical Meeting.

1.4. STRUCTURE

Section 2 of this publication summarizes discussions, conclusions and recommendations from the Technical Meeting. Section 3 of this publication provides the Member States' full papers submitted to and presented during the Technical Meeting; the papers are presented in alphabetical order of the Member States.

2. SUMMARY OF MEETING DISCUSSIONS AND RECOMMENDATIONS

The contributions provided by the participants enabled the Technical Meeting to fulfil its objectives, specifically in:

- Collecting current information from Member States on methodologies and numerical models and codes being used for the assessment and modelling of severe accidents in SFPs;
- Enabling the exchange of information on ongoing R&D in code development and validation, and identification of needs for new experimental data required to more accurately assess the capabilities of the codes dedicated to SFP severe accident analysis.

Discussion sessions enabled the exchange of useful information regarding the analysis of severe accidents in SFPs, the provision of an overview of current R&D activities, and discussion on the planning and execution of further R&D and associated issues.

Throughout the course of discussions, several important recommendations were identified that are outlined in this section.

2.1. AVAILABILITY OF EXPERIMENTAL DATA

For SFP accident analysis, the code development strategy begins with obtaining new data on the thermal-hydraulics and severe accident phenomena in SFPs. These data are then utilised to improve current models or define new ones, a necessary step within the codes. The experimental data are then used for validation prior to performing a benchmark of the code, which may include code-to-code benchmarks.

In order to reasonably describe postulated SFP accident scenarios, the design and execution of specific experiments regarding boundary conditions of SFP accident phenomena are necessary to produce a database of results. The results held within this database can be used to validate extended models for SFP behaviour, or to define new models, both of which could be implemented in the SFP severe accident codes.

In addition to the generation of new experimental data, the release of existing data (such as those from the Sandia National Laboratory experiments [2] or the 'Accidental DENOyage (de-watering) of Nuclear Fuel Storage' (DENOPI) project [3]) would benefit validation processes. These data can be used in benchmark studies to increase knowledge about the influence of boundary conditions on the accident progression and to identify important phenomena in severe SFP accidents. The inclusion of a sensitivity analysis as part of severe accident progression modelling in SFPs could improve understanding, as there is a large uncertainty within the thermal hydraulics description of SFPs that will only be increased during the analysis of the fuel degradation phase.

The meeting participants identified the necessity of defining guidelines for SFP severe accidents modelling as an important task for the code developers. The publication of example input decks for generic spent fuel pools would be beneficial for code users and beginners, as the modification of an existing input deck is more efficient than developing completely new input decks.

2.2. IMPLICATIONS OF REACTOR SHUT DOWN AND DECOMMISSIONING

It was highlighted that once an NPP concludes operations and proceeds toward decommissioning, storage of spent fuel within the SFP will be of increasing importance than it may have been during the reactor's operational phase. There may also be more away from reactor (AFR) storage pools to support reactor decommissioning.

Following shutdown and/or decommissioning of an NPP, some of the operational safety infrastructure may no longer be available. The effect of reduced accident management infrastructure after final shutdown of the reactor on the progression and recovery of postulated SFP accidents is an area that could warrant further investigation.

2.3. SIMULTANEOUS REACTOR AND SPENT FUEL POOL EVENTS

There could be the potential for a postulated severe accident scenario that would affect both the reactor and the SFP (either simultaneous or subsequent); any such event would be power plant and scenario specific. This progression may bear an influence on the overall source term. The simulation of such a postulated accident is more complex than an independent power plant or SFP accident, as two separated 'cores' would have to be modelled.

In a severe accident scenario where there has been a loss of reactor building containment, for fuel stored within an at reactor (AR) pool, the only barrier remaining for the release of fission products from the spent fuel pool would be the cladding of the spent fuel. Due to a possible loss of safety features, a large amount of long-lived fission products (FPs), like Cs-137, could be released into the environment.

Where the SFP is not within a containment (usually an AFR facility), the potential for FP release resulting from an accident is always an issue.

Such an accident scenario would also influence general emergency preparedness; the influence of the dose rate from a reactor accident on mitigation activities in the SFP is an area for investigation.

2.4. LATE PHASE SPENT FUEL POOL ACCIDENT MODELLING

Modelling and analysis of SFP accidents may benefit from the consideration of fuel melting in the later phases. The determination of potential corium-concrete interaction after pool liner degradation is complex due to the elevated position of the SFPs within either the containment or the spent fuel storage building in Pressurised Water Reactors (PWRs) or the reactor building in Boiling Water Reactors (BWR). In the event of the failure of the base of the pool, there are several open possibilities for the relocation of molten corium into different rooms below the SFP.

Criticality in spent fuel pools may be an issue for some storage strategies. Development of a common strategy for spent fuel pools could enable the highest safety standards for the storage of spent nuclear fuel to be reached.

2.5. INFLUENCE OF FUEL ASSEMBLY HISTORY

The influence of fuel assembly history (burn-up) and long-term storage on material properties, potential accident progression, and source term are areas of interest for future investigations.

This includes the improvement of models that address:

- Cladding ballooning and internal fuel relocation at higher burnup (rim effect);
- The formation of porous debris and its subsequent effective heat transfer;
- The kinetics of cladding oxidation in air/steam and in H_2O-N_2-O_2-H_2-CO_X mixtures;
- Associated material properties at high temperatures, especially after long term storage.

Simplified models are required to decrease the calculation time associated with these factors.

Consideration has to be given to probabilistic safety assessment (PSA) aspects during the SFP accident analysis. For PSA studies, the strategy is to improve modelling (new computer codes) and use improved (validated) models from a phenomenological aspect. An increasing number of regulatory authorities are asking for PSA level 2 studies for spent fuel pools. This would include identifying the most important weak points of the severe accident codes for calculating the source term.

The fission product distribution for spent fuel in the SFP is different from the distribution of the short-lived fission products investigated in a reactor accident scenario; the fission product distribution is no longer dependent on the reactor power distribution, but on the fuel burn-up history and fuel storage time in the pool. In addition, air ingress can lead to a change of the fission product chemistry and therefore a change in the release probability of several elements, such as ruthenium. Therefore, the FP release calculations in SFP severe accident models have two main weak points: the wrong FP distribution in the fuel and wrong release constants for more volatile FP oxides in an oxidizing environment. As a result, the FP release calculation would have a high uncertainty and would probably not be acceptable for regulatory authorities.

The development of Severe Accident Management Guidelines (SAMG) for SFP accidents requires qualified and validated computer codes for SFP; this is an immediate requirement for some countries and may be an issue from a regulatory perspective. The application of modelling results to SAMG development, in terms of SFP conditions for mitigation activities (e.g. pool hall dose, temperature, humidity), are necessary to achieve realistic guidelines.

2.6. INFLUENCE OF 3D EFFECTS IN ANALYSIS

A strong influence of 3D effects in large SFPs, e. g influenced by positioning of fuel elements with different irradiation history, was demonstrated by the results of an AC^2 code simulation [4].

The use of computational fluid dynamics (CFD) codes, e.g. Open Source Field Operation and Manipulation (openFOAM), for the support of SFP analysis leads to the question 'is flashing a possibility for a large pool inventory loss?'. One focus for investigation could be the influence of the fuel storage configuration (hot neighbour, cold neighbour) once fuel uncovery has begun. In France, Institut de Radioprotection et de Sûreté Nucléaire (IRSN) has research programme underway on this issue, as such an event could result in lost hours of accident mitigation time.

2.7. CANDU SPENT FUEL POOL MODELLING

Existing models for SFPs are often based on the geometry and operation of LWR pools, with fuel stored upright in racks. The horizontal layout of CANada Deuterium Uranium (CANDU) spent fuel in trays presents a complex geometry of cross-flow, with thermal hydraulics that are not adequately described in existing models. For CANDU SFPs, I-131 release is an issue as fuel assemblies are normally discharged while the reactor is operating. The horizontal fuel orientation and cross-flow influences the rate of SFP accident progression and the subsequent release of fission products. Additionally, collapsing of fuel storage trays during a severe accident with re-immersion of fuel bundles has to be tackled. This presents a need for codes for CANDU SFP, with models to describe the heat transfer taking place by radiation and conduction. These codes would also require subsequent validation, in a process similar to that undertaken in the DENOPI project [3].

Such activities are in the interest of R&D in the small CANDU community, but significant effort is required. A collaboration of all players will be beneficial to speed up the progress

A project to develop a new computer code for the simulation of an accident in a CANDU SFP has commenced in Republic of Korea. Canada has also been active in SFP modelling and research. The Canadian Nuclear Safety Commission (CNSC) and Canadian Nuclear Laboratories (CNL) undertook the OECD/NEA phenomena identification and ranking table (PIRT) process [5]. In general, the PIRT determined that there was the requisite knowledge to begin developing a CANDU SFP accident specific code. However, knowledge gaps exist, in particular in the thermal-hydraulics related to fuel cooling in CANDU open racks. An experimental campaign intending to close this gap is in progress at CNL Chalk River.

2.8. INTERNATIONAL COOPERATION

In addition to the IAEA, there are serval other collaborative approaches in the analysis of SFP severe accidents and cooperation between them is important to ensure the best use of resources and most efficient outcomes for the NPP modelling community. Interested parties include the H2020 Management and Uncertainties of Severe Accidents (MUSA) project (SFP Work Package), OECD/NEA Working Group on Analysis and Management of Accidents (WGAMA), and Nuclear Generation II& III Association (NUGENIA). Possible common strategies in experimental investigation and model-developing programmes for SFP boundary conditions could be developed.

Regular meetings of organisations involved in the analysis of SFP severe accidents would be beneficial to build up a knowledge base; the facilitation of information exchange between research, industry, regulatory authorities, and code developers would be extremely valuable.

Periodic revisions of published status reports [6] and PIRTs for SFP related severe accidents [7] could be used to document progress in the knowledge and modelling of SFP regarded phenomena.

The interaction of probabilistic and deterministic analytical activities may be used to systematically review accident initiators and determine research priorities based on both the frequency and impact represented by potentially occurring phenomena.

Three gaps have been identified in relation to understanding the phenomenology of severe accidents in SFPs that could benefit from a coordinated international effort to address:

- Identifying progress achieved and further needs for R&D on the basis of the OECD/NEA (PIRT);
- Developing a validation matrix and identifying the relevant experimental data for the validation of computer codes applied for the accident analysis in SFPs;
- Code benchmarking against experimental data and code-to-code comparison based on accident scenarios using representative SFP configurations.

REFERENCES

[1] INTERNATIONAL ATOMIC ENERGY AGENCY, Status and Evaluation of Severe Accident Simulation Codes for Water Cooled Reactors, IAEA-TECDOC-1872, IAEA, Vienna (2019).

[2] DURBIN, S. G., ET AL., Spent Fuel Pool Project Phase I: Pre-Ignition and Ignition Testing of a Single Commercial 17x17 Pressurized Water Reactor Spent Fuel Assembly under Complete Loss of Coolant Accident Conditions, NUREG/CR-7215 (2016). DOI: www.nrc.gov/docs/ML1611/ML16112A022.pdf.

[3] MUTELLE, H., ET AL., A new research program on accidents in spent fuel pools. The DENOPI project, 2014 Water Reactor Fuel Performance Meeting / Top Fuel / LWR Fuel Performance Meeting (WRFPM 2014), Paper ID: 100071, Sendai, Miyagi, Japan, 14-17 September 2014.

[4] LOVASZ, L., WEBER, S., KOCH, M.K., New Approach for Severe Accident Simulations in Spent Fuel Pools Using the Code System AC2, 12th International Topical Meeting on Nuclear Reactor Thermal-Hydraulics, Operation and Safety (NUTHOS-12), Qingdao, 14-18 October 2018.

[5] CANADIAN NUCLEAR LABORATORIES, Phenomena identification and ranking table for a severe accident in a CANDU irradiated fuel bay, CW-126800-REPT-001, Rev 0, CNL, Chalk River (2010). http://nuclearsafety.gc.ca/eng/resources/research/research-and-support-program/research-report-abstracts/research-report-summaries-2017-2018.cfm#RSP-602-2.

[6] ORGANISATION FOR ECONOMIC CO-OPERATION AND DEVELOPMENT – NUCLEAR ENERGY AGENCY, Status Report on Spent Fuel Pools under Loss-of-Cooling and Loss-of-Coolant Accident Conditions, NEA/CSNI/R(2015)2, OECD-NEA, Paris (2015). https://www.oecd-nea.org/nsd/docs/2015/csni-r2015-2.pdf.

[7] ORGANISATION FOR ECONOMIC CO-OPERATION AND DEVELOPMENT – NUCLEAR ENERGY AGENCY Phenomena Identification and Ranking; R&D Priorities for Loss-of-Cooling and Loss-of-Coolant Accidents in Spent Nuclear Fuel Pools, NEA/CSNI/R(2017)18, OECD-NEA, Paris (2018). https://www.oecd-nea.org/nsd/docs/2017/csni-r2017-18.pdf.

PAPERS PRESENTED AT THE MEETING

APPROACHES TO THE MANAGEMENT OF SEVERE ACCIDENTS IN SFP AT ARMENIAN NPP

E. YEGHOYAN, A. HOVHANNISYAN
Institute “Armatom”,
Republic of Armenia

1. INTRODUCTION

The nuclear energy sector of Armenia includes one nuclear power plant — Armenian NPP (ANPP). ANPP consists of two units with Soviet design WWER-440/270 model reactor that is a version of the WWER-440/230 serial model with special seismic considerations in the design.

Unit 1 started its commercial operation in 1976 and the Unit 2 in 1980. Both units were shut down shortly after the earthquake of December 7th, 1988. Following the completion of repair and safety upgrading activities Unit 2, after 6.5 years of shutdown, restarted operation in 1995 and it has been operational since then. Unit 1 reactor plant remains in long-term shutdown condition (with no fuel in the core).

The Spent Fuel Pools (SFPs) of both units are currently in operation — the fuel discharged from the operating unit 2 reactor core is put first in the SFP of that unit, then, after several years of storage, is transferred to the SFP of the unit 1. When the decay heat is low enough the spent fuel assemblies are moved from the SFP of the unit 1 to the spent fuel interim ‘dry’ storage facility (Dry Casks for long term Storage of Spent Nuclear Fuel).

2. PLANT LAYOUT

SFPs at Armenian NPP are of ‘at-reactor’ type. The SFPs are located close to the reactor, but outside of the containment hermetic boundary. The pools are constructed of reinforced concrete with a two-layer steel liner – stainless steel and carbon steel with 4 mm of thickness each one and 4 mm gap between them.

The so called ‘Central hall’ of the reactor building, to which the SFPs are connected, is a relatively big area – width 39 m, length 126 m, height 28.3 m (the Central hall is common for two units of the plant; it is an airtight room in the upper part of the reactor building, not designed for overpressure).

When the fuel pool is not in refuelling mode, it is covered by panels (panels don’t ensure tightness of the pool and the pool is considered to be connected to the Central hall).

The simplified layout of the Reactor building is presented in Figure 1.

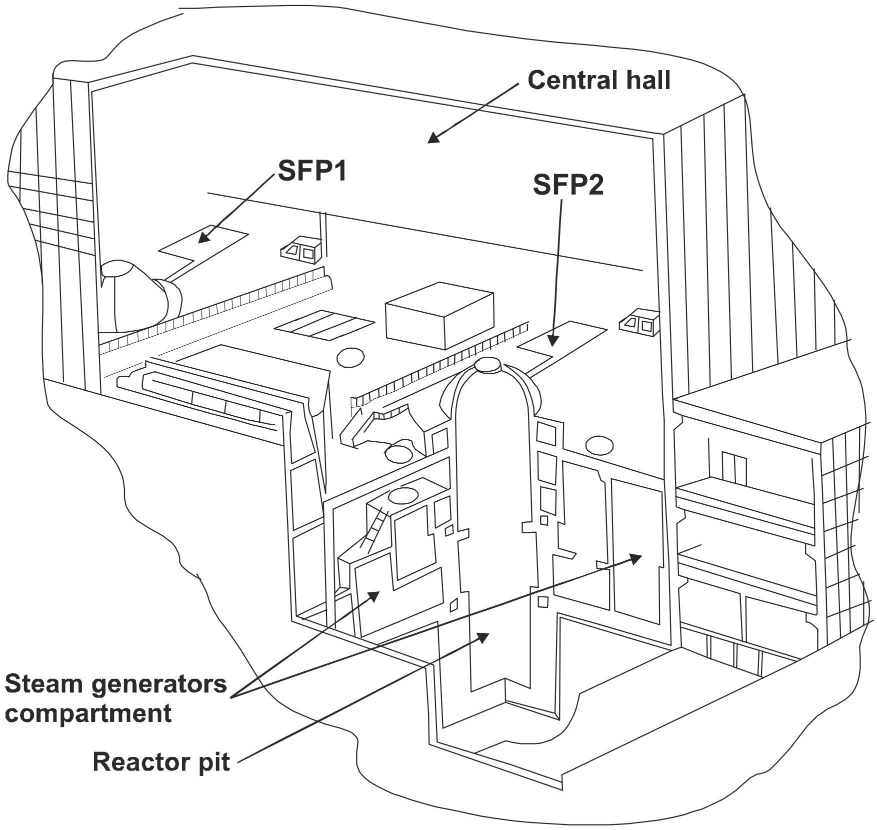

FIG. 1. Layout of the reactor building.

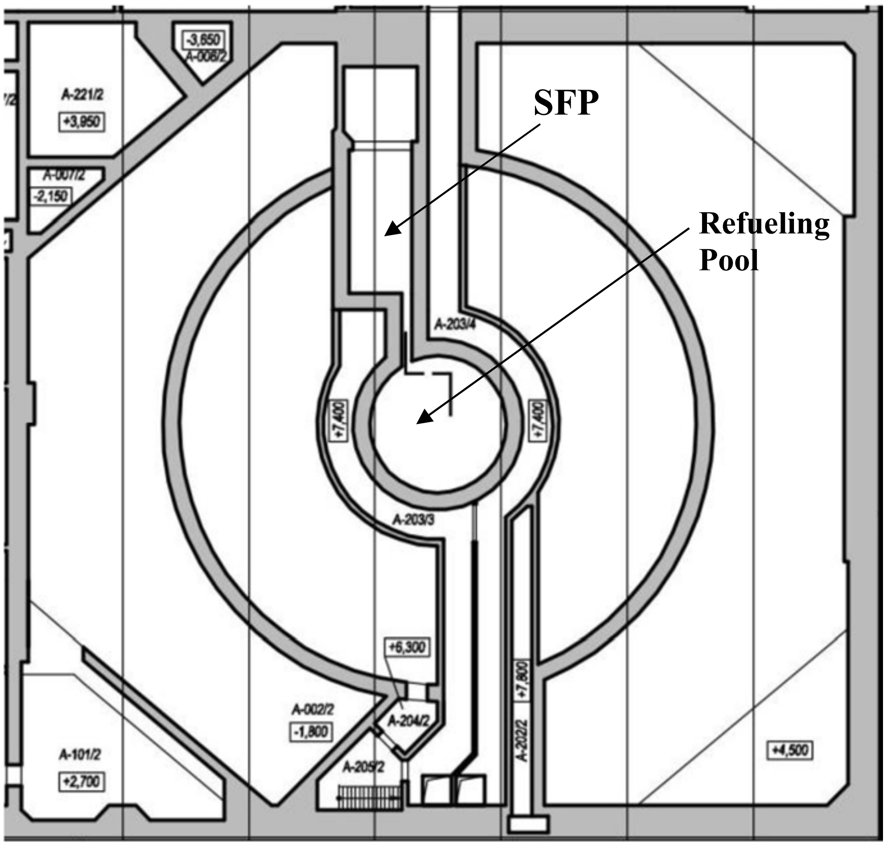

FIG. 2. Section of the reactor building.

3. SFP ACCIDENT STUDY

3.1. Spent fuel pool and cooling system design

The SFP has rectangular form and has 2 separate parts — main pool and container compartment. The length of pool is about 6.5 m, the width is 3.0 m and the full depth is 13.6 m. The racks in the SFP can have 2 levels. The lower level is used for permanent storage of the fuel assemblies, and the upper level of racks is used temporarily; installed and used in short term in case of full off-load of reactor core. The number of fuel assembly cells in the SFP lower racks is 372 and in the upper level 351. The number of fuel assemblies in reactor core is 347. The pools have also several cells for installing special containers in the SFP for the storage of damaged or leaking FAs. Depending on operation mode, different coolant levels are maintained in the pool.

Heat removal from SFPs is ensured by forced circulation of the coolant through the heat exchangers of the dedicated cooling system. The system designation is to keep the coolant temperature in normal operation modes within 50–60 °C. The system includes 2 circulation pumps with 280 m^3/h nominal flow rate each one and 2 heat exchangers. The principal scheme of the system is presented in Figure 3. The lowest level penetration of the pool is the connection of circulation pumps suction line (pool outlet line).

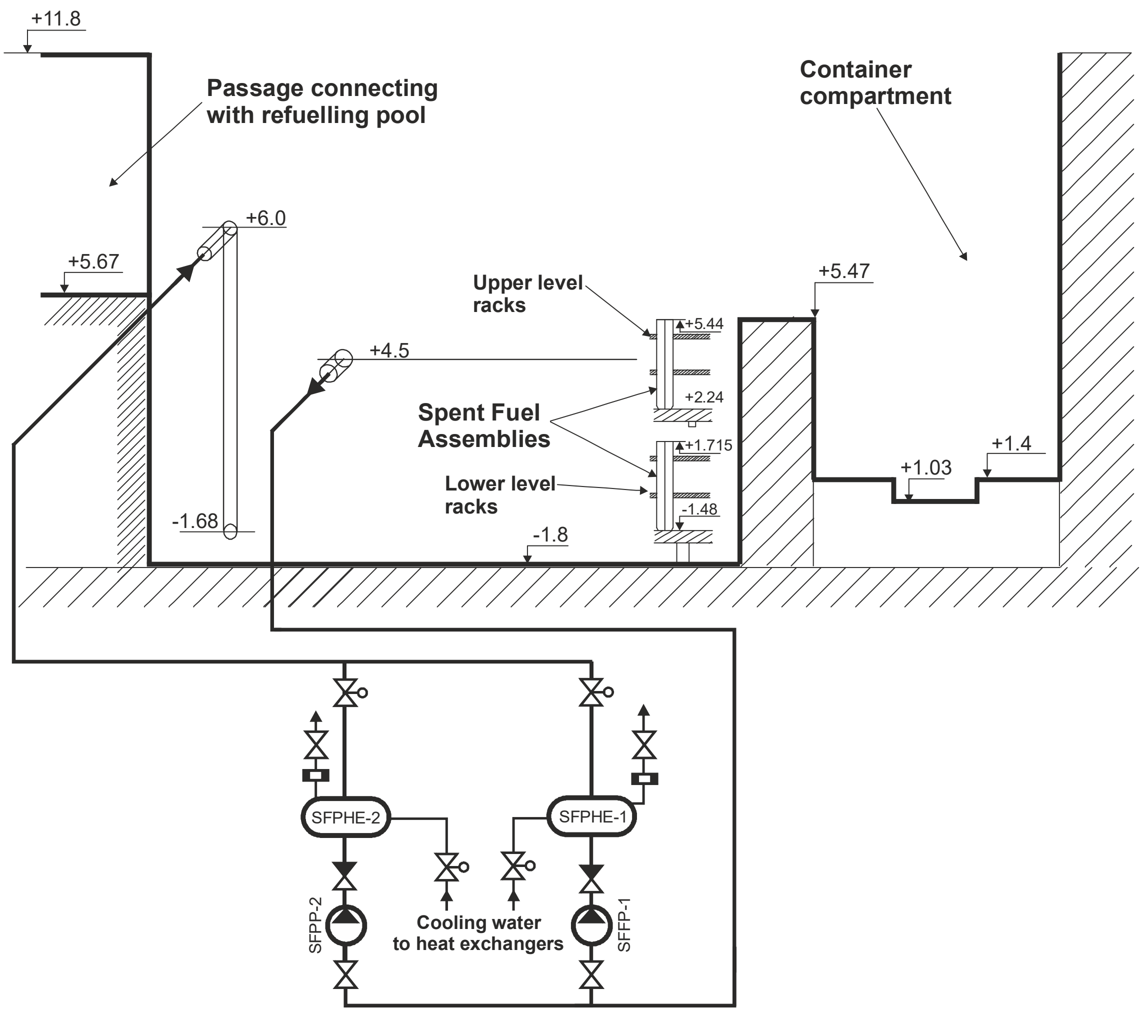

FIG. 3. SFP heat removal system simplified principal scheme.

3.2. Accident scenarios

The main scope of studies of accident scenarios in SFPs is performed within the development of plant EOPs for SFPs and corresponding analytical justification documentation. Main two categories of accident scenarios considered in the studies are 'Loss of SFP coolant' and 'Loss of cooling of SFP'.

'Loss of SFP coolant' scenario can take place in case of a very unlikely break of cooling system tube. For the case of coolant inlet pipe break, in order the siphon effect is 'broken' (and coolant loss is limited) there is special small size line connected to the containment atmosphere which will ensure air inlet to the cooling system in case the highest point is under vacuum. The elevation of tube connection to the pool prevents uncovering of fuel when only lower level racks contain spent fuel assemblies. In such scenario the operators will have several tens of hours before fuel uncovering [1].

The scenario with most serious consequences is the one with both level of racks full of spent fuel assemblies (reactor core off-load mode) and break of cooling system tube (pump suction line). In such a scenario coolant level in SFP decreases fast till reaching the elevation of cooling system suction tube. Thus, the higher part of fuel assemblies in the upper level racks will be uncovered.

The main results of calculations are summarized in Ref. [2] to justify the strategies considered in EOPs. Assumptions made for the considered scenario are presented in Table 1.

TABLE 1. ASSUMPTIONS MADE FOR THE ACCIDENT SCENARIO WITH OUTLET LINE BREAK

Number of fuel assemblies in the lower level racks (discharged from the reactor core during last 4 refuelling outages) – racks contain maximum number of assemblies	372 pcs.
Decay heat of fuel assemblies in the lower level racks (maximum anticipated)	260 kW
Number of fuel assemblies in the upper level racks (full off-load of the reactor core)	347 pcs.
Decay heat of fuel assemblies in the lower level racks (corresponds to the case of reactor core off-load 10 days after the reactor shutdown – maximum anticipated)	3.54 MW
Initial coolant level in the SFP (corresponds to the minimum allowable level for normal operation modes in case of upper level racks installed)	10.2 m
Cooling system tube break size Dn (full cross section break considered - very unlikely for the system operated under atmospheric pressure)	309 mm

Coolant level change in the pool and fuel temperature change during the studied scenario are presented on the figures 4 and 5. According to the calculations' results, in the beginning phase of the transient, decrease of the coolant level in SFP is very fast. The fuel top level is uncovered in less than 5 min. From this moment increase of fuel temperature starts at the uncovered part and takes place significantly fast.

Quick loss of coolant ceases when the coolant level reaches the elevation of the tube connected to the pool. Heat removal from the pool is lost and the coolant temperature increases continuously. Starting from this period, during about 50 minutes the coolant level is unchanged – the loss of coolant through break is almost stopped, and some coolant loss takes place through evaporation; the loss of coolant is compensated by its thermal expansion.

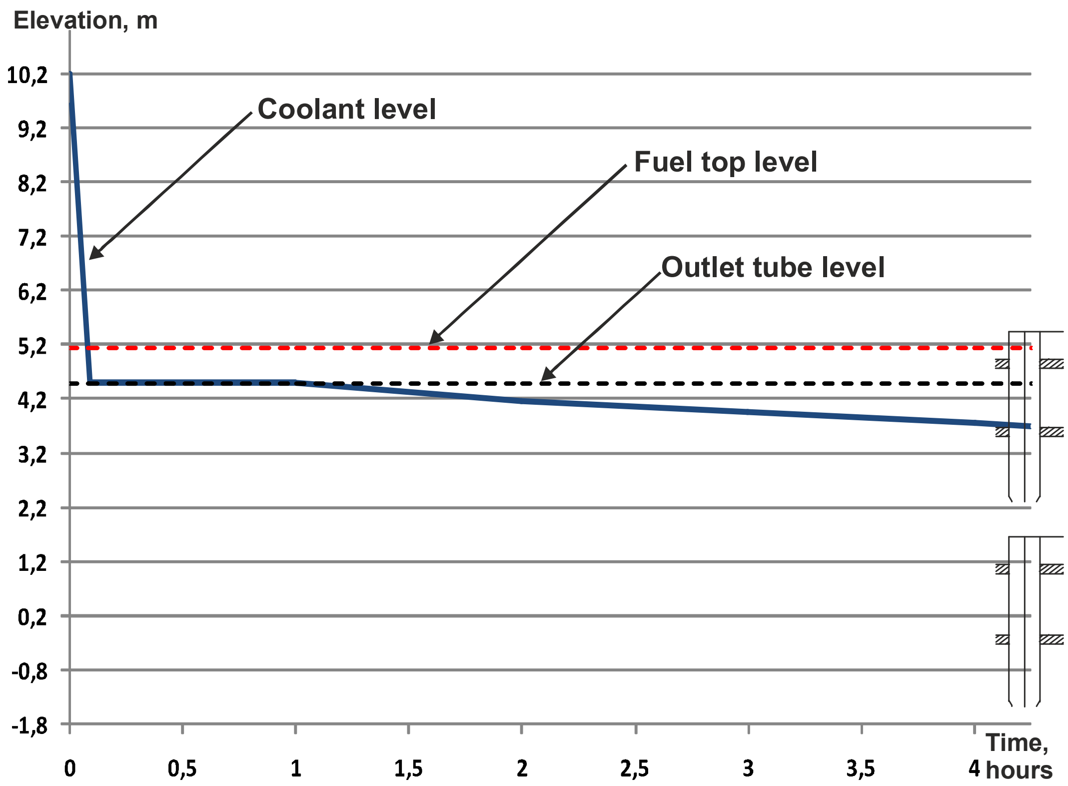

FIG. 4. Change of coolant level in the SFP in the scenario of cooling system tube break (without SFP make-up).

About 1 hour after beginning of the transient coolant temperature reaches the boiling temperature and decrease in coolant level starts again due to more intensive evaporation process (with no more thermal expansion).

In parallel to the overheating (warming up) of the coolant in the lower part of the pool (below upper level racks), the rate of steam generated in the upper level assemblies increases improving the heat removal from the uncovered part of the fuel, and starting from about 45–46 minutes of the transient the fuel temperature starts to decrease. Continuous decrease in coolant level results in less steam generated and bigger part of fuel uncovered, i.e. bigger decay power to be removed by steam. After 25 minutes of fuel temperature decrease, it starts to increase again. Overheating of the fuel cladding till the temperature of 1200 °C takes place about 4.23 hours after starting of the transient.

Another accident scenario with the same initiating event and early SFP make-up was studied. Due to significant loss of coolant through the break the coolant level is almost the same as in the first scenario. Some kind of 'feed-and-bleed' takes place in the pool, and the mean temperature of the coolant does not practically increase. However, heat removal conditions for upper level rack assemblies are deteriorated — low temperature of coolant feeding the upper level assemblies result in low rate of steam generation and, thus, in continuous increase in fuel temperature in the upper uncovered part of fuel. In this second scenario with early pool make-up the conditions of fuel damage are reached significantly earlier (less than 1.5 hours after beginning of the transient) than in the first scenario without any pool make-up.

Based on these calculations' results the priority for recovery actions in the considered 2-level racks configuration would be: first to isolate the break in the cooling system rather than to ensure the pool make-up.

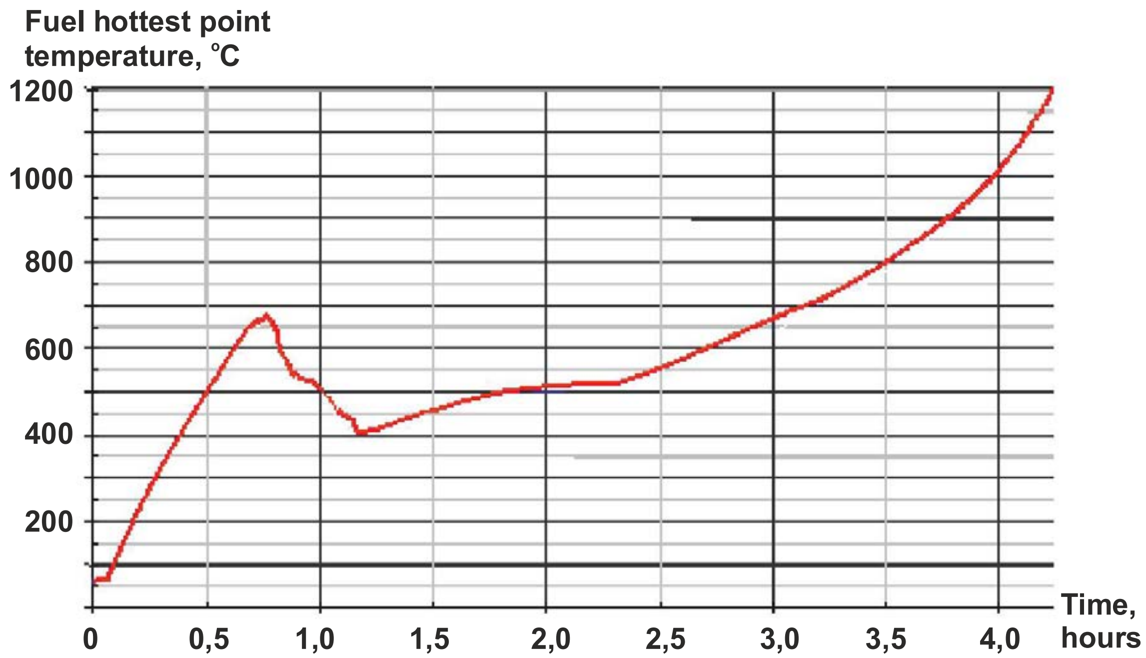

FIG. 5. Change of fuel maximum temperature in the scenario of cooling system tube break (without SFP make-up).

In the scenario with loss of cooling of the SFP, even in case of reactor core full off-load (configuration for higher discussed scenarios), the fuel top part will be uncovered in a time longer than 34 hours (coolant boiling starts about 2 hours and 40 minutes after the beginning of the transient). For the scenarios with only lower level racks containing spent fuel assemblies the cooling system line break will not create quick change of heat removal conditions — at least 2.5 m layer coolant inventory will be available in the beginning phase of the transient.

Severe accidents in SFPs are not studied yet. Draft versions of SFP SAMGs were developed based on known general phenomenology of the accident progression in SFPs. Currently the model is under development (MELCOR 1.8.6 version is used) to support analytical justification of the strategies considered in the SAMGs. In Section 3.3 main approaches for management of severe accidents in SFPs as well as transfer from EOPs to SAMGs are described. In Section 3.4 main tasks defined for analytical part for severe accident management in SFP are discussed.

3.3. Management of severe accident in SFP

Armenian NPP SAMG development program was divided in 2 phases. In phase 1 set of SAMG documentation was developed for conditions of closed reactor and closed (tightened) containment. In the second phase (launched in 2018) draft versions of SAM guidelines were developed based on known phenomenology of the accident progression in SFPs and the approaches to severe accident management used by Westinghouse Owners Group (analytical studies were not performed yet).

The main way to stop the progress of fuel damage in the SFP is providing coolant inventory in the pool to ensure heat removal from fuel — through evaporation in the beginning, then, if the inventory is enough, through circulation of the coolant via cooling system. The attempts to ensure SFP make-up from different sources and through different ways are considered in EOPs that are used before use of SAMGs. If transfer from EOPs to SAMGs was done, this means the attempts were not successful. After the onset of fuel damage in the SFP there are at least 2 phenomena that will influence the priorities of tasks to be completed within the severe accident management — 1) release of radioactive materials from SFP to the Central hall, 2) generation of hydrogen in the SFP and its accumulation in the Central hall. The priorities of strategies comparing to EOPs should be changed making main priority limitation of radioactive releases, both current and potential.

To mitigate the consequences of the severe accident radioactive releases should be limited as much as possible. The way of radioactivity release to the environment is the flow of radioactive materials from SFP atmosphere to the Central hall, and then from there directly to the environment or to the adjacent premises in the reactor building (Central hall is not a hermetic area). If no strategy is implemented, continuous flow of Central hall atmosphere to the environment will take place in result of generation of steam and incondensable gases in the SFP. In the current configuration of the plant, the only way for limitation of releases is the 'direction' of flow through the ventilation system filters.

Although Central hall is not hermetic, it has capability to localize to some extent the radioactive materials and limit the releases. Due to its design, burn of hydrogen even in slow deflagration mode could result in damage of this area boundary and in opening of ways for unobstructed propagation of radioactive materials to the environment. Thus, formation of flammable gas mixture in Central hall should be excluded during the progression of the severe accident.

The major steps considered in draft SAMGs to be implemented within the management of severe accident in SFP are as follows [3]:

- Blocking/closing ways of radioactive materials propagation from Central hall to the environment – depending on the current configuration of the plant different ways for atmosphere propagation could be available; on this step there is need to identify these ways, if any, then close or control them (at the extent possible);
- Organizing filtered venting of the Central hall with the purpose of limiting the unfiltered releases of the gases from the Central hall as well as limiting accumulation of hydrogen in the Central hall and adjacent areas — design of the plant premises and ventilation systems allows to organize flow of atmosphere from Central hall through aerosol filters of reactor building ventilation systems; in case of unavailability of ventilators' power supply, use of vent stack natural draft is considered;
- Identifying/recovering ways for SFP make-up — after completing previous 2 urgent steps related with severe accident phenomena and strongly influencing the consequences of severe accident, there is need to consider the possibilities to recover heat removal from fuel/fuel debris, and the only way is the make-up of the pool;
- Identify and evaluate anticipated impacts of pool make-up at the current conditions and with available means of make-up — during severe accident progression make-up of the SFP is related not only with positive effects or benefits but also with negative impacts; potential benefits are: prevention or delay of fuel melt interaction with concrete basement of the pool; restoration of heat removal from fuel assemblies/fuel debris; ensuring of coolant inventory for the recovery of the mechanism of pool cooling; ensuring coolant inventory to have adequate level of coolant over fuel for scrubbing of fission products; the possible negative impacts are: generation of additional mass of hydrogen and possible increase of radioactive materials release in the beginning phase of the make-up (intensive steam generation in the beginning phase of make-up will result in high speeds of steam-gas flow and, thus, large aerosols and fuel fines could be transported by the flow). Before make-up is initiated the positive and negative effects must be weighed — the negative impacts must be assessed to determine if fission

product releases can be increased or if other recovery actions can be jeopardized by initiating pool make-up;
- Control of the strategy of pool make-up — after initiating the strategy of pool make-up there is need to control the effects; define if the make-up is efficient; define if the tendency of change of parameters is compliant with anticipated tendencies, etc.;
- Transfer of SFP heat removal to its cooling system – after recovery of coolant inventory in the pool there will be needed to make the transfer to the normal pathway of heat removal from the SFP.

During the implementation of the mentioned steps there are 2 main decision points:

- Determine if the available make-up capabilities are adequate. Depending on the conditions in the SFP and anticipated flow rate of make-up, the impacts can be different; e.g., if the fuel assemblies are fully uncovered, there would be air flow through the assemblies ensuring some heat removal from fuel; depending on presence of pathways of coolant loss from pool, their size and location, the make-up with relatively low flow rate can result in limited increase of coolant level in the pool, which will not ensure adequate heat removal but can blockade the air ingress pathway; when assessing the adequacy of coolant inventory available in source of make-up, the minimum desired level in the pool is considered to be at least 0.6 m over fuel assemblies, as according to available analysis data [1] such coolant layer over fuel will prevent increased β- and γ-radiation field;
- Determine the rational for initiating the pool make-up in the current conditions of the SFP and the plant as well as with the current capabilities of make-up — decision on initiating the make-up should be taken based on the following factors:
  - Potential benefits of SFP make-up;
  - Anticipated negative impacts;
  - Consequences of not initiating the make-up;
  - Anticipated timeframes for recovery of other equipment.

Available instrumentation for SFP is as follows:

- Level measurement;
- Coolant temperature measurement.

Figure 6 presents the scheme for transitions from EOPs to SAMG documentation. EOPs documentation includes 3 standard sets of procedures — EOPs on power; Shutdown EOPs; SFP EOPs. Fragmentation of SAM guidelines was made based on anticipated pathway of radioactivity releases: 1) releases from containment, and 2) releases through reactor building Central hall. In the first case the source of radioactivity is the reactor, and in the second case the source of radioactivity can be the reactor (open reactor or closed reactor but open containment - configuration of the plant possible at the end of outage during short time period), SFP of unit 1 and SFP of unit 2.

In ANPP SAMGs plant diagnostics during severe accident will be ensured using 2 different diagnostics flow-charts – DFC and DFC-2. DFC is developed for the configuration of the plant with closed reactor and closed containment using mainly the methodology of Westinghouse Owners Group [4, 5]. It controls such parameters, as dose rate on the plant site, hydrogen concentration in containment, pressure and temperature in containment, steam generators coolant levels, primary pressure, core exit temperature, reactor vessel failure symptoms. DFC-

2 is referenced in case of severe accident in SFP or in open reactor or in closed reactor with open containment. For each of these mentioned cases there is a special guideline which will be used to mitigate the severe accident (transitioned from DFC-2). These guidelines can be used in parallel, if needed, depending on number of facilities containing damaged nuclear fuel. In order to exit SAMGs, conditions of controlled stable state for all 3 facilities containing spent nuclear fuel (reactor plant, SFP1, SFP2) must be met.

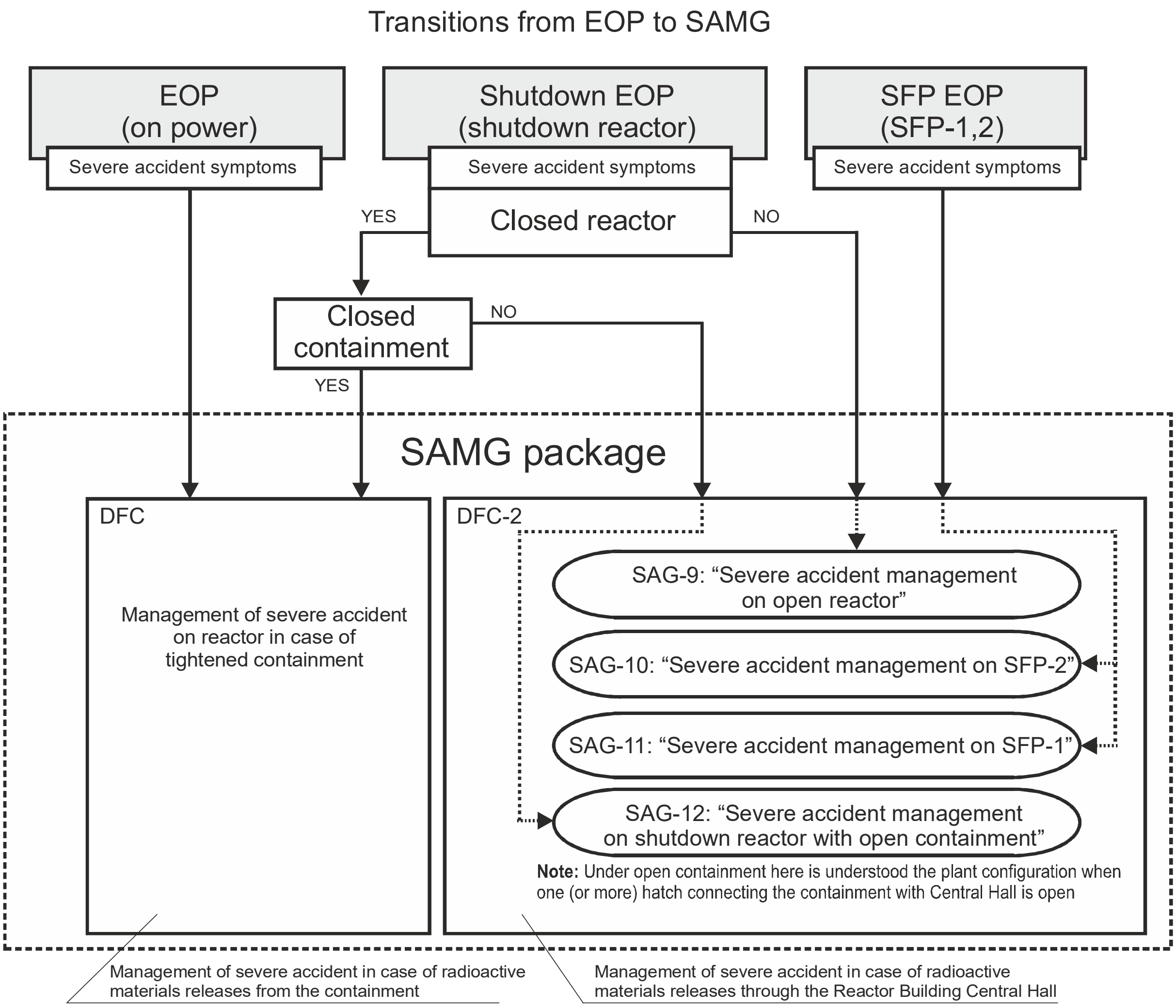

FIG. 6. Transitions from EOPs to SAMGs.

3.4. Main tasks defined for analytical part for severe accident management in SFP

Recently activities for severe accident study for spent fuel pools (SFP) and open reactor configuration started. The MELCOR model (using MELCOR 1.8.6 version) is under development. Below are the main tasks defined by SAMG developers for analytical team, considering the needs of analytical data during the decision making process when using SAMGs.

– The considered configurations of the SFP must include the anticipated conditions with 1) only lower level racks filled with fuel assemblies, 2) the both level racks filled with fuel assemblies (with maximum anticipated number of assemblies as well as maximum total decay heat in both cases);

- The model must include also the ventilation systems (including the vent stack) to ensure the modelling of filtered venting from of the plant Central Hall (through different paths). It must model also the natural draft of the vent stack and, thus, the flow of gazes without operation of the ventilators.
- The model must be detailed enough to ensure the consideration of the possible air ingress into the assemblies from lower head and air circulation through the assemblies;
- The model must consider (at the extent possible) the heat exchange of steam-gas mixture with constructions and walls of the Central Hall (to consider the steam condensation rates and its influence on the flammability of the gas mixture and the scope of releases which will depend on intensity of forcing out the gas media from the Central Hall to the environment by steam generated in the pool);
- The model must include consideration of the Central Hall constructions leakages — justified assumptions must be done;
- The model have to allow to assess the efficiency of the heat removal by air in case the lower heads of assemblies are uncovered and the air ingress into the assemblies is possible (to assess how it can mitigate the heating up of fuel or if it can prevent the overheating of the fuel, what temperatures of cladding are anticipated in case of cooling by air);
- The calculations must include scenarios with loss of heat removal from SFP and loss of coolant. For the case of severe accident during refuelling (with condition of connected spent fuel pool and refuelling pool) simultaneous accident on 2 SFP and Open Reactor must be also considered with applicable assumptions;
- The calculations must include scenarios without any operator actions to assess the phenomenology of the severe accident and different phases of its progression as well as the scenarios with implementation of strategies considered in the guidelines (to assess the positive and negative impacts of the strategies);
- The calculations must reveal the conditions (decreased level of coolant in the pool) when the failure of fuel cladding is anticipated as well as the tendency of change of the temperature in the SFP (thermocouples measurement values) during the heating up of the fuel, the runaway oxidation of fuel cladding and later phases of severe accident. Analytical part has to define the scale of temperature measurements to be sufficient for the severe accident phase;
- The calculations must reveal the quantity (tendency of generation) of the hydrogen that can be generated in the pool in case of different accident scenarios as well as the tendency of hydrogen concentration increase in Central Hall. It must reveal if flammable mixtures can be formed in the Central Hall and the minimal anticipated timeframes for its formation;
- The calculations must reveal the quantity of radioactive materials released from pool to the Central Hall and the influence of aerosols natural deposition;
- The calculations must reveal the efficiency of Central Hall venting — mitigation of releases of radioactive materials and prevention of flammable mixture formation (especially for the case without availability of ventilators and use of vent stack natural draft);
- The calculations must include the reflooding of uncovered fuel, assessment of the volume of coolant needed to reflood the fuel in the pool (a curve for dependency of level on the coolant volume in the pool would be very useful), assessment of the influence of the make-up rate on the accident progression and its mitigation as well as the possible negative impacts like generation of additional quantity of hydrogen,

possible intensive releases during first phases of make-up — increase of aerosols release from pool volume to the Central Hall, and then to the environment, etc;

- Calculations must justify (or disprove) the fact that the make-up of the pool (containing uncovered overheated fuel) with bigger flow rates will result in better results and more favourable negative impacts (this assumption is made based on the worldwide existing studies of severe accidents). It must define the minimum desirable rate of make-up which will ensure effective mitigation of the accident with acceptable negative impacts;
- The minimal rate of SFP make-up for the decay heat removal must be assessed (depending on time and configuration of the SFP).

REFERENCES

[1] ORGANISATION FOR ECONOMIC CO-OPERATION AND DEVELOPMENT NUCLEAR ENERGY AGENCY, Status Report on Spent Fuel Pools under Loss-of-Cooling and Loss-of-Coolant Accident. Conditions, NEA/CSNI/R(2015)2, OECD-NEA, Paris (2015).

[2] ARMENIAN NUCLEAR POWER PLANT, Technical Basis Document for Armenian NPP Units 1,2 SFPs Emergency Operating Procedures, ANPP, Metsamor (2019).

[3] ELECTRIC POWER RESEARCH INSTITUTE, Severe Accident Management Guidance Technical Basis Report, EPRI, Palo Alto, CA (2012).

[4] ARMATOM, Draft of Technical Basis Document for ANPP guideline “Severe accident management on SFP-2”, ARMATOM, Yerevan (2018).

[5] WESTINGHOUSE OWNERS GROUP, Severe Accident Management Guidance - Vol.1 (1994).

SPENT FUEL POOL SEVERE ACCIDENTS MODELLED WITH MELCOR TO SUPPORT A PSA LEVEL 2

N. NUNES ARAÚJO, M. RODRIGUEZ GUAL, M. COELHO MATURANA
Amazonia Azul Technologias de Defesa S.A. (AMAZUL),
Brazil

1. INTRODUCTION

Probabilistic Safety Assessment (PSA) is a key part of a Nuclear Power Plant (NPP) licensing process [1]. It considers the elaboration and updating of probabilistic models that estimate the risk associated to the operation, allowing the risk monitoring from the design to the plant decommissioning, for both operational as regulatory matters. The PSA of industrial installations is a subject that has evolved with the complexity of the systems [2, 3], and presents specific methodologies for some hazard groups, e.g. flood, fire and seismic events.

In nuclear industry, the PSAs are performed for three different levels: from the core damage to a possible radiological release. The PSA Level 1 identifies potential accident sequences and provides an estimate of the frequency they can lead to major fuel failure. After modelling the phenomena that occur due to the sequence of events indicated in PSA Level 1, the PSA Level 2 analyzes the behaviour of containment, evaluates the release of radionuclides, providing frequency estimation and release of radioactive material. The PSA Level 3 analyzes the consequences of a release of radioactive material into the environment and provides an estimate of the effects on public health.

After a safe shutdown of the reactor, heat continues to be generated in the nuclear fuel due to the fission products, so the fuel needs to be cooled continuously, even if its power is low in relation to the power in full operation. If the fuel is not cooled, there will be an increase in temperature in the materials and possible melting.

In most Pressurized Water Reactor (PWR) NPPs, nuclear fuel is removed from the pressure vessel and moved to pools of water, named spent fuel pool (SFP). The fuel is kept in racks in the pool, submerged in water that remains continuously circulated to dissipate the decaying heat of the fuel elements and provide adequate radiological shielding.

For SFP accidents, a set of issues is identified and addressed. If the SFP is located outside the containment, the potential release paths to the environment depend very much on plant specific properties, e.g. ventilation systems, building doors, roof under thermal impact, size of rooms on the path, etc. [4]. In any case the impact of very hot gas and of hydrogen has to be considered. Besides, the PSAs Level 2 require a detailed knowledge of severe accident phenomena and analysis of the design vulnerabilities to the severe accidents — given the complexity of these phenomena, some computer codes were developed to support these analyses (e.g., MELCOR [5], ASTEC [6], etc).

This paper discusses the initial studies for a Shutdown PSA Level 2, considering an SFP, and the preparation of a model in MELCOR that will be used to simulate different types of severe accidents in a reference NPP in the design phase, to support the PSA, as described in NUREG 0800 [1]. Thus, next section presents the reference NPP, focusing its SFP cooling systems and, after that, this paper presents the failure sequences for the mentioned systems —

as obtained from the Shutdown PSA Level 1 for the reference NPP — and a discussion on the severe accident phenomena that could occur in the reference plant SFP.

2. SFP COOLING SYSTEMS

The reference NPP is a PWR in the design phase with 48 MW of thermal power. The reactor will consist of 21 fuel elements with uranium oxide (UO_2) fuel rods enriched at about 5%. The SFP will have a storage capacity of 378 fuel elements of the 17 × 17 fuel type, enough for thirty years of operation.

In order to ensure the operability and safety conditions, five systems are associated with the SFP. The systems related to the cooling of the SFP are the Spent Fuel Pool Cooling System (SFPCS), designed to remove the residual heat from the existing spent fuel elements caused by the decay of fission products, the Safety Water Cooling System (SWCS) serve as a source of cooling water for the SFPCS heat exchangers. The other systems present are the Cleaning and Purification System (CPS), Sampling System (SS), Drainage System (DS).

Since the water cooled by the SFPCS will be in direct contact with the fuel elements, only this system will be modelled in MELCOR, and the other systems will be considered as contour condition variables – in the first approach for the PSA Level 2. Thus, this section presents this system in more detail.

2.1. System description

The scheme presented in Fig. 1 was developed to facilitate the SFPCS description — the equipment involved in the operation can be identified by the following codes:

– FE: fuel element;
– T: heat exchanger;
– B: pump;
– V: valve.

In this scheme, the continuous lines represent the pipes considered in this work and the dashed lines represent the pipes of the systems associated with the SFPCS.

Among the characteristics of the SFPCS deemed important for the operation design, the following were highlighted:

System functions: it cools the compartments in which the FEs with residual heat are located in normal and degraded operation, thus maintaining the water temperature below 41°C; during a transition — which may occur between normal and degraded operation — it keeps the water temperature in the SFP below 60°C. The SFP is expected to receive an annual load of FE;

Compartments to be cooled: The FE can be in four compartments of the SFP, called SFP-I (Compartment I), SFP-II (Compartment II), SFP-III (Compartment III) separated by watertight gates and interconnected by a TC (Transfer Channel) — these compartments are identified in Fig. 1. Only the TC will not be cooled directly — the FE will remain shortly in this compartment. It is important to note that the TC is the physical connection between the SFP compartments, and that, during the cooling operation, these compartments are isolated. Thus, in Fig. 1, the compartments were presented isolated;

The SFP-II is intended to receive all spent fuel elements after being initially removed from the reactor and then transferred to their appropriate compartments. During the reference NPP shutdown phase all the fuel is moved into the SFP-II, so only the cooling to SFP-II is included in the Shutdown PSA Level 1 [7].

System operation: all actions of the components depend on manual actuation, with the exception of automatic pump shutdown (B1 and/or B3) in case of low flow downstream, and actuation of the pump on standby — B2, in case of failure of B1 (B1 and B2 are 100% redundant), and/or B4, in case of failure of B3 (B3 and B4 are 100% redundant). The valves are actuated locally, and the pumps can be actuated either locally in panel P1, or remotely in panel P2. After the first actuation, the pump B1 (and/or B3) remains at low speed provided that there is no need to cool the SFP by the SFPCS, whereas the pump B2 (and/or B4) remains off, and will be actuated only in case of failure of pump B1 (and/or B3) — a controller deactivates the pump B1 (or B3) and activates the pump B2 (or B4) by a low flow signal received from the sensors;

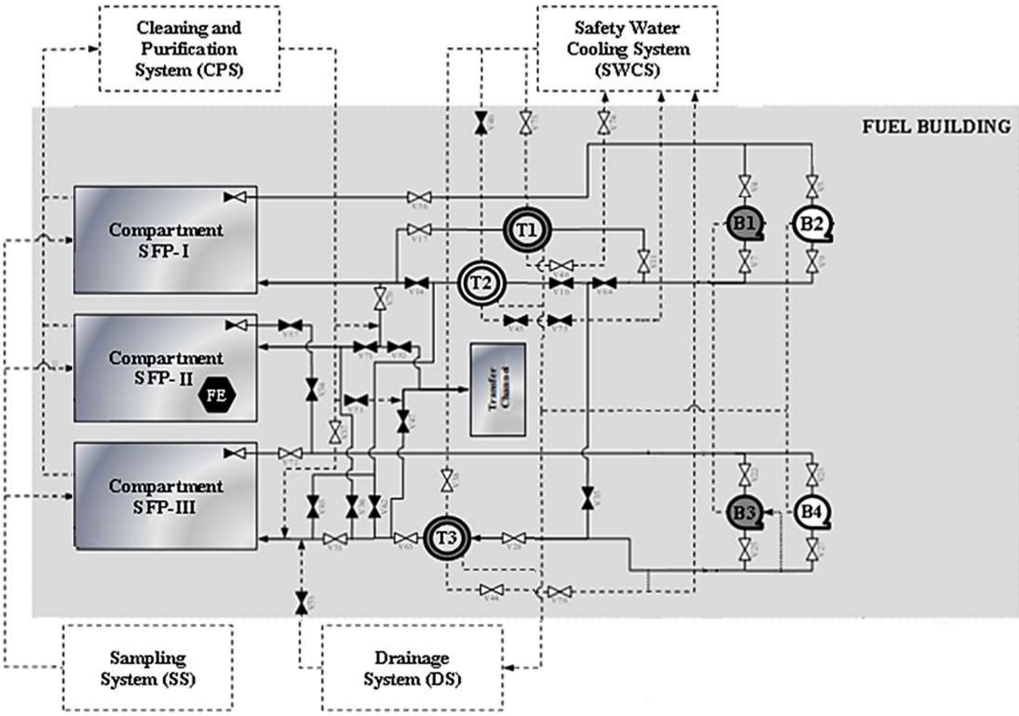

FIG. 1. SFPCS schematic arrangement [8].

Heating and cooling time: SFPCS is considered to have the ability to cool the largest SFP compartment from 41–37 °C in 4 hours. The SFP temperature, without SFPCS performance, rises from 37–41 °C in 8 hours, and from 41–60 °C in 38 hours (in the most adverse design condition, i.e., considering the higher ambient temperature of the historical series and the highest possible power for the FE). Additionally, the FE may exhibit negligible residual heat within 10 days, which does not exceed the natural capacity for heat dissipation in the SFP. Thus, considering that the system does not operate continuously, the expected actuation time for the SFPCS is 80 hours;

Interfaces with other systems: in addition to the ES (Electrical System) — not shown in Fig. 1 — which feeds the equipment connected to the panel P1 and the equipment present in the CR, the following systems interface with the SFPCS: a) CPS; b) SWCS; c) SS, and; d) DS;

Operational modes: In addition to the normal operation, Table 1 shows the equivalent modes (which cool the same compartments) for degraded operation. Degraded modes can be identified by the same letter accompanied by a number (e.g., modes 'B.1', 'B.2' and 'B.3' are the possible degraded modes for cooling the SFP-II compartment). To successfully cool the fuel elements in the SFP-II, one of the two circulation pumps B3 and B4 and one of the two heat exchangers, T2 and T3, must be successful.

TABLE 1. SFPCS OPERATIONAL MODES

Operational Mode	Cooled Compartments	Description
B	SFP-II	Normal operation. Circulation by pump B3. Cooling by the heat exchanger T2.
B.1		Degraded operation. Circulation by pump B3. Cooling by the heat exchanger T3.
B.2		Degraded operation. Circulation by pump B4. Cooling by the heat exchanger T2.
B.3		Degraded operation. Circulation by pump B4. Cooling by the heat exchanger T3.

Maintenance procedure: it is expected the conditions of the SFPCS equipment to be checked immediately before its operation. However, in this work, the maintenance procedure is not developed, and it is considered that the equipment will be as good as new immediately after the maintenance procedure — though the possibility of a failure on demand is considered for the equipment which presents mobile parts (valves, panels and pumps), whereas a failure on demand for heat exchangers, for example, is not being considered.

2.2. Design constraint

In addition to the aforementioned characteristics, the following restrictions for the system operation design are presented as follows:

Reliability: the probability of not cooling the FE with significant residual heat must be less than 1.00E-07 in a year's time — this condition is presumed when the SFP water temperature exceeds 60ºC. The SFPCS failure rate must be less than 1.00E-03 in a year's time;

Fluid mixing: in order to minimize the generation of tailings, the fluids in the different compartments must be independently cooled, e.g., the same heat exchanger or circuit section must not participate in the cooling of two compartments simultaneously.

The reliability criterion (which was presented in the first topic above) summarizes the concern about the lack of FE cooling due to the failure of different systems, e.g., in addition to SFPCS, ES, CPS. According to this criterion, the frequency of cooling lack should be less than 1.00E-03 in a year's time, specifically for the SFPCS. Note that the lack of water cooling by the SFPCS does not necessarily result in a lack of FE cooling, i.e., the lack of cooling by the SFPCS is an initiating event for other actions, including the SFPCS recovery through corrective maintenance, for example, and / or its operating without meeting the non-mixing criteria. These conditions will be considered in the Shutdown PSA Level 2, in a Plant Response Model (PRM) development.

3. FAILURE SEQUENCES

The PSA Level 1 involves the development of potential accident sequences and solution to evaluate the frequency of an end state of core damage as well as an understanding of the ability to achieve safe-stable state to protect plant staff and the public. The accident sequence delineation on PSA Level 1 consisted of the development of functional event trees that outline the necessary functions and the top logic development that defines how plant systems perform those functions. The event trees are coupled with the system models through fault tree linking to develop a comprehensive, integrated model. The relative importance of systems and components, initiating events, etc. are obtained from the cutsets. For the Level 1 model, each event tree sequence represents either a success or a fuel damage event. This model does not assess other outcomes, such as economic risk or plant personnel risk. The system success criteria are performed using a best estimate approach.

The reference NPP is not currently an operating plant, system unavailability are not based on plant experience but rather on conservative assumption. Thus, the Shutdown PSA Level 1 will need to be validated upon completion of the installation using an acceptable thermo-hydraulic analysis code, simulator experience, or documented manual calculation. In the Shutdown PSA Level 1, the SFPCS system was identified as the most important system with respect to core damage contribution from a system during shutdown. A failure to remove decay heat from the fuel pool will ultimately lead to damaging the fuel elements in the SFP.

Table 2 provides six cutsets (from Shutdown PSA Level 1) in order of descending frequency of fuel damage at the SFP – listing the individual events making up a cutset and which, occurring together, may cause core damage and the correspondent probability. As part of the PSA Level 2 first approach, these SFP fuel damage events will be modelled by a dedicated code for severe accidents. In Table 2, Shutdown Phase II, III, IV duration refers to the time in which the FE is in the SFP.

Still in the Shutdown PSA Level 1, the second highest Common Cause Failure (CCF) Event, based on Fussell-Vesely importance, is the B3 and B4 circulation pumps from SFPCS failing to start – if these pumps fail to start, the SFPCS system will fail to remove decay heat from SFP-II. In Table 2, this event is included in cutset number 4.

TABLE 2. SHUTDOWN PSA LEVEL 1 TOP 6 SFP FUEL DAMAGE FREQUENCY CUTSETS

Cutset Number	Event Description	Frequency (yr)
1	Failure to open the manual valve 036 and consequent loss of SFPCS.	7.79E-06
2	Failure to open the manual valve 034 and consequent loss of SFPCS.	7.79E-06
3	Failure to open the check valve 032 and consequent loss of SFPCS.	3.33E-06
4	Motor-Driven Pumps B4 and B3 failure to start due to CCF and consequent loss of SFPCS.	3.12E-06
5	Motor-Driven Pump (Running) B4 failure to Start and Pump B3 unavailable due to testing and maintenance. Loss of SFPSC.	4.55E-07
6	Motor-Driven Pump (Standby) B3 failure to Start and Pump B4 unavailable due to testing and maintenance. Loss of SFPSC.	4.27E-07

4. MELCOR CODE

Analyses of SFP accident processes in the case of a loss of coolant with no heat removal are a concern in the nuclear industry and have been studied [9–11]. The loss of cooling accident (LOCA) is typically induced from a complete loss of SFP safety/cooling systems. In the case of LOCA, the time to the pool uncover is obviously dependent on the level of decay heat load [12] — it is increased by, for example, the decrease in the time after the shutdown (for the full core offloading), or the increase in the fuel burn up.

Loss of cooling can be caused by the loss of SFP cooling flow, or because the heat generated in the SFP is not fully transferred to the ultimate heat sink. In the first case, the loss of SFP coolant flow can be due to several reasons, such as loss of electrical power to the cooling pumps, pump failure, flow blockage, loss of suction caused by the loss of water level, or a diversion in the SFP cooling system. In the second case, loss of heat sink can be due to the lack of enough cooling flow in the heat exchangers, or due to heat loads higher than the system design capacity. Any degradation of the heat removal characteristics, such as heat exchanger fouling, insufficient coolant flow, etc. can result in increased water temperature in the SFP [13].

The MELCOR can be used to confirm the Shutdown PSA Level 1 success criteria and accident sequence development activities and all aspects of the SFP deterministic accident progression modelling, supporting the Shutdown PSA Level 2 [1].

MELCOR is a fully integrated, engineering-level computer code whose primary purpose is to model the progression of accidents in Light Water Reactor (LWR) NPP [5]. Aiming supporting the severe accidents investigations, several new features of MELCOR model has been added to simulate both Boiling Water Reactor (BWR) fuel element and PWR 17 × 17 fuel element in an SFP rack undergoing severe accident conditions [14]. Versions of the MELCOR code has been developed by Sandia National Laboratories for plant risk assessment and source term analysis since 1982. This code uses the approximation of point kinetics for neutron calculations. The default decay heat curves and radionuclide inventories were obtained from ORIGEN [15] calculations.

MELCOR is composed of several modules, called packages, responsible for modelling a different portion of the accident phenomenology. The MELCOR thermo-hydraulic packages are composed of control volumes, CV, and, flow paths, FL, which represents the fluid paths from one control volume to another. The packages are integrated in a suitable way to model the pool. There are special packages that are specific to engineered safety features such sprays, fan coolers, passive autocatalytic hydrogen recombiner, among others.

The SFP modelling in MELCOR consists of the cells modelled in the core (COR) package, associated to CVH package that represented the water of the SFP. This association allows the modelling of the heat transfer between core structures and control volumes, volume changes and the blocking of the refrigerant due to the reallocation of the corium.

The COR package represents the components of the core and its lower region, subdivided into axial levels and radial rings specified by users. The radial rings are numbered consecutively from the centre line of the core outwards — the axial levels are numbered from the bottom to the top. Each axial level at each radial level represents a cell. Each cell allows the modelling of one or more components such as fuel rod, cladding, fuel element, support structures, rack, etc.

5. SFP MODELLING IN MELCOR

The fuel elements in the reference SFP of this work are divided into 3 radial rings and 12 axial levels for the MELCOR COR nodalization. The flat lower head wall directly below the core was divided into 6 segments associated with a lower cavity, modelled by the cavity (CAV) package. The SFPCS circuit is closed and the pipes are modelled from control volumes and heat structures. The pump, the heat exchangers and the valves are modelled through specific options in the flow path package.

The thermal-hydraulic diagram of the SFP nodalization is shown in Figure 2. There are eleven control volumes, the CV-1 and CV-2 models portions of the water of the pool, the CV-3 models the bottom of the SFP, the CV-4, CV-6 and CV-8 are associated with the radial rings of the core nodalization and models the fuel channels, the CV-5, CV-7 and CV-9 represents the bypass, the CV-10 models the upper region of the SFP above the fuel elements and the CV-11 represents the atmosphere. Nineteen flow paths, represent by the arrows on the Fig 2, are modelled. The floor and the walls surround the pool are modelling by heat structures of concrete and stainless steel.

Twenty-one fuel elements, equivalent to one core, are considered to be in the SFP-II compartment with decay heat correspondent to 5 days. The simulated accident scenario consists in the loss of cooling of the entire SFP-II, representing the top six sequences of the PSA level 1.

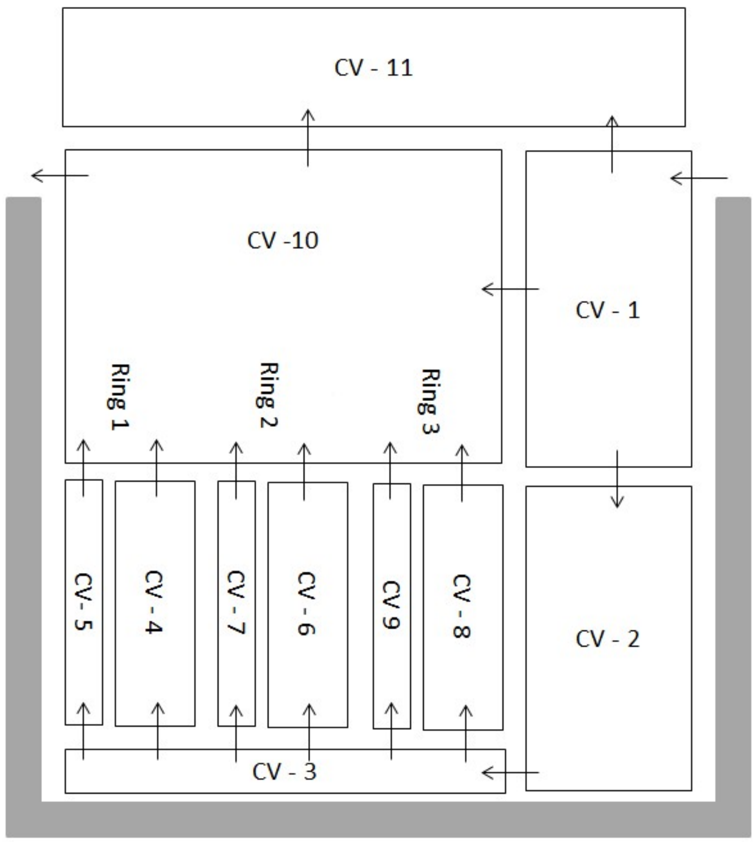

FIG. 2. Thermal-hydraulic nodalization of the SFP in MELCOR.

6. RESULTS OF THE SIMULATION

The accident is assumed to occur at 0 seconds in the simulation. The water in the SFP starts to heat immediately after the beginning of the accident because of the decay heat of the fuel elements, Fig. 3.

The Fig. 4 presents the trend of the SFP water level decrease for four control volumes. The increase in level is due to the thermal expansion until saturation conditions are reached and then a decrease in level. The core start to be uncovered at about 83 hours after the loss of the pool cooling and the SFP runs out of liquid water at about 97.22 hours.

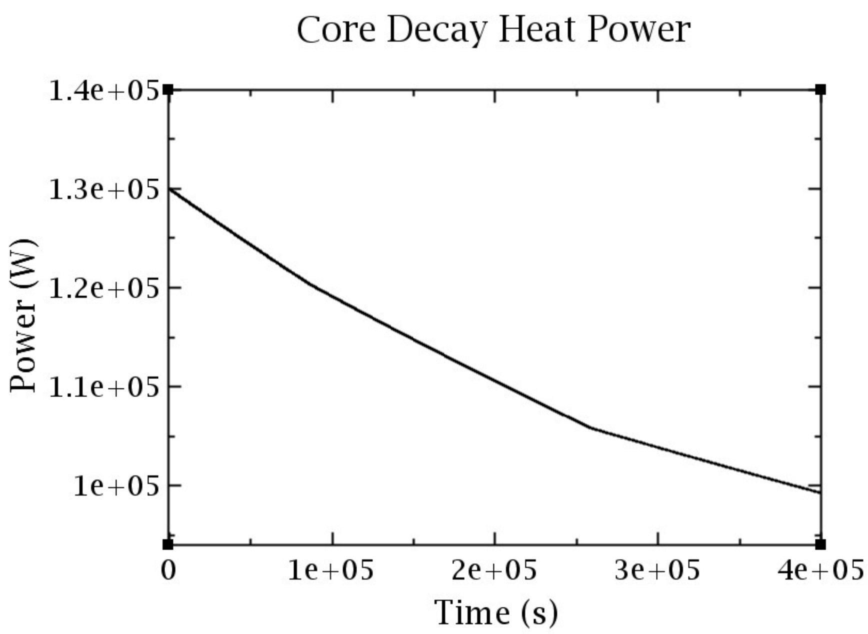

FIG. 3. Total core decay heat power of the FE in the SFP.

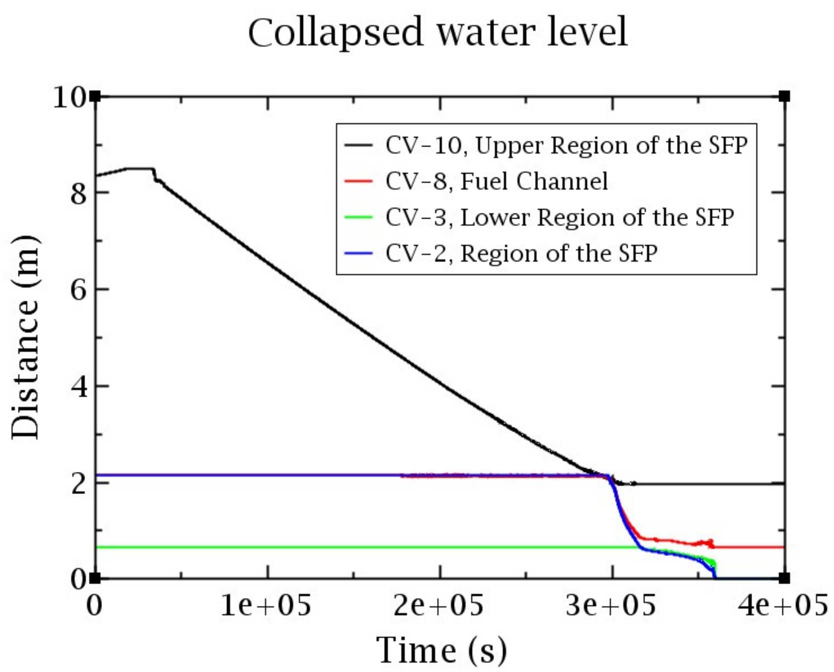

FIG. 4. Collapsed water level of the reference SFP under accident scenario.

The Fig. 5 shows the gradual temperature increase up to the saturation temperature. The temperature remains the same until the FE are uncovered, resulting a sharp increase in fuel cladding temperature. The maximum cladding temperature reaches 1700 K after the core is uncovered (t>83 h). The fuel claddings are partially melted.

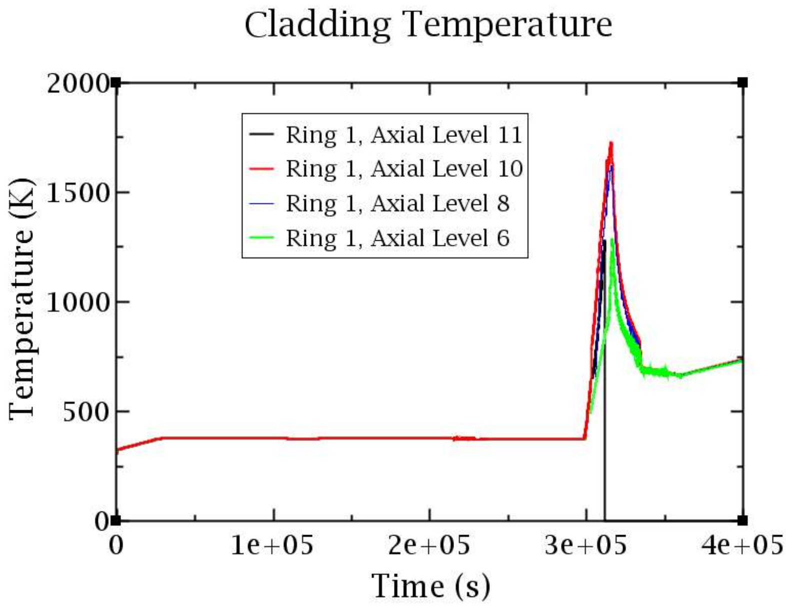

FIG. 5. Fuel cladding temperature under accident scenario.

The generation of hydrogen starts at 87 hours. The total cumulative amount of hydrogen produced by the zirconium oxidation and the steel oxidation during the progress of the accident is 10.7 kg, and the mass of hydrogen in the atmosphere of the building is 8.2 kg (Fig. 6 and Fig 7).

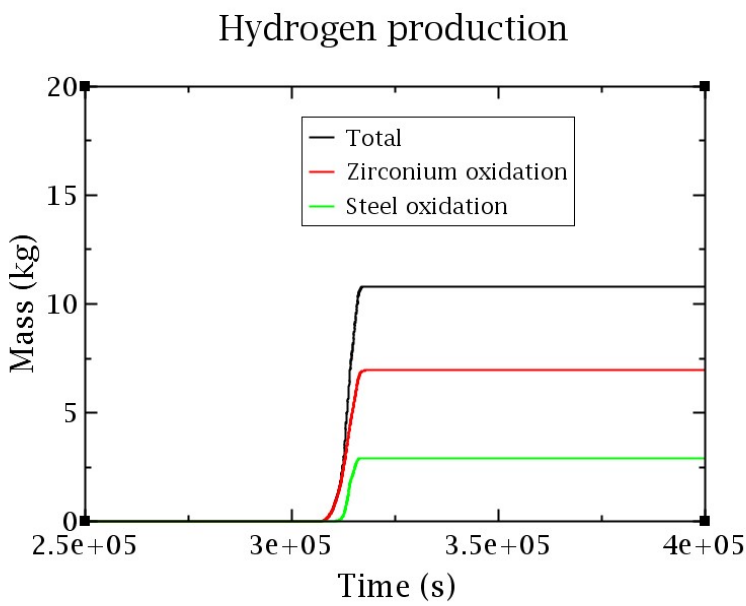

FIG. 6. Total cumulative hydrogen production in the SFP.

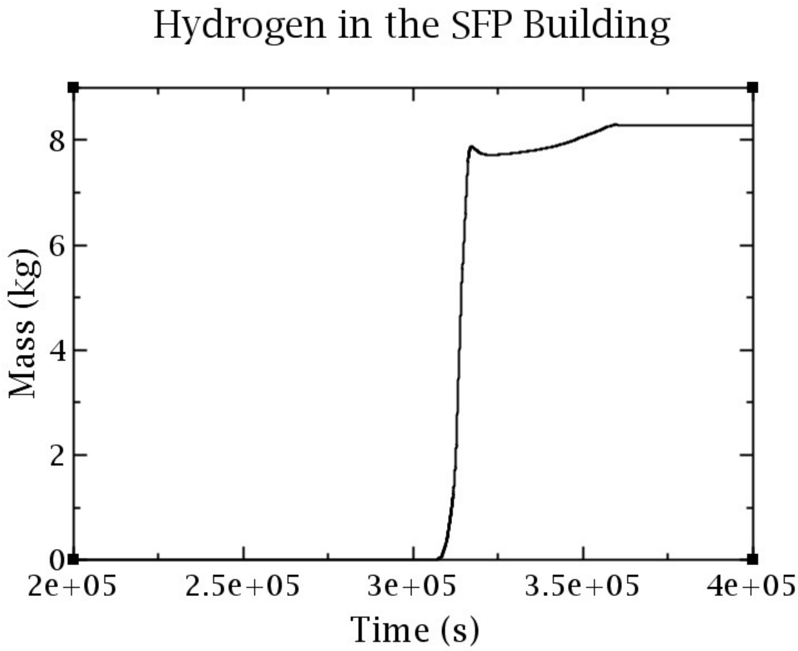

FIG. 7. Total cumulative hydrogen production in the SFP.

CONCLUSIONS

The severe accidents simulation using MELCOR code to support a Shutdown PSA Level 2 of a reference NPP — based on the information presented in the Shutdown PSA Level 1 was successfully developed.

The severe accidents simulated promoted realism in the treatment of the overall site risk and a better understand of the physical phenomena.

The calculations predicted the core degradation and hydrogen production on severe accident inside SFP. The evaluation of SFP accidents without taking into account the effectiveness of accident management measures after fuel damage may result in overestimation of risk.

The resulting MELCOR model will be applied in the PRM development, which will be useful for the calculation Large Early Release Frequency (LERF) of the reference NPP. The calculations of containment failure frequencies and mitigation of accident progression to a reference NPP will be based on the results of this simulation.

REFERENCES

[1] UNITED STATES NUCLEAR REGULATORY COMMISSION, Probabilistic Risk Assessment and Severe accident Evaluation for New Reactors, NUREG-0800, Section 19.0, USNRC, Washington, DC (2007).

[2] HAYNS, M. R., The Evolution of Probabilistic Risk Assessment in the Nuclear Industry, Trans. IChemE **77** B (1999) 117–120.

[3] MARTINS, M. R., MELO, P. F. F., MATURANA, M. C., “Methodology for system reliability analysis during the conceptual phase of complex system design considering human factors”. Proc. Int. Topical Mtg on Probabilistic Safety Assessment and Analysis (PSA 2015), ANS, LaGrange Park, IL (2015).

[4] KUMAR, M., LÖFFLER, H., MORANDI, S. GUMENYUK, D., DEJARDIN, P., YU, S., et al., Complement of existing ASAMPSA2 guidance for Level 2 PSA for shutdown states of reactors, Spent Fuel Pool and recent R&D results, IRSN/PSN-RES-SAG 2017-00005, EURATOM ASAMPSA_E 7th Framework Programme, Contract 605001 (2016).
[5] HUMPHRIES, L. L., BEENY, B.A., GELBARD, F., LOUIE, D.L., PHILLIPS, J., MELCOR Computer Code Manuals Vol. 1: Primer and Users' Guide Version 2.2.9541, SAND2017-0455 O, SNL, Albuquerque, NM (2017).
[6] CHATELARD, P., REINKE, N., ARNDT, S., BELON, S., CANTREL, L., et al., ASTEC V2 severe accident integral code main features, current V2.0 modelling status, perspectives, Nucl. Eng. Des. **272** (2014) 119–135.
[7] YOUNG, V. T., Appendix E: Low Power and Shutdown Analysis, Revision 0, RSC Engineers Inc., RSC 11-29 (2011).
[8] MATURANA, M. C., Consideração da confiabilidade humana na concepção de sistemas complexos: desenvolvimento e aplicação da TECHR, São Paulo (2017) *(In Portuguese).* http://www.teses.usp.br/teses/disponiveis/3/3135/tde-29062017-082417/pt-br.php
[9] STEINRÖTTER, T., Application of MELCOR to Severe Accident Analyses for Spent Fuel Pools of German Nuclear Power Plants, Presented at 4th European MELCOR User Group (EMUG), 16-17 April 2012, Cologne.
[10] KIM, W.T., SHIN, J.U., AHN, K.II, Development of Methodology for Spent Fuel Pool Severe Accident Analysis Using MELCOR Program, Proc. Transactions of the Korean Nuclear Society Spring Meeting , 6-8 May 2015 Jeju, Korea, KNS, Daejeon (2015).
[11] ALCARO, F., STEMPNIEWICZ, M. M.., SFP LOCA Analysis with MELCOR, Presented at 8th European MELCOR Group User Group(EMUG), 6-7 Apr 2016, London.
[12] AHN, K.II, KIM, W.T., The plant-specific Spent Fuel Pool severe accident analysis to support a SFP risk and accident management, Proc. 23 Conf. Structural Mechanics in Reactor Technology (SMiRT-23), Int. Assn. for Structural Mechanics in Reactors Technology, Raleigh, NC (2015).
[13] INTERNATIONAL ATOMIC ENERGY AGENCY, OECD-IAEA Paks Fuel Project Final report, IAEA, Vienna (2010).
[14] CARDONI, J., MELCOR Model for an Experimental 17×17 Spent Fuel PWR Assembly, SAND2010-8249, SNL, Albuquerque, NM (2010).
[15] OSTMEYER, R. M., An Approach to Treating Radionuclide Decay Heating for Use in the MELCOR Code System, NUREG/CR-4169, SAND84-1404, SNL, Albuquerque, NM (1985).

CLADDING BEHAVIOUR UNDER SEVERE ACCIDENT CONDITIONS IN SFP

B. JÄCKEL, T. LIND
Paul-Scherrer-Institute,
Villigen
Switzerland,
Email: bernd.jaeckel@psi.ch

M. STEINBRÜCK
Karlsruhe Institute of Technology,
Eggenstein-Leopoldshafen,
Germany,
Email: martin.steinbrueck@kit.edu

1. INTRODUCTION

While in a reactor accident the reactor pressure vessel and the containment are barriers for the fission product release, the cladding of the fuel in a spent fuel pool is the only barrier between the fission products and the environment. Therefore cladding integrity is of high importance for the wet and dry storage of nuclear spent fuel. Since more than 10 years Paul-Scherrer-Institute (PSI) is involved in research activities to investigate and model phenomena, which are of great importance for the cladding integrity under spent fuel pool conditions. Part of the phenomena like air oxidation and break away of oxide layer were not modelled in the severe accident codes [1] and so a new model, which was primarily thought for air ingress during a reactor accident or a mid-loop accident during maintenance, was developed using separate-effect test data from IRSN, France [2] and KIT, Germany [3]. This new model was implemented in the severe accident codes SCDAP/RELAP5 and MELCOR [4, 5]. Then the focus of the severe accident research group (SACRE) concentrated more on the “Benchmark Study of the Accident at the Fukushima Daiichi Nuclear Power Station (BSAF) Project” and on the spent fuel pool and possible accident scenarios with the participation in the OECD/NEA SFP project [6, 7]. After the Fukushima accident, the SACRE group was involved in an IAEA project to collect, analyze and assemble data from Fukushima Daiichi spent fuel storage facilities [8, 9]. The knowledge gained during that time was applied in several international projects [10–13]. A NUGENIA project with a severe accident code benchmark exercise [14] followed these activities and finally a phenomena identification and ranking table [15] was produced during an OECD/NEA project. As a result of the ranking table, a project for the investigation of the nitrogen influence on the cladding degradation was started with an experimental program at KIT, Germany, and a nitriding model development at PSI, Switzerland.

2. BACKGROUND

The effect of nitrogen was observed as catalyzing effect during oxidation of cladding materials with air without reaching starvation conditions of the oxygen. As was found in the off-gas analysis of the SFP project Phase II, nitrogen was consumed when oxygen starved conditions were reached [7]. This effect implies a direct reaction of cladding materials with nitrogen. Small-scale experiments conducted at KIT, Germany, were used to extract temperature dependent reaction rates for the production of a nitriding model [16, 17]. In these experiments a one cm long tube of the cladding material was adjusted to a constant temperature in argon atmosphere. After reaching the selected temperature level (900–1200°C) an oxygen flow with argon as carrier gas was initiated for the pre-oxidation in Phase I. Then the oxygen flow was stopped, and nitrogen was used for Phase II of the test again with argon as carrier gas. In Phase III again oxygen was used for the re-oxidation of the partially nitrided sample without nitrogen flow, but with argon as carrier gas. For optical investigations of the nitriding history several tests were stopped at different times in Phase II.

At the beginning of the model development, a standalone computer code was written to recalculate the mass gain data from the about 70 separate-effect tests (SETs). The program was able to calculate most of the mass gain curves without problem, but it did not match the first strong oxidation after the oxygen reaches the sample in the pre-oxidation phase. The reason for this behaviour was the temperature increase of the sample due to the chemical energy released from the oxidation of the fresh metal. Therefore, the nitriding model had to be implemented into a computer code, which was able to calculate the temperature increase, and due to that, the increase of the reaction rates, in a reasonable way. The MELCOR code version 1.8.6 was selected for this project due to the availability of the source code of this program version.

3. NITRIDING MODEL DESCRIPTION

In case of presence of an oxidant (oxygen or steam) at the reaction level no zirconium nitride can be produced in presence of nitrogen. In this case the nitrogen can only be used as catalyst for the oxidation reaction [4, 5]. This means, that generation of zirconium nitride can only happen under starvation of oxygen and steam. The SETs conducted at KIT [16] showed, that two different nitriding mechanisms can be identified.

The mass gain curve (Fig. 1) of a separate-effect test at 1100°C shows a first strong mass gain due to the 10 minutes pre-oxidation time (Phase I), which is then followed by the nitriding in the argon-nitrogen atmosphere (Phase II) and at the end, the re-oxidation in Phase III. The nitriding reaction can be clearly separated into a fast nitriding reaction for the about first two hours with a following transition to a slow nitriding for the remaining time in phase II. This slow reaction can be interpreted as nitriding of zirconium metal with a strongly (factor ~20) reduced reaction rate compared with the fast nitriding.

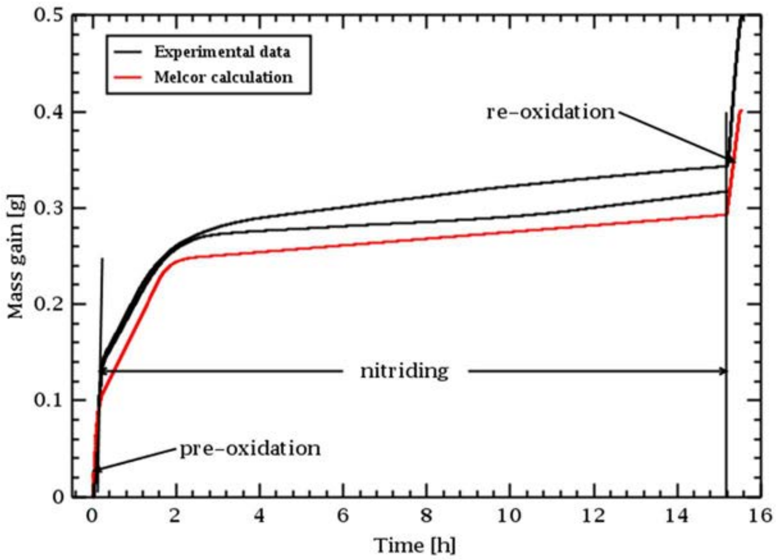

FIG.1. Mass gain data at 1100 °C.

The first (fast) reaction mechanism is interpreted as the nitriding of sub-stoichiometric zirconium oxide and oxygen stabilized alpha zirconium (α-Zr(O)). At temperatures of 1100°C and above the nitriding begins from the outer surface (Fig. 2) due to the high diffusion velocity of oxygen from the zirconium dioxide layer to the zirconium metal.

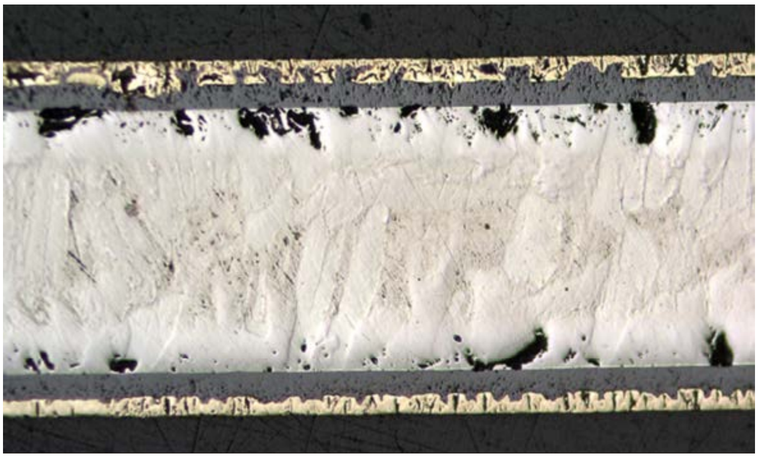

FIG. 2. Pre-oxidation and nitriding at 1100°C, stopped during Phase II (0.5 h).

The zirconium nitride is visible as golden layer which is attacking the grey coloured zirconium dioxide. The white coloured zirconium metal and α-Zr(O) are difficult to distinguish.

After the nitriding reaction has broken the oxide layer (upper part of Fig. 3) the nitrogen is then reacting with the α-Zr(O) layer between the ZrO_2 layer and the zirconium metal. It can be seen, that no nitriding reaction occurs between the ZrO_2 layer and the zirconium metal if the zirconium dioxide layer has not been broken (lower part of Fig. 3). Due to the cutting process small pieces of material can be broken from the sample. These are shown as 'holes' in the micro graph. After different times of nitriding (Figs. 3 and 4) the increasing zirconium nitride layer can be observed. Unfortunately the contrast in Fig. 4 does not allow to recognize the inner part as zirconium metal as it is compared with the measured mass gain of the sample (Fig. 1).

FIG. 3. Pre-oxidation and nitriding at 1100°C, stopped during Phase II (1.0 h).

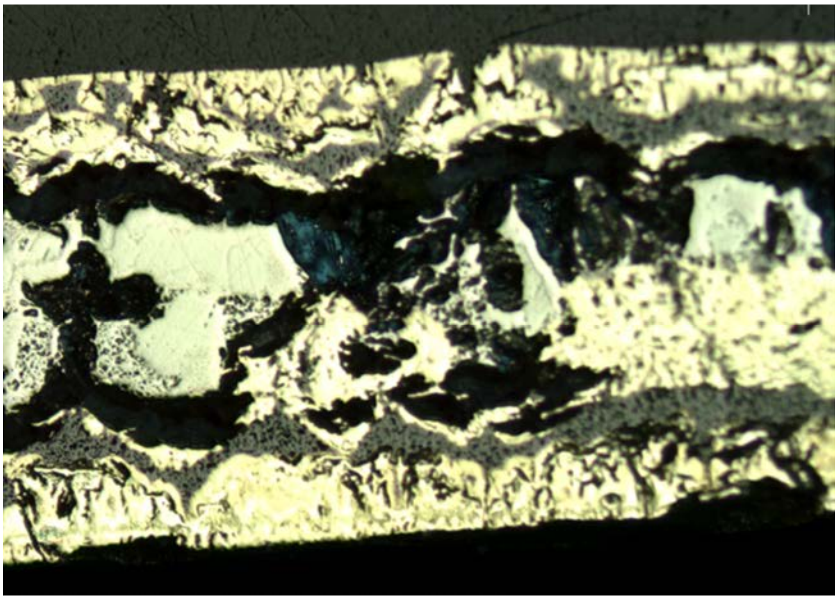

FIG. 4. Pre-oxidation and nitriding at 1100 °C, stopped during Phase II (3.0 h).

For the recalculation of the mass gain data with the MELCOR code (Fig. 1), the test had to be separated into different phases. After adjusting the temperature of the sample in the facility under argon atmosphere a valve was opened to start the oxygen flow to the sample. The reaction of the zirconium metal with the oxygen leads to a temperature increase of up to 40 K (Fig. 5). Due to the exponential temperature dependence of the reaction rate, this temperature increase is influencing the calculation of the mass gain.

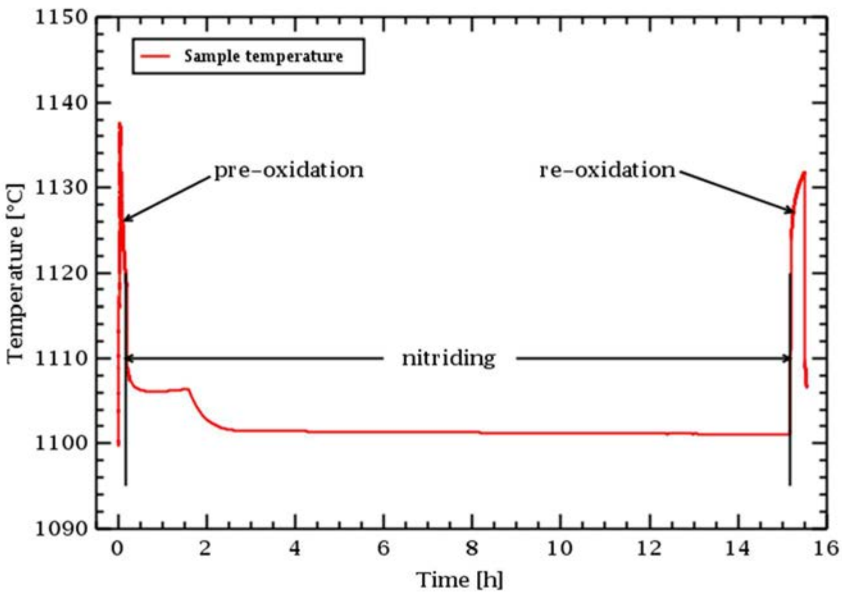

FIG. 5. Temperature history during pre-oxidation, nitriding and re-oxidation at 1100°C calculated by MELCOR.

The temperature increase in the MELCOR calculation is underestimated, because a support plate of the sample had to be modelled due to input requirements. This support plate removes some heat from the sample via heat conduction, which is not the case in the experiment.

Therefore, the oxidation phases will show an under estimation in the temperature increase and also in the calculated mass gain during pre-oxidation and re-oxidation after nitriding (Fig. 1). The nitriding phase is almost not affected because of the very small temperature increase during nitriding reaction.

The temperature dependent reaction rates for the fast nitriding reaction and the slow nitriding reaction (Fig. 6) differ by about a factor of 20.

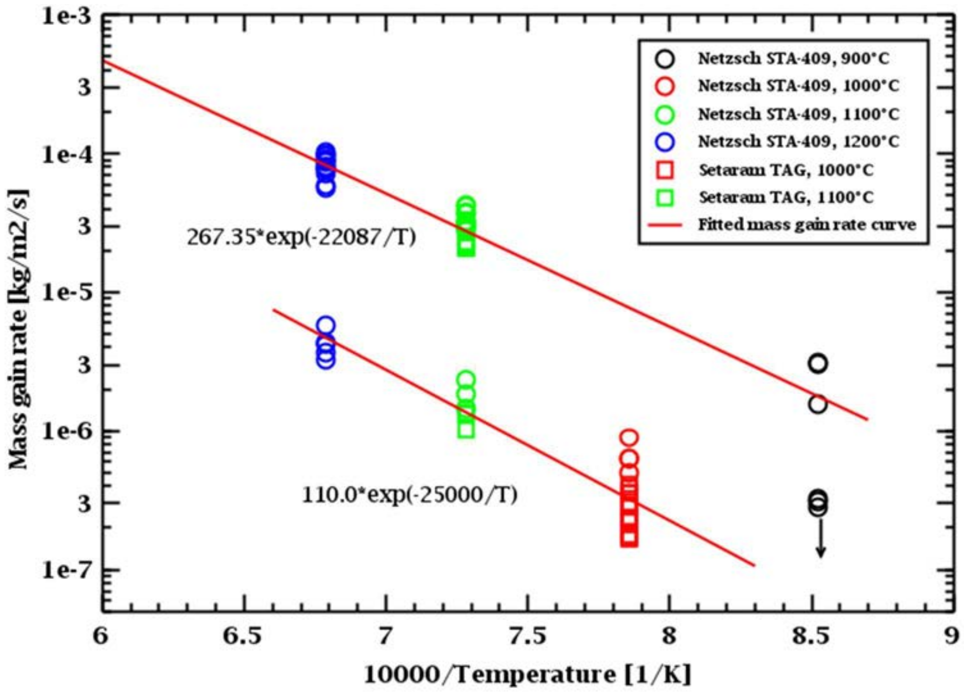

FIG. 6. Temperature dependence of nitriding rate.

A nonlinear behaviour of the nitriding rates (Fig. 6) during the SETs could not be observed and therefore it is assumed, that the nitriding reaction is linear instead of parabolic like the oxidation reaction of zirconium. Experiments with nitriding of pure α-Zr(O) [18] show decreasing reaction rates at temperatures above 1300°C. Therefore, the reaction rates for high temperatures for zirconium based cladding materials are also limited in the model, even if experimental nitriding data with zircaloy tubes at that temperatures are not yet available.

4. APPLICATION ON SANDIA FUEL PROJECT PHASE II

The OECD/NEA SFP experiment [7], which showed the consumption of nitrogen, was used to assess the nitriding model on a large scale test. In this experiment a spent fuel rack with one electrically heated original 17 × 17 PWR fuel assembly (FA) in the centre was surrounded by four unheated fuel elements in the neighbouring rack cells to model the cold neighbour policy of spent fuel storage. The experiment started in dry environment to simulate a total loss of coolant accident in a spent fuel pool. The cooling of the FAs was due to convectional heat loss by buoyancy driven air flow. The heated as well as the unheated FAs were instrumented by a large number of thermocouples. The flow velocity through the bundles was measured at the inlet of the bundles as well as the off-gas composition at the outlet. Unfortunately, all the thermocouples failed after the zirconium fire had ignited and passed their position because of the very high temperatures. Also the gas flow measurement at the inlet of the experimental facility failed due to liquid aluminium from the neutron absorber sheets was dropping downwards onto the measurement device. The only measurement device working until the end of the experiment was the off-gas analysis.

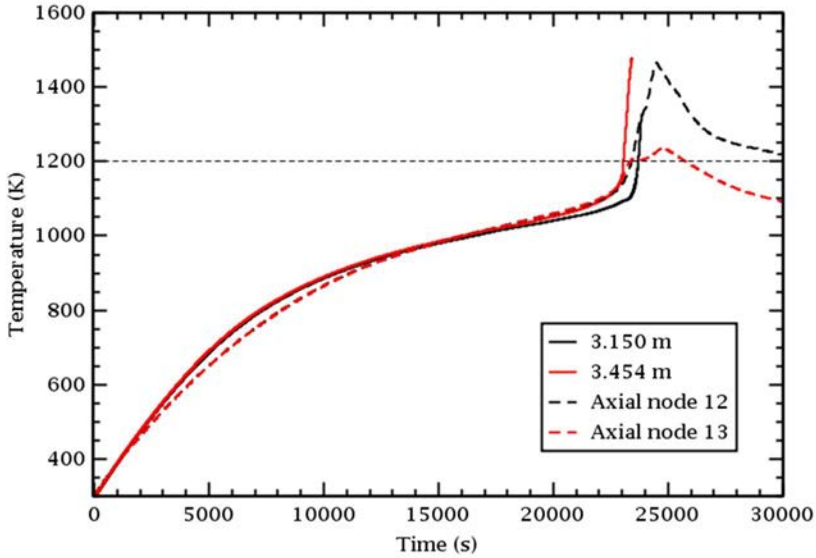

FIG. 7. Ignition calculation and comparison with experimental data.

The calculation of the SFP experiment could be done with the nitriding model, implemented in the local version of MELCOR 1.8.6 at PSI. The comparison with experimental data (Fig. 7) shows a good estimation. Until that time the nitriding model was not activated because oxygen starvation in the bundle was only reached after ignition has occurred. The temperature history in the centre of the heated bundle (Fig. 8) showed the ignition in node 14, which is at about 90% elevation of the heated bundle. Then the temperatures are showing the downward propagation of the zirconium fire until the lowermost node 4 of the cladding is reached. Now the oxidation front is moving upward until all the cladding material is oxidized. At temperatures above 1500 K the sub stoichiometric zirconium oxide and the α-Zr(O) is nitrided until almost all of the metal is consumed. The experiment stopped after about 70 hours when only zirconium dioxide was left from the cladding material.

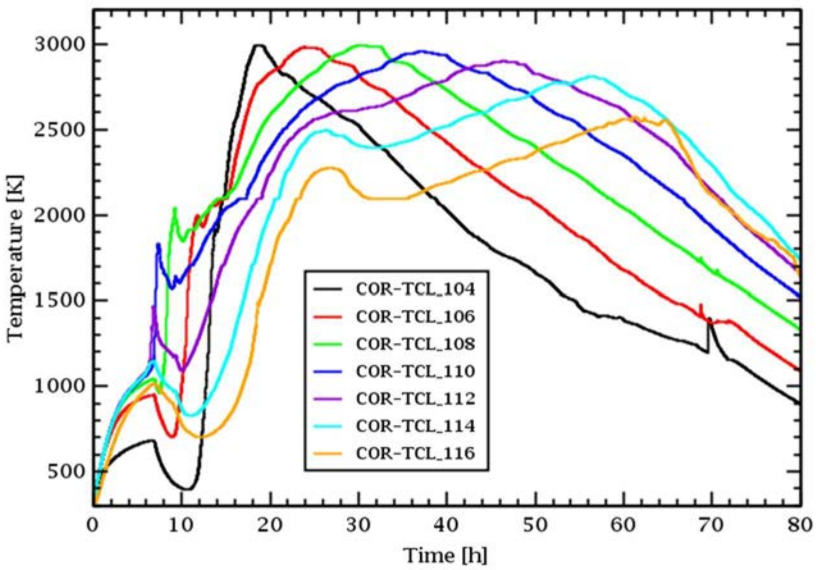

FIG. 8. Temperature history of the center of the heated FA.

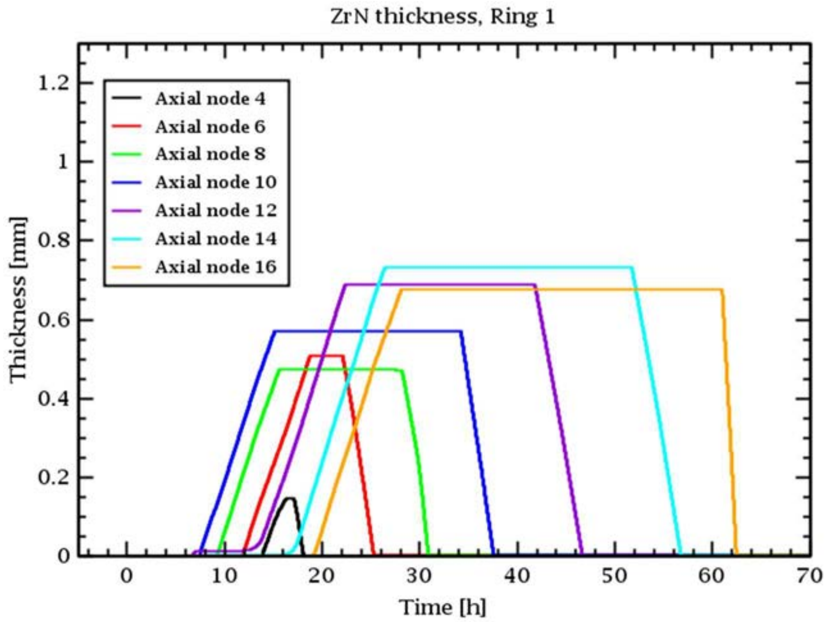

FIG. 9. Zirconium nitride generation in the centre of the heated FA.

The nitriding of the remaining metal (Fig. 9) led to a complete consumption of the metallic cladding between 15 and 28 hours (Fig. 10). The effect of the absence of metal is, that in the late phase of the experiment, when temperatures above the melting point of metallic zirconium is reached, the candling of liquefied metal cannot occur anymore. The melting temperature of zirconium nitride is at about 3250 K, while the melting temperature of the zirconium metal is at about 2130 K. In the post-test examination no hint for cladding melting and relocation could be found.

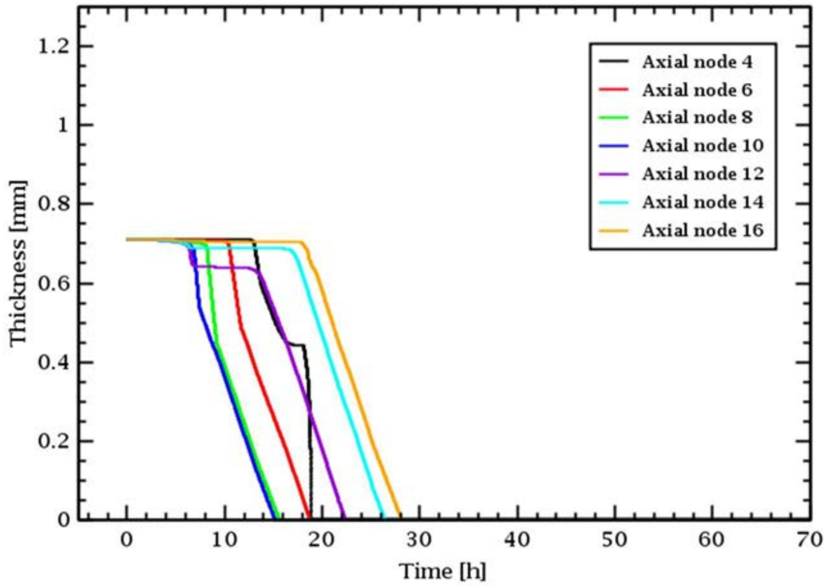

FIG. 10. Thickness of remaining metal in the centre of the heated FA.

The normalized off-gas analysis of the SFP experiment phase II [7] shows the complete consumption of oxygen after ignition at about 6 hours. The nitrogen consumption starts only marginally later. The 'recovery' of oxygen at about 10 hours is explained with the consumption of nitrogen, which opens the possibility of counter current flow from the upper end of the bundle to the section, where the off-gas samples are taken. When the zirconium fire front reaches the lower end of the bundle at 18 hours (Fig. 8), the consumption of nitrogen reduces and the counter current flow of air into the upper part of the bundle stops. The calculation with the nitriding model (Fig. 11) shows a good qualitative estimation with the measured consumption of oxygen and nitrogen.

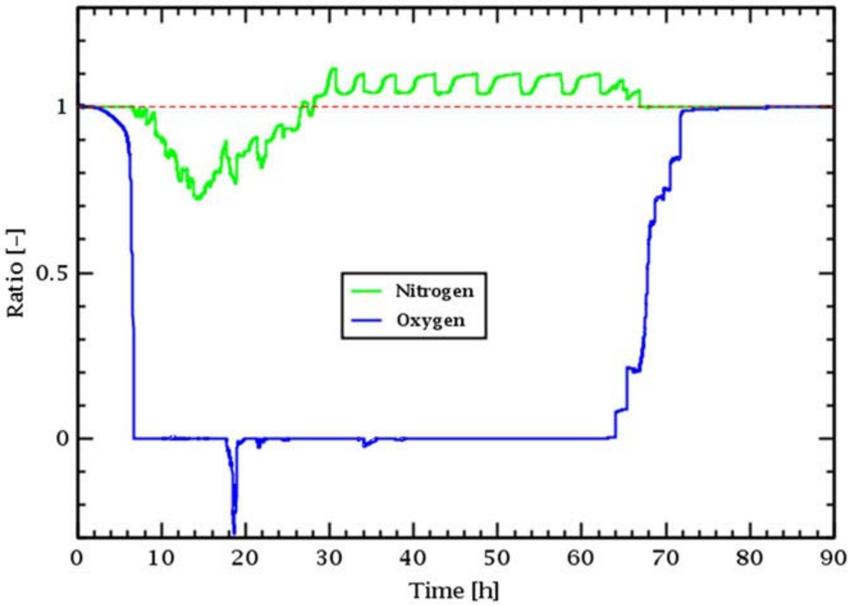

FIG. 11. Ratio of gas outlet flow divided by gas inlet flow (centred channel).

Even if MELCOR is not a CFD program, some advice for counter current flow could be observed with the negative flow ratio at about 18 hours.

CONCLUSIONS

The comparison of the results of the nitriding model implemented in a local version of MELCOR 1.8.6 with the experimental data shows the capability of the new model to describe the oxidation and nitriding reactions observed in the SFP Phase II experiment. The almost full nitriding of the cladding material in the phase of the zirconium fire downward propagation explains the fact, that no significant melting and relocation in the experiment was observed. The model will be published and prepared for the implementation in an official release of the newest MELCOR 2 version.

ACKNOWLEDGEMENT

The authors like to thank the Swiss nuclear regulatory body ENSI for the financial support of the experimental part as well as for the nitriding model development. The authors also like to thank KIT, Germany, for the support during the separate-effect tests.

REFERENCES

[1] HASTE, T., BIRCHLEY, J., Code assessment Programme for MELCOR 1.8.6, Contribution to HSK, 2007 Annual Research and Experience Report HSK-AN-6502 (2008) ISSN: 1661-2884.

[2] DURIEZ, CH., DUPONT, T., SCHMET, B., ENOCH, F., Zircaloy-4 and M5® high temperature oxidation and nitriding in air, J. Nuc. Mat. **380** (2008) 30.

[3] STEINBRÜCK, M., Prototypical experiments relating to air oxidation of Zircaloy-4 at high temperatures, J. Nuc. Mat. **392** (2009) 531.
[4] BIRCHLEY, J., FERNANDEZ-MOGUEL, L., Simulation of air oxidation during a reactor accident sequence: Part 1 - Phenomenology and model development, Ann. Nucl. Energy **40** (2012) 163.
[5] FERNANDEZ-MOGUEL, L., BIRCHLEY, J., Simulation of air oxidation during a reactor accident sequence: Part 2 - Analysis of PARAMETER-SF4 air ingress experiment using RELAP5/SCDAPSIM, Ann. Nucl. Energy **40** (2012) 141.
[6] UNITED STATES NUCLEAR REGULATORY COMMISSION, Spent Fuel Pool Project Phase I: Pre-Ignition and Ignition Testing of a Single Commercial 17x17 Pressurized Water Reactor Spent Fuel Assembly under Complete Loss of Coolant Accident Conditions, NUREG/CR-7215, US NRC, Rockville, MD (2016).
[7] UNITED STATES NUCLEAR REGULATORY COMMISSION, Spent Fuel Pool Project Phase II: Pre-Ignition and Ignition Testing of a 1×4 Commercial 17×17 Pressurized Water Reactor Spent Fuel Assemblies under Complete Loss of Coolant Accident Conditions, NUREG/CR-7216, US NRC, Rockville, MD (2016).
[8] JÄCKEL, B., Status of the spent fuel in the reactor buildings of Fukushima Daiichi 1-4, Nucl. Eng. Des. **283** (2015).
[9] JÄCKEL, B., BEVILAQUA, A., DUCROS, G., GAUNTT, R., STUCKERT, J., Land contamination activity data interpretation from Fukushima Daiichi accident, Nucl. Eng. Des. **300** (2016).
[10] FLEUROT, J., et al., Synthesis of spent fuel pool accident assessments using severe accident codes, Ann. Nucl. Energy **74** (2014).
[11] ORGANISATION FOR ECONOMIC CO-OPERATION AND DEVELOPMENT NUCLEAR ENERGY AGENCY, Status Report on Spent Fuel Pools under Loss-of-Cooling and Loss-of-Coolant Accident Conditions, OECD-NEA Report, CSNI/R(2015), OECD-NEA, Paris (2015).
[12] ADORNI, M., et al., OECD/NEA Sandia Fuel Project phase I: Benchmark of the ignition testing, Nucl. Eng. Des. **307** (2016).
[13] BEUZET, E., et al., Cladding oxidation during air ingress. Part II: Synthesis of modelling results, Ann. Nucl. Energy **93** (2016).
[14] COINDREAU, O., et al., Severe accident code-to-code comparison for two accident scenarios in a spent fuel pool, Ann. Nucl. Energy **120** (2018).
[15] ORGANISATION FOR ECONOMIC CO-OPERATION AND DEVELOPMENT NUCLEAR ENERGY AGENCY Phenomena Identification and Ranking Table: R&D Priorities for Loss-of-Cooling and Loss-of-Coolant Accidents in Spent Nuclear Fuel Pools, OECD-NEA Report, NEA No. 7443, OECD-NEA, Paris (2018).
[16] JÄCKEL, B., LIND, T., FERNANDEZ-MOGUEL, F., STEINBRÜCK, M., PARK, S., Development of a Computer Code Model for Nitriding and Re-Oxidation of Cladding Materials under Severe Accident Conditions, 27th NENE Conf., Portoroz, Slovenia (2018).
[17] JÄCKEL, B., LIND, T., FERNANDEZ-MOGUEL, F., STEINBRÜCK, M., PARK, S., Application of a newly developed computer code model for nitriding and re-oxidation of cladding materials on separate effect tests and integral experiments, 9th ERMSAR Meeting, Prague, Czech Republic, (2019).
[18] STEINBRÜCK, M., High-temperature reaction of oxygen-stabilized a-Zr(O) with nitrogen, J. Nucl. Mater. **447** (2014.)

SIMULATION AND DESIGN STRATEGY FOR THE DEVELOPMENT OF ADVANCED FUEL POOL COOLING SYSTEMS

K. GAUTER, T. FUCHS
Framatome GmbH,
Germany

1. INTRODUCTION

Fuel pool cooling is an essential task in the scope of nuclear power applications. During the first years of commercial nuclear power implementation robust fuel pool cooling systems have been developed and used for several decades. Two decades ago the development of a new cooling technology/concept was initiated to ensure prevention of accidents, including fuel damage. The so-called advanced cooling technology offers a modular design system which enables tailor-made robust and cost efficient cooling solutions. However, all the advanced cooling systems feature an indispensable and distinctive fall back option of a passive heat removal in case of a station blackout as most important feature.

In contradiction to conventional cooling systems the advanced cooling solutions use immersed heat exchangers to establish an additional safety barrier inside the heat removal chain. This results in the necessity of a free convective heat transfer on pool water side. This in turn requires a special design approach and methodology. Because of the huge nominal heat load and the size of the heat removal systems itself full size test are under economical aspects nearly impossible. In this paper a purpose-built simulation and design methodology is presented, which has been developed and proved in the scope of several first-of-a-kind projects during the last years.

2. DESIGN METHODOLOGY

The procedure for system pre-sizing is based on a combination of different approaches and tools. Thus, a straight-lined, cost effective, and reliable design process is guaranteed. The following lines give a simplified summary of the design process.

In a first step rough calculations define the basic parameters, geometrical system boundaries as well as thermal hydraulic boundary and initial conditions. Subsequently, the major physical effects are determined (e.g. by dimensional analysis) so that the system can be divided into different phenomenological sections or areas. For these sections the best fitting approach (methodology, numerical code, etc.) is selected. This approach is called adaptive design technology. For instance, a system of two heat exchangers (HX) connected via piping is divided into three parts. The HX require a high local (numerical) resolution to describe the heat transfer mechanisms inside the thermal boundary layer at the HX's surface. Inside the piping system heat transfer mechanism are of smaller importance, so that usually a 1D or 2D approach is sufficient. Thus, a combination of different tools is reasonable, physically adequate and cost and time efficient. In contrast, a high resolution approach of the whole system results in long and expensive calculation times without a gain in precision or system understanding.

The adaptive design methodology was for example applied during the development of Framatome's Advanced Cooling Tube (ACT) modules. ACT modules are HX with the outer shape of fuel assembly that are arranged inside the fuel racks, see Chapter 3.

However, to model such sophisticated systems a lot of experience in terms of numerical and physical knowledge is essential. Especially the strong coupling between energy and mass transfer inside the components but also in the complete system needs special attention. Active systems are less ambitious especially in terms of design optimization because of less parameter interdependency.

In the scope of Framatome's advanced cooling activities, during the last years different first-of-a-kind technologies have been developed and successfully implemented. In all cases the projected performances have been accomplished without the need of rework due to design flaws. The reliance in the utilized design tools is very important, because in case of passive heat removal systems a readjustment is nearly impossible after implementation. Performance deficiencies result in deconstruction of the whole system (including civil structures). To achieve the necessary confidence, a combination of different design and simulation methodologies is essential. Furthermore, a re-investment of measured data from commissioning activities and normal operation for the enhancement of the design and calculation tools is important. For this purpose a combination of small-scale-, semi-scale- and full-scale-tests in combination with a special numerical approach was used. Several R&D activities have been performed to understand the basic effects in the field of passive and/or hybrid systems. As result, different new numerical approaches have been implemented in the in-house design codes. In addition, the development test facilities have been adapted and improved.

Fig. 1 shows an overview of the developed and refined design thinking process. From left to right the timeline is plotted with a correlated increasing size of the (test) facilities. Furthermore, the horizontal split differentiates between experimental (grey boxes) and numerical (blue boxes) development tasks. The two green arrows show the iteration steps from a small scale facility to the full scale facility. The immanent linkage between experimental and numerical tasks is the key to a fast and reliable product development. With this approach Framatome developed a tailor made first-of-a-kind diversified fuel pool cooling system within only three years — from the first idea over the licensing to the successful commissioning of the system (see Section 3). In terms of nuclear standards this short development period can be seen as outstanding.

In summary, the design of advanced cooling systems is challenging and requires an adequate knowledge about material properties, numerical approaches as well as an advanced understanding of flow and thermal hydraulic phenomena.

The two general concepts of direct cooling (chillers outside pool) and indirect cooling (immersed coolers) can be subdivided in three different categories of heat transport mechanisms within the heat removal chain: active, passive or hybrid. In case of an active mechanisms or system, components like electrical pumps induce a forced flow/convection to transport the thermal energy. The technical requirements and components are well known. In case of a station blackout (SBO), however, measures have to be implemented to ensure the electrical power supply for the active components to sustain the heat removal.

In contrast, passive heat removal systems utilize a part of the provided thermal energy (decay heat) to induce a flow inside the system. Depending on the system configuration the IAEA categories B to D can be achieved (category A is limited to a very small number of applications due to the restricted transport potential of conduction and radiation). Passive systems offer advantages, because the heat transfer is independent from an electrical power supply. On the other side, the design of such systems is challenging. All operational modes and boundary conditions have to be covered by a simple geometrical closure (pipes and HXs). After the design phase only marginal modifications are possible to trigger the behaviour of the system.

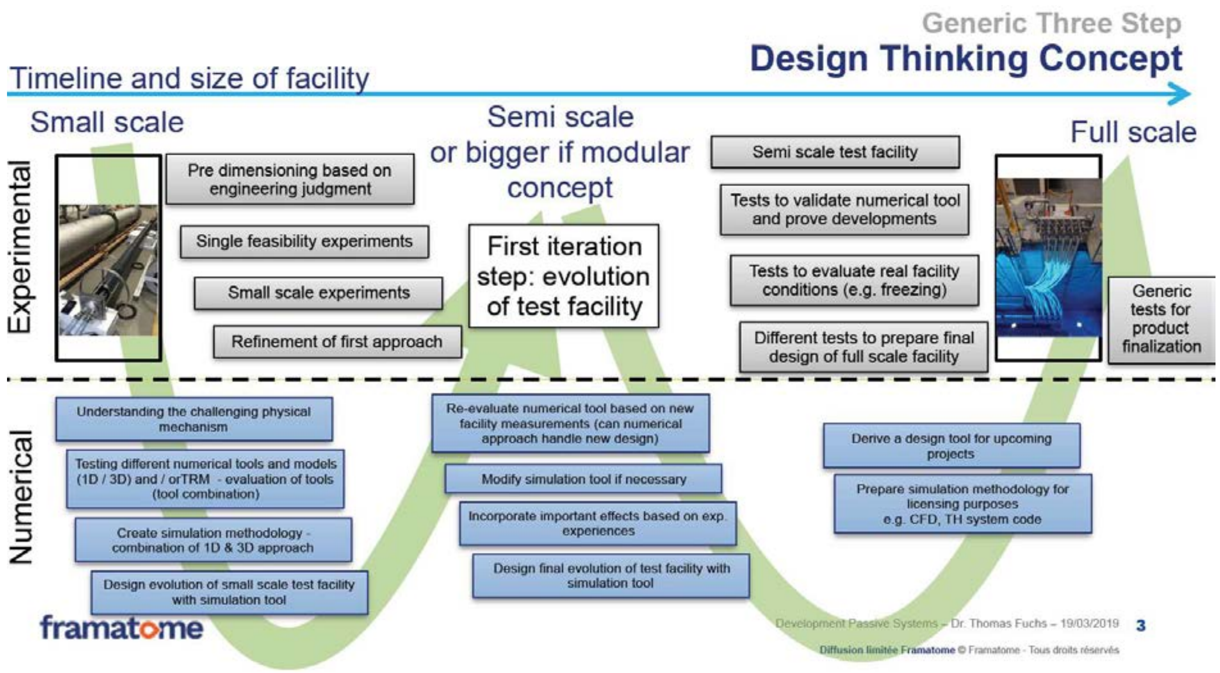

FIG. 1. Overview "Agile Nuclear Design Thinking Concept".

The two general concepts of direct cooling (chillers outside pool) and indirect cooling (immersed coolers) can be subdivided in three different categories of heat transport mechanisms within the heat removal chain: active, passive or hybrid. In case of an active mechanisms or system, components like electrical pumps induce a forced flow/convection to transport the thermal energy. The technical requirements and components are well known. In case of a station blackout (SBO), however, measures have to be implemented to ensure the electrical power supply for the active components to sustain the heat removal.

In contrast, passive heat removal systems utilize a part of the provided thermal energy (decay heat) to induce a flow inside the system. Depending on the system configuration the IAEA categories B to D can be achieved (category A is limited to a very small number of applications due to the restricted transport potential of conduction and radiation). Passive systems offer advantages, because the heat transfer is independent from an electrical power supply. On the other side, the design of such systems is challenging. All operational modes and boundary conditions have to be covered by a simple geometrical closure (pipes and HXs). After the design phase only marginal modifications are possible to trigger the behaviour of the system.

The third heat transport mechanism is a combination of active and passive mechanisms or systems. The combination can be based on different local system parts but also on a chronological sequence of operating modes. That means a system can work in an active mode under normal operating conditions and switch to a temporary passive mode if the electrical power supply is interrupted. Fig. 2 shows the different relations and combinations of the concepts and mechanisms.

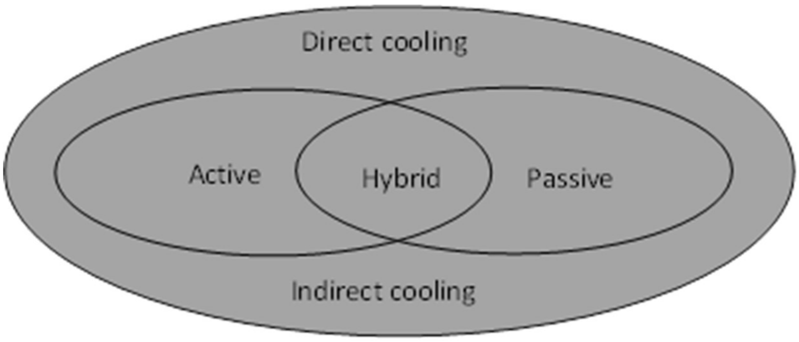

FIG. 2. Schematic of different relations and combinations of the general concepts and mechanisms of fuel pool cooling.

3. CASE STUDY "ADVANCED COOLING TUBE"

3.1. Basics

Framatome's Advanced Cooling Tube (ACT) is a modular heat exchanger, developed as a retrofit spent fuel pool cooler. Its implementation requires no changes to the pool and thus no re-certification. ACT-modules are placed into free spaces of the existing fuel assembly storage racks. The cooling system is sized via the number of ACT modules, not the ACT design. This allows for parallel design of ACT module and system (time saving approx. 3 months in a project's planning phase). Here, the numerical treatment of the ACT-module is described for a first-of-a-kind customer project, designing a retrofit fuel pool cooling solution. An implementation example is shown in Fig. 3.

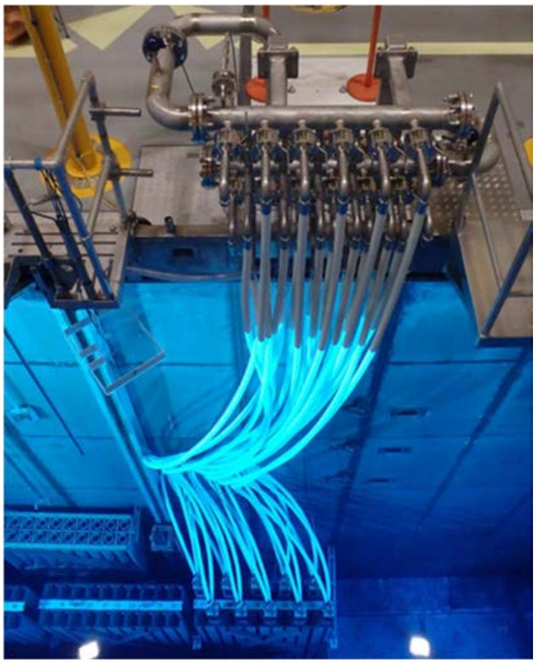

FIG. 3. Implemented and commissioned Advanced Cooling Tube system (upper part: collector and distributor, lower part: Cooling Tubes inside the fuel racks).

Thermal hydraulic calculations yield the heat transfer performance in the context of system design. These calculations use experimental results. This is described in more detail in Sections 3.5 and 3.6. *CFD calculations* are applied in order to judge the interaction of the cooling system and the flow patterns inside the fuel pool. Since the orders of magnitude for the numerical models for ACT-module and fuel pool differ, a two-step approach is used for the CFD calculations.

Based on the challenging task to simulate the whole spent fuel pool, the calculation domain was split into different parts (domain separation), see Fig. 4. In a first step some raw calculations with 1D heat transfer correlations were performed to proof the concept and to detect the first geometrical dimensions. In a second step the cooling tube itself was designed with the in-house developed system code STADRU. For this task several parameter variations were necessary to establish an optimized geometrical configuration (component optimization). Due to the high number of varied parameters (>10) the combination results in 10^5 to 10^6 single calculations. The execution of this task is practically not possible with a 3D CFD approach because of the required time and resulting costs.

After the determination of an optimized cooling tube configuration (geometry) the geometrical specified HX itself was modelled and calculated with StarCCM+ (3D CFD code). The outcome of this development step was a parameter field containing the thermal performance of the cooling tube mainly depending on mass flow rate and fluid inflow temperature of the cooling tube itself. The results were in good agreement with thermal hydraulic calculation results for the same HX geometry. In a last step the whole spent fuel pool was modelled (StarCCM+) excluding the volume of the cooling tubes. This domain was coupled under conservation of mass, momentum and energy with the already calculated parameter field (domain separation). Even with such a sophisticated approach the numerical simulations needed a significant amount of calculation time.

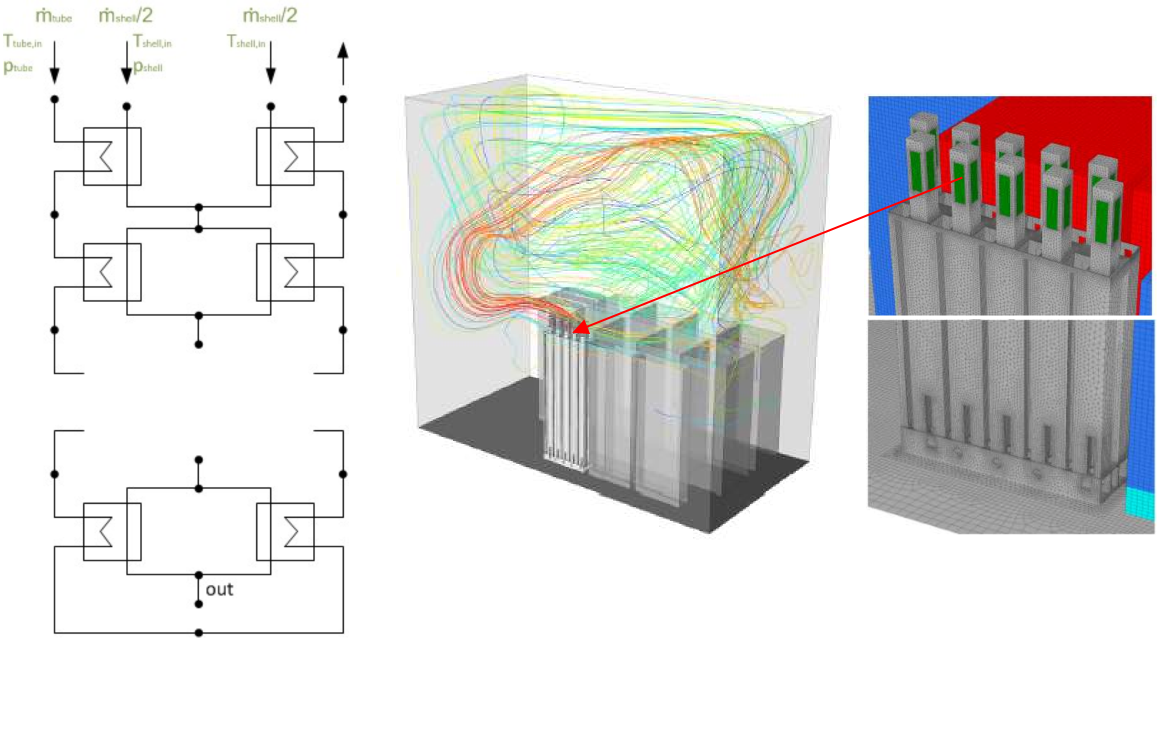

FIG. 4. Methodology of Framatome's Advanced Cooling Tube development (left side: geometry optimization with the system code STADRU, right side: subsequent StarCCM+ treatment).

3.2. Motivation for ACT-module design

The ACT-module is designed specifically for retrofit fuel pool cooling requirements. The retrofit fixation of immersed coolers generally requires:

- The penetration of the liner;
- The welding of mounts;
- Under water assembly;
- In the last consequence a re-certification of the liner.

All these measures are expensive and time consuming up to the point of fulfilling economic or schedule-related no-go criteria or both.

In order to avoid all the mentioned measures, the ACT-modules are placed into fuel racks. These existing structures are already licensed for the use with fuel assemblies, which are by a large margin heavier than the ACT-coolers. Therefore, also earthquake safety issues are covered.

3.3. Description and main features of the ACT cooling system

The ACT cooling system uses the indirect cooling method. The coolers, i.e. the ACT-modules, are immersed into the pool water and act as a barrier between the pool water and the cooling water. The pool water remains inside the pool, even in case of a leakage in the cooling system. Sufficiently high pressure on the tube side of the ACT-modules prevents an ingression of pool water into the cooling system. This enhances the safety because of pool water drainage prevention.

The ACT-Modules are designed to have an outer shape similar to that of a fuel assembly. Rough designs exist for BWR, PWR and VVER types, see Fig. 5. Outer size, foot and header with bow for crane handling are considered. The detailed design is adjusted to plant-specific requirements.

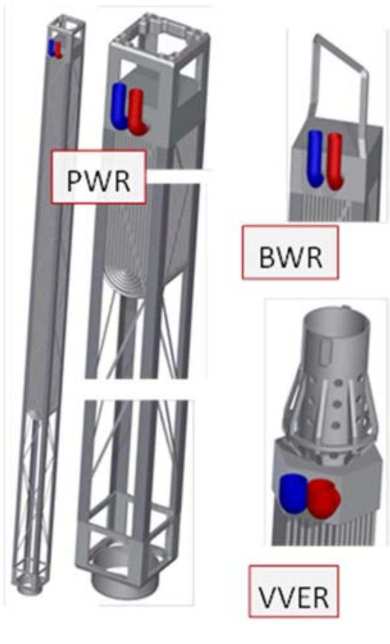

FIG. 5. Basic design ACT-modules for PWR, BWR and VVER.

The modular character allows for a parallel development of the mechanical ACT-module design and the sizing of the system. Since the system is scaled to heat removal requirements by adjusting the number of ACT-modules, the sizing of the system is independent of the detailed design of the ACT module. Therefore the duration of project start to commissioning may be reduced by a roughly one third.

The ACT module itself is a kind of U-tube bundle heat exchanger with, both, inlet and outlet at the top for easy access. This also allows for the application of different operation modes with flow in both directions.

The flow on the shell side is induced by natural convection (passive shell flow). Therefore, the ACT module requires a chimney-like shell with inlets at the top and outlets at the bottom, such as shown in Fig. 6. In case the fuel rack already provides such a chimney, it may be used as the shell of the ACT module. The shell should be longer than the U-tube bundle to improve the shell side flow rate, since this passive flow rate (induced by natural convection) is limiting the ACT module heat transfer capacity.

The foot and the shell are designed for placement into a fuel rack position and stable stand without the need for additional fixation, similar to that of a fuel assembly.

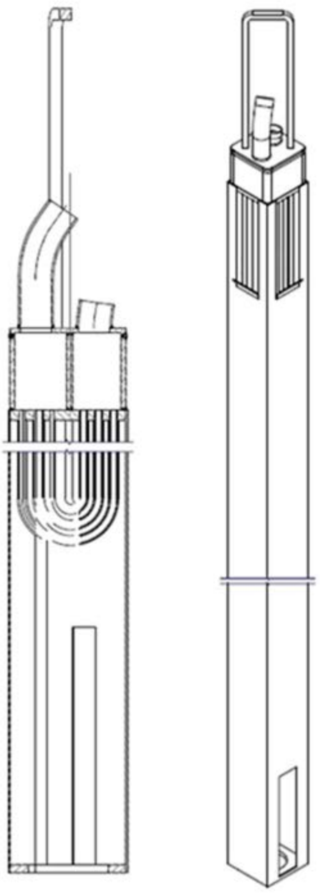

FIG. 6. Schematic of an ACT-Module for BWR type NPP.

3.4. Design procedure – experimental part

3.4.1. First experimental examinations as part of a feasibility study

The first feasibility study was a cost efficient set of experiments, using already available parts as far as possible. It took place in the R&D phase of the technology development.

Fig. 7 shows a schematic of the experimental setup used for the experimental part of the feasibility study. Measurements were collected in several experimental series, varying heating capacity and mass flow rate and feed temperature on the tube side ($T_{tube,in}$). Mass flow rate and inlet and outlet temperature on the shell side and outlet temperature on the tube side adjust accordingly. All but the mass flow rate shell side are measured. In addition, the temperature profiles over the height of the ACT-module in the shell and in the vessel simulating the pool were measured.

When a steady state is reached, while keeping one set of defined parameters constant, the results form one data point for the operational characteristic diagram, schematically shown in Fig. 8.

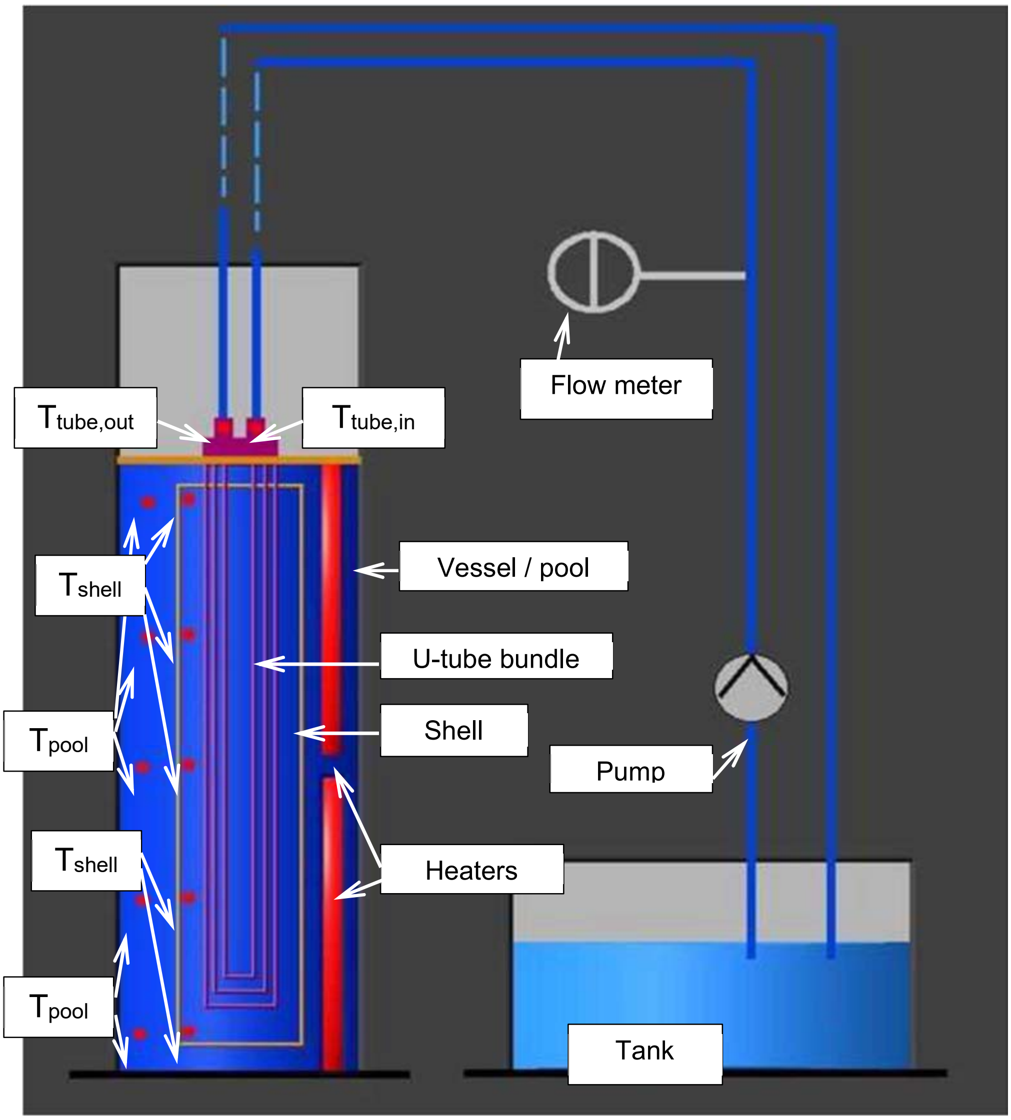

FIG. 7. Experimental set-up for feasibility study (schematic).

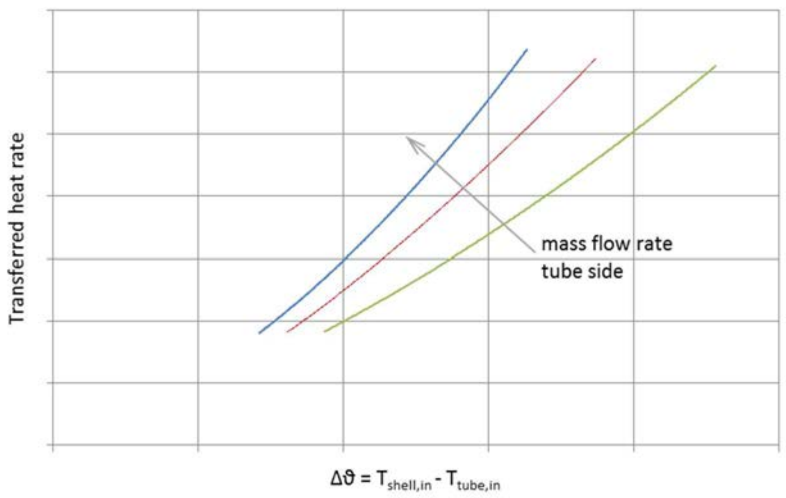

FIG. 8. Schematic set of operational characteristic curves determined by experiments.

3.4.2. Customer specific design requirements

The geometric design requirements for the reference project did not allow the use of the experimental ACT module of the feasibility study. The ACT module has to fit into the already installed fuel racks with a usually quadratic inner cross section area. This defines or limits the outer ACT geometry. Channel length and U-tube bundle geometry are optimized by a detailed parameter variation with the aid of the thermal hydraulic code STADRU. The header is designed according to plant space and handling requirements.

In order to cover any slits and gaps over the height of the fuel rack structure, an outer channel is required, the ACT module shell. The shell inlets and outlets are designed to fit gaps in the fuel rack structure.

Because of the modular character of the immersed ACT coolers, the sizing of the system is done through the adaptation of the number of ACT modules. Determining for the sizing of the system are:

- the difference between maximum allowed pool temperature and tube side feed temperature;
- the maximum heat removal rate.

In addition, the available positions and heights for piping and components and for their handling (installation, testing etc.) need to be discussed in detail, especially for plants already in operation.

3.4.3. Test stand setup and results for customer specific ACT geometry

The experimental setup is similar to the one of the feasibility studies shown in Fig. 7. The main addition is a cooler in the return line to facilitate a constant feed temperature on the tube side.

Fig. 9 shows a typical example of temperature profiles over tube bundle elevation (measurement results of test stand, schematized). The area between the shell side temperature and the pool side temperature is proportional to the driving force for pool water flow (natural convection). This illustrates the small static pressure differences over the cooler height, caused by the density differences (shell side to pool side) because of temperature differences. An accurate numerical prediction of the driving forces is essential to the cooler design, since small absolute errors lead to large errors in per cent.

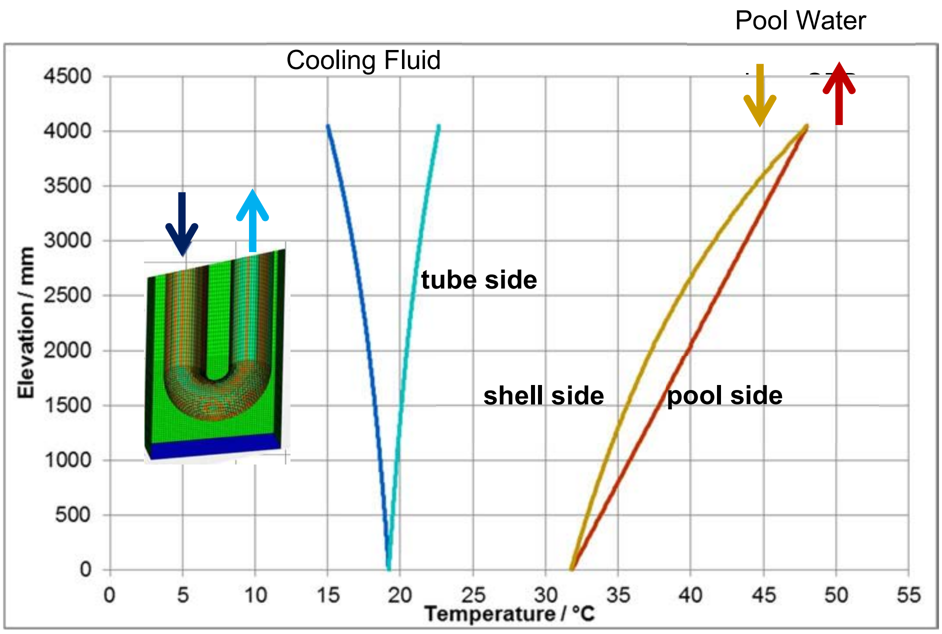

FIG. 9. Temperature profiles for tube, shell and pool flow inside and around ACT-module for the elevation of the U-tube bundle.

3.5. Thermal hydraulic calculations for system design

3.5.1. Thermal hydraulic calculation tool

The tool applied for thermal hydraulic calculations of large piping networks with a large number of components is an in-house development. Especially the heat exchanger components require the use of this tool.

The geometric model of large piping networks can be built by direct import of geometric CAD data from the Framatome plant data base. This reduces the time required for the build-up of large geometric model considerably (time needed approx. 5% to 10% as compare to manual approach).

The tool provides a large set of components, such as various types of valves, orifices, single-cell heat exchangers and pumps. Dissipation is considered through implemented equations. It contains a steady state 3D piping network solver for the mass, energy and momentum conservation equations and is used for system design, layout, pressure loss calculations, pressure / temperature / mass flow distribution and orifice design or calculation.

Additional numerical modules also allow for transient 3D piping network calculations, including the transient treatment of large heat exchanger components, as well as smaller scale two-phase calculations (water/steam: evaporation, condensation, flashing) under possible consideration of inert gas components.

3.5.2. Geometric model of the ACT-module

Because of the location of a U-tube bundle inside a single shell, one side of the ACT-module acts as a co-current heat exchanger and the other side acts as a counter flow heat exchanger, without division and therefore with mixing shell flow, as shown in Fig. 10. Another aspect to be considered is the length of the U-tube bundle of considerable 4 m.

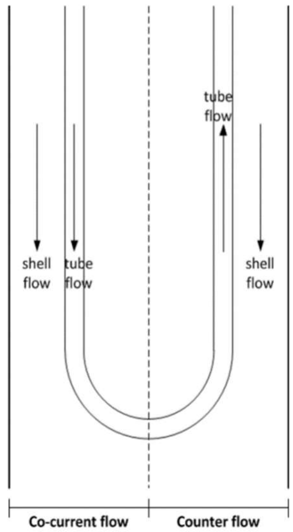

FIG. 10. Schematic of the flow patterns inside the ACT-module.

This type of heat exchanger cannot be modelled by a single-cell unit. In order to accommodate all these features, the geometric model of the ACT module is built by 10 single-cell co-current and 10 counter flow elements, connected in series on the tube side. For the shell mixing is allowed. The geometric model used for the ACT-module heat transfer calculations is shown in Fig. 11. The boundary conditions are marked in green. For each geometric parameter variation the single-cell units' geometry differs.

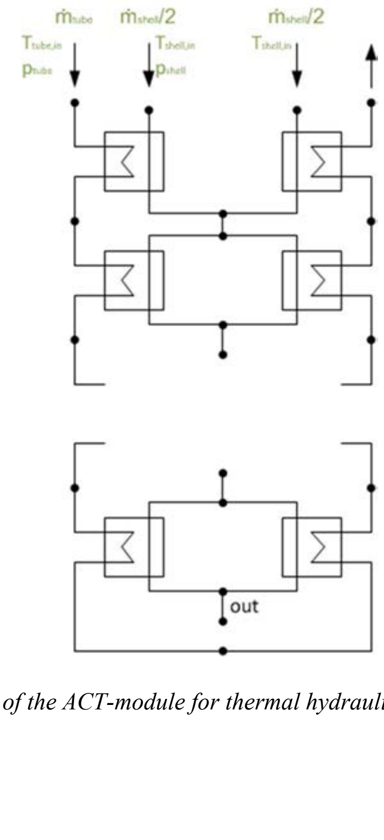

FIG. 11. Geometric model of the ACT-module for thermal hydraulic heat transfer calculations.

3.5.3. Required boundary conditions

Heat transfer calculations require a certain set of influencing boundary conditions:

- Heat exchanger geometry;
- Mass flow rate on the tube side;
- Mass flow rate on the shell side;
- Inlet temperature at the tube side;
- Inlet temperature at the shell side.

The *heat exchanger geometry* is given by the ACT design. The single heat exchanger elements in Fig. 10 are sized such that they add up to the dimensions of the ACT-module.

The *mass flow rate* on the *tube side* is a controlled and therefore known parameter (active flow). It is in the order of magnitude of 1 kg/s for each ACT module. For the numerical calculations it is applied to the tube inlet of the geometric model in Fig. 11.

The *mass flow rate* on the *shell side* is induced by natural convection and realistic measurement cannot be achieved with justifiable effort. It remains *unknown*. Its value must be determined by an adequate method, see Section 3.6. Because of the division into a co-current and a counter flow regime, the mass flow on the shell side is divided in half and applied to both shell sides of the geometric model, as shown in Fig. 11.

The *inlet temperature* on the *tube side* is a controlled or at least measurable quantity. It is set as a boundary condition for the numerical calculations at the tube inlet, the same location as the mass flow rate on the tube side. It is usually a quantity provided by the customer.

The *inlet temperature* on the *shell side* is the temperature of the fuel pool water entering the ACT shell at the top. It is in the range of 20°C to a maximum of 80°C. The outlet temperature on the shell side can be determined by measurement, although measurement results include inaccuracies because of incomplete mixing of the shell flow at the outlet. The measured temperature value slightly depends on the specific measurement location.

The *pressures* at tube and shell side are required for thermal hydraulic calculations but do not influence the heat transfer calculations in an essential way. The use of approximate values is sufficient.

3.6. Thermal hydraulic calculation method

3.6.1. General approach

On the tube side the mass flow rate is known. In the experimental set-up it is measured and in the plant, it is controlled. Therefore, together with the inlet temperature given by the customer and an approximate pressure all required boundary conditions are given. On the shell side, however, only the inlet temperature is given (maximum allowed pool temperature). The mass flow rate of this passive flow will settle at equilibrium conditions, where the pressure loss equals the driving pressure difference between shell and pool side.

The driving pressure difference is determined from experimental results by

$$\Delta p_{driving} = 9.81\frac{m}{s^2} \cdot \sum_{i=2}^{n}\left(\bar{\rho}_{shell,i} - \bar{\rho}_{pool,i}\right) \cdot (h_i - h_{i-1}) \tag{1}$$

with the densities as functions of the measured temperatures (shell and pool side) at measuring level i, i.e. at height h_i. The pressure loss Δp_{loss} is therefore also known, since for natural convection it is equal to $\Delta p_{driving}$. In order to determine the pressure loss coefficient ζ on the shell side via

$$\Delta p_{driving} = \Delta p_{loss} = \frac{1}{2} \cdot \zeta_{shell} \cdot \left(\frac{\dot{m}_{shell}}{2}\right)^2 / [\rho \cdot (A)^2] \tag{2}$$

with the cross sectional area A given by geometry and the mass flow rate $\dot{m}_{shell}$ is calculated via

$$\Delta\dot{Q}_{tube} = \dot{m}_{tube} \cdot c_p \cdot \left(T_{tube,out} - T_{tube,in}\right) = -\Delta\dot{Q}_{shell} = \dot{m}_{shell} \cdot c_p \cdot \left(T_{shell,out} - T_{shell,in}\right) \tag{3}$$

Given the pressure loss coefficient shell side, the calculation tool of Section 3.5.1 together with the geometric model (Section 3.5.2), and the boundary conditions of Section 3.5.3 delivers a field of result sets with varying shell side inlet temperatures and with varying tube side mass flow rate as shown schematically in Fig. 8.

3.6.2. Calculation of the heat transfer capacity

The heat transfer capacity (or heat transfer rate) depends on the mass flow rate on the tube side (usually not varied during operation, but a design value to be defined) and the temperature difference between cooling water (tube side) and pool water (shell side) inlet temperatures.

Using the boundary conditions derived in Section 3.5.3, the equations in "VDI Wärmeatlas" [1] yield the outlet temperatures on tube and shell side and the transferred heat rate for each single-cell heat exchanger element. Outlet temperatures of a previous heat exchanger element enter the piping connecting the 20 heat exchanger elements as shown in Fig. 11. The outlet temperatures on the tube side each yield the inlet temperatures (tube side) of the next heat exchanger element downstream. The shell side mixing of flows yield the inlet temperatures (shell side) for the next heat exchanger elements downstream. Finally the tube side and shell side outlet temperatures are determined. This yields temperature profiles over the tube length, i.e. HX height and, by addition, the total transferred heat rate.

The mass flow rate shell side is a required input parameter, although unknown. Therefore, it is set to an assumed value in a first step. It is determined by iteration via the pressure loss calculated by the tool together with the requirement for natural convection

$$\Delta p_{driving} = \Delta p_{loss} = \frac{1}{2} \cdot \zeta_{shell} \cdot \left(\frac{\dot{m}_{shell}}{2}\right)^2 / [\rho \cdot (A)^2] \tag{4}$$

Commissioning results and 3D CFD calculations showed a very good agreement with the results obtained.

4. CASE STUDY "HIGH PERFORMANCE COOLER"

As a second example the design process of Framatome's High Performance Coolers is presented. In contradiction to the Advanced Cooling Tubes the High Performance Coolers are developed to remove high heat loads with a compact component design. One cooler with the outer dimensions of 2 m × 2.5 m × 0.5 m is able to remove 3–10 MW depending on the cooling water capacities. In accordance with the mindset of an additional safety barrier the heat exchangers are realized as immersed units. Thus, on the pool water side a free convective flow has to be handled.

4.1. Numerical design tool and validation

On the test stand in Karlstein (Germany) a full scale component was measured. This task was accompanied by 3D CFD simulations. However, within the tests only one geometrical configuration was investigated. To offer customers the best fitting configuration, a thermal - hydraulic tool has been derived to calculate the component performance under deviating geometrical and thermal hydraulic boundary conditions. Furthermore, design optimizations can be handled by parameter deviation studies (10E+06 optimization calculations). The tool follows a 1D approach with the conservation of mass, energy and momentum. In addition, special correlation for the heat transfer as well as pressure drop were incorporated.

Fig. 12 and Fig. 13 show the validation of the tool by a comparison to the full scale tests. The free convective mass flow rate as well as the cooling capacity are in good accordance (within the bandwidth of the error of measurement). Taking into account the complexity of such a system (e.g. multi-dimensional effects), the tool shows impressive results. This tool facilitates a fast a reliable design of tailor made cooling solutions. Also combinations of different cooling systems for different operating modes can be evaluated (promising new concepts are possible). With this design approach wet spent fuel storages with a heat load of 10 MW to above 20 MW have been evaluated.

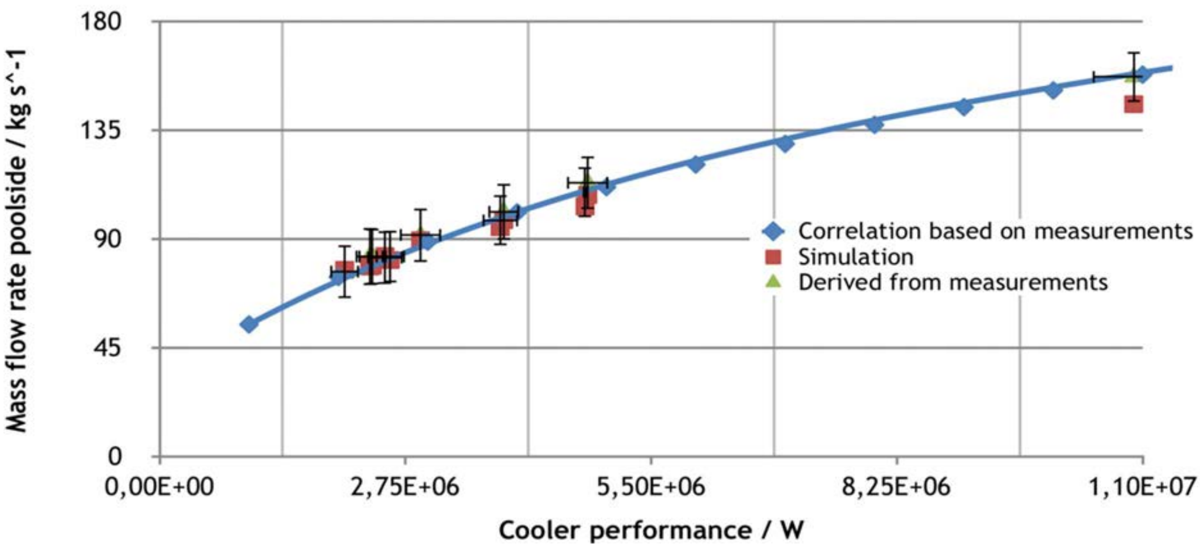

FIG. 12. Validation of numerical model - mass flow rate pool water side versus cooler performance (experiments carried out at Framatomes's full scale test facility in Karlstein, Germany).

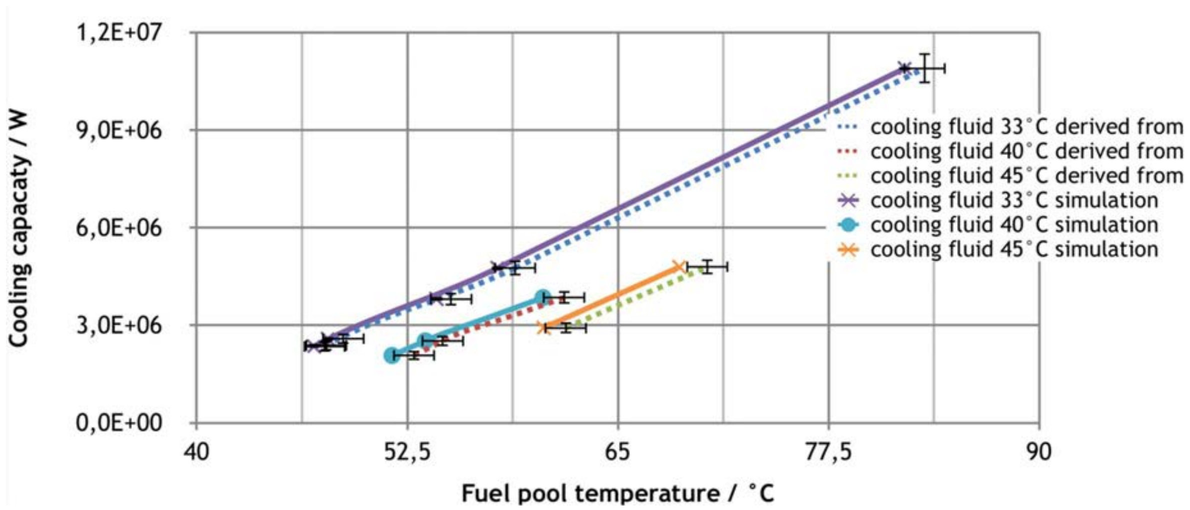

FIG. 13. Validation of numerical model - cooling capacity over fuel pool temperature (experiments carried out at Framatome's full scale test facility in Karlstein, Germany).

CONCLUSIONS

During the last two decades for the cooling of spent fuel pools new advanced concepts have been developed, realized and successfully commissioned. For the design of the partially passively working heat removal systems new sophisticated concepts were necessary. Especially the large scale free convective flows inside the system have to be predicted in a reliable way. In this scope an agile three step design thinking concept has been developed and proven. This concept combines numerical and experimental design steps on different scale levels. The system has been refined by the re-investment of experimental, commissioning and operational measurements. Based on the reliability of the predicted physical phenomena tailor made cooling concepts but also combinations are possible to fulfil the individual requirements of the customers.

REFERENCES

[1] VDI-GESELLSCHAFT VERFAHRENSTECHNIK UND CHEMIEINGENIEURWESEN (Hrsg.), VDI-Wärmeatlas, 7th ed., Springer-Verlag, Berlin Heidelberg (1994).

OVERVIEW OF FRAMATOME'S SIMULATION-ASSISTED WORKS TO IMPLEMENT SFP RELATED POST-FUKUSHIMA MEASURES

M. BRAUN
Framatome GmbH,
Erlangen,
Germany

Abstract

In the aftermath of the Fukushima Daiichi accident, operators of nuclear power plants were confronted with numerous regulatory questions concerning the safety of the fuel assemblies stored in the on-site spent fuel pools. As prior to the accident the spent fuel pool was not considered to be a serious fission product release source, the data basis to answer many of these questions was rather weak. After a clear picture was developed regarding which spent fuel pool related scenarios are of relevance and how to accurately represent a spent fuel pool with existing simulation software, it became possible to answer many of these regulatory questions. The results of simulations were subsequently used to develop spent fuel pool related (severe) accident mitigation guidelines and to extend the qualification of existing hardware and components. Due to the extensive research and development following the Fukushima events, nowadays, the spent fuel pool related accident preparedness and accident management planning is considered to have a very high level of maturity.

1. INCIDENTS AND ACCIDENTS IN SFP USUALLY CONSIDERED IN EOP / SAMG

In a nuclear power plant the spent fuel assemblies (FAs) are stored for several years in a dedicated water-filled spent fuel pool (SFP). The SFP is located either within the containment, within the reactor building, or within a dedicated fuel building. During the storage time, the radioactive decay of fission products within the used FA continuously releases heat, which gets absorbed by the pool water. For a stable and safe storage of the FAs, this heat has to be removed from the SFP by a residual heat removal system and evaporated/vaporized water has to be replaced.

After the accidents in Fukushima Daiichi, the topic of safety in the SFP attracted more attention. The reason for this increased interest was that during the accidents in Fukushima Daiichi, the uncertainty about the integrity of the SFPs on one side encumbered the overall accident mitigation, and on the other side caused an increased public awareness that the SFP also represents a possible large source of fission product release.

After Fukushima, many utilities, in expectation of upcoming regulations, expanded the scope of their emergency operation procedures (EOP) and / or their severe accident management guidelines (SAMG) to also include outage states as well as accidents in the SFP. For this expansion of scope to the SFP EOP / SAMG, several different spent fuel related incident/accident scenarios are conceivable on the service floor, which could endanger the safe and stable storage of the nuclear fuel:

– Long-term boiling of a SFP with replenishment of the lost water;
– Boiling and dry-out of the SFP;
– Water leakages from the SFP causing a sudden drop in pool liquid level;
– Loss of core or SFP cooling during outage with open reactor pressure vessel (RPV) (connected or disconnected to the SFP);
– Re-criticality within the SFP;
– Mechanical or thermal damage of one or few fuel elements (e.g. load drop, handling error, failure of fuel handling equipment, …).

The most frequent occurrence of an incident in an SFP or generally on the service floor arises from FA handling errors or fuel handling equipment failure. Such events already occurred e.g. in the NRU Reactor (1958) [1], Bohunice A1 (1976) [2], Paks (2003) [3], and other nuclear installations. However, these incidents or accidents only affect one to few fuel elements and usually do not impair the activity retention capabilities of the (reactor) building. Therefore the fission product release from such a handling error or equipment failure can usually be contained within the controlled area, and thus, the environmental impact of these more likely occurrences is low. As the mitigation or confinement of the consequences of these incidents are mostly already covered by existing operation guidelines, these handling incidents are of less interest for EOP / SAMG extensions.

A re-criticality within the SFP is practically excluded in modern light water reactors with reasonable margins of sub-criticality in the SFP. Even the drop of a fuel element on top of the storage racks is considered a design base accident, thus a re-criticality in such a case must be excluded by design. In general, a re-criticality in the SFP would only be conceivable in case of a massive deformation or destruction of the spent fuel racks, e.g. by a large load drop into the SFP like a dry storage cask or similar massive object. However, load drops are mostly excluded by administrative measures, i.e. by ensuring that a dry storage cask is never lifted over stored FAs. Additionally, the accidents in Fukushima demonstrated that even the collapse of the entire roof structure of three reactor buildings, including the overhead crane, do not cause the corresponding damage to the stored FA for a re-criticality to occur. Thus, for SFPs well-designed with regard to the exclusion of re-criticality such a scenario is considered to be highly unlikely.

A rather fast escalation of a nuclear incident into a nuclear accident can occur in case of a loss of core or SFP cooling during outage directly after opening the RPV prior to flooding the reactor well. Then possibly only a comparably small water reservoir is available, and the FAs still have a high decay heat due to the only recently terminated power production. This could result in core damage with fission product release within few hours, significantly limiting the time available to mitigate the accident by emergency actions. Thus these outage phases are now often included in the plant EOP / SAMG. However, after flooding the reactor well above the opened RPV, incidents in the reactor well are to a large degree physically comparable to incidents in the SFP. Thus, in the following, when discussing incidents / accidents in the SFP, many of the mentioned aspects are also valid for incidents in the reactor well.

In case of e.g. a long-term station blackout, the loss of all SFP cooling systems leads to an uncontrolled heat-up of the SFP water. In the long term, without any mitigative actions, such an occurrence would lead to a dry-out of the SFP, resulting in uncovering of the stored FA and thereafter a substantial thermal FA damage. As the SFP is (depending on the plant design) often not hermetically isolated from the environment by a containment, an accident with substantial thermal FA damage would have major environmental consequences. However, the grace period for a dry-out of the SFP is very long, on the scale of days to weeks, depending on the decay power of the stored fuel. Even in very detrimental environmental conditions as experienced in Fukushima, it was well possible to prevent a dry-out of the SFP by replenishing the evaporated water. Therefore the scenario of an uncontrolled dry-out of the SFP after a loss of cooling capabilities appears to be highly unlikely. Instead, much more likely (by a conditional probability evaluation) the outcome is that after the loss of SFP cooling, a sort of water make-up will be established. In the following, the SFP will be cooled by evaporation or vaporization of water for a long time, a situation described as ‘long-term boiling SFP’. The necessary preparation steps for the reliable mitigation of such a long-term boiling SFP scenario are discussed in Section 4.

A complication concerning the mitigation of a long-term boiling SFP may be that the accessibility of the service floor (and/or adjacent compartments) by plant personnel could become limited by high temperature and humidity. The relevant processes for energy transfer from the pool to the service floor atmosphere will be discussed in more detail in Section 2.

The severity of a leakage of the SFP strongly depends on the location and size of the leakage. It is not uncommon that in installed base nuclear power plants minor leakages of the SFP liner occur. Such small leakages represent a design base condition (DBC) as the water loss can be replaced, and the SFP level does not drop, i.e. the safe operation of the plant is not endangered. Further, these small leakages can be reliably repaired [4].

Even a large loss of SFP water, e.g. via the break of the slot gate, may still be considered a DBC, as long as the SFP water level does not drop into the active zone of the FA and as long as the water is lost into adjacent pools like the reactor well or the storage pool. In these cases a flooding of the affected pools can re-establish the SFP water level, ensuring the safe storage of the spent fuel.

The DBC is departed if the SFP leakage is sufficiently large, that it cannot be compensated by injection systems, and the water drains uncontrolled into an open room area, e.g. the lower reactor building. If the SFP level significantly drops, the SFP leakage additionally induces a loss of all closed loop SFP cooling systems. The water extraction ports of the SFP closed loop cooling systems are located on the top of the pool to prevent a siphon effect in case of pipe rupture. If the SFP level drops, the water extraction ports may get exposed, and thus the SFP closed loop cooling systems cease to operate already after a few meters drop of the SFP liquid level.

An additional possible complication in case of a significant SFP level drop may be that a lack of water coverage leads to insufficient shielding of the direct radiation form the spent fuel elements. Thus the service floor may become inaccessible for personnel due to radiation, limiting the options for a repair of the leakage.

As long as the leakage is located above the top of the active fuel, such a large-break loss of SFP coolant may result either in a long-term boiling scenario or a long-term overfeeding scenario.

A hard to mitigate accident sequence would be a substantial damage to the fuel building with a low-lying leakage of the SFP within or below the active zone of the FA. A lack of submergence of the active FA region represents a substantial risk for cladding heat-up and thermal FA damage, possibly resulting in a large release of fission products. The limitations of FA cooling, depending on the leakage location and the storage time of the FA are discussed in Section 3. The occurrence of such an event however is highly unlikely. A large low-lying SFP leakage would practically require the destruction of one of the SFP walls, which consist typically of 1–2 m thick heavily steel-reinforced concrete. This makes a penetration of an SFP wall rather unlikely even in case of e.g. an airplane crash.

Nevertheless, if a low-lying leak in the SFP is assumed to occur, there are only limited possibilities/measures available to maintain or re-establish FA cooling. These measures include mobile water cannons as e.g. introduced by some Japanese plants or dedicated pool spraying systems [5] as e.g. installed in the U.S. as post-9/11 measures. While the water cannon approach relies on the assumption that the roof of the service floor will also be lost, the pool spray system approach relies on the assumption that the spray system itself survives the massive initiating event despite not necessarily being qualified against the corresponding loads. Instead of such a pool spraying approach, which has significant intrinsic uncertainties, modern plants like the EPR reactor rely on excluding such a scenario altogether by hardening the fuel building with an airplane crash protection shell rated against military as well as large commercial aircrafts [6].

After this short general introduction about the SFP-related incident / accident sequences to be considered in EOP / SAMG the structure of the next chapters is as follows:

- Section 2: In this chapter the SFP behaviour during the accidents in Fukushima Daiichi is examined with the purpose of quantifying the efficiency of evaporative cooling of large bodies of water and deducing recommendations on how to model a SFP in a lumped parameter code as e.g. MELCOR.
- Section 3: This chapter presents studies and simulations performed to evaluate the limitations of FA cooling, in case of a large low-lying leakage of the SFP. As example, boiling water reactor FAs are considered.
- Section 4: This chapter deals with the necessary steps to ensure suitable plant capabilities to mitigate a long-term boiling SFP.

2. LUMPED-PARAMETER SFP MODEL DEVELOPMENT BASED ON THE BEHAVIOUR OF THE FUKUSHIMA DAIICHI SFPS

During the reactor accidents in Fukushima Daiichi, after a loss of all cooling systems the SFP temperature started rising. After a few days the SFP temperatures stabilized due to evaporative cooling well below the actual water boiling temperatures at 47°C/70°C/62°C/87°C respectively, see Fig. 1. For the next month the pool temperatures remained mostly constant, aside from the phases where the lost water was replenished with cold fresh water. Only after re-establishing a closed loop cooling several months after the accident the pool temperatures dropped consistently to values of 30–40 °C.

To explain this behaviour of the pools the specific process of water evaporation at the phase boundary must be considered. Nearly independent of the temperature water diffuses fast through the phase boundary so that directly above the water surface the relative air humidity always approaches 100%. The absolute steam partial pressure in this humid air layer is given by the saturation pressure of steam at the respective water temperature.

Two regimes can be differentiated:

- If the SFP is below saturation temperature, only a thin layer of humid air can form above the water surface. A natural convection flow of air then transports the humid air layer away from the pool surface, and brings new dryer environmental air in contact to the water surface. The ‘evaporation’ rate from the water surface is thus determined by the strength of the convective air flow. If the decay heat in the pool is low and the water surface sufficiently large, the decay heat can be removed from the SFP by evaporative cooling well below the pool saturation temperature.
- If the evaporative cooling is insufficient to remove the decay heat, the pool sooner or later reaches saturation temperature. Then, the steam partial pressure in the humid layer directly above the water surface equals the pressure of the surrounding environment.

Thus, the steam layer on top of the pool starts pushing away the environmental atmosphere, and new water can continuously 'vaporize' from the pool. As the energy release from the water surface into the atmosphere is not limited anymore by an air convection flow, the vaporization occurs on a faster time scale as the only remaining limitation for the vaporization rate is given by the energy input into the pool itself. Thus, the SFP temperature stabilizes at the water saturation temperature.

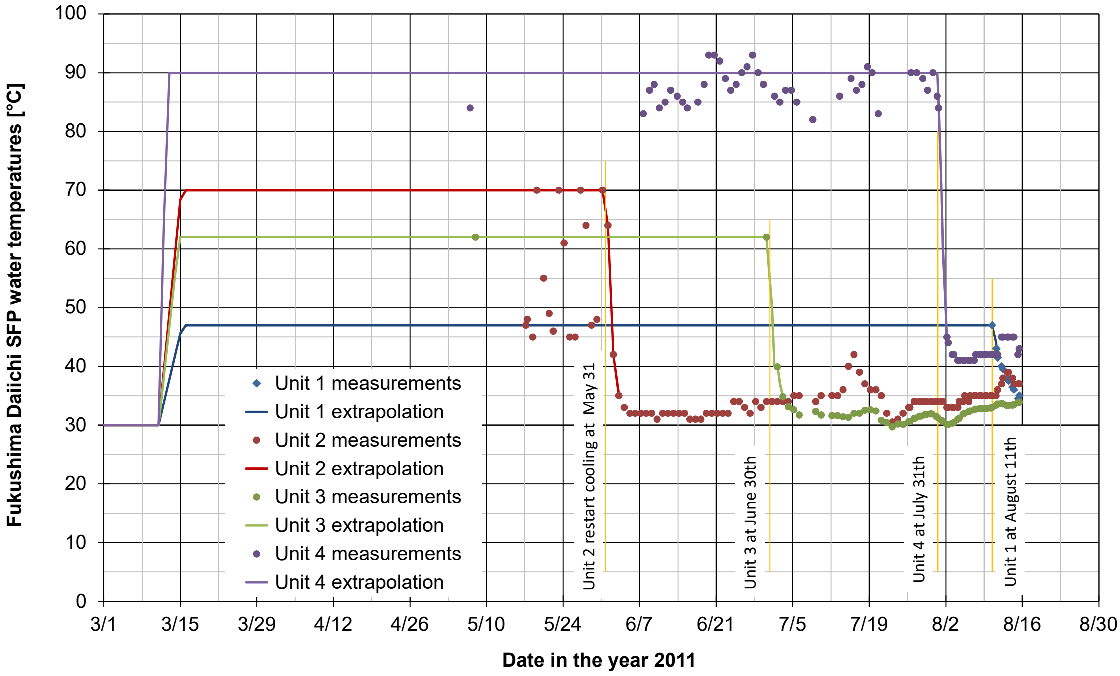

FIG. 1. Temperature history of the Fukushima SFPs.

As general language convention 'evaporation' characterizes the carry-over of water into the atmosphere below water saturation temperature, and 'vaporization' characterizes the steam production when the water is boiling. Note that the rate of loss of water is nearly independent of the question of whether the SFP water is vaporized or evaporated but is given by the decay heat which must be removed from the pool.

As long as the entire core is not unloaded into the SFP, it can be expected that the evaporation of water already below the boiling temperature is sufficient to completely remove the decay heat. The sub-cooled evaporation rates of water were e.g. measured in small scale experiments by Boelter et al. [7], see blue dots in Fig. 2. Thereby Boelter correlated the measured evaporation rates in units of mass flow rate per surface area versus the difference between the absolute humidity in saturation and the absolute humidity of the surrounding atmosphere. The absolute air humidity is an indication for the density difference between the surrounding atmosphere and the humid air layer directly above the water surface and thereby a measure for the buoyance force driving the air convection above the water surface.

From these experiments Boelter et al. have derived a phenomenological correlation for the evaporation e in units of kg/(h·m^2):

$$e = 38.2 \frac{\mathrm{kg}}{\mathrm{h{\cdot}m^2}} \cdot \left[\frac{C_\mathrm{W} - C_\mathrm{atm}}{\mathrm{kg/m^3}}\right]^{1.25} \tag{1}$$

where C_W is the absolute humidity in units of kg_{H2O} / m^3_{air} directly above the water surface (corresponding to 100 % of relative humidity at an air temperature which equals the water temperature) and C_{atm} is the absolute humidity of the surrounding air.

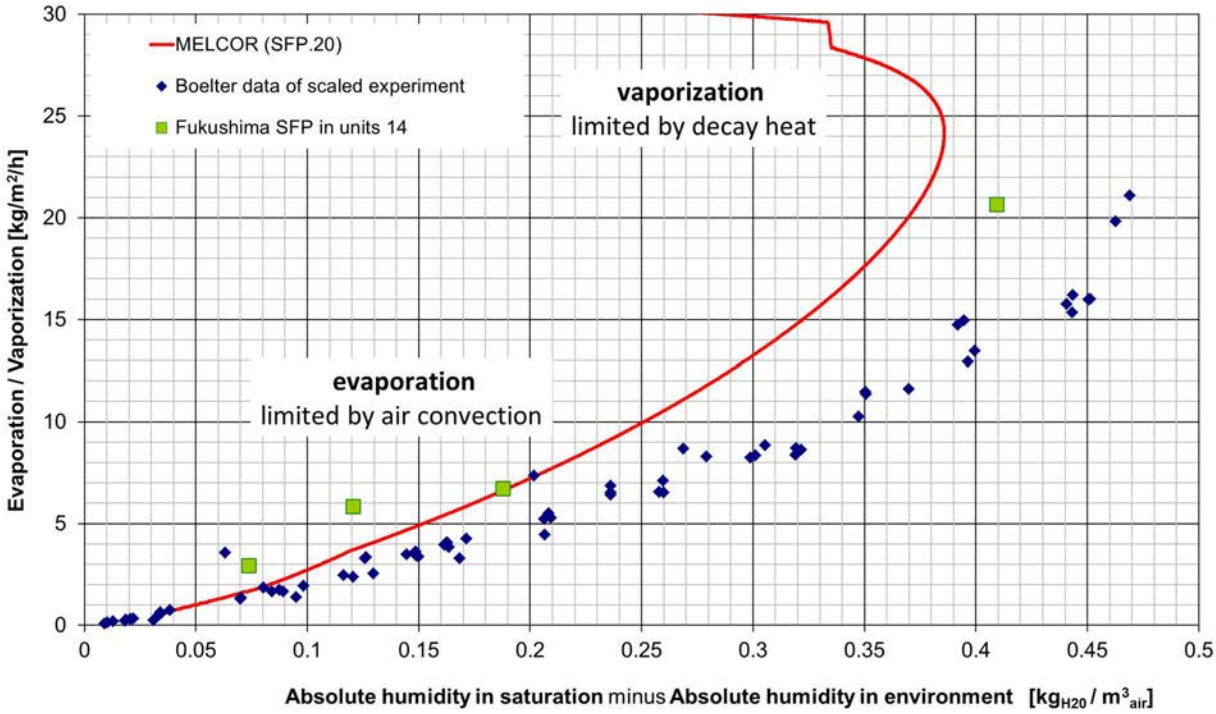

FIG. 2. Correlation of evaporation rates versus air humidity differences.

In Fig. 2 also the four uncooled spent fuel pools of Fukushima Daiichi are depicted as green squares. Due to the low decay heat in the SFP and the good air exchange of the service floor with the environment (after failure of the roofs), subcooled evaporation dominated in Fukushima, leading to maximum SFP temperatures well below the saturation temperature, compare Fig. 1.

Beside the results of Boelter et al., also other alternative correlations were developed, e.g. by Shah [8]. These correlations may be more or less accurate in certain parameter regimes but do not predict significantly different pool behaviours.

To plan / support emergency actions and to define grace periods of service floor accessibility on a best-estimate basis, lumped parameter codes are used like e.g. MELCOR. In these lumped parameter codes complex geometries are represented by control volumes in which physical parameters are represented close to equilibrium conditions. The control volumes are connected with flow paths allowing for transfer of gas / water / steam. Reasonable reproduction of the evaporation cooling effect in a lumped parameter code requires special attention on how to couple the water pool to the atmosphere of the service floor.

The simplest approach is to represent the SFP together with the service floor above as one control volume, partially filled with water up to the top elevation of the pool, see Fig. 3a. As this nodalization approach does not differentiate between a humid air layer above the condensed water and the rest of the atmosphere, it will significantly overestimate the diffusion-driven evaporation of coolant from the pool. Thus the simulation results are conservative in respect to the accessibility of the service floor (humidity & temperature), but predict optimistically low SFP water temperatures.

Another approach is to split the SFP and the service floor in two control volumes, and connect these by one flow path, Fig. 3b. As a flow paths usually allows only the transfer of one phase in one direction, this nodalization inhibits any closed-loop air convection flow, and thus suppresses evaporation cooling altogether. Therefore the SFP will always reach saturation condition until the decay heat can be removed from the SFP control volume by vaporization of pool water. This modelling approach predicts conservatively high SFP water temperatures, but optimistically long periods of accessibility of the service floor.

A minimum viable best-estimate nodalization is shown in Fig. 3c. The pool and the service floor are represented as one control volume each, and the interface between the SFP and the atmosphere contains (at least) two independent flow paths so that an air convection loop can develop. However, lumped-parameter codes often over-predict the speed of convection. Therefore these two flow paths have to be defined in a suitable way.

In the experience of Framatome [9], to reasonably reproduce the experimental data of Boelter et al., the connecting flow paths in MELCOR can be defined with a flow path area of 0.5 meters times the short side length of the fuel pool (representing the cross section area of the convection flow above the water surface), a flow path length of 0.25 times the long SFP side (representing the average in-flow and out-flow length of the convective air flow), and a hydraulic diameter in the range of 1 m to 0.1 m to create a suitably large major loss, slowing down the air convection to reasonable levels. The resulting predicted evaporation rates for a generic SFP are plotted in Fig. 2. as red line. Note that with increasing the decay heat in the SFP, MELCOR also describes the transition from evaporative cooling to boiling.

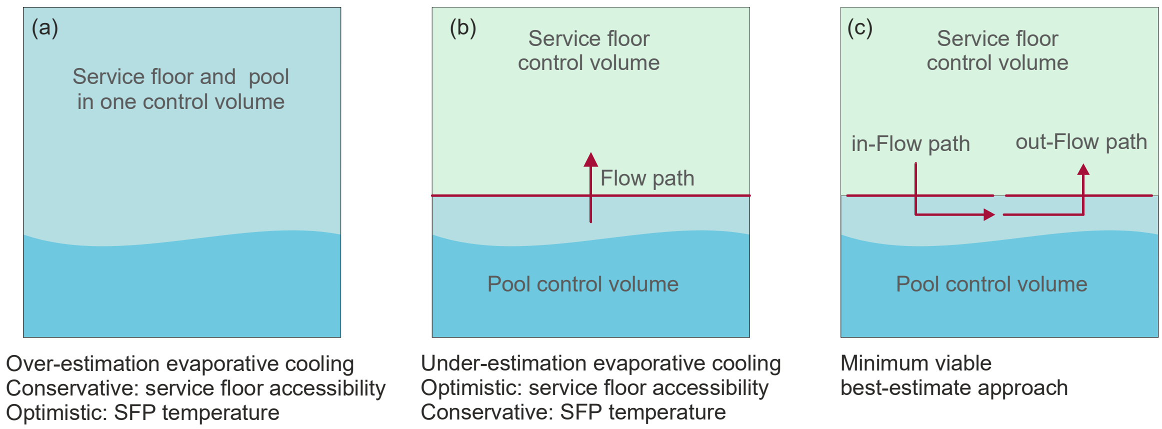

FIG. 3. Lumped parameter modelling approach of a SFP surface.

Again, note that the nodalization example in Fig. 3c only represents a minimum viable approach.

As supporting works for developing SFP-related accident mitigation measures, Framatome conducted MELCOR simulations of the service floor in response to a heat-up of the SFP. The main interest thereby was the determination of grace periods concerning accessibility and the impact of a restart of the building heating ventilation and air conditioning (HVAC) system. A typical nodalization scheme of the SFP and the service floor for a boiling water reactor (BWR) to be used for developing SFP-related SAMG is shown in Fig. 4.

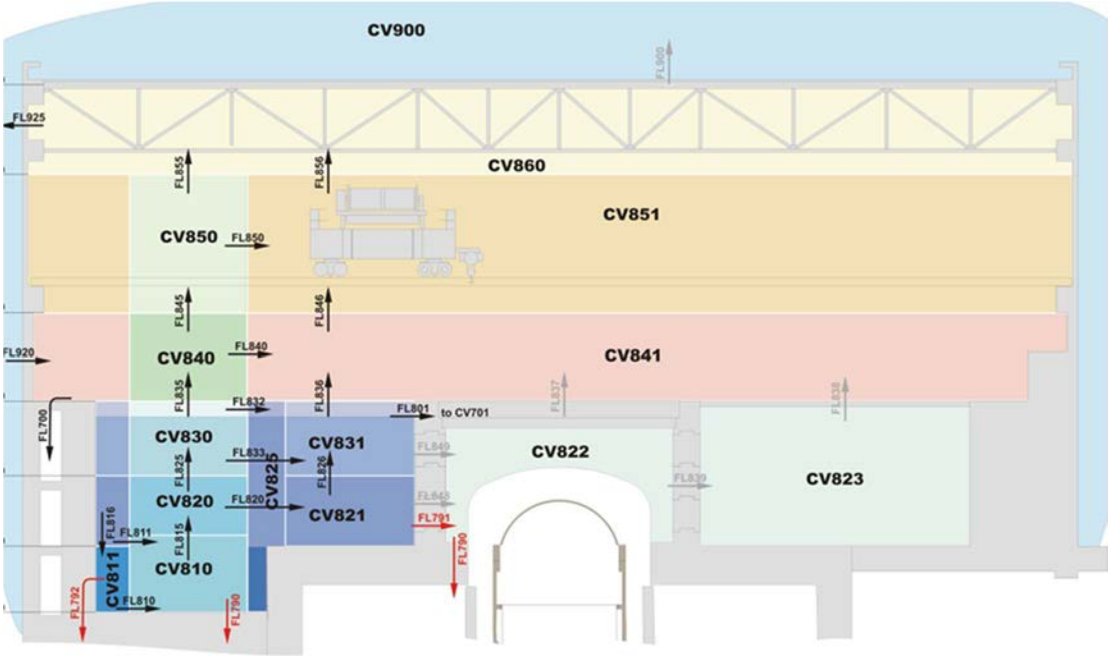

FIG. 4. Typical MELCOR model used in the development of SFP SAMG.

3. LIMITS OF FA COOLING AFTER LOW-LYING LEAKAGE OF A BWR SFP

In this section the scenario of a large low-lying leakage of the SFP is discussed. The leak drains SFP coolant into an open volume, e.g. the reactor building at a rate higher than injection systems can re-inject the coolant. This results in a rapid drop of the SFP level to a nearly constant elevation at the level of the leak.

As long as the SFP liquid level exceeds the FA canister height in a BWR or the rack height in a pressurized water reactor (PWR) (see Fig. 5a), natural convection of water through the FA sufficiently cools the FA, independent of the current water temperature. If, due to the reduced overall SFP level, the swell level inside the FA drops below the FA canisters or even the storage rack top, the water recirculation flow through the FA breaks down. Thereafter other FA cooling mechanisms are of relevance.

With an only partial uncovering of the FA, the dominant FA cooling mechanism is steam cooling, see Fig. 5b. The lower still submerged part of the FA vaporizes water. The released steam is forced through the upper FA part, cooling it while the steam gets superheated. The efficiency of this cooling however depends strongly on how far the liquid level dropped into the active zone. The partial steam cooling of the FA causes a strongly inhomogeneous temperature profile along the FA. This inhomogeneity drives thermal conduction along the FA, canister, and rack structures (see Fig. 5c). Additionally, after a sufficient heat-up the top of the FA starts radiating heat into the service floor (see Fig. 5c). The heat-up of the gases within the FA can drive an additional internal gas convection, which however turned out to not contribute significantly to the overall heat transport within or out of the FA (see Fig. 5d).

In case of a complete drainage of the SFP (see Fig. 5e), a natural convection of air can efficiently cool older low-power FA. Further, FA positioned at the edge of a storage rack can be cooled by an air convection in between the racks (see Fig. 5f).

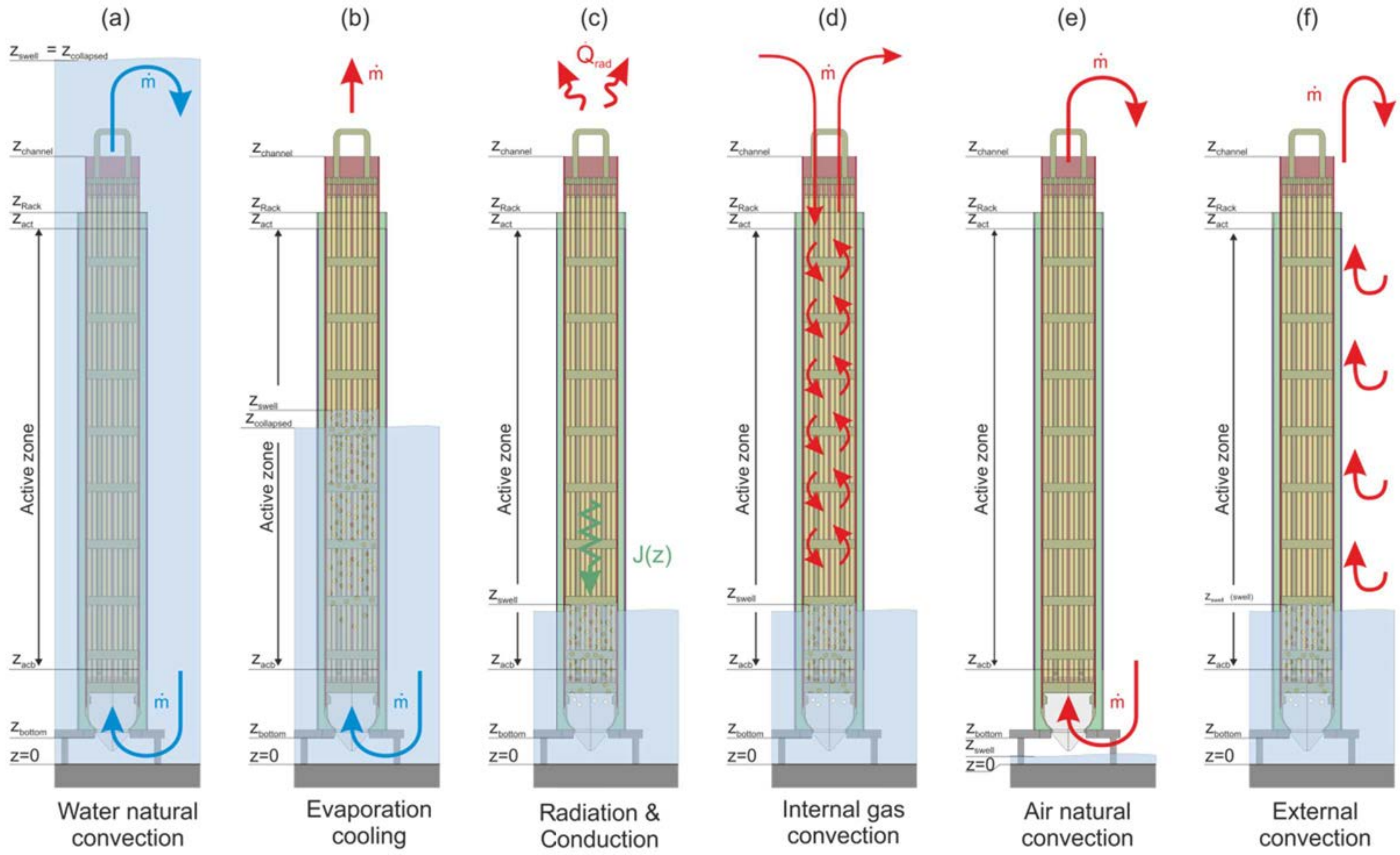

FIG. 5. Different FA cooling mechanisms.

As supporting works for developing SFP-related accident mitigation measures, Framatome conducted MELCOR simulations to determine the accessibility of the service floor (see Fig. 4 and compare Section 2) and to explore the bounding cases of a sufficient FA cooling.

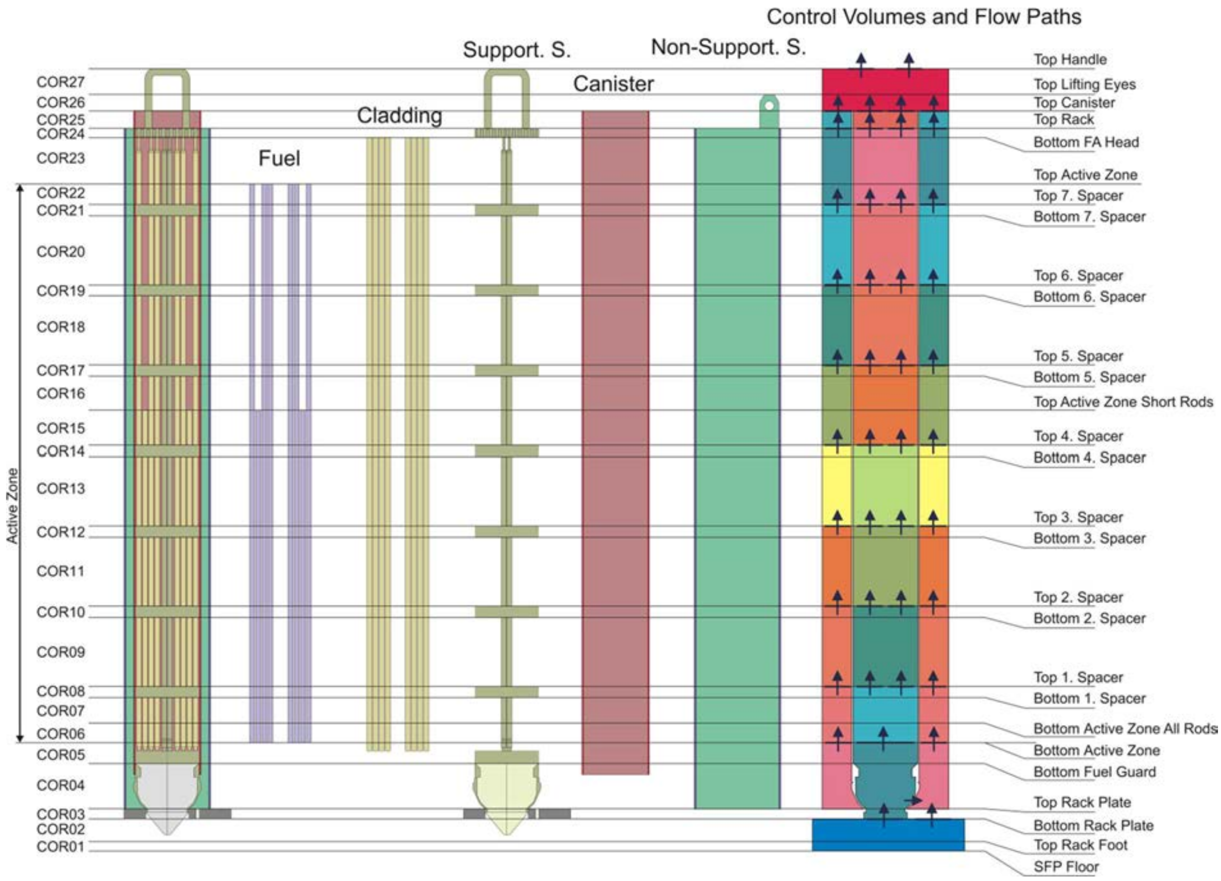

FIG. 6. MELCOR COR nodalization of a single BWR FA.

All relevant heat-transmitting phenomena are either intrinsically included in the MELCOR code or can be added through a suitable nodalization [9, 10]. An individual FA was modelled. The used nodalization is shown in Fig. 6. As conservative bounding assumption it was considered that the FA is located at the centre of a rack. Thus the radial boundary condition was chosen to be periodic i.e. insulating, and no heat loss due to inter-rack air convection was credited.

The primary goal of the simulations was to determine thresholds up to which design-exceeding situation a suitable cooling of the FA is still possible and at which state a significant release of fission products must be expected. This may affect the initiation criteria for external civil protection measures in case of emergency.

Two different cases were examined:

- Section 3.1 – Drop of the SFP liquid level into the FA active zone;
- Section 3.2 – Total drainage of the SFP.

3.1. Drop of the SFP liquid level into the FA active zone

If the swell level in the FA has fallen into the active zone, only the decay heat generated below the swell level in the FA is removed by vaporizing water. The generated vapour is forced through the upper part of the FA. There the steam absorbs the decay heat from the exposed fuel rods and gets superheated.

When ignoring axial heat conduction, heat radiation, internal convection, and radial heat losses, the FA outlet temperature in a partially exposed FA can be estimated analytically by an energy balance. The fraction n $[0 \leq n \leq 1]$ of the total decay heat $\dot{Q} = \int \dot{q}(z) \cdot dz$ in the submerged lower part of the FA is given by

$$n \cdot \dot{Q} = \int_0^{z_{\text{swell}}} \dot{q}(z) \cdot dz \tag{2}$$

where $\dot{q}(z)$ is the decay power per FA length at the elevation z, and z_{swell} is the swell level of the SFP within the FA. The vapour production rate $\dot{m}$ inside the FA, generated below the water level, is given by the decay power input $n \cdot \dot{Q}$ divided by the evaporation enthalpy

$$\dot{m} = \frac{n \cdot \dot{Q}}{h_{\text{v}} - h_{\text{W}}} \tag{3}$$

where h_{v} is the specific vapour enthalpy, and h_{W} is the specific enthalpy of liquid water at saturation condition. The remaining part of the decay power $(1-n) \cdot \dot{Q}$ is released in the exposed top part of the FA. This energy can be absorbed by overheating of the vapour which is generated in the lower part. If the vapour mass flow $\dot{m}$ is known, the superheating of the vapour, equalling the FA outlet temperature at elevation z_{Canister} can be determined through an energy balance

$$(1-n) \cdot \dot{Q} = \dot{m} \cdot \left(h_{\text{v}}|_{T(z_{\text{Canister}})} - h_{\text{v}} \right) \tag{4}$$

where $h_{\text{v}}|_{T(z_{\text{Canister}})}$ is the specific vapour enthalpy at the FA outlet temperature $T(z_{\text{Canister}})$. Through the elimination of the vapour mass flow, the equation for the outlet steam enthalpy can be transferred to

$$h_{\text{v}}|_{T(z_{\text{Canister}})} = \frac{(1-n)}{n} \cdot (h_{\text{v}} - h_{\text{W}}) + h_{\text{v}} \tag{5}$$

The result is interesting as the FA outlet temperature only depends on the relative behaviour of the decay power fractions released above or below the water surface, and not on the total decay power $\dot{Q}$ of the FA. The higher the FA's total decay power, the higher is the required vapour flow in order to cool the exposed top part of the FA. However, with a higher total decay power, more vapour is also produced in the covered part of the assembly. For FAs that have a longer storage time, a lower vapour flow through the FA is needed. However, in this case also less vapour is produced. The expected vapour outlet temperature is therefore independent of the total decay power of an FA.

Assuming a homogeneous power distribution in the FA, the FA outlet temperature $T(z_{\text{Canister}})$ is plotted versus the liquid level in a BWR SFP as a blue-dashed line in Fig. 7. Because of the cladding tube's low heat flux density, the surface temperature of the tubes is approximately equal to the steam temperature. The analytical estimate predicts that a FA, independent of its decay power, can fall dry by 1/4 (25%) without suffering damage from structurally dangerous temperatures (assumed beyond 650°C). Up to this fraction of submersion, the water/vapour cooling is sufficient.

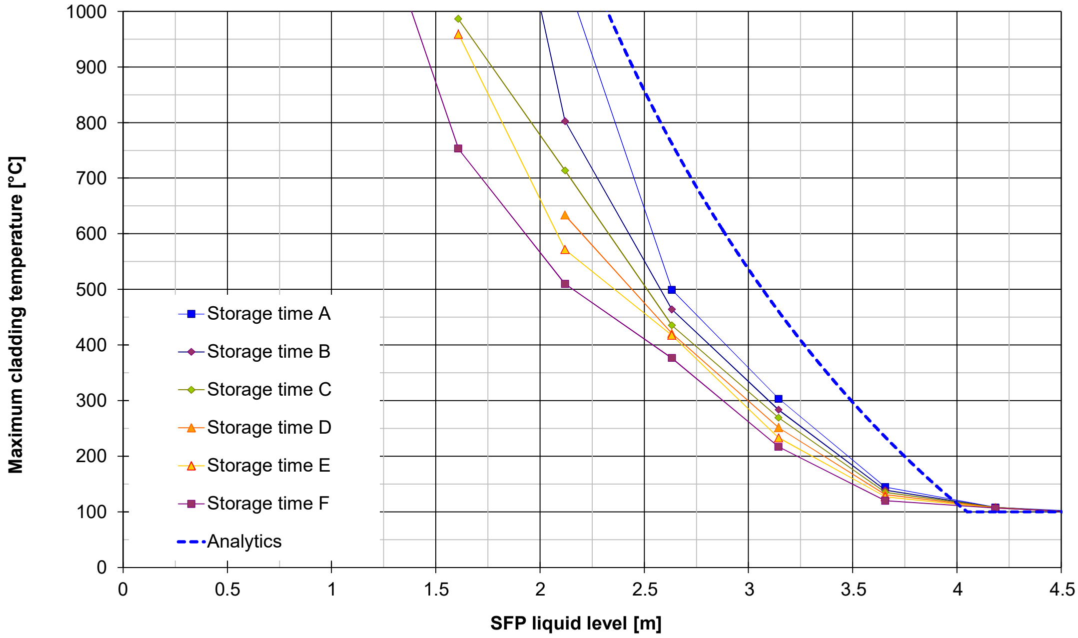

FIG. 7. FA outlet temperature as function of the SFP liquid level.

However, the analytical evaluation conservatively neglects axial heat conduction, radiation losses and internal gas convection. Thus the analytical prediction is conservative. When calculating the peak cladding temperatures in a FA with the MELCOR code on a best estimate-basis, lower FA exit temperatures are predicted, see Fig. 7. In contrast to the steam cooling, the above mentioned cooling mechanisms are primarily driven by the temperature gradient within the FA. Thus, the relative importance of axial heat conduction, radiation losses and internal gas convection are higher for FA with low total decay power. Therefore FAs can be exposed to a higher degree (up to 50% total height after storage time F) and still be efficiently cooled when having subsided for a sufficiently long time in the SFP before the assumed accident.

3.2. Total drainage of the SFP

If an event is strong enough to penetrate the SFP walls well below the top of the active fuel, compare Section 3.1, then it is quite likely that also the SFP floor gets damaged. Thus a total drainage of the SFP in the aftermath of an external event is probably more likely than a low-lying leakage. This can be beneficial concerning the coolability of the FA. After a total drainage of the pool a natural convection of air can circulate through the FA, see Fig. 5e.

The air volume flow through a FA is determined by the competition between the buoyancy of the heated gas and the flow resistance of the FA structure. The water flow resistance of fuel elements is well examined, as this is an important quantity for power operation. It is predominantly determined by minor losses. However, the air flow resistance, dominated by the major loss / friction loss, is known to a much lower accuracy. Thus, to determine the air flow resistance the hydraulic diameter of a FA was examined with analytical calculations in comparison to computational fluid dynamics (CFD) simulations [9, 10].

After determination of the air friction loss of a FA, the air mass flow and thus the FA outlet temperature was analytically calculated (with certain simplifications). Additionally, the more precise loss coefficients were implemented in the MELCOR model, and the air flow and FA outlet temperature were simulated. The results of the simulation and the analytical calculation agree reasonably well, see Fig. 8.

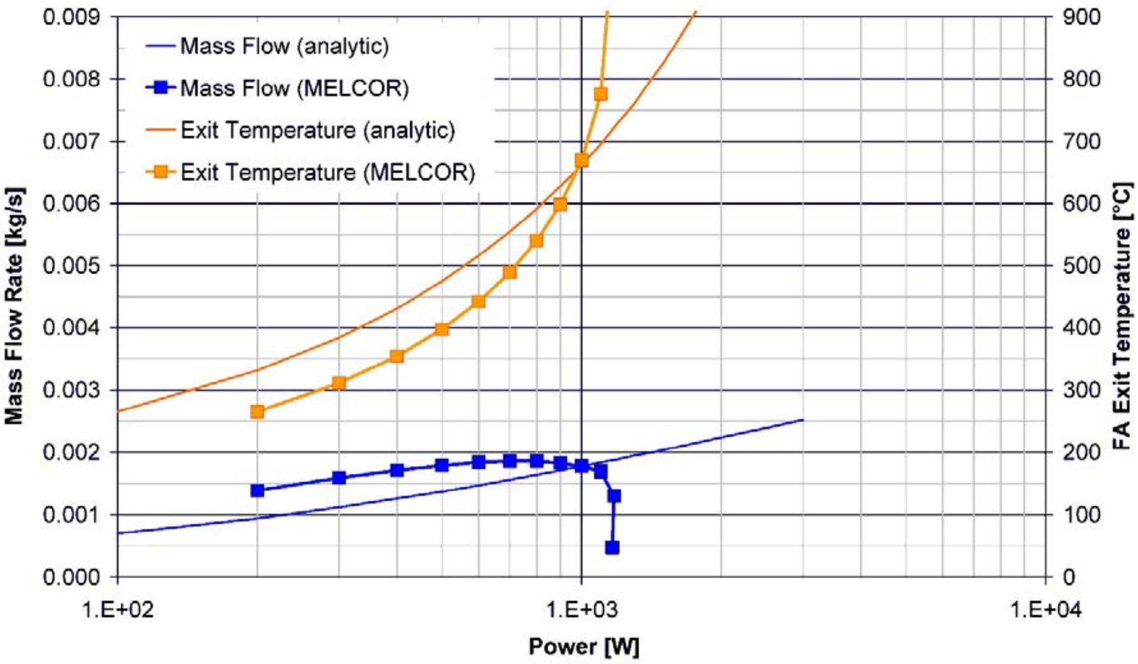

FIG. 8. FA outlet temperature in case of air cooling the FA.

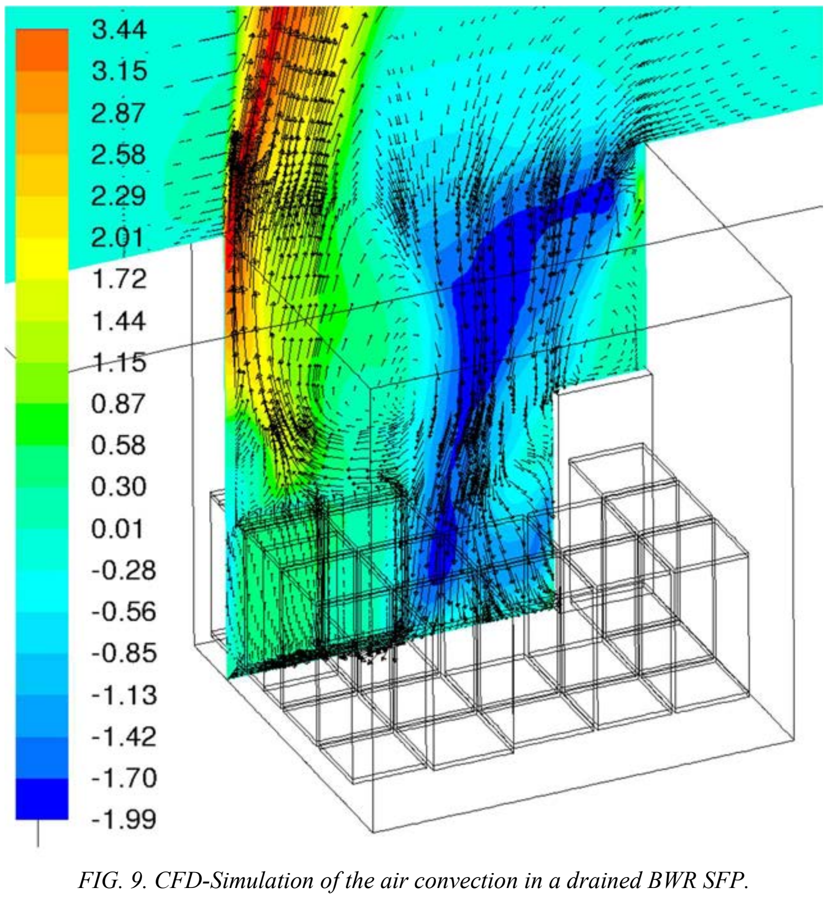

FIG. 9. CFD-Simulation of the air convection in a drained BWR SFP.

It turns out that up to a decay heat of about 1 kW per BWR FA, the cladding remains reasonably intact (temperature remains below ~650°C) [10]. While this result excludes the possibility of air-cooling freshly unloaded FA, it shows that in case of a total drainage of the SFP only the FA unloaded within about the last 12 months cannot be cooled efficiently. The FA, unloaded before and stored for a longer duration can be expected to remain intact.

An extrapolation of this MELCOR simulation for a single FA to the entire SFP geometry was done using CFD tools, see Fig. 9. This CFD simulation thereby fully confirmed the MELCOR simulation results concerning the temperatures within the FA and additionally confirmed that there is a suitable convection loop to transport the heat out of the SFP room into the upper service floor.

4. MITIGATION OF A LONG-TERM BOILING SPENT FUEL POOL

As experienced in Fukushima, a long-term station blackout leads to an uncontrolled heat-up of the spent fuel pool. There, it was possible to establish a water makeup to the affected SFP in units 1 to 4, so that a dry-out of the pools was avoided, and a 'long-term boiling SFP' situation occurred (for simplicity the notation of 'boiling' is used in the following even if evaporative cooling keeps the SFP below saturation condition).

Thereby it needs to be considered that in Fukushima the circumstances for the SFP feeding were in some aspects detrimental and in some aspects beneficial. Strongly detrimental were the general environmental conditions on the plant site, i.e. the damaged infrastructure due to the tsunami, scattered contaminated debris from the failed roof structures, the elevated radiation levels due to the core damage events in Units 1 to 3, the unavailability of resources due to the efforts to secure the reactor cores, and the complete lack of plant instrumentation. Beneficial were the good accessibility to the pools by concrete pumps for injecting water, the good ventilation of the service floors limiting the pool temperatures well below the boiling condition, and the ability to visually "measure" the pool liquid levels. These three aspects were directly caused by the failure of the roof structures in the plant (respectively the opened blow-out panel in Unit 2).

As the long-term boiling SFP is one of the (conditionally) more likely nuclear incident / accident sequences with respect to the SFP (compare also the discussion in Chapter 1), many plant utilities, with support by Framatome, have implemented emergency measures to reliably mitigate such an event. Thereby the implementation of a reliable emergency measure to mitigate a boiling SFP requires the following prerequisites:

- Access of plant personnel (possibly limited by temperature, humidity, and radiation) to the SFP itself or an interconnected cooling system to establish the water makeup;
- Availability of suitable hardware / equipment like fire engines or diesel-driven pumps;
- Surveillance of the current pool water level (at best qualified for the expected environmental conditions);
- Preparation of a suitable steam release path from the plant buildings into the environment;
- Confirmation that the pool liner and load-bearing concrete structures can endure the increased water temperature (to not induce an additional pool leakage).

The accessibility to the SFP or systems interconnected to the SFP may be limited for several reasons. A failure of the roof structure, as occurred in Fukushima, cannot be credited for emergency planning, especially not for plants where the SFP is enclosed in an airplane resistant building. But when the building which houses the SFP remains intact, a heat-up of the SFP will cause high temperatures and high humidity levels, possibly requiring suitable personal protection equipment to enter the building. However, planned emergency works to be performed in heavy protection equipment should be avoided as far as possible. Furthermore, the boiling of the SFP is likely not an isolated incident, but a consequence of a large-scale accident situation on the plant site. Thus, in parallel to the boiling SFP, damages to the plant site infrastructure must be anticipated, requiring simultaneous execution of other emergency actions like e.g. feeding the reactor core / steam generators. This effectively limits the availability of plant equipment and personnel. Additionally, the release of fission products may limit the accessibility of the plant site and execution of emergency measures.

When access of personnel is ensured, the personnel needs suitable hardware to establish a water injection into the SFP, e.g. mobile diesel-driven pumps, and a dedicated injection path into the SFP. Depending on the plant layout this may be realized e.g. by an additionally installed dry pipe directly leading into the SFP or by installing a connection flange to a system which is connected to the SFP.

The emergency preparedness should foresee dedicated sources for coolant, e.g. the condensate storage tanks in BWRs or the emergency feedwater tanks in a PWR. Also the injection of fire water or drinking water is possible. In general, due to the low surface area heat flux in used fuel elements, water impurities do not endanger the cooling of the FA so that even non-purified surface fresh water can be used to feed an SFP. However, impurities increase the risk for corrosion in the long term. For water makeup in a boiling SFP, unborated water is preferable for BWR as well as for PWR. Due to the evaporation / vaporization of water from the SFP, boric acid possibly present in the SFP water remains in the pool. By adding more and more borated water to the pool over a time span of weeks to month, the boric acid would accumulate, and in the long term could lead to a re-crystallization risk. However, depending on the design basis of the spent fuel storage racks, the injection of unborated water into a PWR fuel pool should be covered in the emergency planning by suitable analysis excluding a re-criticality risk.

To maintain a controlled liquid level in the pool, a sufficiently robust and accurate measurement is stringently necessary. This level measurement must avoid an accidental unobserved under-feeding of the pool (compare e.g. the SFP liquid level in Fukushima Unit 4 for the first month after the tsunami [11]) as well as to prevent an excessive over-feeding of the pool, causing a flooding risk or an occupational hazard within the building. In case the existing fuel pool instrumentation is not considered sufficiently robust (with respect to the environmental conditions or with respect to administrative boundary conditions like a non-available main control room) suitable strengthening / back-fitting measures are to be considered. Framatome developed accident tolerable level measurement devices [12] as well as a severe accident tolerable level measurement system [4].

It further must be evaluated how the steam generated by the SFP is released to the environment. For the steam release an operating active HVAC system cannot be credited due to its dependency on AC power. In some plant designs like the German PWR, the VVER, or the MARK III BWR the SFP is located inside the containment. For these plants a boiling SFP may even cause a pressurization of the containment.

Typically lumped-parameter codes (e.g. MELCOR, WAVCO, COCOSYS,…) are used to address the thermal-hydraulic behaviour of the fuel building, the reactor building, or the containment building response to events such as high-energy pipe breaks. These codes can also be used to simulate the building response to a boiling SFP. A typical lumped-parameter code nodalization scheme is shown to simulate the containment of a German PWR for system design purposes. Note that the SFP and the service floor are represented as a single control volume. This nodalization was chosen on purpose, not to get best-estimate simulation results, but to over-predict sub-cooled vaporization and thus gain conservative results concerning containment pressure build-up, compare the discussion in Section 2.

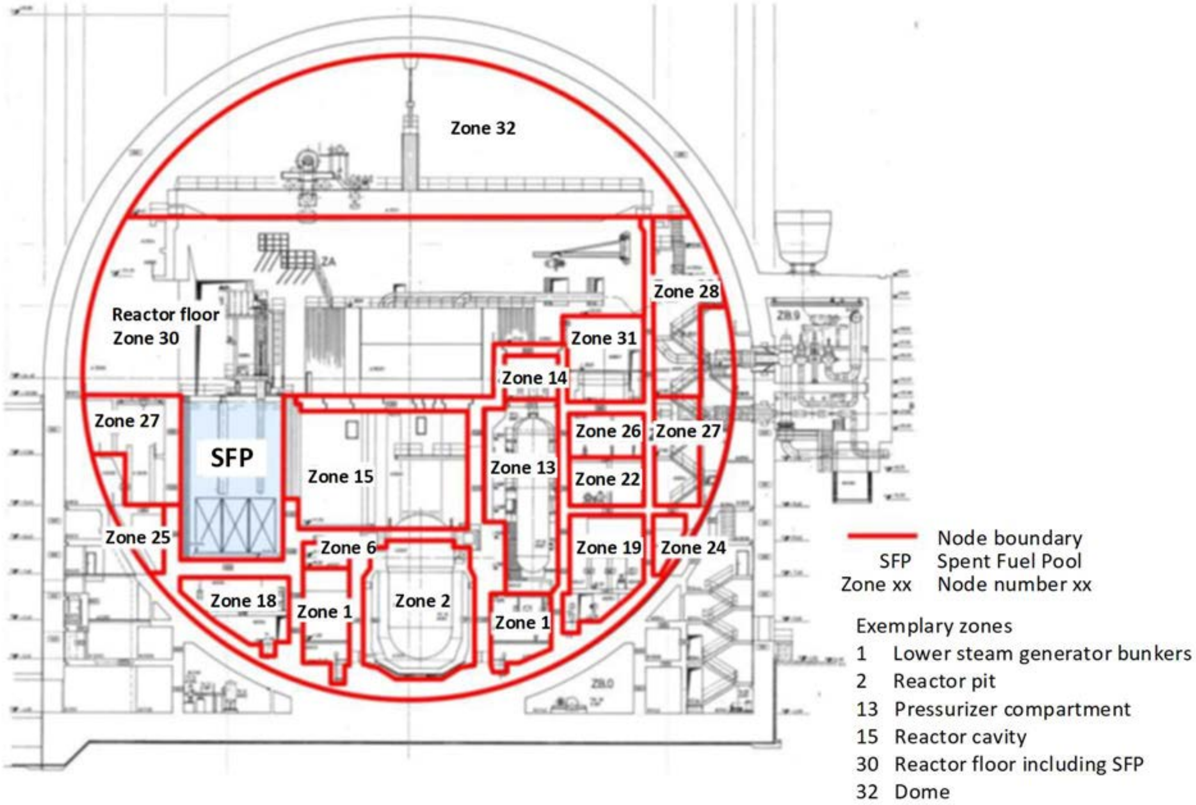

FIG. 10. Typical (conservative) containment nodalization scheme for a German PWR.

Based on such building response simulations the necessary flow rate for a steam release path can be balanced versus the level of impact a boiling SFP can have onto the building (e.g. which humidity levels in a reactor building or what pressure build-up inside the containment can be accepted). After determining the necessary steam release flow rate, it can be evaluated if an existing operational (but non-active) HVAC system can be credited for steam discharge, whether existing emergency hardware like a filtered containment venting system can be used, or if a new steam release path is back-fitted.

At last, when planning to mitigate a long term boiling SFP, it must be confirmed that the SFP liner as well as the structural support concrete structure can endure the expected temperatures for a long duration. It must be excluded that an excessive heat-up induces additional leakages of the SFP. SFP were often constructed under the requirement to store only subcooled water, e.g. ≤80°C in Germany [13] (due to the post-Fukushima revision the German nuclear regulations nowadays also foresee higher SFP temperatures, see Ref. [15]).

In Fukushima the SFP in Unit 4 endured temperatures in excess of 90°C. Thereby no additional large leakages induced by the high temperature were observed. However, it is unclear if this observation can be generalized also to other plants. Furthermore, in case of a non-ventilated fuel building the SFP will likely approach 100°C after the building atmosphere reached 100% air humidity. And in plants where the SFP is located within the containment even higher pool temperatures are expectable, depending on the containment pressure build-up.

To ensure that a long-term boiling does not impair the leak-tightness of the SFP, the liner and the structural concrete can be numerically examined by finite element methods, and the resulting material strains and stresses can be compared to the allowed limits. In the experience of Framatome, it is often possible to back-qualify an existing SFP to water temperatures above the maximum expected temperatures in a long-term boiling SFP event.

Based on all the above listed tasks, in part supported by numerical studies, a nuclear power plant can be enabled to mitigate a long-term boiling SFP with a very high reliability.

SUMMARY

The paper gives an overview of the Framatome experience concerning analytical and numerical studies in the overall context of spent fuel pool (SFP) incidents and accidents. Respective simulations are performed and used in the frame of developing SFP-related (severe) accident management guidelines (SAMG), and to support the back-fitting of emergency operation actions to reliably mitigate a long term boiling SFP.

In Section 2 the recordings during/after the accidents of Fukushima Daiichi are used to develop and qualify the thermal-hydraulic modelling of a spent fuel pool, especially the transition from evaporation to vaporization. This is a necessary prerequisite to make reliable predictions concerning the increase of temperature and humidity on the service floor. With these information grace periods are deduced how long an accessibility of the service floor by plant personnel can be credited.

In Section 3 the limits of coolability of FA are evaluated in the frame of the introduction of SFP-related SAMG in boiling water reactors. These studies are used to narrow down the criteria in which situations an extended FA damage event must be expected. Thus, these studies have a direct impact on the planning of civil protection actions in case of a SFP-related design extension condition event.

In Section 4 the necessary steps to implement the reliable ability of a plant to mitigate a long-term boiling of an SFP is examined. These steps include the clarification of accessibility of personnel to relevant locations, the availability of equipment like pumps and injection lines, the preparation of a suitable steam release path to the environment, the qualification of the pool liner / concrete structure to the expected temperatures and to ensure the availability of a suitably robust SFP level measurement.

REFERENCES

[1] WERNER, M.M, MYERS, D.K., MORRISON, D.P., Follow up of AECL employees involved in the decontamination of NRU in 1958, AECL-7901, Atomic Energy of Canada Limited, Chalk River, ON (1982)

[2] HARTUNG, J., RUTHERFORD, P., Lessons Learned from Major Core Damage Accidents, Transactions of ANS **43** (1982) 676–677.

[3] INTERNATIONAL ATOMIC ENERGY AGENCY, OECD-IAEA Paks Fuel Project, IAEA, Vienna (2010).

[4] FRAMATOME GMBH, Silicone-Based Adhesive Technology, Leakage Mitigation for Reactor Cavity Liners and Transfer Canal Liners, Framatome (2018) **Error! Hyperlink reference not valid.**http://www.framatome.com/customer/liblocal/docs/KUNDENPORTAL/PRODUKTBRPRODUKTBR/Broschüren%20nach%20Nummer/PS-G-0005-ENG-201807-Silicone%20Based%20Adhesive%20Technolgy.pdf
[5] HARTMANN, C., VUJIC, Z., Retrofitting a spent fuel pool spray system for alternative cooling as a strategy for beyond design basis events, ATW - Internationale Zeitschrift für Kernenergie, **62** 6 (2017) 392–396.
[6] AREVA, UK-EPR Fundamental Safety Overview, Volume 1 Chapter A: EPR Design Description http://www.epr-reactor.co.uk/ssmod/liblocal/docs/V3/Volume%201%20-%20Overview/1.A%20-%20EPR%20Design%20Description/1.A%20-%20EPR%20Design%20Description%20-%20v3.pdf
[7] BOELTER, L.M.K., GORDON, H.S., GRIFFIN, J.R., Free Evaporation into Air of Water from a Free Horizontal Quiet Surface, Ind. Eng. Chem. **38** (1946) 596–600.
[8] SHAH, M.M., Analytic Formulas for Calculating Water Evaporation from Pools, ASHRAE Transactions, **114** 2 (1981) SL08-062.
[9] FRAMATOME GMBH (formerly AREVA GmbH), Aspects of Modeling a Spent Fuel Pool, Presented at European MELCOR User Group Meeting, KTH Stockholm, Sweden, May 2nd–3rd 2013. https://www.psi.ch/sites/default/files/import/emug/Emug2013EN/EMUG2013_Aspects_of.pdf
[10] FRAMATOME GMBH (formerly AREVA GmbH), Cool-ability of used fuel in storage racks, Presented at European MELCOR User Group Meeting, Cologne, Germany, April 17th 2012. https://www.psi.ch/sites/default/files/import/emug/Emug2012EN/EMUG2012_AREVA_Loeffler.pdf
[11] TOKYO ELECTRIC POWER COMPANY, INC, Fukushima Nuclear Accident Analysis Report, June 20, 2012, TEPCO, Tokyo (2012).
[12] FRAMATOME GMBH (formerly AREVA GmbH), Spent Fuel Pool Level Instrumentation, EA-12-0051 / REC. 7.1. http://us.areva.com/home/liblocal/docs/Solutions/Product%20Sales/SFP-Instrumentation_By_AREVA_Presentation_V0.pdf
[13] KERNTECHNISCHER AUSSCHUSS, Sachstandsbericht zu KTA-BR 2 „Kühlung der Brennelemente“, KTA-GS-72, Stand: April 2004. http://www.kta-gs.de/d/versch/kta-gs-72%20br2.pdf
[14] KERNTECHNISCHER AUSSCHUSS, Sicherheitstechnische Regel des KTA “Wärmeabfuhrsysteme für Brennelementlagerbecken von Kernkraftwerken mit Leichtwasserreaktoren, KTA 3303, Fassung 2015-11. http://www.kta-gs.de/d/regeln/3300/3303_r_2015_11.pdf

RECENT DEVELOPMENTS OF AC^2 FOR SPENT FUEL POOL SIMULATIONS

T. HOLLANDS, L. LOVASZ
Gesellschaft für Anlagen- und Reaktorsicherheit (GRS) gGmbH,
Garching
Germany
Email: thorsten.hollands@grs.de

Abstract

System codes are used worldwide to assess the safety of nuclear power plants. The system code AC^2 is capable of simulating design basis accident (DBA) and beyond design accident (BDBA) scenarios in a nuclear power plant. Historically, similarly to the other major code systems, AC^2 was optimized to simulate the relevant processes within the reactor circuit. However, the accident at the Fukushima Daiichi nuclear power plant heightened awareness regarding a possible severe accident scenario in a spent fuel pool. Some limitations of AC^2 regarding adequate modelling of the accident phenomena inside a spent fuel pool were identified. Therefore, major code developments were carried out at GRS in the recent years to eliminate these limitations. The paper summarizes these limitations, introduces the developments and new features of AC^2 for spent fuel pool calculations, presents a verification sample calculation, and gives an insight about needed/possible further works.

1. INTRODUCTION

The environmental impact of the accident at the Fukushima Daiichi nuclear power plant developed from the processes linked to the failure of fuel assemblies within the reactor vessel. The cooling of the spent fuel pools (SFP) was disrupted in parallel to these events. Fortunately, the cooling of the fuel assemblies inside the spent fuel pools was restored before fuel damage could occur.

Scenarios are possible, however, where either due to loss of coolant or due to loss of cooling the fuel assemblies become dry, which can result in fuel degradation and release of fission products. Modelling and simulating such accident scenarios in a spent fuel pool was not in focus of research, but the accident in Fukushima Daiichi nuclear power plant highlighted the possibility of such scenarios. This gave spent fuel pools a larger safety relevance and a good motivation to use code systems to analyze BDBA also in spent fuel pools.

AC^2, similarly to other major code systems [1–3], were developed and optimized mostly for simulating accident phenomena within the reactor cooling circuit. Some of the implemented models take advantage of the typically cylindrically symmetrical geometry inside of a reactor vessel, the usual nodalization of the core region is, therefore, also cylindrically symmetrical. This is, however, in most cases not true for spent fuel pools, where the geometry of the pool and the position of the stored fuel assemblies are typically not cylindrically symmetrical. The adequate representation of the fuel assemblies using the standard 'ring-like' nodalization of AC^2 is not possible. Due to this reason, a new option was implemented in the developer version of ATHLET-CD (which is the part of the code system AC^2 that is responsible for the simulation of severe accident phenomena) that departs from the typical "ring-like" nodalization and allows the user to define the core nodes flexibly. This allows a more adequate representation of accident scenarios without cylindrically symmetrical conditions.

The paper presents the basic idea and implementation of the new and flexible nodalization scheme in the developer version ATHLET-CD. The capabilities of the new feature are shown on verification sample calculations. Furthermore, the limitations, which still exist, and future tasks are addressed.

2. AC²/ATHLET-CD

The code system AC² is primarily developed by the Gesellschaft für Anlagen- und Reaktorsicherheit (GRS) GmbH and consists of three major modules: **A**THLET, ATHLET-**C**D and **C**OCOSYS. The three modules are dedicated to simulating different stages of a nuclear accident:

- ATHLET covers all the relevant processes during a DBA inside the reactor cooling circuit and the balance of plant (BOP). Core degradation effects are not taken into account, fission product release and transport processes are not considered;
- ATHLET-CD uses as basis the original ATHLET input for the calculation of the thermodynamic phenomena and extends the models of ATHLET to be able to calculate processes during a severe accident: core degradation including fission product release and transport inside the cooling circuit;
- COCOSYS simulates the main phenomena in the containment under DBA and BDBA conditions. If not used in stand-alone mode, COCOSYS receives the thermohydraulic, melt and fission product data from ATHLET/ATHLET-CD.

By coupling all these modules the user can simulate the whole extent of a nuclear accident. However, the user can also use the modules individually. This paper focuses on ATHLET-CD.

ATHLET-CD was optimized for reactor applications; therefore, the core is nodalized horizontally in concentric rings and axially in different levels (Fig. 1). There are different materials considered in these nodes: fuel rods, control rods/blades and canister walls. There are many materials defined into a horizontally and axially defined 'ring' and it is assumed that all fuel rods/control rods/canister walls behave identically in such a node, respectively. Simulating these structures individually would be very time consuming. Grouping many of the structures in a ring is a valid assumption as long as the modelled scenario is cylindrically symmetrical. The ATHLET-CD structures are located in ATHLET thermohydraulic volumes and the heat transfer from these structures to the fluid is calculated by ATHLET.

Without going into detail, ATHLET-CD specific modules calculate phenomena related to severe accident phenomena:

- Heat transport of solid and molten structures;
- Mechanical fuel rod behaviour (ballooning);
- Oxidation/nitride formation of zirconium and boron carbide (melt and solid state);
- Hydrogen production;
- Melting of metallic and ceramic components;
- Relocation, freezing, re-melting and re-freezing;
- Formation and dissolution of blockages;
- Fission product release and transport in the cooling circuit;
- Relocation of molten material into the lower plenum;
- Lower plenum phenomena including wall ablation and vessel failure.

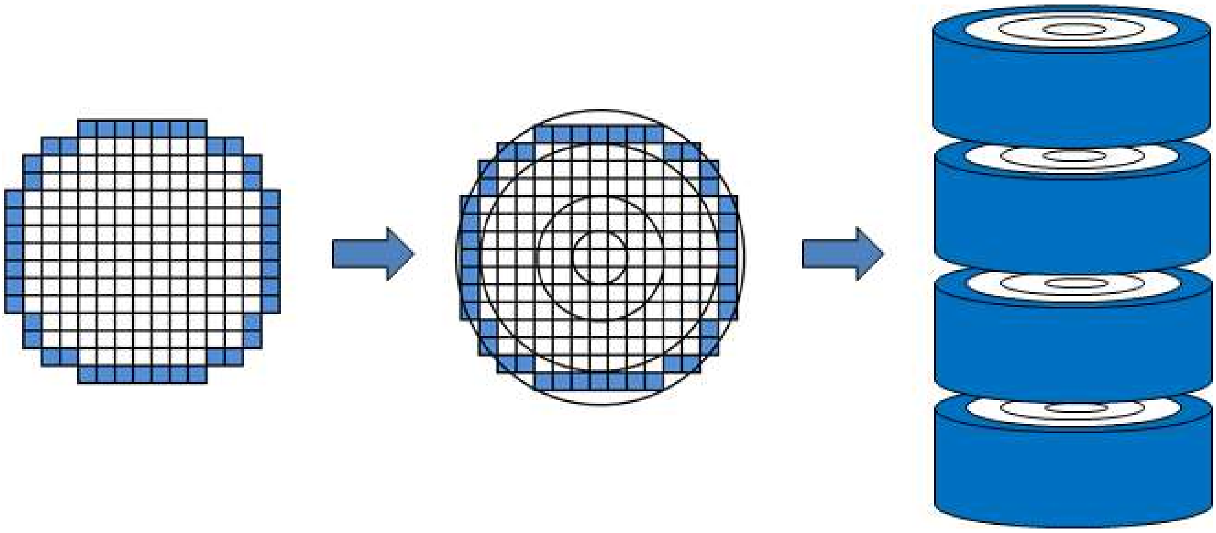

FIG. 1. State of-the-art nodalization of the core [4].

3. SEVERE ACCIDENTS IN SPENT FUEL POOLS

3.1. ATHLET-CD/AC^2 version 2019

Modelling severe accidents in spent fuel pools using major severe accident codes (for example: ASTEC, MELCOR, ATHLET-CD) [1–3] is possible, but the user is required to make simplifying assumptions, mostly due to the typically non-cylindrical geometry of spent fuel pools and due to non-uniform power distributions of the stored fuel assemblies. Applying the previously shortly described 'ring-like' nodalization adequately in spent fuel pools is difficult. Fig. 2 shows an example of a nodalization of a generic spent fuel pool (based on the spent fuel pool of the nuclear power plant Fukushima Daiichi unit 4) with the 'ring-like' nodalization.

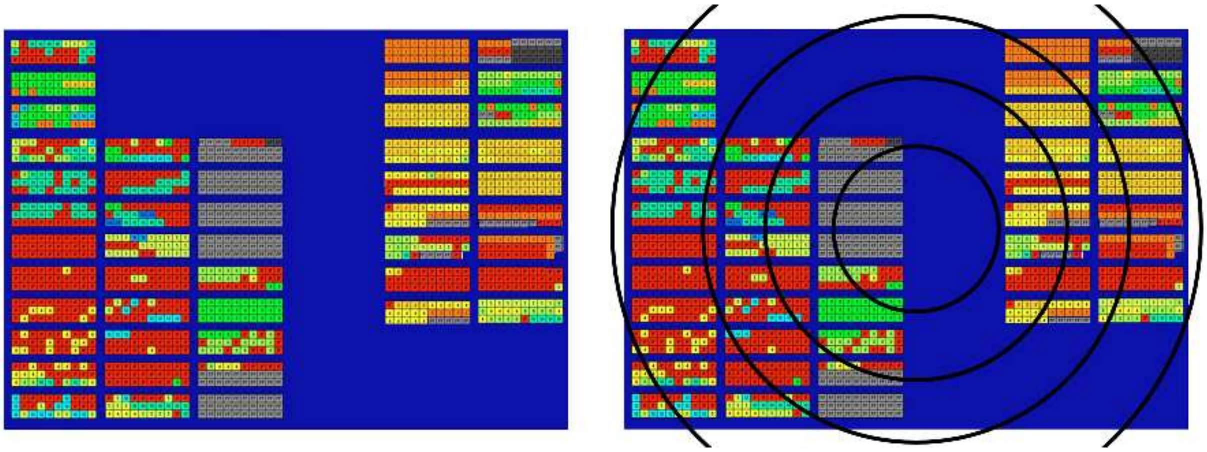

FIG. 2. Nodalization of a spent fuel pool with the "ring-like" method [5].

The figure shows the top view of a spent fuel pool, dark blue areas represent empty (filled with water only) spaces, while the areas marked with small red/green/yellow/grey squares represent the fuel assemblies with different decay heat (red – high, green – low and grey – no decay power).

It is clearly visible that the geometry of the spent fuel pool is not cylindrical and the distribution of the stored fuel assemblies are also far from an axisymmetrical state. Using the 'ring-like' nodalization under such circumstances does not necessarily model the reality correctly. As visible on the right side of Fig. 2, fuel assemblies with completely different properties have to be assigned to a ring, which artificially distributes uniformly the fuel assemblies in that ring, local information is lost. Also, if the spent fuel pool is rectangular, like in Fig. 2, rings can also extend beyond the physical boundaries of the spent fuel pool.

In order to use the standard 'ring-like' nodalization for spent fuel pools the user has to artificially reposition the fuel assemblies with similar properties, similarly as shown in Ref. [6]. To model the spent fuel pool more adequately a flexible nodalization scheme has to be allowed that can take local effects into account.

3.2. ATHLET-CD/AC^2 developer version

Recently a new feature has been added into the developer version of ATHLET-CD which allows the user to define the core nodes flexibly. The user can explicitly define the cartesian coordinates of rectangular nodes (the defined nodes do not have to be of equal size). This creates an option for the user to take the local properties of the spent fuel pool also into account. Fig. 3 shows an example of the possible new nodalization of the same spent fuel pool as depicted previously. The rectangular nodes have the advantage that they can fit better to the typical rectangular geometry of the spent fuel pools. The flexible definition of the node coordinates allows the user to take the different local effects of the spent fuel pool into account. This results in a more realistic nodalization, like seen on the right side of FIG. . There for example: 'Node 2' consists of almost only fuel assemblies with high decay heat, while 'Node 11' represents the stored fresh fuel with practically no decay heat. 'Node 12' is an empty node, containing only water.

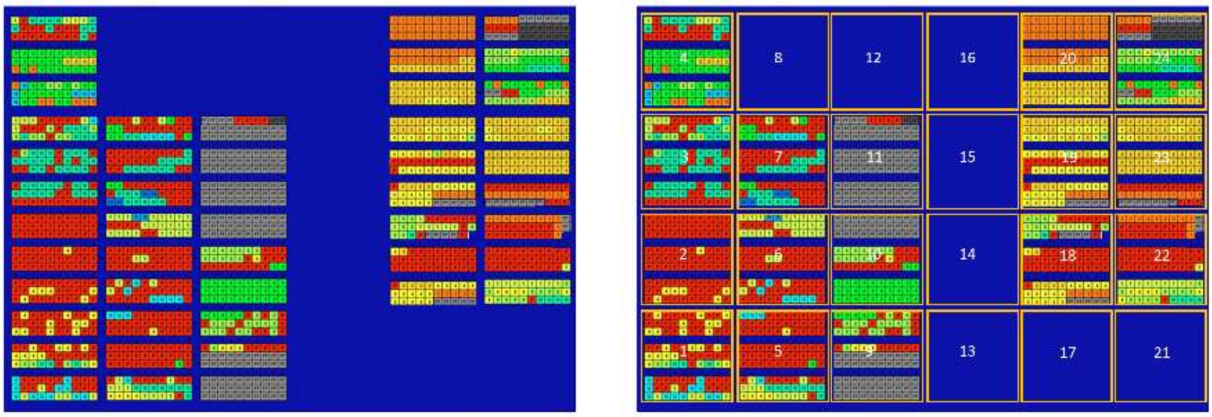

FIG. 3. Nodalization of spent fuel pool with the flexibly nodalization method [5].

The departure from the hardcoded ring-like nodalization of ATHLET-CD had several consequences on the models that take advantage of cylindrically symmetrical configurations. These models have to be adjusted / replaced. However, only two such models were identified, because:

– Within a node most of the phenomena are calculated pin-wise, the results are multiplied by the number of rods assigned to the node. These phenomena are: convective and conductive heat transfer, rod deformation, oxidation/nitride formation, fission product release and melting processes in axial direction.

- Physical modes don't have to be changed, because a different nodalization scheme only changes the number of rods assigned to a node.
- The thermohydraulic volumes to which the core nodes are assigned to are already flexibly definable.
  - Physical models are not affected by the nodalization change.

Physical models are however affected if they describe the data exchange between two nodes, like heat radiation and horizontal movement of molten material between nodes. Currently, a new heat radiation model was developed and implemented for testing into the developer version of ATHLET-CD. The new model for the simulation of horizontal movement of molten material in a flexible defined nodalization is still under development.

3.2.1. New heat radiation model

In the current release version of ATHLET-CD heat radiation between rings is considered. If a node melts, the radiative heat transfer is automatically calculated towards the next intact node. It is basically always heat radiation from a cylinder surface to another cylinder surface. Analytical solutions are available for such relatively simple geometry to determine the radiative heat transfer rate. Shadowing effects (where a still intact node blocks the heat radiation from one node to another) do not exist.

Using a flexibly defined nodalization the calculation of radiative heat transfer can be complex between nodes, shadowing effects can also occur in a constantly changing geometry. Fig. 4 shows an example of a possible complex geometry. Left side of the figure shows the top view of a hypothetical meltdown scenario in a spent fuel pool, where the red zones indicate molten nodes. Heat radiation (indicated with blue line) from one side to another is blocked by a still intact node. The right side of the figure shows the same problem but from a side view. Heat radiation can also be blocked in diagonal direction.

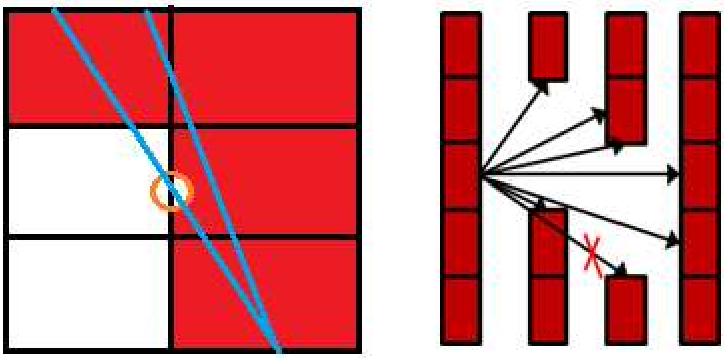

FIG. 4. Top and side view of a partially molten spent fuel pool – heat radiation paths with shadowing effects [4].

There are no analytical solutions to determine the required view factors for such a potential complex geometry, while also taking shadowing effects three-dimensionally into account. A fast running numerical method was therefore implemented in ATHLET-CD to determine the view factors for the radiative heat transfer calculation. The developed numerical method takes the boundaries of the nodes as flat surfaces into account. The underlying consideration behind this assumption is the following: the fuel rods assigned to a node have the same temperature and there are typically many rows after each other, therefore, the incoming heat radiation is absorbed by the node. This also gives a limitation to the model, because this model can be used as long as there are at least three rows of fuel rods in a node, otherwise some portion of the heat radiation can pass through the node, which is not covered by this model. The sum of view factors from a node has to be 1.0, if the results of the numerical view factor calculation are outside of the range 0.9–1.1 for any side, the calculation is repeated with a more detailed calculation, automatically. The numerical method is reasonably fast, but the calculation of view factors cannot be performed every timestep. The view factors are updated if there is a significant geometry change, which means, if 70% of the node is already relocated.

Furthermore, the implemented new heat radiation model uses the following assumptions:

- The fluid is transparent, the emissivity of the structures is defined by the user.
- Temperature of fuel, cladding and structure material are currently considered, heat radiation to melt and crust is taken into account only in an indirect way (radiation to structures, heat transfer from structures to melt/crust). Direct radiation to melt/crust is topic of future development.
- Radiative heat transfer horizontally to the core surroundings is taken into account, but those purely ATHLET-structures cannot relocate as melt if they reach their melting temperature.
- In spent fuel pool calculations the radiative heat transfer to the environment above and below the pool is calculated currently only by a user defined temperature as boundary.

3.2.2. Spent fuel pool specific changes

The implementation of the flexible nodalization and the new heat radiation model were the largest and most necessary changes in ATHLET-CD to be able to model severe accidents in spent fuel pools. There were, however, several smaller, but also relevant changes regarding spent fuel pool configurations.

In the currently released version of ATHLET-CD empty core nodes cannot be specified. A node in the core region has to contain fuel assemblies. In the developer version it was made possible for the user to define empty (only water filled) nodes. These nodes still have to be defined as regular core nodes, but the user has to define explicitly zero fuel rods to that node. An empty node is transparent for the heat radiation.

The canister walls of fuel assemblies are made of zirconium by default, their material properties and oxidation capabilities had to be changed.

The number of thermohydraulic connections of a node in the core were limited to four, to avoid input errors. This is a good help for the user using a ‘ring-like’ nodalization, however in a flexibly defined nodalization a node can have potentially more than four neighbouring nodes

4. VERIFICATION EXAMPLE

In order to demonstrate the importance of the adequate spent fuel pool nodalization and the functionality of the new model, series of simulations are presented. Each simulation calculates the same scenario in the same spent fuel pool, the only difference between the calculations is the power and spatial distribution of the stored fuel assemblies. The simulations were terminated after the molten mass reached 50% of the total mass in the spent fuel pool.

A generic spent fuel pool model was developed, with a side ratio of 6.75 m × 9.87 m. The total power of the simulated spent fuel pool was 2.345 MW and 1440 out of the possible 2160 spent fuel assemblies were stored in it. These parameters are comparable with the parameters of the spent fuel pool of Fukushima Daiichi Unit 4 [7]. The postulated accident is a loss of coolant scenario, the assumed leak mass flow rate was 10 kg/s. The spent fuel pool was divided into 24 equal rectangular nodes, using the new, flexible nodalization method. Each node consists of 90 fuel assembly positions.

Three different fuel assembly configurations were analyzed, they are depicted in Fig. 5. 'Configuration 1' is the closest to the spent fuel pool configuration of Fukushima Daiichi Unit 4 regarding fuel assembly and power distribution. 'Configuration 2' had the same spatial distribution of fuel assemblies as 'Configuration 1', but a perfect mixture of fuel assemblies was assumed, creating an average power for all non-empty nodes. 'Configuration 3' has a new spatial distribution of the fuel assemblies. The aim was to distribute the empty spaces along the spent fuel pool to be able to analyze the potential cooling effect of the empty nodes. Still, all the non-empty nodes have the same power. The used power distribution in the different configurations is summarized in Fig. 5. Thermohydraulically, all nodes are connected with all their neighbouring nodes, however cross-flow is limited, as long as canister walls are intact in the nodes. Fig. 5. shows only the top view of the fuel assembly region, there are two other water volumes, one above this region and one below this region. Along the sides of the pool four downcomer nodes are defined. ATHLET-heat objects are defined in the downcomer nodes, they represent the walls of the spent fuel pools. They are simulated as a flat wall, with 1 cm thickness of steel and 1 m thick concrete. The outside temperature of 20°C is set as a boundary condition. Above the pool air at atmospheric pressure is defined. The leak is defined at the bottom of the pool.

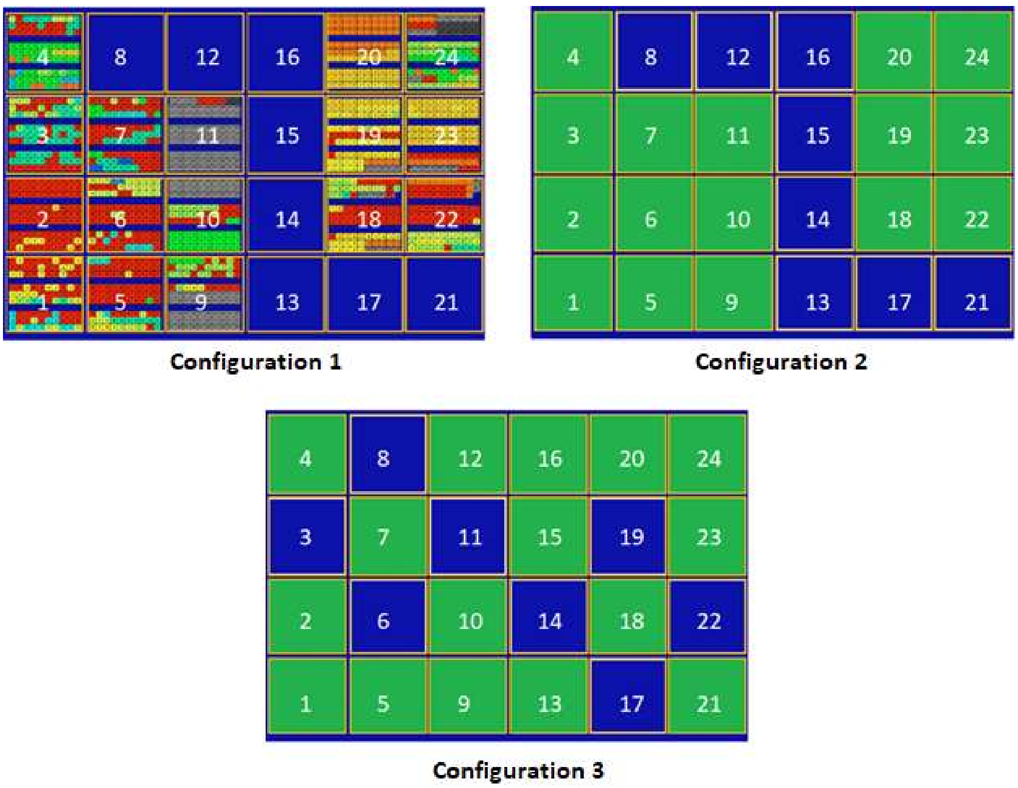

FIG. 5. Top view of the analyzed fuel assembly configurations in the spent fuel pool. Colours indicate the power of the node: red – high power, yellow – medium power, green – low power, dark blue – empty node (filled with water).

If there are no fuel assemblies defined to a node, then the power of that node is zero, they are considered empty (blue nodes in Fig. 5). Exception is the node 11 in 'configuration 1', because it represents a node filled with fresh fuel, without any decay power.

Thermohydraulically, all nodes are connected with all their neighbouring nodes, however cross-flow is limited, as long as canister walls are intact in the nodes. Fig. 5. shows only the top view of the fuel assembly region, there are two other water volumes, one above this region and one below this region. Along the sides of the pool four downcomer nodes are defined. ATHLET-heat objects are defined in the downcomer nodes, they represent the walls of the spent fuel pools. They are simulated as a flat wall, with 1 cm thickness of steel and 1 m thick concrete. The outside temperature of 20°C is set as a boundary condition. Above the pool air at atmospheric pressure is defined. The leak is defined at the bottom of the pool.

TABLE 1. POWER DISTRIBUTION OF THE SPENT FUEL POOL IN DIFFERENT CASES

	Power (W) 'Configuration 1'	Power (W) 'Configuration 2'	Power (W) 'Configuration 3'
1	186 230	146 572	146 572
2	304 800	146 572	146 572
3	135 710	146 572	0
4	177 240	146 572	146 572
5	297 270	146 572	146 572
6	287 160	146 572	0
7	192 140	146 572	146 572
8	0	0	0
9	63 790	146 572	146 572
10	64 640	146 572	146 572
11	0	146 572	0
12	0	0	146 572
13	0	0	146572
14	0	0	0
15	0	0	146 572
16	0	0	146 572
17	0	0	0
18	155 790	146 572	146 572
19	79 280	146 572	0
20	76 260	146 572	146 572
21	0	0	146 572
22	186 600	146 572	0
23	90 250	146 572	146 572
24	47 990	146 572	146 572
Sum of power (W):	2 345 150	2 345 152	2 345 152

Fig. 6 shows the evolution of the maximum cladding temperature in the different configurations. As it is clearly visible, as long as the fuel assemblies are covered by water, their cooling is sufficient. The water level reaches the top of the fuel assemblies at approximately 30 000 seconds after the start of the LOCA scenario. The heat up of the upper parts of the fuel assemblies is not significant at the beginning, due to their relatively low decay power and due to the fact that the parts below are still cooled. The generated heat can be removed by axial conduction. As larger parts of the fuel are uncovered, the temperatures rise and the first differences occur due to the unequal efficiency of the cooling via heat radiation. At about 64 000 seconds after the initiating event the whole fuel assembly is uncovered. The disappearance of the water plug in the bottom part of the fuel assemblies allows the air to flow through completely. This leads to a natural circulation, which increases the coolability of the spent fuel assemblies. The cooling effect of the natural circulation can be seen in Fig. 6 at around 64 000 seconds, because the maximum cladding temperatures decrease temporarily. The natural circulation is, however, not strong enough to cool the spent fuel pool in the long term. Therefore, after a short temperature decrease the fuel assemblies start to heat up again.

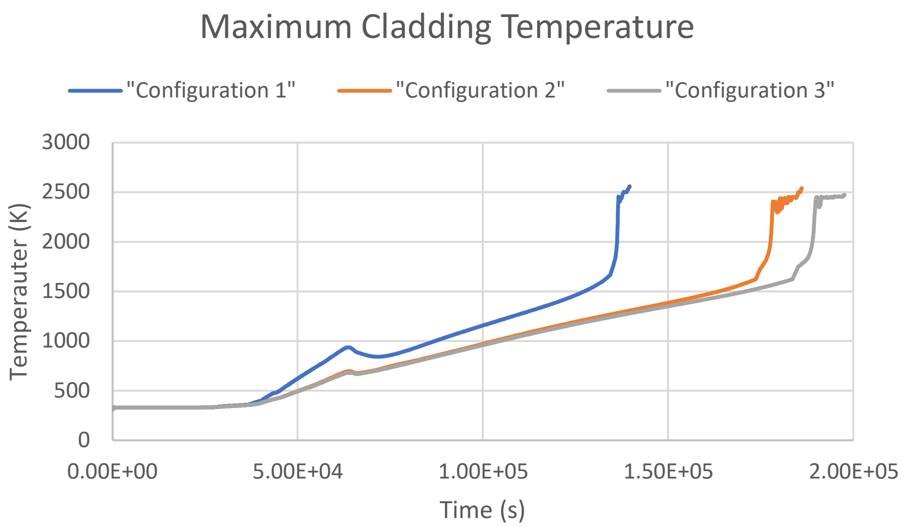

FIG. 6. Evolution of maximum cladding temperatures in different configurations.

The slow but continuous temperature increase lasts until the temperature of the hottest zone reaches the breakpoint, where oxidation processes start to dominate. There are, however, significant time differences when this point is reached.

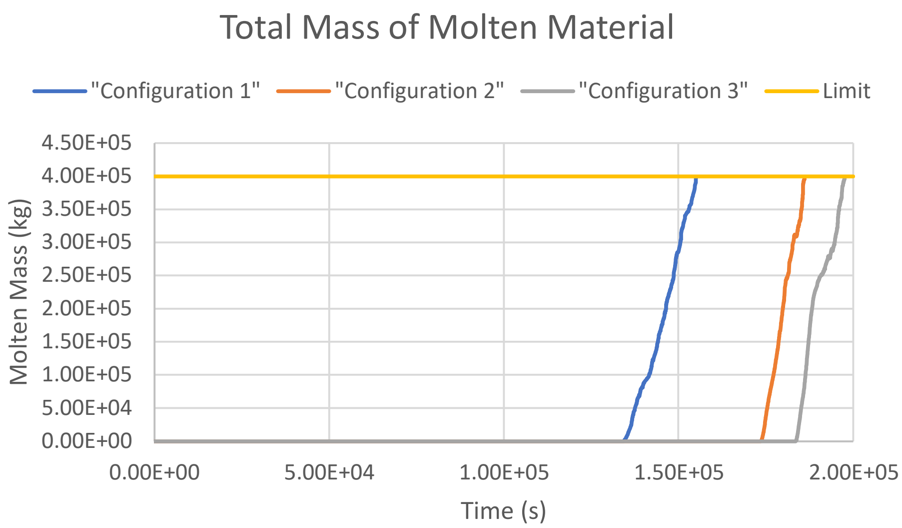

FIG. 7. Evolution of molten mass in different configurations.

Fig. 7 shows the evolution of molten masses in the spent fuel pool. At around the start of oxidation the canister walls melt, then after an excessive heat generation due to the oxidation, also the cladding and the fuel start to melt.

As it was expected, the earliest melt formation is in ‘Configuration 1’ and the first melt formation occurs in the node 6 at around 135 000 seconds. In ‘Configuration 1’ that node has one of the highest powers and its neighbours have also relatively high decay power. Therefore, it cannot be cooled effectively by thermal radiation, which leads to an early melt formation. In ‘Configuration 2’ all the nodes have the same decay power, but node 6 is the only node that has no cold neighbours. Therefore, in this configuration also the first melt formation occurs in the node 6. However, approximately 40 000 seconds later than in ‘Configuration 1’. In ‘Configuration 3’ the first melt occurs later, at around 184 000 seconds in the node 16. In ‘Configuration 3’ this node has the least cold neighbours (similarly to node 9, which melts soon after node 16).

The main events of the accident scenario are summarized for the different configurations in Table 2.

TABLE 2. SUMMARY OF MAIN EVENTS IN DIFFERENT CONFIGURATIONS

	Configuration 1	Configuration 2	Configuration 3
Water level at the top of fuel assemblies	30 000 s	30 000 s	30 000 s
Water level at the bottom of fuel assemblies	64 000 s	64 000 s	64 000 s
Excessive oxidation start	135 000 s	175 000 s	185 000 s
First melt occurrence	135 000 s	175 000 s	185 000 s
First node to melt	6	6	16 / 9
50% melt mass limit reached	156 000 s	186 000 s	198 000 s
Time between first melt occurrence and 50% melt mass limit reached	22 000 s	12 000 s	14 000 s

The simulations showed that spent fuel pool configurations can have a large influence on the accident evolution. Distributing spent fuel assemblies uniformly in a spent fuel pool can provide significant amount of extra time to prevent fuel degradation. If melt starts to form in a spent fuel pool with uniformly distributed fuel assemblies, then the rate of melt formation is faster. The reason for this is that due to the more or less equal power distribution the temperature of the stored fuel is similar.

The simulations were performed using the newly implemented external numerical toolkit of ATHLET-CD [7]. The numerical toolkit “ATHLET-NuT” could accelerate the calculations by approximately 30%. Simulating the scenarios for the different configurations took about 2.5 days each, on a normal PC, with four cores. Dividing the spent fuel pool into 24 core nodes and defining cross connection between all nodes is maybe more detailed than it is needed for plant applications. Using this detailed subdivision of the spent fuel pool could however demonstrate the applicability of the new nodalization method in spent fuel pool configurations and show possible future applications. Also, the simulations delivered expected results qualitatively, therefore, the study could have been also used for verification purposes. [5].

5. FUTURE TASKS

The verification calculations performed using the previously described flexible nodalization show promising results (one of them is shown in this paper), but an in-depth validation of the newly implemented feature is still missing. Unfortunately, the lack of experiments with local effects make the validation work difficult.

As mentioned before, the horizontal relocation of melt in a flexibly defined nodalization is still under development, so far accidents assuming only axial melt relocation can be simulated.

Melt relocation from the bottom of the fuel assemblies to the bottom of the spent fuel pool is not possible yet, because if melt relocation outwards of the core is modelled, it is currently automatically relocated to the lower plenum of the reactor with hemispherical or elliptical bottom.

Heat radiation to the environment is currently taken into account via a user-defined temperature. In the future ATHLET-object and/or COCOSYS objects should be defined that emit/absorb heat radiation.

Analyzes of the effect of the nodalization on the fission product release for the containment source term.

Currently, the user has to define explicitly the coordinates of the core nodes, as well as the initial connections of all sides. This is currently very error prone, therefore, a simplified input method has to be developed. The flexible nodalization allows to gather 3D information about the spent fuel pool, however, the graphical tools for the representation of the accident evolution cannot depict this information. New graphical tools have to be developed.

Experience has to be gathered on how to create an ideal nodalization of a spent fuel pool, because results of the verification tests show large nodalization dependency.

CONCLUSIONS

After the accident in the Fukushima Daiichi nuclear power plant awareness rose regarding a possible meltdown scenario in a spent fuel pool. The currently widely used code system to assess the safety of nuclear power plants are only partly usable for spent fuel pool configurations. These limitations were identified for ATHLET-CD/AC^2. A new option was implemented into the developer version of ATHLET-CD which allows a flexible node definition in the core region. This eliminates/reduces the effects of the limitations mainly caused by the hardcoded “ring-like” nodalization of the currently released version of ATHLET-CD. A series of verification calculations was shown at the current stage of the development, which delivered interesting and plausible results. However, there are still some model improvements to be made before the accidents in a spent fuel pool can be addressed realistically. An in-depth validation of the developed new features has to be performed.

REFERENCES

[1] AUSTREGESILO, H., ET AL., ATHLET-CD User's Manual, July 2016, GRS-P-4/VOL. 1.

[2] CHATELARD, P., ET AL., ASTEC V2 severe accident integral code main features, current V2.0 modeling status, perspectives, Nuclear Engineering and Design **272** (2014) 119–135.

[3] HUMPHRIES, L.L., ET AL., MELCOR Computer Code Manuals Vol. 1: Primer and Users' Guide Version 2.2.9541 2017, January 2017.

[4] LOVASZ L., ET AL., "New Approach for Severe Accident Simulations in Spent Fuel Pools Using the Code System AC^2", Presented at 12^{th} International Topical Meeting on Nuclear Reactor Thermal-Hydraulics, Operation and Safety (NUTHOS-12), Qingdao, China, October 14–18 (2018).

[5] LOVASZ L. ET. AL., Investigation of the Effect of the Spent Fuel Pool Configuration on Fuel Degradation, Proc. Mtng ERMSAR-2019, Prague, Czech Republic, 18–20.03.2019, AF Power Agency, Prague (2019).

[6] JÄCKEL, B., ET AL., D6.8.4 Report on the benchmark (including criticality risk assessment), Spent Fuel Pool behaviour in loss of cooling or loss of coolant accidents (AIR-SFP), NUGENIA-PLUS Project, European Commission 7th Framework Programme, Grant Agreement No. 604965, V1/30092016, September 2016.

[7] ORGANISATION FOR ECONOMIC COOPERATION AND DEVELOPMENT NUCLEAR ENERGY AGENCY, Status Report on Spent Fuel Pools under Loss-of-Cooling and Loss-of-Coolant Accident Conditions, Final Report, Nuclear Safety NEA/CSNI/R(2015)2,OECD-NEA, Paris (2015).

LOSS OFF COOLANT AND LOSS OF COOLING ACCIDENT RESEARCH: THE DENOPI PROJECT

C. MARQUIE, N. TREGOURES, J. MARTIN, G. BRILLANT, C. DURIEZ
Institut de Radioprotection et de Sûreté Nucléaire (IRSN),
Saint-Paul-lez-Durance
France

1. CONTEXT

Since the Fukushima Daiichi accident, increased attention has been paid to the vulnerability of the Spent Fuel Pools (SFP). This vulnerability is a concern for SFPs safety because generally the fuel clad is the sole barrier against fission product release in case of dewatering. Also, the potential source term is several times the one present in the reactor vessel. For example, French SFPs can harbour up to 2.5 times the number of fuel assemblies present in the core of a 900 MW(e) reactor.

The IAEA "International Experts Meeting on Strengthening Research and Development Effectiveness in the Light of the Accident at the Fukushima Daiichi Nuclear Power Plant" [1], held in Vienna in 2015, concluded that one priority is to investigate SFP loss of coolant and loss of cooling accidents. The OECD/NEA edited a Status Report on Spent Fuel Pools under Loss-of-Cooling and Loss-of-Coolant Accident Conditions [2] and afterward gathered and expert group to establish a Phenomena Identification and Ranking Table on Spent Fuel Pools under Loss-of-Cooling and Loss-of-Coolant Accident Conditions [3]. Several R&D programs dealing with SFP accidents were carried out. This PIRT concluded to the needs of further R&D concerning SFP accidental conditions and prioritized the topics to be investigated.

After the Fukushima Daiichi accident, the French government decided to encourage research efforts aiming at safety improvement of nuclear facilities in the light of this accident by a specific call for projects under the aegis of the National Research Agency (ANR). Within this context, IRSN proposed the DENOPI Project for that call and the project has been accepted.

2. OBJECTIVES OF THE DENOPI PROJECT

The DENOPI project aims at improving the knowledge of phenomena involved in SFP accident prior to the severe accident phase (clad failure), to evaluate mitigation by water spraying and to develop and validate thermohydraulic models. The DENOPI project is organized around three axes that investigate three consecutive phases of the accident and three different scale of interest. In axis 1 is devoted to study phenomena at pool-scale before uncovering of the fuel assemblies is studied. Axis 2 is devoted to the study of phenomena at assembly scale before fuel degradation and finally axis 3 is devoted to the oxidation of the cladding. Work is done by IRSN and its academic partners: ARMINES (Ecole des Mines de Saint-Etienne), LEPMI (CNRS Grenoble), LVEEM (University of Auvergne), and PROMES (CNRS Perpignan).

3. AXIS 1: POOL SCALE PHENOMENA

3.1. Objectives

In case of loss-of-cooling, the pool water is gradually heated up and natural convection is developing between the FAs (heat source) placed at the bottom of the pool and the free surface. Despite its relative apparent simplicity, natural convection in the pool is complex.

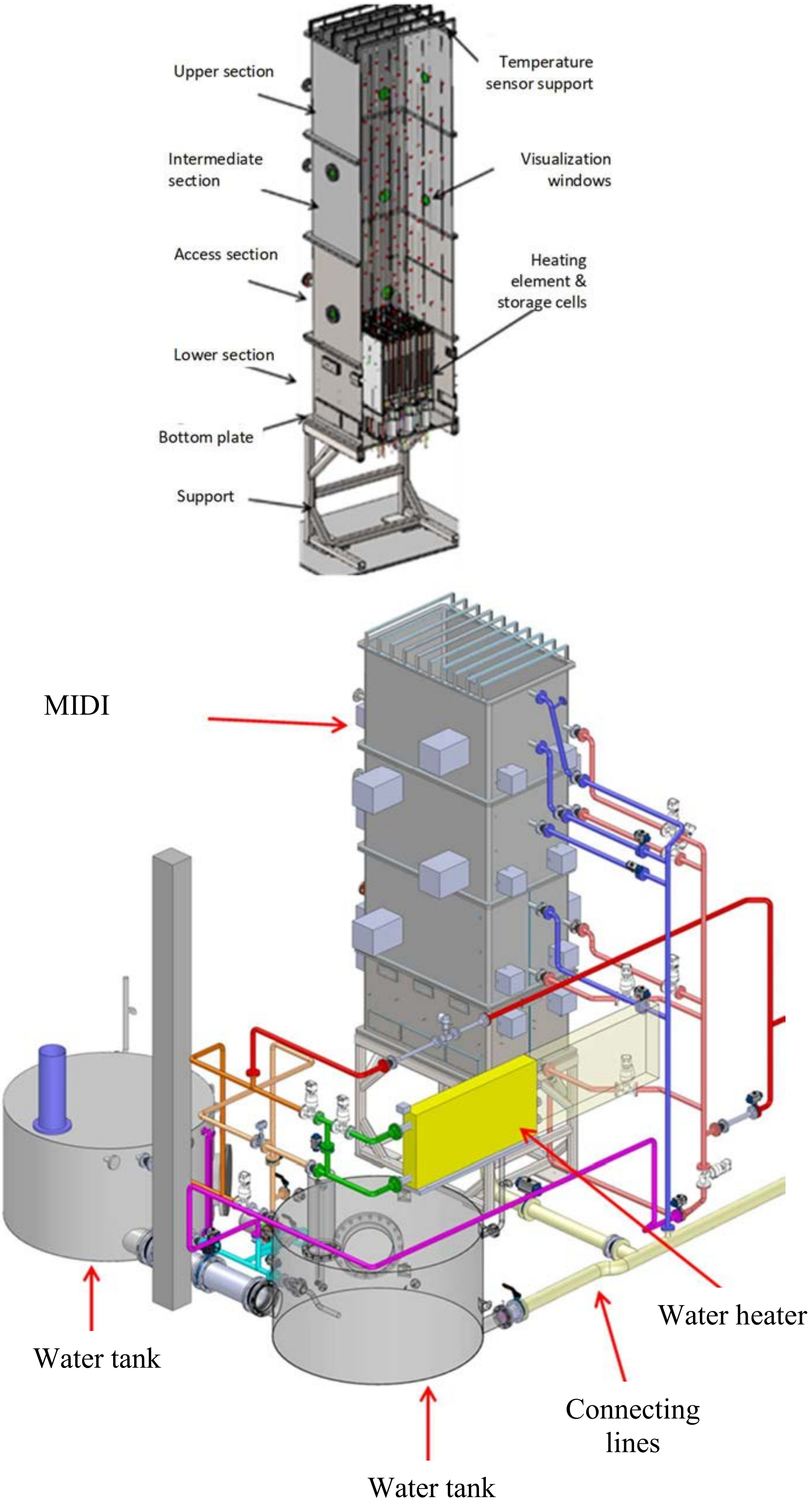

FIG. 1. MIDI facility – top: view of MIDI pool – bottom: general overview.

First, the overall flow structure is function of the distribution of decay power in the pool. The flow is rising more vigorously above the hot fuel assemblies than over the colder ones. Vaporization can occur near the surface by evaporation, in the upper volume as the fluid temperature overpasses saturation temperature or in the storage cells (nucleate boiling). Very few data are available concerning diphasic natural convection at such a large scale and low pressure. Natural convection in a spent fuel pool is poorly known and is mainly evaluated on the so-called expert judgment. The objective of DENOPI axis 1 is to validate CFD models or system codes for typical SFP conditions based on the results of experimentation performed in the MIDI facility.

3.2. The MIDI facility

The MIDI facility is a scaled-down SFP pool with electrically heated assemblies. The scaling of the MIDI facility was based on similitude-like approach and simplified calculations of accidental scenarios.

The chosen compromise between better representativeness and the overall cost of the facility was a one-third scale on the vertical axis and a one-sixth scale on the other axes. Thus, based on the design of a French 900 MW(e) NPP SFP, the MIDI facility is a 12 m^3 pool with 21 heating assemblies (each constituted of 3 × 3 rods) placed in their storage cells. The power of each assembly can be independently controlled with an overall limitation to 300 kW, thus allowing to simulate different loading patterns. The MIDI facility can simulate loss of cooling conditions and retrieval of cooling system.

In the water volume above the assemblies, the instrumentation is composed of temperature sensors, pressures sensors and water level sensors. Windows are placed on MIDI walls in order to visualize the steam bubbles. In each cell, measurements include water and wall temperatures, inlet flowrate and pressures. The void fraction at cell's outlet will be determine with abacus function of flowrate, pressure (water level) and assembly power, established in a specific device. The MIDI facility is under construction and experimentation is planned in 2021.

4. AXIS 2: ASSEMBLY SCALE PHENOMENA

4.1. Objectives

The behaviour of fuel assemblies fully uncovered was studied at Sandia National Laboratories in the framework of the OECD-NEA SFP project [4]. Experiments included separate and integral effect tests and investigated zirconium fire propagation between adjacent assemblies. On the other hand, the behaviour of spent fuel pools with FAs fully or partly covered by water is relatively unknown despite the challenges associated. Particularly, the efficiency of spray water cooling in such conditions is still a pending question, that was identified as a priority research need by the OECD PIRT [3].

Within the DENOPI project, the objective is to study the efficiency of water spray cooling of a fuel assembly partially or totally uncovered inside its storage cell. To achieve this goal, a progressive multi-steps approach was chosen.

In the first step, water spray penetration and repartition in the assembly is studied under isothermal conditions (room temperature) with an ascending air flow simulating the vaporization of water, in the MEDEA facility. In the second step, the air flow is replaced by a controlled steam flow also in the MEDEA facility. In the last step, the steam is generated by an electrically heated assembly and cooling is directly assessed in the ASPIC facility.

4.2. The MEDEA facility

The MEDEA facility represents the top 1 m of a 17 × 17 PWR fuel assembly in its storage cell at full scale, with prototypical grids and top nozzle. The fuel rods are simulated by unheated steel rods. At the bottom of the assembly, it is possible to inject an air or steam flow. At the top, a modular spray system is placed. It is possible to change the shape of spray, droplet size and the position of the spray. Also it is possible to change the cross-trough section of the top nozzle to simulate different types of nozzles or partial flow blockage at the top of the assembly.

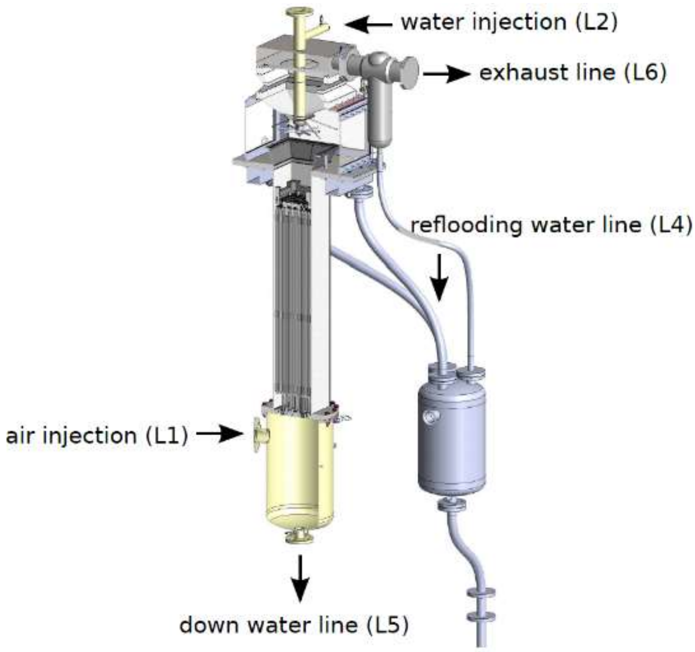

FIG. 2. MEDEA test section.

The experimental parameters are the injection flowrate (air or steam), the temperature of the injected steam up to 200°C (air is injected at room temperature), the top nozzle geometry, the spray topology features, the spray flow and the spray temperature (up to 100°C). The instrumentation allows measuring of injection and spray flowrate and temperature, temperatures inside the test section, the flow of water collected at the bottom of the assembly, water flowrate ejected at the top of the test section, flowrate in the exhaust pipe, and pressures in the test section. For air experiments it is also possible to collect the water dripping along each rod.

4.3. Main learnings from MEDEA experimentation

With air tests, it was first confirmed, as expected from literature correlations, that the risk of CCFL (Counter Current Flow Limitation) is excluded under SFP accidental conditions. However, it has been observed that this conclusion is no longer true when debris are present at the top of the fuel assembly.

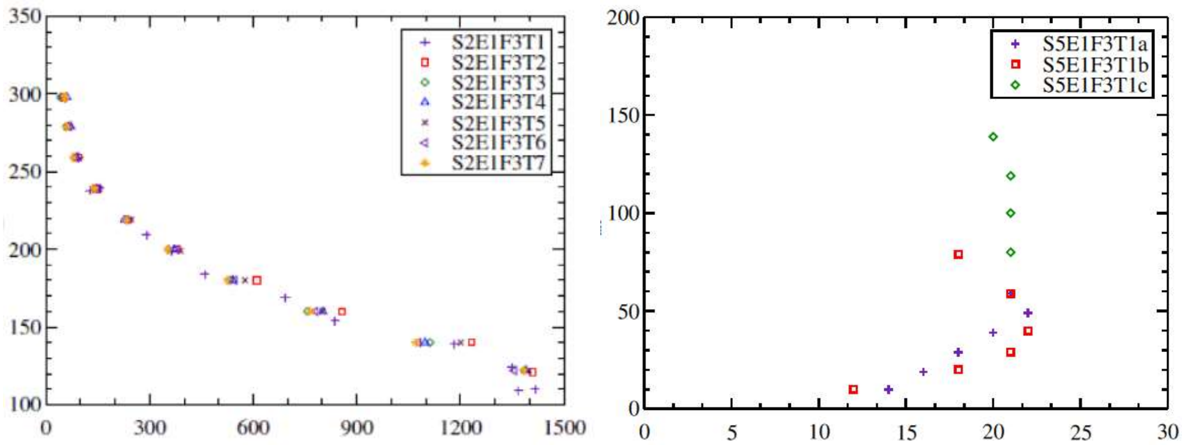

FIG. 3. Flooding curve without debris (left) and with debris (right) showing CCFL occurrence in the MEDEA experiments.

Moreover, our tests evidence chaotic behaviour of water flow inside the fuel assembly both in time and space: watered and un-watered areas variate randomly and are not reproducible between two tests under the same conditions. Nevertheless cooling by spray is quite efficient with quick cooling by wetting or slow cooling by conduction/convection (steam). Some areas can encounter new dewatering during the experiment.

The water repartition inside the bundle showed, as expected, a preferential path at the outer of the assembly. Interpretation of tests are still going on.

4.4. The ASPIC facility

The ASPIC facility represents a full-scale 17 × 17 PWR assembly with electrically heated rods to simulate the residual power. As in MEDEA, a spray system is placed at the top of the assembly.

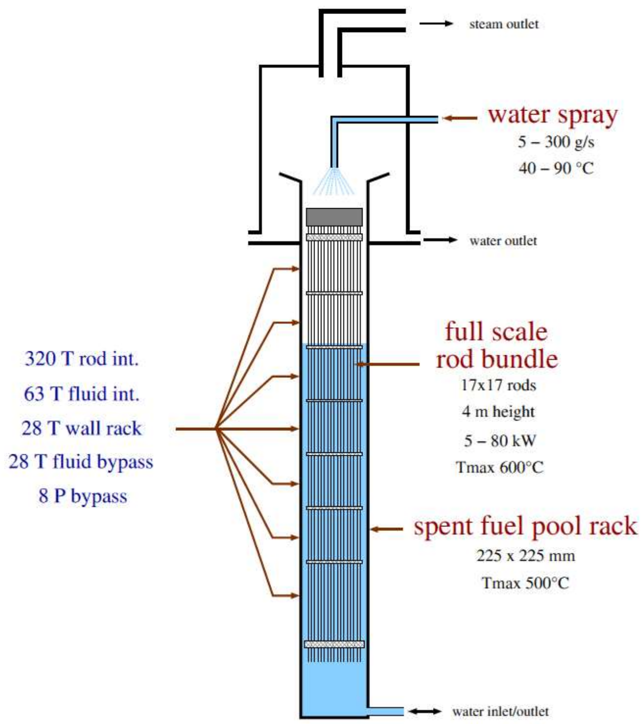

FIG. 4. Schematic view of ASPIC facility.

The test section is connected to a water tank, which allows for different boundary conditions: fixed water level, ‘natural evolution’ resulting from the balance between vaporization and spray, simulation of a leakage, etc. The tank has been designed to be representative of the inertia due to water outside the storage cell. It is possible to simulate no, partial or total uncovering of the assembly.

ASPIC instrumentation is composed of thermocouples (rods, fluid, walls…), pressure sensors (to measure water level and average void fraction), flowmeters etc. The main experimental parameters are the heating power, the boundary conditions, triggering parameter (e.g. when clad temperature reaches a predetermined value) for spray, spray flow and temperature etc. The ASPIC facility is currently under fabrication. Start of experimentation is planned in 2020.

5. AXIS 3: CLADDING SCALE PHENOMENA

5.1. Objectives

After assembly uncovering, from about 700–800°C, the oxidation kinetic of the zirconium alloy cladding material becomes significant and heat generated by zirconium oxidation can contribute noticeably to the overall heating power. Hydrogen production might also be an issue, as the result of the contribution of the oxidation reaction ($2\ H_2O + Zr \rightarrow ZrO_2 + 2H_2$): part of the hydrogen generated is integrated in the cladding (zirconium hydrides) and part is released in the atmosphere.

The objective of DENOPI axis 3 is to determine kinetics laws of Zircaloy 4 (Zy-4) alloy under mixed air-steam atmosphere, to understand the protective effect (or its absence) of the pre-existent oxide layer formed during in-reactor irradiation (called pre-oxide hereafter). Axis 3 studies were realized in collaboration with Ecole des Mines de Saint-Etienne (ARMINES), the University of Auvergne (LVEEM) and Grenoble University (LEPMI).

5.2. Experimentation within axis 3

The first stage of experimentation was the preparation of Zy-4 specimens, i.e. the pre-oxidation of the specimen and the characterization of this pre-oxide. Several protocols were compared to autoclave oxidation, supposedly producing the closest to real in-reactor oxide. Oxidation under steam conditions at 450°C was found as a best compromise. Several types of specimens were tested: plates, tubes and balls.

FIG. 5. Specimen for axis experiments (before high temperature oxidation).

Then high temperature oxidation (i.e. the oxidation during the accident) was performed with different apparatuses:

- Inside a thermogravimetric (TGA) apparatus under controlled atmosphere (partial pressure of O_2, N_2 and H_2O);
- Inside an in-situ DRX apparatus in order to measure stress evolution inside the oxide layer.

To understand the contribution of the pre-oxide, the oxygen and steam oxidation with ^{18}O was correlated with Raman spectrometry [5].

5.3. Main learnings from axis 3 experimentation [6]

DENOPI axis 3 experiments evidenced the importance of specimen preparation. At the same pre-oxide thickness, behaviour strongly changes between two different protocols. Oxidation under steam should be favoured as more representative of real pre-oxide layer. The role of Nitrogen in the oxidation process is now well understood. N_2 diffuses "quickly" through the pre-oxide layer and forms zirconium nitride at the interface metal/oxide. Experiments demonstrated the contribution of steam in the cladding oxidation with incorporation of hydrogen in the cladding and releasing in the atmosphere prior to recombination with the oxygen. But the main outcomes concern the effect of defects or singularities of the pre-oxide. First, on tube or plate specimens, oxidation clearly begins from the edges. To discard experiment artefact, tests were performed with Zy-4 spherical beads to eliminate by definition the edges. The protective effect is then linked to the presence of pre-existing defects. It is expected that in real fuel rods, such defects might be pre-existing or created by clad swelling due to heat-up.

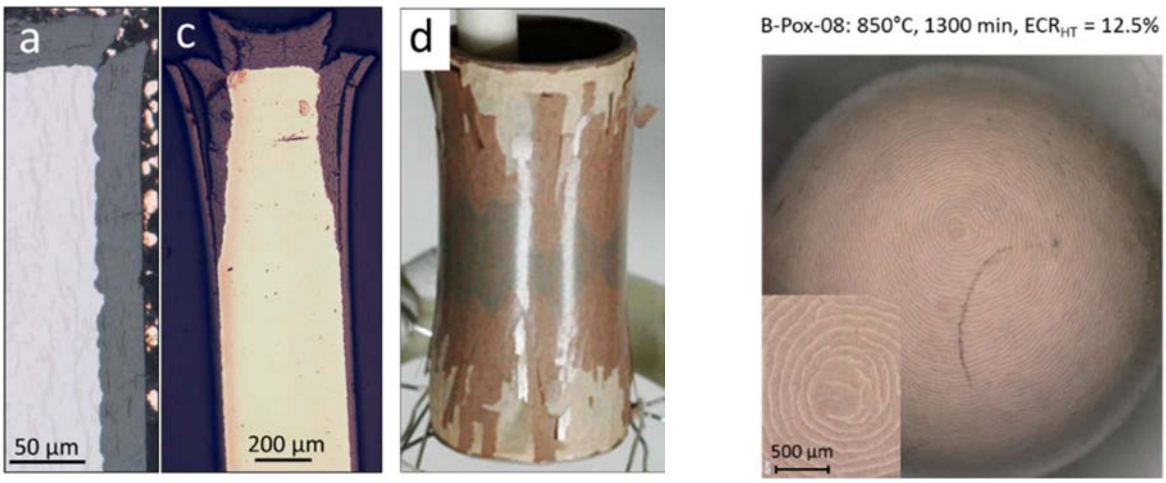

FIG. 6. Cuts and pictures of oxidized samples a, c and d: tube sample before oxidation (a), after high temperature oxidation (cut in b and overview in c) right: scale of oxide on Zy-4 bead sample at the onset of pre-oxide breakdown.

Finally, a kinetic model taking into account the influence of the partial pressure of oxygen and steam has been developed for implementation in the ASTEC code developed by IRSN [7].

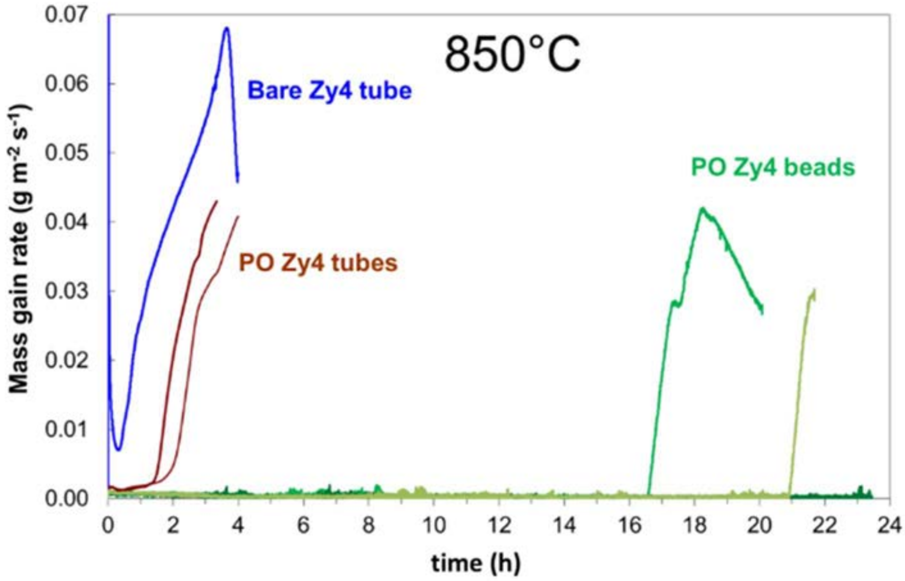

FIG. 7. Oxidation tests (TGA) of bare Zry tube, pre-oxidized Zy-4 tubes and pre-oxidized Zry-4 beads.

CONCLUSION AND PERSPECTIVES

Following the accident of Fukushima Daiichi, IRSN launched the DENOPI project, devoted to the study of SFP accidents 4. The project is fully or partly supported by ANR, US-NRC, EDF and Bel-V. The project is organized in three axes dealing with three scales of interest: pool-scale, assembly-scale and clad-scale. Similitude-like studies allowed to define the MIDI facility scaling down of a spent fuel pool. The test device is currently under construction. Experimentation is expected in 2021. Within axis 2, devoted to water spray assessment at assembly scale, two facilities are used: MEDEA and ASPIC. Experimentation with MEDEA facility is achieved. It allowed to characterize water repartition in a partially uncovered unheated assembly. The ASPIC facility is under fabrication and experimentation would start second part of 2020. Finally testing within axis 3 of Zy-4 oxidation under mixed air-steam atmosphere is finished. It allowed to determine kinetics laws and evidenced the crucial effect of defects of the pre-oxide layer (pre-existing or created during the accident).

The overall project is expected to be achieved by the end of 2021. The OECD/NEA PIRT report listed and prioritized R&D needs concerning SFP accident scenarios that go well beyond the DENOPI Project. In this respect, IRSN is considering a follow-up program to be proposed to the international community. Let's finally note that the issue of radioactive release from accidental situation in SFP, and safety measures to mitigate the consequences of such release, was not in the scope of the PIRT. IRSN is going to address this issue in the frame of a European project starting in September 2019, where the efficiency of innovative mitigation measure will be evaluated.

REFERENCES

[1] INTERNATIONAL ATOMIC ENERGY AGENCY, IAEA Report on Strengthening Research and Development Effectiveness in the Light of the Accident at the Fukushima Daiichi Nuclear Power Plant, IAEA, Vienna (2015).
[2] ORGANISATION FOR ECONOMIC CO-OPERATION AND DEVELOPMENT NUCLEAR ENERGY AGENCY, Status report on spent fuel pools under loss-of-cooling

and loss-of-coolant accident conditions, Report NEA/CSNI/R(2015)2, OECD-NEA, Paris (2015).
https://www.oecd-nea.org/nsd/docs/2015/csni-r2015-2.pdf
[3] [2] ORGANISATION FOR ECONOMIC CO-OPERATION AND DEVELOPMENT NUCLEAR ENERGY AGENCY, Phenomena Identification and Ranking Table. R&D Priorities for Loos-of-Cooling and Loss-of-Coolant Accident in Spent Nuclear Fuel Pools, Report NEA No. 7443, OECD-NEA, Paris (2015). https://www.oecd-nea.org/nsd/docs/2017/csni-r2017-18.pdf
[4] DURBIN. S., LINDGREN, E., Sandia Fuel Project Phase II: Pre-Ignition and Ignition Testing of a Commercial 17×17 Pressurized Water Reactor Spent Fuel Assembly under Complete Loss of Coolant Accident Conditions, Sandia report, SAND2013-2537, SNL, Albuquerque, NM (2013).
[5] KASPERSKI, A., DURIEZ, C., MERMOUX, M., Combined Raman imaging and 18O tracer analysis for the study of Zircaloy-4 high temperature oxidation in spent fuel pool accident, Selected technical papers from 18th International Symposium on Zirconium in Nuclear Industry (COMSTOCK, R.J., MOTTA, A.T., Eds), ASTM, West Conshohocken, PA (2018).
[6] DURIEZ, C ET AL., Zircaloy-4 high temperature oxidation in atmospheres representative of SFP-LOCA: Investigation of the influence of a low temperature pre-oxidation scale, J. Nucl. Mater. **513** (2019) 152–174.
[7] CHATELARD, P., ET AL, ASTEC V2 severe accident integral code main features, current V2.0 modelling status, perspectives, Nucl. Eng. Des. **272** (2014) 119–135.

PHENOMENA IDENTIFICATION AND RANKING TABLE: R&D PRIORITIES FOR LOSS-OF-COOLING AND LOSS-OF-COOLANT ACCIDENTS IN SPENT NUCLEAR FUEL POOLS

N. TRÉGOURÈS
Institut de Radioprotection et de Sureté Nucléaire (IRSN),
France
on behalf of the OECD/NEA/CSNI

1. INTRODUCTION

Spent fuel pools (SFPs) are large accident hardened structures that are used to temporarily store irradiated nuclear fuel. Due to the robustness of the structures, severe accidents involving SFPs are generally regarded as highly improbable events. The safety and security of spent fuel pools are continuously re-assessed as new information becomes available or the operating conditions of the plants or pools change. For example, the terrorist attacks in the USA on September 11, 2001, prompted studies on the vulnerability of spent fuel storage facilities to potential terrorist attacks in many countries [1]. More recently, the Fukushima Daiichi nuclear accident [2] that followed after the Tohoku earthquake on March 11, 2011, has renewed international interest in the safety of spent nuclear fuel stored in SFPs under prolonged loss-of-cooling conditions [3], although the SFPs and the fuel stored in the pools remained safe during the accident.

1.1. Context

Following the 2011 accident at the Fukushima Daiichi Nuclear Power Station, the Nuclear Energy Agency (NEA) Committee on the Safety of Nuclear Installations (CSNI) of the Organisation for Economic Co-operation and Development (OECD) launched several activities to help contribute to the post-Fukushima accident decision making process. Among other things, a status report on spent fuel pools (SFPs) under loss-of-cooling and loss-of-coolant accident conditions was produced in order to summarize the current state of knowledge about such accidents [3]. One of the recommendations given in the report was to produce a Phenomena Identification and Ranking Table (PIRT) in order to systematically identify phenomena that are of both high importance and high uncertainty, and thus of primary interest for further studies. The CSNI endorsed the recommendation and a PIRT was produced from early 2016 to mid-2017 by an international panel of experts consisting of members of the OECD NEA CSNI Working Group on Fuel Safety (WGFS) and Working Group on Analysis and Management of Accidents (WGAMA) as well as invited experts from industry, research organizations and nuclear regulatory bodies. Altogether 23 organizations from 15 countries were represented in the panel. The resulting “Phenomena Identification and Ranking Table (PIRT) on Spent Fuel Pools under Loss-of-Cooling and Loss-of-Coolant Accident Conditions” report [4] is summarized in the present paper.

1.2. Objective, scope, procedure

The main objective of the PIRT is to identify research and development priorities related to loss-of-cooling and loss-of-coolant accidents in spent fuel pools. This is done by applying a PIRT process methodology [5] to identify phenomena that are both of high safety importance and of high uncertainty and therefore deserve further comprehensive analytical and/or experimental studies.

The PIRT process is applied to at-reactor SFPs. The study is generic with regard to reactor and fuel design, it covers boiling water reactor (BWR), pressurized water reactor (PWR), Russian-type pressurized water reactor (VVER) and Canada Deuterium Uranium (CANDU) reactor power plants. Two general types of accidents are studied: a loss-of-coolant accident with fast drainage of the pool water, and a loss-of-cooling accident with slow uncovery of the spent fuel by gradual water evaporation and boil-off. Three separate sub-PIRTs are developed for three consecutive phases of the considered accident scenarios: the pre-uncovery phase, the uncovery phase, and the fuel damage phase. This temporal subdivision is made, since the three phases can be dominated by different phenomena.

The study is restricted to phenomena that occur in the spent fuel pool. Phenomena occurring predominantly outside the SFP, e.g. heat and mass transfer in the pool building, are beyond the scope of the study. However, these phenomena are discussed in terms of boundary conditions to the SFP, when they are deemed to be important to the in-pool accident progression.

2. EXPECTED ACCIDENT PROGRESSION AND PHENOMENA

There are two principal categories of accidents that may lead to loss of adequate cooling of the spent fuel in an SFP: malfunction of the pool cooling system (loss-of-cooling accident) and sudden loss of the pool water inventory by leaking (loss-of-coolant accident) [2]. The two types of accidents are similar with regard to involved phenomena, but the progression may be significantly faster for the loss-of-coolant accidents. This is indicated in Figure 1, which schematically illustrates the phenomenology of SFP accidents. Unmitigated accidents are expected to evolve from a single dominant phenomenon in the early stages to a progressively more complex situation with several interdependent phenomena.

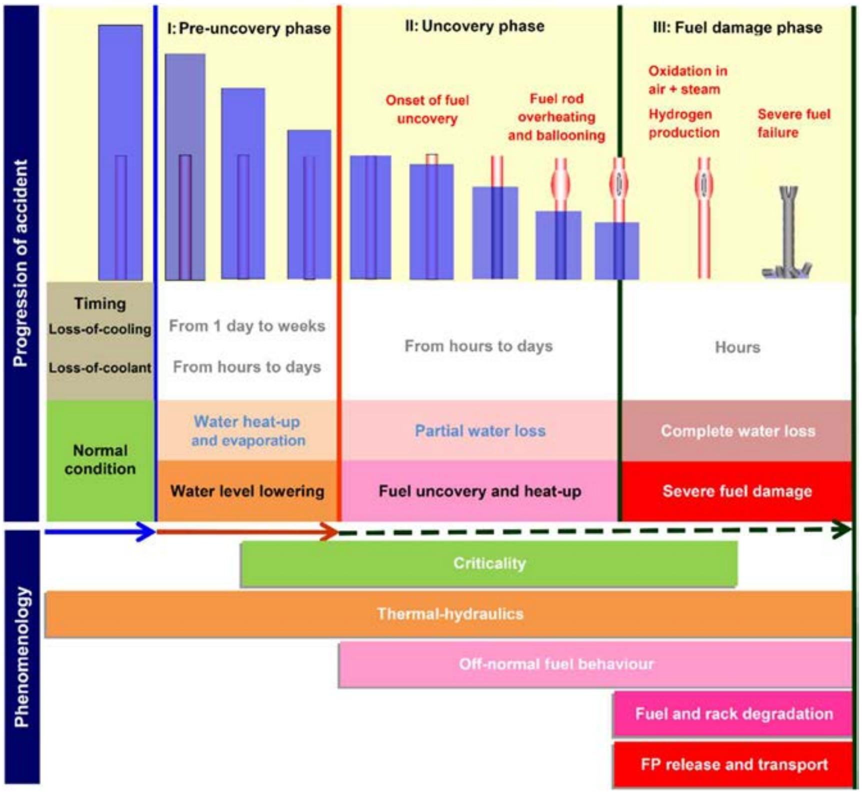

FIG. 1. Temporal phases and phenomenology of SFP loss-of-cooling/coolant accidents.

2.1. Pre-uncovery phase (Phase I)

The first phase of the accident (the pre-uncovery phase) is dominated by thermal-hydraulic phenomena. Safety issues concern increased release of radiolytic hydrogen, tritium and radioactive contaminants from the pool water as it heats up, and the strong radiation field that would arise if the pool water level drops to less than about half a meter above the spent fuel assemblies (FAs). Furthermore, the increasing water temperature and decreasing water level in the SFP could make it impossible to recover cooling of the SFP by restarting the normal cooling system, e.g. because of pump cavitation or loss of suction to the intake strainers in the upper part of the pool.

2.2. Uncovery phase (Phase II)

As the accident enters into the second phase, the spent fuel assemblies start to be uncovered. The elevated temperature experienced by the fuel during the uncovery phase will accelerate the exothermic oxidation of the cladding and its creep deformation that reduces the cross-sectional area for coolant flow through the fuel assembly. For high burnup light water reactor (LWR) fuel, fine fragments of the fuel pellets can relocate axially downward within the distending cladding tube, therefore increasing the risk for cladding failure and the amount of ejected fuel material. When the spent FAs are completely uncovered, natural convection by air and radiation are the dominating cooling mechanisms. Analyses suggest that a large-scale flow pattern develops inside the pool building.

2.3. Fuel damage phase (Phase III)

During the fuel damage phase of the accident, the phenomena are expected to be similar to those in reactor loss-of-coolant accidents, but since the decay heat is much lower, damage phenomena occurring at relatively low temperature (<1200 K) become comparatively more important. Moreover, fuel in an SFP accident may be exposed to air, which speeds up UO_2 fuel degradation and volatilization of fission products by oxidation, and may increase the release. As damage progresses in the upper part of the fuel assembly, debris may relocate downward and obstruct the axial flow through the fuel assembly. If melting occurs, the molten material will flow downwards and solidify in cooler regions of the fuel assembly. If water remains at the bottom of the pool, hot relocated material may cause a strong steam production and possibly energetic interaction if it drops into water. Uncertainty exists whether the specific decay heat of spent fuel would be sufficient to cause degradation of the concrete floor in the pool. If degradation occurs, the phenomena would be similar to those known for molten corium concrete interaction.

3. METHODOLOGY

The step-wise procedure applied in the study follows the generally accepted methodology for PIRT development [5]. During the application of the different steps, the international panel of experts have defined the SFP designs (a generic at-reactor SFP of rectangular shape and a length/width/depth of about 12/8/11 m), the spent fuel inventories (two postulated inventories of spent fuel, representing a worst case and a typical heat load of the pool, respectively) and two general accident scenarios that may lead to loss of adequate cooling of the spent fuel in a SFP: sudden loss of pool water inventory (loss-of-coolant accident) and failure of the pool cooling system (loss-of-cooling accident). Since the relative importance of phenomena changes with time as the accident progresses, accident scenarios were partitioned into three temporal phases: the pre-uncovery phase, the uncovery phase, and the fuel damage phase leading to three separate sub-PIRTs.

The international panel of experts responsible for the PIRT consisted of members of the OECD NEA CSNI WGFS, WGAMA as well as invited experts from industry, research organizations and nuclear regulatory bodies. Table 1 shows the composition of the panel.

TABLE 1. ORGANIZATIONS REPRESENTED IN THE INTERNATIONAL PANEL OF EXPERTS

Country/organization	Participating organizations
Belgium	BEL V
Canada	CNL, CNSC
Czech Republic	UJV
European Commission	JRC
France	CEA, EDF, IRSN
Germany	GRS
Hungary	MTA-EK
Italy	NINE
Japan	IAE, JAEA, MNF, S/NRA/R
Republic of Korea	KAERI
Russian Federation	NRCKI
Slovenia	JSI
Spain	CIEMAT, CSN
Sweden	QT
Switzerland	PSI
USA	U.S. NRC

All panellists were asked to identify phenomena that they deemed relevant to each of the three temporal phases of the accident, and propose them for subsequent ranking and inclusion in the three sub-PIRTs. To ensure completeness, this was done in a brain-storming manner and no screening or ranking of the suggested phenomena were attempted at this stage. The study was restricted to phenomena that occur in the spent fuel pool.

Evaluation criteria for the ranking were selected with the aim to address safety issues, while at the same time being generic with regard to fuel and SFP design. The expert panel decided to use the following evaluation criteria: source term (release of radionuclides and hydrogen from the SFP), fuel damage (loss of cladding integrity, loss of geometry, melting), accident progression (timing of events that lead to a new phase of the accident) and water density (important primarily to the subcriticality margin in the SFP, but also to the operation of SFP cooling systems). In the ranking process, three-level scales were used with regard to the importance level (High, Medium, Low importance), see Table 2, and the knowledge level (Adequate, Some, None) of each phenomenon, see Table 3. The knowledge level was assessed with regard to availability of both data and models.

TABLE 2. THREE-LEVEL SCALE USED FOR PHENOMENA IMPORTANCE RANKING

Rank	Weight	Definition	Implication
High (H)	1.0	The phenomenon has a dominant impact on any of the evaluation criteria.	The phenomenon should be explicitly considered in experimental programmes and modelled with high accuracy in computational tools.
Medium (M)	0.5	The phenomenon has only a moderate impact on the evaluation criteria.	Experimental studies and analytical modelling are required, but the scope and accuracy may be compromised.
Low (L)	0.0	The phenomenon has small or no impact on the evaluation criteria.	The phenomenon should be exhibited experimentally and considered in computational tools. However, almost any model will be sufficient.

TABLE 3. THREE-LEVEL SCALE USED FOR RANKING THE CURRENT KNOWLEDGE LEVEL OF PHENOMENA. THE RANKING WAS PERFORMED WITH REGARD TO BOTH EXPERIMENTAL DATA AND COMPUTATIONAL MODELS

Rank	Weight	Definition - data	Definition - models
Adequate (A)	1.0	The phenomenon is well understood. Data obtained for SFP accident conditions are available in sufficient range, quantity and quality.	Models that are validated for application to SFP accident conditions are available.
Some (S)	0.5	Data obtained for SFP accident conditions are available, but not in sufficient range, quantity or quality. Alternatively, data pertinent to other conditions exist and can be extrapolated to SFP conditions.	The phenomenon can be approximately modelled, e.g. by lower order models or models for similar phenomena that can be extrapolated to SFP conditions.
None (N)	0.0	No relevant data exist, and the phenomenon is poorly known.	No validated models exist.

The importance level and knowledge level (IL and KL) for each phenomenon was determined by averaging the panellists' votes. The colour-coding used for the importance and knowledge levels is defined in Table 4.

TABLE 4. KEY FOR THE COLOUR-CODING USED IN THE PIRTS

Parameter range	Importance/knowledge level	
	IL	*KL*
< 1/3	Green	Red
1/3 – 2/3	Yellow	Yellow
> 2/3	Red	Green

As a panellist may be an expert in some of the identified phenomena, but less familiar with others, all panel members were invited to consult with other experts in their home organizations and instructed to vote only if they had sufficient knowledge with the phenomenon in question. The panellists were also instructed to focus solely on the importance of the phenomenon relative to the evaluation criteria when casting their votes. Only one vote per participating organization was accepted, which means that each organization had to internally agree on a specific vote.

Following the voting, the panel was convened to discuss the outcome. The discussion focused on phenomena that had received high importance level (*IL*) and/or low knowledge level (*KL*), and for which there seemed to be significant disagreement between the panellists. These phenomena were identified by use of two screening parameters [4]. The first one, R, was used as a measure for the *relative relevance* of each phenomenon. The second screening parameter, D, addressed the *relative dispersion* of votes for each phenomenon, i.e. the scatter in experts' opinion regarding importance level and knowledge level.

4. RESULTS AND DISCUSSION

Altogether 130 phenomena were identified and ranked by the expert panel [4]. The phenomena are distributed over the three consecutive phases of the considered accident scenarios as 31/38/61. About 25 of the phenomena are common to Phase II and III, meaning that they initiate with undamaged fuel and continue after cladding integrity is lost, possibly with increasing complexity as the fuel damage progresses.

Twenty phenomena were identified by the panellists as having priority research needs, since they were judged to be important and at the same time having a low level of knowledge with regard to available data and/or computational models. The identified high-priority phenomena are listed in Table 5. Two of the phenomena are common to Phase II and III of the accident (II.9-III.7 and II.37-III.59). Ten of the phenomena in Table 5 are important to both of the considered accident scenarios, while the remaining ten are specific to either the fast drainage or the slow uncovery scenario. The differences between these accident scenarios are relevant mostly for phenomena pertaining to the early phases of the accident: for Phase III, most of the identified high-priority phenomena are deemed important to both scenarios. The phenomena are distributed among the three phases of the accident as follows:

Pre-uncovery phase:
- Non-uniform natural circulation cooling flow distribution between FAs;
- Flow instabilities within the spent FAs at low liquid level;
- Multi-dimensional interaction of different temperature zones within the pool;
- Radioactive aerosol formation due to bubble breakup processes at the free surface;
- Leakage due to pool concrete and liner deterioration and cracking by temperature rise.

Uncovery phase:
- Development of two-phase natural circulation in FAs, storage racks and SFP;
- Air cooling of the FAs and storage racks after complete pool drainage;
- Fuel fragmentation and relocation during ballooning, before cladding rupture;
- Cladding oxidation under air and/or (steam+hydrogen)-mixture environment;
- Nitrogen assisted oxide breakaway at low temperature;
- Fuel cooling by water spray: water injection above the FAs.

Fuel damage phase:
- Stop of natural circulation of air through the FAs by water, injected or sprayed as mitigation measure;

- Air cooling of the FAs and storage racks after complete pool drainage;
- Coolability of almost completely uncovered FAs, with their bottom ends immersed in water;
- Influence of geometry changes during degradation on heat transfer;
- Radiative heat transfer from uncovered fuel assemblies to other FAs, racks and SFP structure;
- Re-oxidation of ZrN by steam/oxygen;
- Fuel volatilization and behaviour of fuel fines;
- Loss of subcriticality due to relocation of absorber materials;
- Fuel cooling by water spray: water injection above the fuel assemblies.

A majority of the phenomena identified as having priority research needs are related to fuel damage phase (Phase III) of the accident. This is partly a consequence of the evaluation criteria used for ranking the importance level of each phenomenon. Since two of these criteria are related to fuel damage and source term, many phenomena occurring in the fuel damage phase inevitably become important. Nevertheless, five phenomena from Phase I and six phenomena from Phase II are included in Table 5. Most of these phenomena have a moderate importance level, but, on the other hand, also a low level of knowledge. Since it is generally difficult to accurately assess the importance of poorly known phenomena, the expert panel preferred to give some priority to these phenomena when identifying those with high research needs. It should also be remarked that not only the importance and knowledge levels, but also the dispersion in the panellists' votes regarding these levels was accounted for when identifying phenomena with priority research needs. The high-priority phenomena in Table 5 were generally identified with a fairly high consistency among the panellists' votes.

Half of the phenomena in Table 5 concern thermal-hydraulics and heat transfer. From the Table 5, it is clear that these disciplines are important for all phases of the accident. The situation is somewhat different for the phenomena related to fuel behaviour in Table 5, which are important mainly for Phase II of the accident. The reason is that the listed fuel behaviour phenomena are expected to affect the time to cladding tube rupture, and hence, will be important to the accident progression rate for Phase II.

In order to assess the consistency of the votes, a dispersion analysis of the results was performed. The analysis showed that there is a significant dispersion in the votes for many of the ranked phenomena. In some cases, the spread may be explained by the phenomenon being design dependent, and that panellists have different views of its importance and level of knowledge, depending on the SFP technology that they are familiar with. In other cases, the dispersion of votes suggests that the phenomenon is poorly known.

In the pre-uncovery phase, the most dispersed phenomena are associated with the pool concrete and liner deterioration. The high relative dispersion is due to disagreement among the panellists regarding both the importance level and the availability of data and models. For the uncovery and fuel damage phases, the criticality-related phenomena are the most dispersed. For the uncovery phase, the dispersion seems to be caused mainly by an inconsistent view on the availability of data among the voters. For the fuel damage phase, the dispersion also includes disagreement on the importance level for some criticality phenomena.

TABLE 5. PHENOMENA WITH PRIORITY RESEARCH NEEDS

Phenomena by category	#	Scenario	Importance ranking				State of knowledge: Availability of data				State of knowledge: Availability of models				Screening parameters	
			L	M	H	*IL*	N	S	A	KL^D	N	S	A	KL^M	*R*	*D*
1. Thermal-hydraulics																
Non-uniform natural circulation cooling flow distribution between fuel assemblies.	I.5	SU	2	7	10	0.711	8	9	0	0.265	3	11	3	0.500	1.000	0.296
Flow instabilities within the spent FAs at low liquid level. Includes flow reversal and flow excursions.	I.6	SU	7	7	3	0.382	12	3	0	0.100	5	9	1	0.367	0.834	0.248
Multi-dimensional interaction of different temperature zones within the pool.	I.15	SU	1	9	7	0.676	5	11	0	0.344	2	12	2	0.500	0.850	0.202
Development of two phase natural circulation in FAs, storage racks and SFP. Including liquid water, steam and H_2.	II.3	SU	4	8	7	0.579	7	10	0	0.294	3	14	1	0.444	0.850	0.321
Stop of natural circulation of air through the FAs by water, injected or sprayed as mitigation measure.	III.3	SU	2	6	10	0.722	8	9	1	0.306	6	12	0	0.333	0.813	0.369
		FD	0	4	14	0.889	8	9	1	0.306	6	12	0	0.333	1.000	0.224
2. Heat transfer																
Air cooling of the FAs and storage racks after complete pool drainage.	II.9	FD	1	3	15	0.868	4	8	6	0.556	1	13	5	0.605	0.571	0.402
Air cooling of the FAs and storage racks after complete pool drainage.	III.7	FD	0	2	17	0.947	5	9	5	0.500	4	11	4	0.500	0.576	0.280
Coolability of almost completely uncovered FAs, with their bottom ends immersed in water (partial drain down).	III.8	SU	3	2	12	0.765	5	10	1	0.375	5	8	3	0.438	0.653	0.584
		FD	2	2	13	0.824	5	10	1	0.375	5	8	3	0.438	0.704	0.513
Influence of geometry changes during degradation on heat transfer (both in water and air/steam).	III.11	SU	0	6	13	0.842	9	8	1	0.278	4	13	1	0.417	0.862	0.269
		FD	0	6	13	0.842	9	8	1	0.278	4	13	1	0.417	0.862	0.269
Radiative heat transfer from uncovered fuel assemblies to other FAs, racks and SFP structure.	III.12	SU	0	6	13	0.842	7	11	0	0.306	2	15	1	0.472	0.750	0.177
		FD	0	3	16	0.921	7	11	0	0.306	2	15	1	0.472	0.820	0.139

TABLE 5. CONT.

Phenomena by category	#	Scenario	Importance ranking				State of knowledge: Availability of data				Availability of models				Phenomena by category	
			L	M	H	*IL*	N	S	A	KL^D	N	S	A	KL^M	*R*	*D*
3. Fuel behaviour																
Fuel fragmentation and relocation during ballooning, before cladding rupture.	II.18	SU	2	9	7	0.639	0	17	1	0.528	5	11	2	0.417	0.659	0.171
		FD	2	10	6	0.611	1	16	1	0.500	5	12	1	0.389	0.699	0.214
Cladding oxidation under air or/and (steam + hydrogen) mixture environment, influence of nitriding.	II.23	FD	0	7	12	0.816	1	14	4	0.579	2	15	2	0.500	0.643	0.207
Nitrogen assisted oxide breakaway at low temperature.	II.24	FD	3	6	9	0.667	3	8	4	0.533	4	11	0	0.367	0.738	0.429
Re-oxidation of ZrN by steam/oxygen.	III.22	SU	0	9	9	0.750	6	11	1	0.361	11	7	0	0.194	0.938	0.263
		FD	0	8	9	0.765	5	12	1	0.389	10	8	0	0.222	0.883	0.256
4. Radioactivity release issues																
Radioactive aerosol formation due to bubble breakup processes at the free surface.	I.23	SU	5	7	5	0.500	4	7	3	0.464	3	8	3	0.500	0.513	0.522
Fuel volatilization, behaviour of fuel fines.	III.49	SU	5	5	7	0.559	8	8	0	0.250	6	9	2	0.382	0.629	0.519
		FD	4	6	7	0.588	8	8	0	0.250	6	9	2	0.382	0.662	0.489
5. Pool concrete and liner effects																
Leakage due to pool concrete and liner deterioration and cracking by pool temperature rise.	I.28	SU	4	7	6	0.559	7	3	3	0.346	5	5	5	0.500	0.699	0.752
6. Criticality issues																
Loss of subcriticality due to relocation of absorber materials.	III.58	SU	2	6	8	0.688	9	2	2	0.231	4	4	5	0.538	0.593	0.832
		FD	2	6	8	0.688	9	2	2	0.231	4	4	5	0.538	0.593	0.832
7. Mitigation																
Fuel cooling by water spray; water injection above the FAs.	II.37	SU	0	5	11	0.844	3	11	1	0.433	2	11	2	0.500	0.895	0.229
		FD	0	5	11	0.844	3	11	1	0.433	2	11	2	0.500	0.895	0.229
Fuel cooling by water spray; water injection above the FAs.	III.59	SU	0	4	14	0.889	5	12	0	0.353	3	14	1	0.444	0.776	0.168
		FD	0	3	15	0.917	5	12	0	0.353	3	14	1	0.444	0.801	0.151

CONCLUSIONS

The results of the PIRTs [4] summarized in this paper were developed with the overall objective to guide future experimental and modelling efforts relating to SFP loss-of-cooling and loss-of-coolant accidents. An international panel of experts identified and ranked more than a hundred physical phenomena with regard to their safety importance and current level of knowledge, with the aim to identify phenomena that should be prioritized in future experimental and/or analytical studies. A well-established PIRT methodology was used to identify these phenomena, which are deemed to be of high potential safety importance and low level of knowledge as measured by the availability of experimental data and/or computational models. The study was generic with regard to reactor and fuel design, but restricted to phenomena that occur in the spent fuel pool. Phenomena occurring predominantly outside the SFP, e.g. heat and mass transfer in the pool building or to the environment, were beyond the scope of the study.

Altogether eighteen unique phenomena were identified as having priority research needs; see section 4. About half of these phenomena are related to thermal-hydraulics and heat transfer in the SFP, and they are judged to be important to the coolability of the spent fuel in loss-of-cooling and/or loss-of-coolant accidents. Experimental studies of these phenomena generally call for costly large-scale integral tests, and it is therefore expected that associated computer models and supporting databases will evolve slowly. However, there are also phenomena with high priority research needs that can be studied in fairly simple separate effect tests, for example fuel volatilization, cladding oxidation in mixed steam-air environment and nitrogen-assisted oxide breakaway at moderate temperature.

The expert panel also opines that phenomena related to spent fuel emergency cooling by water spray are among those with priority research needs. Quite a few of the phenomena identified by the expert panel as having priority research needs are currently being investigated in ongoing research projects or will be studied in near-term programmes. This is no coincidence, since many of the panellists are involved in or aware of these programmes. Hence, the ranking results reflect the current (early 2017) understanding of involved phenomena and the current perception of their importance. This implies that the PIRTs include only phenomena for which there exists some knowledge base. It also implies that the ranking of certain phenomena will most likely change as the results of new research become available. Hence, it should be recognized that the PIRTs in this report are inevitably based on incomplete information and that they have to be re-evaluated as the knowledge base is extended. Most of the knowledge base behind the PIRTs in this report is documented in Ref. [3].

The study addresses the research needs on SFP accidents from a general point of view. It has a wide scope in that it is generic with regard to the design of the considered at-reactor SFP, the storage racks and the spent fuel. It also considers two general types of accidents, each taking place with a spectrum of postulated initial and boundary conditions in terms of fuel heat load and storage configuration. In general, there is a risk that results of generic PIRTs tend to become inconclusive or too imprecise to be useful [5]. In the present study, the confidence of the ranking results can be assessed through the dispersion of the panellists' votes. Most of the eighteen phenomena that were found to have priority research needs were identified with a high degree of agreement among the panellists, which lends confidence to the main results of the PIRTs. It is therefore likely that further research on these eighteen phenomena will improve our understanding and modelling capacity of SFP accidents for a wide range of designs and accident scenarios.

On the other hand, there is a large dispersion of the votes on phenomena that may potentially lead to loss of subcriticality in the SFP. A plausible reason is that these phenomena have a particularly strong dependence on the design and/or accident scenario. We recall that our study covers SFPs using both borated and un-borated water, all kinds of storage rack designs, all kinds of LWR fuel, and even CANDU fuel, for which criticality in the SFP is not an issue at all. More design specific and/or scenario specific studies are needed to produce useful PIRTs for criticality issues under SFP accidents.

Based on the results of the presented study, the following recommendations are given:

- A CSNI state-of-the-art report on SFP loss-of-cooling and loss-of-coolant accidents should be written as the results of ongoing and planned research programmes become available. An appropriate starting time for this activity would be 2020–2022.

- Ongoing separate effect tests that address cladding chemical reactions with mixed steam-air environments should be supported, and it should be ensured that the testing programmes cover all type of fuel cladding present in SFPs and also the low temperature range, which is of interest for many SFP accident scenarios.

- Integral tests at and above the scale of fuel assemblies should be conducted to further investigate thermal-hydraulic and heat transfer phenomena with importance to the coolability of partly or completely uncovered fuel assemblies. The need for such tests is most apparent for CANDU fuel and rack designs, for which the results of recently conducted Sandia tests on LWR fuels and racks do not apply.

- Properly scaled experiments should be carried out to study the thermal-hydraulic behaviour and the large-scale natural circulation flow pattern that evolves in the SFP under the pre-uncovery phase of loss-of-cooling accidents. These experiments are needed, in the first instance for validating 3D models in thermal-hydraulic system codes, and later, for formulating and validating models in computational fluid dynamics codes under development.

- Spray cooling of uncovered spent fuel assemblies in typical storage rack designs should also be experimentally studied. Experiments are needed at and above the scale of fuel assemblies and they should be done with heat loads typical for spent fuel. In a first step, the tests should address the coolability of the fuel, with the aim to generate suitable data for development and/or validation of empirical spray cooling models in severe accident codes and thermal-hydraulic system codes. Later, more detailed experiments are needed, on several length scales, for formulation and validation of mechanistic models for spray cooling.

- Sensitivity and uncertainty analyses should be considered an integral part of computer code applications for SFPs in loss-of-cooling and loss-of-coolant accidents conditions. These analyses should be directed towards submodels and phenomena for which the most substantial uncertainties are known to exist. The results presented in the PIRT report provide some general guidance in identifying these phenomena.

REFERENCES

[1] THE NATIONAL ACADEMIES PRESS, Safety and security of commercial spent nuclear fuel storage, Public report ISBN 0-309-09647-2, The National Academies Press, Washington, DC, (2006).

[2] ATOMIC ENERGY SOCIETY OF JAPAN, The Fukushima Daiichi Nuclear Accident: Final report of the AESJ investigation committee, Springer Japan, Tokyo (2015).
[3] ORGANISATION FOR ECONOMIC COOPERATION AND DEVELOPMENT NUCLEAR ENERGY AGENCY, Status report on spent fuel pools under loss-of-cooling and loss-of-coolant accident conditions, Report NEA/CSNI/R(2015)2, OECD-NEA, Paris (2015).
https://www.oecd-nea.org/nsd/docs/2015/csni-r2015-2.pdf.
[4] ORGANISATION FOR ECONOMIC COOPERATION AND DEVELOPMENT NUCLEAR ENERGY AGENCY, Phenomena Identification and Ranking Table. R&D Priorities for Loos-of-Cooling and Loss-of-Coolant Accident in Spent Nuclear Fuel Pools, Report NEA No. 7443, OECD-NEA, Paris (2018) https://www.oecd-nea.org/nsd/docs/2017/csni-r2017-18.pdf
[5] WILSON, G.E. and BOYACK B.E., The role of the PIRT process in experiments, code development and code applications associated with reactor safety analysis. Nuclear Engineering and Design **186** (1998) 23–37.

VVER-440 SPENT FUEL POOL CALCULATIONS WITH THE MAAP5-VVER CODE

Z. TÉCHY, G. LAJTHA
NUBIKI, Budapest

L. TARCZAL
Paks NPP, Paks

Hungary

Abstract

Severe accident analyses for the spent fuel pool of the VVER-440/213 plant have been performed with the MAAP5-VVER code. The selected sequence was an unmitigated loss-of-cooling accident. MAAP5 modelling of the SFP is quite advanced due to several features including the possibility of modelling rectangular pool geometries. The SFP input deck for the MAAP5 code has been set up using plant specific data concerning SFP dimensions, parameters and materials. Accident progression has been analyzed by tracking thermal-hydraulic parameters and fission product release during the sequence. Results of the calculations have been found physically reasonable. Additional check of the results has been performed via code-to code comparison with a similar MELCOR analysis. Computer run times of MAAP5-VVER for a typical SFP transient lasting 200 h have been less than 20 min on a usual PC under Microsoft Windows. Graphical capabilities of the code are flexible and efficient enabling the analyst to review and study physical parameters.

1. INTRODUCTION

MAAP5 computer program is the intellectual property and solely licensed by the Electric Power Research Institute (EPRI). The code has been developed for simulation of severe reactor accidents, the thermal-hydraulic and fission product phenomena in the western type PWR and BWR power stations [1].

Under an agreement between EPRI and Paks NPP a VVER-specific MAAP5 code version (MAAP5-VVER v5.03) development has been started in 2017 [2] leading to the issue of the final version of the code in 2019. This paper is based on a report devoted to VVER Spent Fuel Pool (SFP) calculations with the MAAP5-VVER code [3].

2. VVER-440/213 SPENT FUEL POOL

2.1. Geometry of the spent fuel pool

The Spent Fuel Pool (SFP) is situated in the reactor building (Fig. 1) [4]. The SFP compartment is situated between architectural levels +7.30 m (bottom) and +22.37 m (top). The SFP is outside of the containment boundary and it is connected with the Reactor Hall. Plan view of the SFP is shown in Fig. 2 [4]. The SFP has the form of a truncated rectangle with a length 6.0 m at the longer side, but the lengths of the shorter side are 3.76 m at the lower part and 4.76 m at the upper part of the pool. Fuel racks are of two types, regular or operational racks and reserve racks. Reserve racks serve to incorporate the whole reactor core (in addition to the regular spent fuel contingent) during full maintenance, i.e. once every fourth fuel cycle, or in case of an emergency reload. Reserve racks are installed onto the top of regular racks in case these operations are requested. This report on MAAP5 SFP application is limited to modelling the regular SFP configuration.

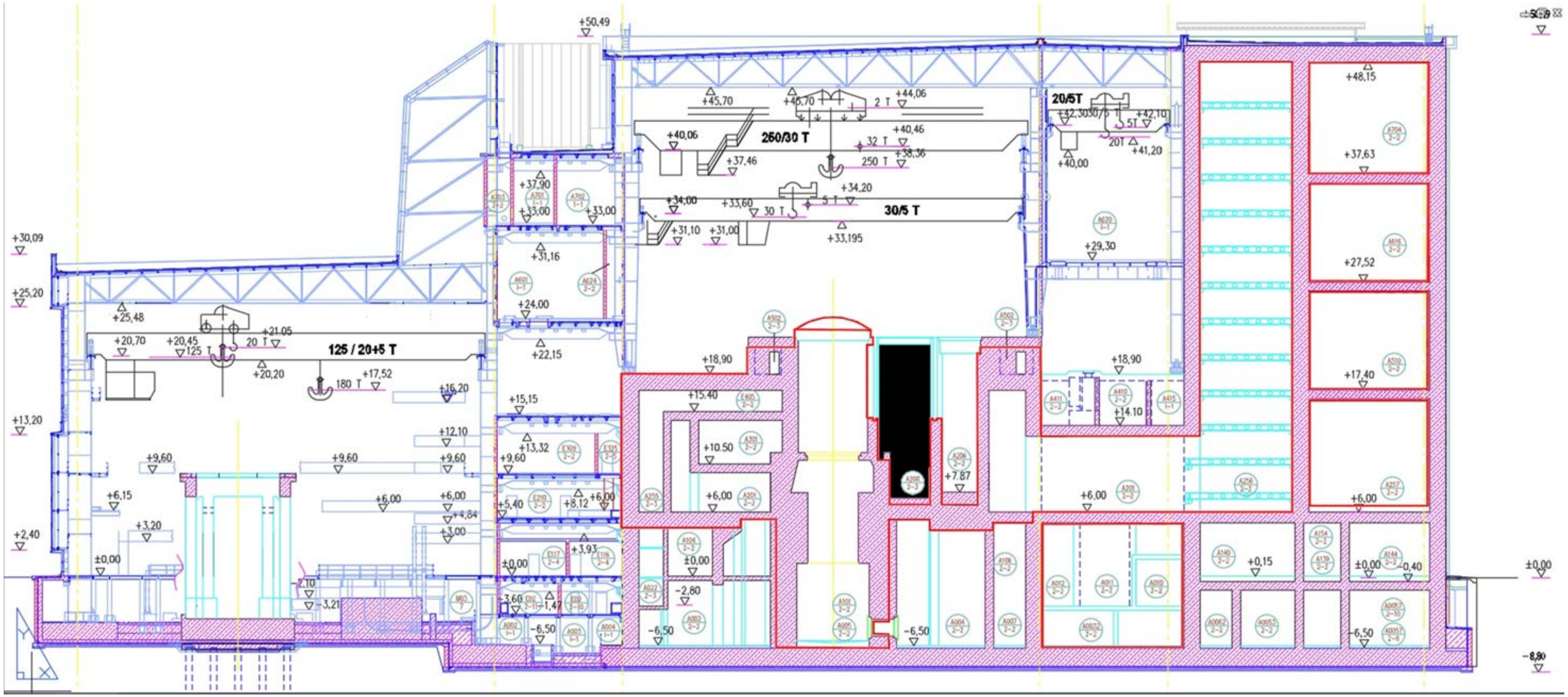

FIG. 1. Cross section of the Reactor Building. Spent fuel pool compartment is highlighted with black colour.

Regular racks consist of the bottom plate, the top plate and hexagonal tubes called absorber tubes made of boron steel. Each absorber tube may incorporate a fuel assembly. The total capacity of the regular racks is 650 fuel assemblies. In addition to the storage of spent fuel, there are 56 slots for storing the so called hermetic canisters and 5 slots to store specific tools used for reload operations. Geometric dimensions of the absorber tubes are as follow: length 3050 mm, distance across flats is 150 mm (inside dimension), pitch of racks is 160 mm and the wall thickness is 3 mm.

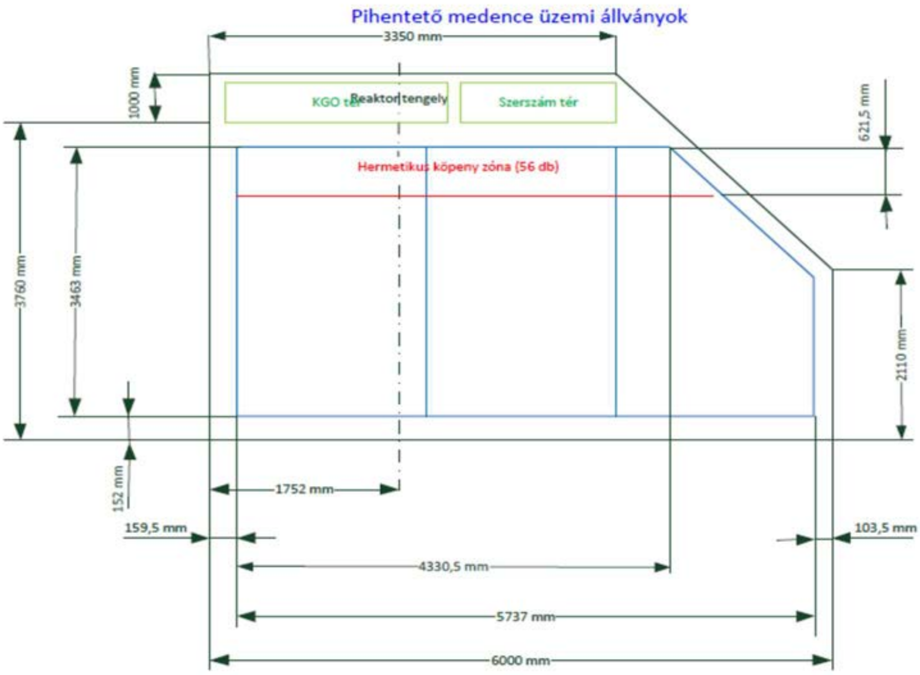

FIG. 2. Plan view of the spent fuel pool with dimensions.

2.2. Positioning of fuel assemblies in the SFP

Considering the structure of the fuel assemblies stored in the SFP, we relied to a great extent on a study presented in Ref. [5]. The actual storage contingent used in the model is presented in Table 1. There are five FA types characterized by cooling time duration in the spent fuel pool.

TABLE 1. TYPES OF FUEL ASSEMBLIES STORED IN THE SFP

Type	Cooling time (d)	Number of FAs
1	135 h	88
2	425	101
3	850	102
4	1275	102
5	1700	257
Total		650

Fuel assemblies fill altogether 650 racks. The remaining 61 racks of the SFP are reserved for hermetic canisters and specific tools.

Positioning of the fuel assemblies in the SFP is illustrated in Fig. 3.

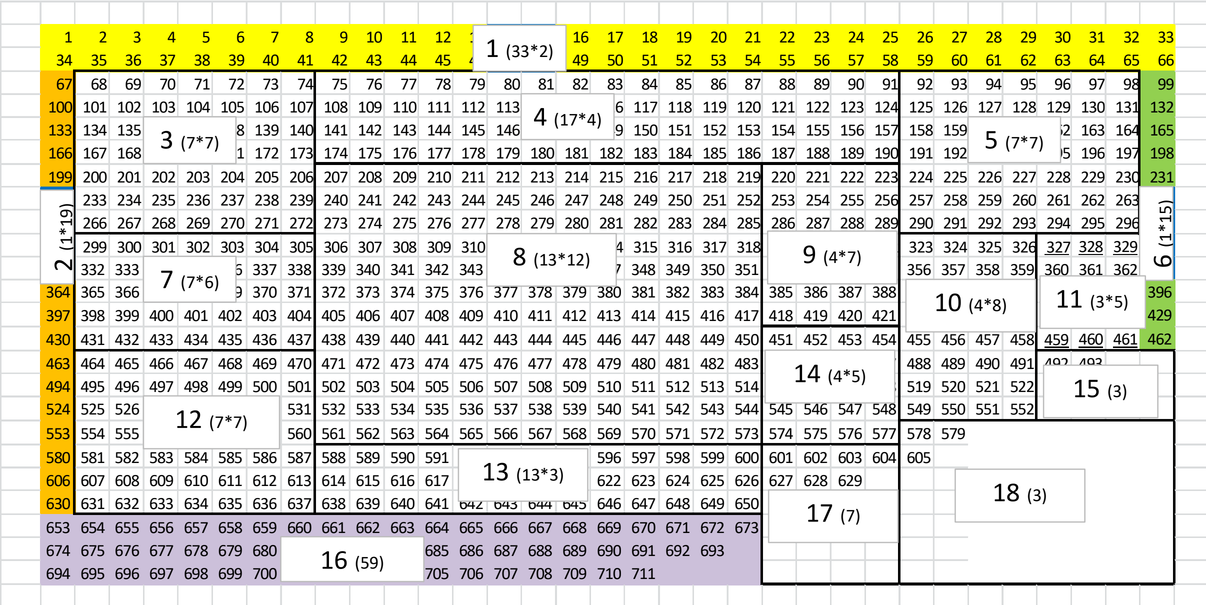

FIG. 3. Positioning of the fuel assemblies in the Spent Fuel Pool.

Each fuel rack has an individual number. MAAP5 modelling uses the convention of fuel channels containing a specific number of fuel assemblies or fuel racks. In the above Fig. 3 the SFP is subdivided into 18 channels. Fuel racks are numbered in increasing sequence, so the SFP is populated with 650 racks containing fuel assemblies, 56 racks for storing hermetic canisters and 6 racks for the storage of specific equipment, altogether 711 storage slots. Racks are numbered consecutively in row-major order.

Channel labels in Fig. 3 include rack numbers in the x and y directions for fully populated channels or the total number of the assemblies at the truncated side of the SFP. With the selected subdivision of the entire storage pool into channels we aimed to set up separate treatments for the racks situated at the borders and for those in the inner regions of SFP.

Fuel assemblies have been assumed to undergo three operational cycles, each lasting 425 days. Burn-up values associated with the operational cycles have been assumed 16.83, 33.09 and 47.57 MWd/kgU along with 4.7% of enrichment for each assembly.

Concerning the distribution of fuel assemblies in the SFP, the older FAs have been positioned predominantly into the channels at the borders of the SFP and the more energetic fresh FAs placed mainly into the middle channels.

3. RESULTS OF MAAP5/VVER SFP CALCULATIONS

MAAP5-VVER code calculations have been performed for a loss-of-cooling sequence selected on the basis on an SFP PSA study. MAAP5 parameter and input files have been set up to match the setup and arrangement of the fuel in the SFP as described above.

3.1. Thermal-hydraulic results of the loss-of-cooling sequence

The loss-of-cooling sequence of the spent fuel pool with regular configuration has been calculated. The calculation was conducted with the following boundary conditions (Table 2).

TABLE 2. BOUNDARY CONDITIONS FOR LOSS OF COOLING SEQUENCE, SFP WITH REGULAR CONFIGURATION

Parameter	Value
SFP configuration	Regular
SFP initial thermal power (kW)	1600
Number of FAs	650
Configuration of fuel bundles	Fresh FAs: 88 FAs at 1 year cooling time 101 FAs at 2 year cooling time 102 FAs at 3 year cooling time 102
SFP initial water inventory	146 m^3
Water volume above the FAs	73 m^3
SFP initial temperature	25°C
SFP cover	removed (open pool)

Most important events of the calculation are presented in Table 3. Upon loss of cooling the temperature of the spent fuel pool is increasing and the saturation temperature is reached at 9.7 h after the initiating event. The temperature of the water is not changing until the depletion of the coolant inventory. The top of the fuel assemblies will be uncovered at 54.4 h and the melting of fuel, indicated by exceeding the temperature of 2500 K, reached at 78.3 h, followed by fuel relocation from 80 h. The spent fuel pool water dryout occurs at 85.4 h and the bulk fuel relocates to the bottom of SFP at 110 h. Erosion of the concrete floor starts later, at 203 h.

TABLE 3. MAIN EVENTS OF THE LOSS OF COOLING SEQUENCE, SFP WITH REGULAR CONFIGURATION

Event	Time (s)
Initiating event: loss of cooling	0
Start of boiling of SFP inventory	34875
Top of fuel (TOF) uncovered	195695
Start of Zr-H_2O reaction	249930
Gap release starts $T_{clad} > 1173$ K	271700
Start of fuel degradation, $T_{fuel} > 2250$ K	281917
Start of fuel melting, $T_{fuel} > 2500$ K	281928
Fuel debris relocation started	288000
Coolant level at bottom of fuel (BOF)	306530
SFP water dryout	307490
Bulk of debris relocated to the bottom of the SFP	396000
Concrete erosion started	732565

Decay heat generated in the Spent Fuel Pool calculated by MAAP5-VVER is shown in Fig. 4.

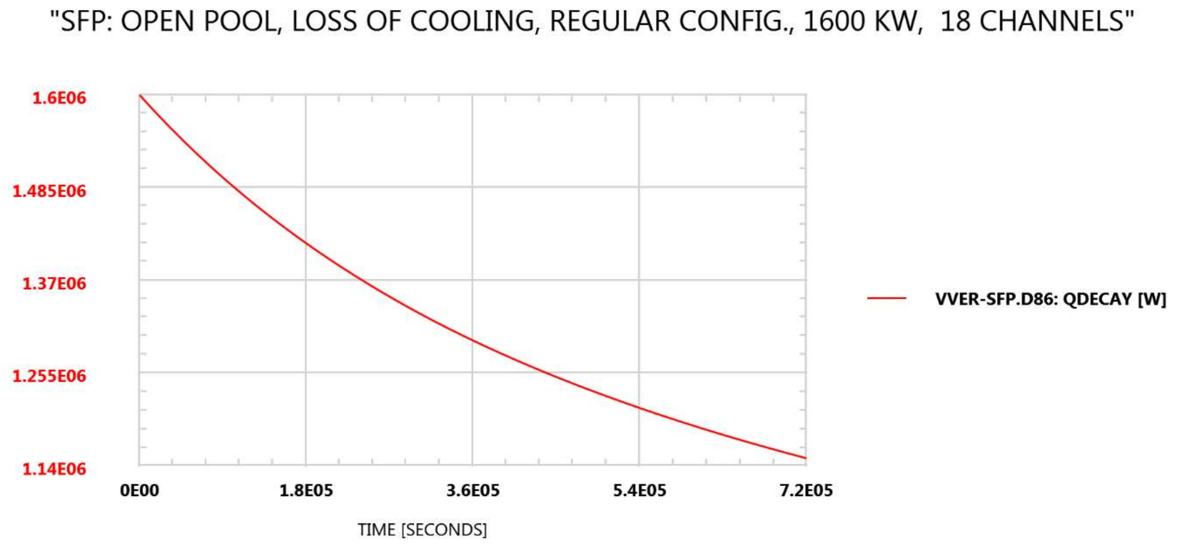

FIG. 4. Decay heat.

The decay heat is 1600 kW in the Spent Fuel Pool at the beginning of the calculation and it decreases to 1149 kW by the end of the calculation (200 h or 720 000 s).

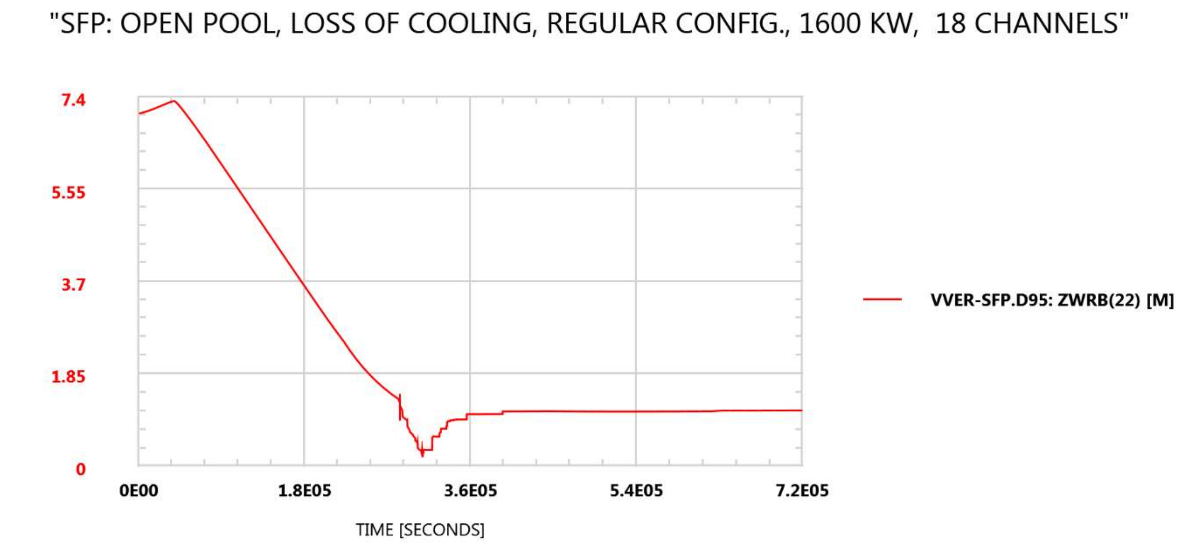

FIG. 5. Water level in SFP.

Fig. 5 includes the level history from the beginning of the transient. The water level in the SFP (ZWRB(22)) starts at the 7.07 m relative level (from the SFP floor at +7.30 m). Initial level swell corresponds to the heat expansion of the coolant. Top of fuel (3.595 m) is reached at 180 214 s. This time is less than the uncovery time (185 695 s), but this is consistent with the fact that ZWRB(22) refers to collapsed water level, while the uncovery time corresponds to a boiled-up level.

The diagram shows that the pool level decreases quite sharp from the uncovery of the fuel. The summary file provides the precise time of uncovery at 195 695 s. After the dryout of the pool the ZWVRB parameter corresponds to the height of the debris on the SFP floor.

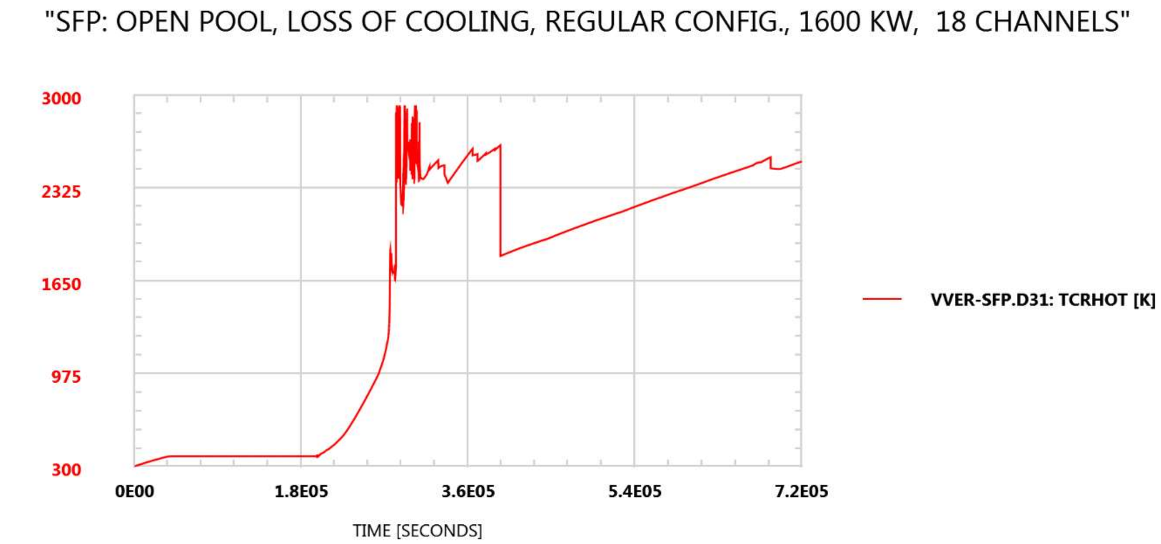

FIG. 6. Maximum fuel temperature in SFP.

Fuel temperatures start to rise at the time of the fuel uncovery (195 695 s). Gap release temperature (1173 K) is reached at 271 700 s and rise further up to and beyond 2500 K, the value identified with fuel melting, at 281 928 s (Fig. 6).

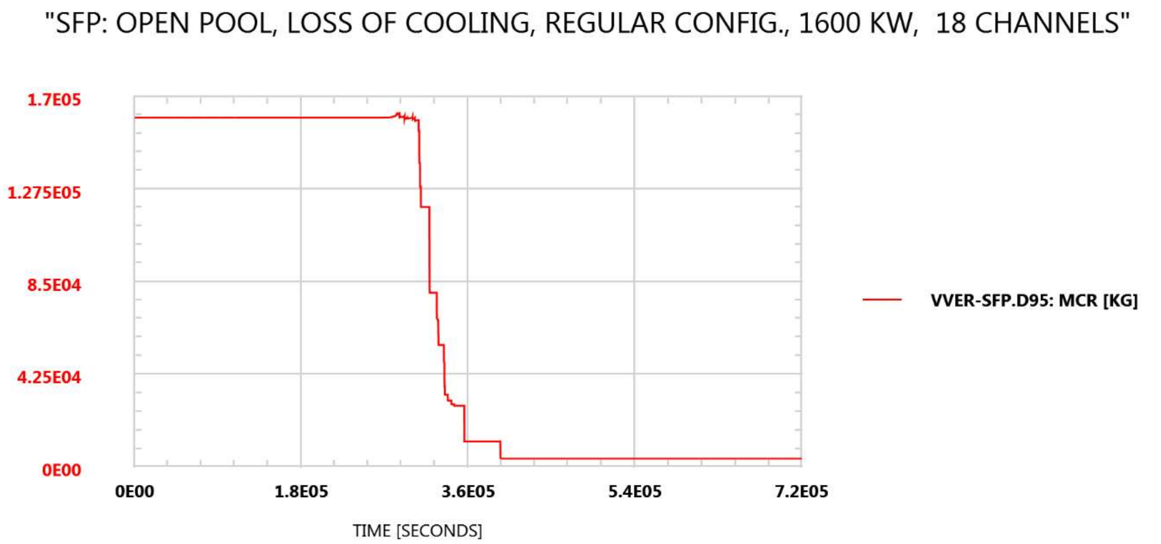

FIG. 7. Total mass of fuel material remaining in place.

Fuel slumping is progressing relatively slow from around 288 000 s and continuing in several steps until around 396 000 s with a certain part remaining in place until the end of the calculation (Fig. 7). Integrated amount of hydrogen is represented in the next plot.

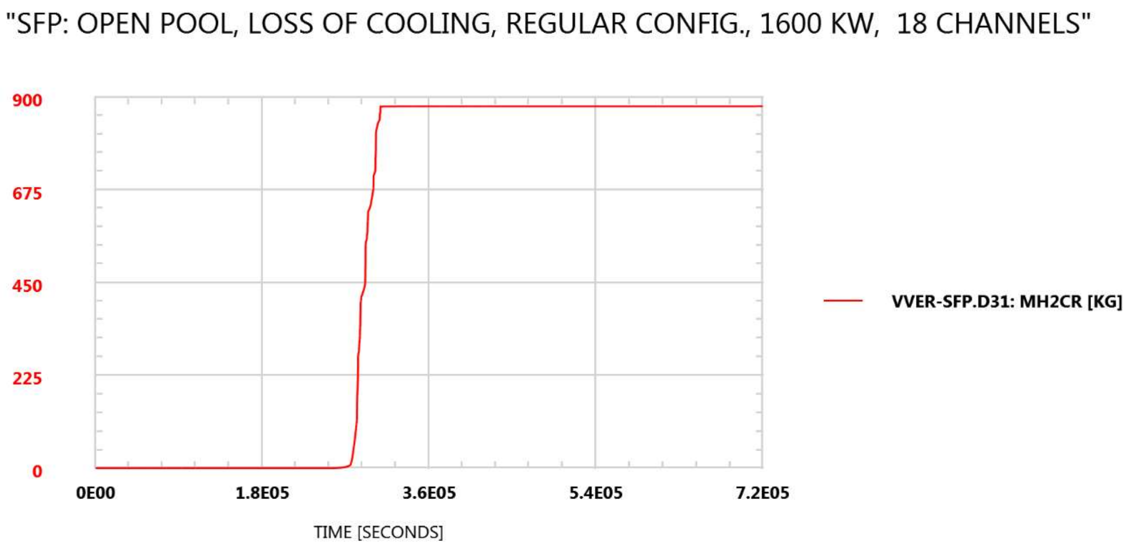

FIG. 8. Integrated mass of hydrogen generated in SFP.

Total amount of the generated hydrogen becomes 879 kg by the end of fuel degradation (Fig. 8).

3.2. Fission product release

MAAP5 considers the release of fission products (FPs) (25 fuel and control rod elements in various chemical compositions) that are distributed into 18 fission product groups based on similar chemical and physical behaviour (Table 4).

TABLE 4. MAAP5 FISSION PRODUCT GROUPS

Group number	Elements or chemical compounds
1	Xe, Kr
2	CsI, RbI
3	TeO_2
4	SrO
5	MoO_2, RuO_2, TcO_2, RhO_2
6	CsOH, RbOH
7	BaO
8	La_2O_3, Pr_2O_3, Nd_2O_3, Sm_2O_3, Y_2O_3, ZrO_2, NbO_2, AmO_2, CmO_2
9	CeO_2, NpO_2, PuO_2
10	Sb
11	Te_2
12	UO_2 (fuel, not FP)
13	Ag (control rod material, not FP)
14	I_2 (iodine in elemental form)
15	CH_3I (iodine in organic form)
16	Cs_2MoO_4
17	RuO_2
18	PuO_2 (fuel, not FP)

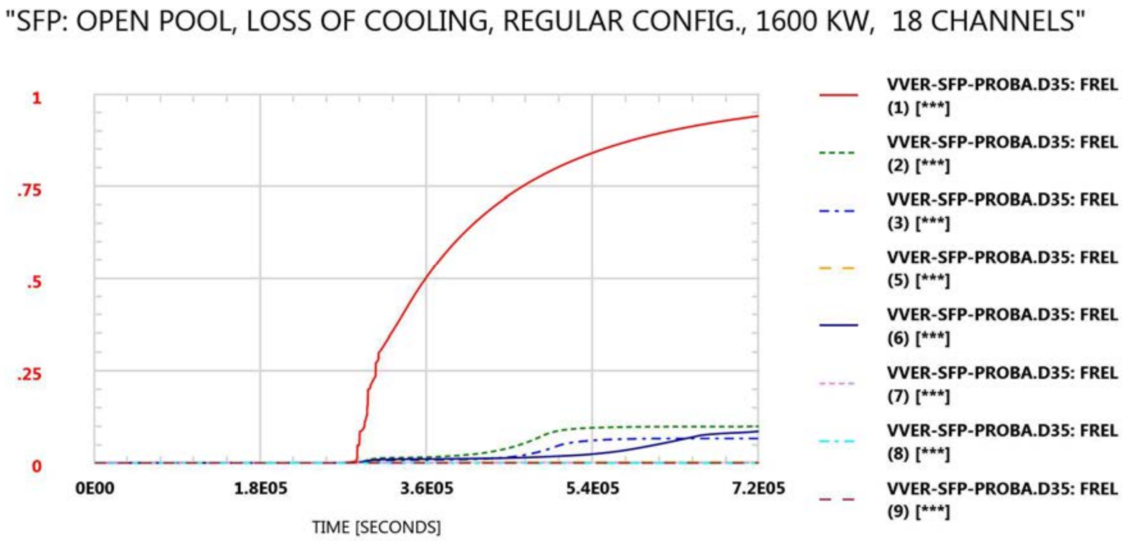

FIG. 9. Release fractions of fission product groups into the environment.

Most important fission product groups are shown in Fig. 9. As expected, noble gas (group 1) release rates are most prominent, 82% by the end of the sequence. Caesium (groups 2 and 6) release rates are smaller, 6.3% and 5.5%, similarly to the TeO_2 (group 3, 4.7%), due to the fact that these aerosols are mainly deposited on the walls of Reactor Hall. Other isotopes belong to the semi-volatile or non-volatile category therefore they do not represent any significant release fraction. Volatile radioactive products released into the Reactor Hall are plotted in Fig. 10.

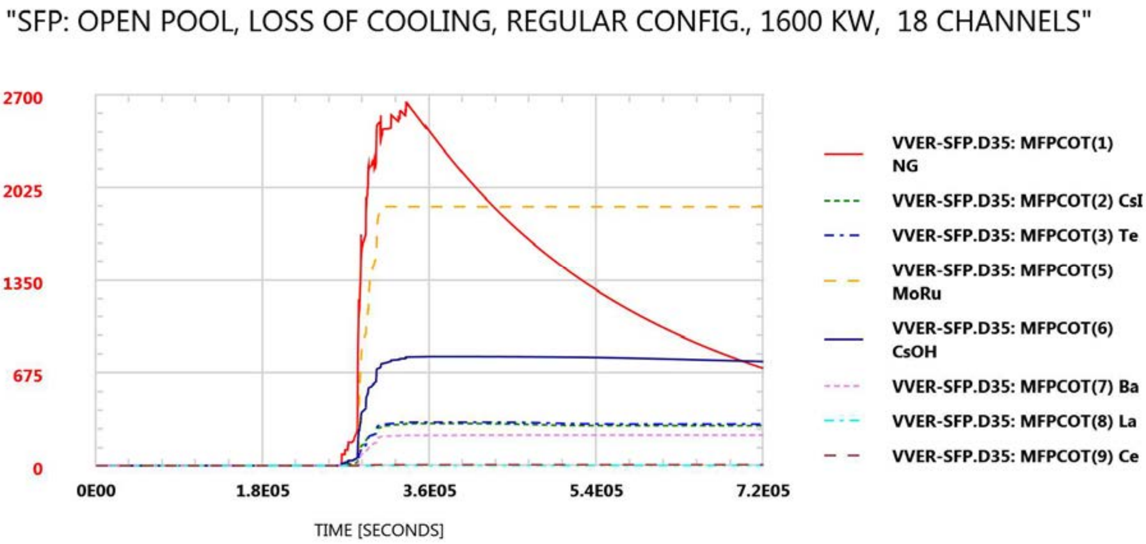

FIG. 10. Total fission product mass in Reactor Hall.

Noble gas (Xe and Kr) mass is increasing at the degradation of the fuel, but it is receding later due to the release to the environment. Other volatiles as CsI, CsOH and Te are staying at stable amounts, since these species are mostly deposited on the walls.

4. COMPARISON OF MAAP5-VVER AND MELCOR CALCULATION RESULTS

In Table 5 MAAP5 main events presented in a previous section have been compared to the results of a similar analysis performed for spent fuel pool accidents using the MELCOR 1.8.6 code [6]. The MELCOR code uses cylindrical model for SFP calculations.

Start times of boiling vary due to the difference of the initial water inventories assumed in the calculations, therefore this time shift between subsequent events should be taken into account. That said, the events up to the start of Zr-H2O reaction are relatively well correlated. Later event timings, however, differ to a much greater extent, than the initial time shift. Start of the fuel degradation, for instance, occurs later according to MAAP, and the difference is more than 4 h. which is likely due to modelling differences, including the cooling effect of the walls. Coolant levels at the bottom of the fuel are reached at 85.1 h in MAAP vs. 78.3 h in MELCOR. Complete dryout of the SFP water inventory is predicted at 85.4 h for MAAP and at 95.9 h for MELCOR, with a delay of more than 10 h. All these deviations can be attributed to modelling differences including the cooling effect of the walls to the modelling of fuel and structure slumping.

TABLE 5. MAIN EVENTS OF THE LOSS OF COOLING SEQUENCE, SFP WITH REGULAR CONFIGURATION

Comparison of MAAP and MELCOR results Event	MAAP5 Time (h)	MELCOR Time (h)
Initiating event: loss of cooling	0	0
Start of boiling of SFP inventory	9.7	11.4
Top of fuel (TOF) uncovered	54.4	52.8
Start of Zr-H2O reaction	69.4	71.4
Gap release starts T_{clad} > 1173 K	75.5	71.6
Start of fuel degradation, T_{fuel} > 2250 K	78.3	74.2
Start of fuel melting, T_{fuel} > 2500 K	78.3	-
Fuel debris relocation started	80	-
Coolant level at bottom of fuel (BOF)	85.1	78.3
SFP water dryout	85.4	95.9
Bulk of /all debris relocated to the bottom of the SFP	110	92.6
Concrete erosion started	203.5	-
End of calculation	200	95.9

Distribution of the main fission product groups (percent of initial inventory) between the fuel debris, the Reactor Hall and the environment for MAAP5 and MELCOR calculations are presented in Table 6.

Because the presentation of the various isotope groups in the MAAP5 and MELCOR models are somewhat different, the structure of the table is not fully identical. The difference concerns mainly the representation of the caesium and iodine isotopes. The MELCOR part of the table includes the Cs and I contributions recalculated for the corresponding chemical elements, whereas they appear as chemical compounds in MAAP5 results.

Noble gases are released in most prominent portions from the fuel. For these elements MAAP5 predicts no retention at all in the corium. However, according to MELCOR calculations, 12.83% of the nobles still remain in the corium at the end of the sequence. There is another great difference in the amounts of the nobles retained in the reactor hall and released into the environment; MAAP5 predicts 17.6% retention in the reactor hall and 82.4% release to the environment, MELCOR, in its turn calculates an opposite proportion, i.e. 71.38% are retained in the building and just 15.77% released to the environment. However, the sequence calculation times for MAAP5 and MELCOR analyses have been different: 95.6 h for MELCOR and 200 h for MAAP5. The amount of the noble gases in the building (Fig. 9) is increasing during fuel degradation and then slowly receding due to dilution and release to the environment. The noble gas proportions calculated by MAAP5 at the same time, i.e. 95.6 h, are as follow: 64.1% retained in the building and 35.9% released to the environment. The latter values are closer to those calculated with MELCOR. However, the results still deviate due to other modelling differences.

TABLE 6. DISTRIBUTION OF THE MAIN FISSION PRODUCT GROUPS OBTAINED IN MAAP5 AND MELCOR ANALYSES

MAAP5				MELCOR			
Group	Corium (%)	Reactor Hall (%)	Environment (%)	Group	Corium (%)	Reactor Hall (%)	Environment (%)
Xe+Kr	0.00	17.60	82.40	Xe+Kr	12.83	71.38	15.77
CsI	6.97	86.74	6.29	Cs	12.55	83.11	4.24
TeO_2	0.00	93.81	6.19	Te	18.80	77.74	3.41
Mo+Ru	49.69	49.96	0.36	Mo	67.24	31.31	1.39
CsOH	6.97	87.59	5.44	Ru	100	0	0
BaO	82.94	16.93	0.13	Ba	98.46	1.47	0.06
La_2O_3	99.95	0.05	0.00	La	99.99	0	0
CeO_2	99.40	0.60	0.00	Ce	100	0	0
				I	13.01	82.68	4.28

Caesium and iodine are grouped differently for MAAP5 and MELCOR calculations, but all taken into account MELCOR predicts a greater retention in the fuel amounting to 12–13%, while MAAP calculates around 7%. Retentions of the caesium and iodine isotopes in the reactor hall are similar, 83–88 % for both calculations. Released amounts of Cs and I are somewhat different: 5.5–6.3% are released in MAAP5 and just around 4.2% in MELCOR calculations. However, if MAAP and MELCOR releases were compared at the same accident time, then the difference would be greater: MAAP releases amount to just 1.2–1.4% at this time.

CONCLUSIONS

Severe accident analyses for the spent fuel pool of the VVER-440/213 plant have been performed with the MAAP5 code. The selected sequence was an unmitigated loss-of-cooling accident. The objective of the study was testing of the performance of the code for a VVER specific SFP application.

The SFP input deck for the MAAP5 code has been set up from scratch. Genuine plant specific data concerning SFP dimensions, parameters and materials have been used for the input. In terms of the fuel composition of the SFP we relied on a previous study [5].

MAAP5 modelling of the SFP is quite advanced and straightforward in comparison with either MAAP4 or MELCOR models. The statement concerns first of all the possibility of modelling a rectangular pool without forcing the dimensions into cylindrical geometry and subdivision of the various fuel types into specific rack groups called channels. This and many other SFP specific features provide the analyst with a truly flexible and efficient tool for modelling phenomena and performing analyses.

Results of the calculations have been found physically reasonable. Additional check of the results has been performed via a code-to code comparison with similar MELCOR analyses.

The results of the MAAP5 and MELCOR calculations agree in broad lines, although the actual numerical values obviously deviate to some extent due to modelling differences.

Computer run times for a typical SFP transient lasting 200 h have been less than 20 min on an ordinary PC under Microsoft Windows. Graphical capabilities of the code are flexible and efficient enabling the analyst to review and study physical parameters.

REFERENCES

[1] ELECTRIC POWER RESEARCH INSTITUTE, Modular Accident Analysis Program 5 Version 5.05 (MAAPv5.05) – PWR/BWR – Windows, EPRI, Palo Alto, CA, March 2019 (3002015307).

[2] ELECTRIC POWER RESEARCH INSTITUTE Modular Accident Analysis Program for VVER Reactor (MAAP5-VVER), Version 5.03-Windows, EPRI, Palo Alto, CA, January 2019 (3002015055).

[3] LAJTHA, G., TÉCHY, ZS., Using MAAP5-VVER for Spent Fuel Pool Accidents, Technical report 211-713-00/3, NUBIKI (2018).

[4] MAGYAR VILLAMOS MŰVEK ZÁRTKÖRŰEN MŰKÖDŐ RÉSZVÉNYTÁRSASÁG, Paks Nuclear Power Plant, Final Safety Analysis Report, Vol. 9.1.2. Spent Fuel Storage, MVM Paks (1998).

[5] TARCZAL, L., Decay heat power calculations for the spent fuel pool, Paks NPP FEO, e-mail message (2015).

[6] HORVÁTH, G.L., KOSTKA, P., TÉCHY, ZS., Analysis of the progression of severe accidents and radioactive releases of spent fuel pool, Safety analysis report (in Hungarian), 212-522-00/2, NUBIKI (2016).

SCENARIO IDENTIFICATION, ANALYSIS AND MITIGATION MEASURES RELATED TO SPENT FUEL POOL FOR VVER-1000

P. KRISHNA KUMAR, Y.K. PANDEY, G. BISWAS
Engineering – LWR Directorate,
Nuclear Power Corporation of India Ltd,
Anushakti Nagar, Mumbai
India.

1. INTRODUCTION

The Indian Nuclear Power Programme started with the Tarapur boiling water reactor (BWR). Subsequently the main thrust of our nuclear power programme has been design, construction and operation of CANDU type pressurized heavy water reactors (PHWR). Today we operate 22 nuclear power units with net installed capacity of 6780 MW(e). These include 18 PHWRs, two BWRs and two VVERs (VVER-1000). A total of seven reactors (2 × VVER-1000, 4 × 700 MW(e) PHWRs and 1 fast breeder reactor (FBR) of capacity 500 MW(e)) are under construction.

The Kudankulam Nuclear Power Project (KKNPP), VVER type (Vodo-Vodyanoi Energetichesky Reacktor, water-water power reactor) belongs to family of Pressurized Water Reactor developed by OKB Gidropress, Russian Federation and its Version V-412 type reactor. The reactor plant consists of four circulating loops and a pressurizing system connected to the reactor with each loop containing a horizontal steam generator, a main circulating pump as shown in Figure. 1. Each KKNPP units have the rated power of 3000 MW(th) and enriched uranium (3.92% U-235) in oxide form is used as fuel with light water as moderator and coolant. The heat produced is then transferred to primary coolant. The Primary coolant then rejects its heat in Steam generator to produce steam and gets itself cooled [1].

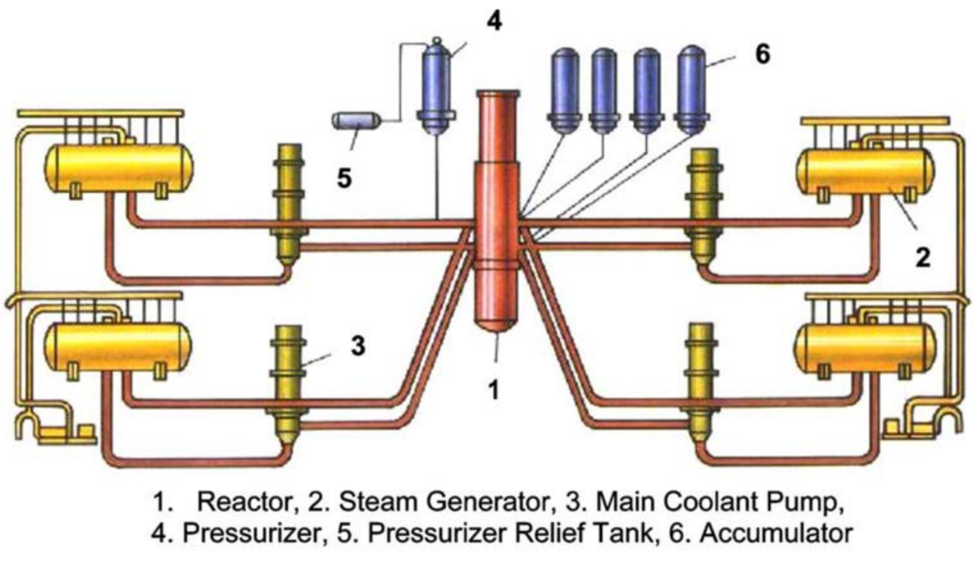

FIG. 1. Simple schematic of KKNPP-1&2 reactor primary circuit.

During refuelling outage, spent fuels are taken out of the reactor and kept for storage in the spent fuel pool. In VVERs, spent fuel pool (SFP) is located in the reactor hall inside the containment close to reactor cavity. After discharge from reactor cores, the spent fuel is stored in spent fuel racks in spent fuel pools which are separate for each unit. The leaky fuel will be stored in special bottles. After getting cooled for at least 5 years, the fuel can be transferred by spent fuel transportation casks to an away from reactor (AFR) facility for further storage till its transfer from facility.

This paper describes the features of VVER 1000 spent fuel pool, scenario identified for various plant states, event progressions, analysis results, prevention and mitigation measures for spent fuel pool related events. Also gap areas are identified for evaluating scenarios including partial/full fuel melt & improvements in code modelling for the simulation of spent fuel pool events.

2. SPENT FUEL POOL IN VVER

The fuel pool in VVER is an in-containment spent fuel storage system is designed to cool the spent fuel taken out of the reactor in order to reduce the former's activity and residual heat to the values that are permissible at transportation.

The design criteria for the SFP is for

1. Provide shielding in accessible spaces adjacent to the SFP (including the operating floor above) to ensure that when the pool is at design fuel assembly inventory and at minimum design water depth, the expected direct radiation dose rate from the stored fuel assemblies is not more than prescribed value;
2. Retain pool water such the water contaminated with radioactive material is not inadvertently released. The pools should be designed for zero leakage;
3. Retain SFP water level such that it is maintained above the top of stored fuel during all storage conditions to prevent overheating.

The spent fuel storage racks are for

1. Maintain the capability to remove and insert fuel assemblies and prevent physical damages to stored fuel;
2. Maintain the stored fuel in a proper geometry to ensure adequate cooling;
3. Maintain the stored fuel in a sub critical configuration for all plant conditions.

The in-containment spent fuel storage system is designed to keep and cool the spent fuel inside the reactor building considering the scheduled fuel reloading and the whole core unloading at any moment of NPP operation. The fuel pool is lined with stainless steel to provide a leak tight barrier. Spent fuel assemblies are kept in the racks. The storage bay has capacity to store spent fuel discharged for about 7 reactor years of operation in addition to provision for unloading of one full core load in case of emergency. The structures, systems and components (SSCs) of SFPs have been designed for design basis earthquake and design basis flood levels.

The spent fuel pond cooling system is designed for residual heat removal from the spent fuel that are located in the SFP under all the operating conditions as well as under the design basis accidents and design extension conditions.

In the fuel pool, spent fuel assemblies (SFA) are stored in closely packed racks maintaining a pitch of 300 mm in a triangular lattice, which provides K_{eff} below 0.95 in case of racks completely loaded with fuel having maximum enrichment and being submerged into boron-free water. To provide radiation and nuclear safety in the course of fuel storage, the fuel pond is filled with boric acid solution of 16 g/kg concentration.

All pipelines at inlet and outlet of fuel compartments penetrate fuel pool from its top such that their ruptures would not result in level decreasing below 3 m above the active lengths of SFAs. Besides, pressure pipelines going inside the fuel pool down to compartment's bottom, are provided with siphon break device. A simple schematic of spent fuel pool along with the reactor pressure vessel (RPV) are shown in Figure 2.

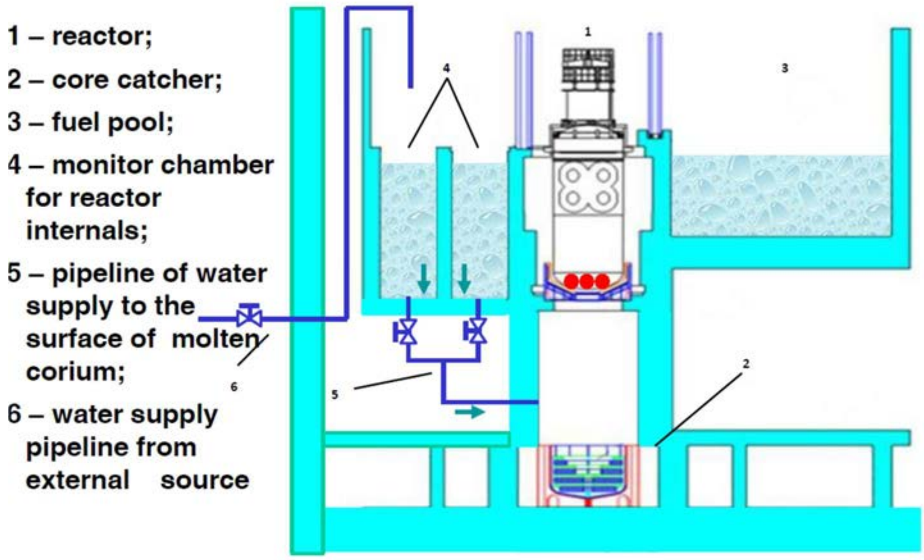

FIG. 2. Simple schematic of KKNPP-1&2 Spent Fuel Pool and RPV.

3. SCENARIO IDENTIFICATION UNDER DIFFERENT PLANT STATES

For the design basis of each plant, plant states are identified and grouped into a limited number of categories according to their likelihood of occurrence and defence in depth (DiD). The categories typically cover

– Normal Operation;
– Anticipated Operational Occurrences (AOO);
– Design Basis Accidents;
– Design Extension Conditions, including Severe Accidents with significant degradation of the reactor core.

Acceptance criteria are assigned to each plant state, such that frequently occurring plant states has no, or only minor, radiological consequences and plant states that could give rise to serious consequences have a very low frequency of occurrence. A safety analysis of the design for the nuclear power plant is conducted, in which methods of both deterministic analysis and probabilistic analysis are applied to enable the challenges to safety in the various categories of plant states to be evaluated and assessed.

The above philosophy is also applicable to the events related to the SFP. Over and above, there are some of the events will be considered under practically eliminated events for spent fuel pools. The practically eliminated events/event sequences are the conditions that could result in an early radioactive release or a large radioactive release. The possibility of certain events occurring is considered to have been practically eliminated if it is physically impossible for the conditions/phenomena to occur or if the events can be considered with a high level of confidence to be extremely unlikely to arise.

Considering the above methodology, the events related to spent fuel pool have been identified under different plant states and provided below.

Internal events

– Compensable leak in SFP;
– Failures of SFP cooling system;
– Boric acid dilution in SFP;
– Supporting system failures (loss of service water to heat exchangers);
– Loss of on-site electrical supply failure;
– Extended station black out;
– Non-compensable leak of SFP facing.

In the above, station black out and non-compensable leak of SFP facing are under design extension conditions. The remaining events mentioned above are under anticipated operational occurrences (AOO).

4. ANALYSIS ON LOSS OF COOLING/INVENTORY EVENTS IN THE SFP

SFP related events have been analyzed under two broad categories:

a. Loss of cooling in the SFP;
b. Loss of inventory from SFP.

Under loss of cooling, extended station black is also being considered.

4.1. Failures of spent fuel pool cooling system

4.1.1. Causes and description of the event

The function of SFP cooling is performed by the emergency and planned cooling down of primary circuit and fuel pool cooling system (JNA) in VVER-1000. Availability of four independent channels provides fulfilling the function of SFP cooling by JNA system under all design conditions including accidents not connected with the primary circuit leak. JNA system does the functions of Emergency core cooling and Fuel pond cooling.

The present section deals with the loss of SFP cooling during the primary circuit coolant leak (LOCA), when heat is not removed from the SFP that result in heating the coolant in the SFP and its boiling. This is AOO type of event.

Under the conditions of the primary circuit coolant leak with decrease in margin to saturation at any hot leg of the loops or increase in the gauge pressure under the containment, the valves on the JNA system pipelines for cooling water in the SFP are closed automatically. They are switched over to borated water supply from the SFP into the primary circuit. When the pressure under the containment exceeds 0.3 MPa, the gate valves under the sprinkler pumps pressure head open automatically and the borated water begins to enter the JMN sprinkler system from the SFP. After water intake from the SFP by ECCS active system and sprinkler system in the volume of 750 m^3 the water intake is stopped. In this case the water level in the SFP is minimum and this case envelops all the Loss of cooling type events. The present calculation estimates the flow rate of the required SFP water make-up and available time for its connection (time before beginning the FA fuel part uncovering). There are two cases have been considered,

Case 1: Complete filling of 'small' compartment (after planned refuelling) with SFAs is considered. 49 SFAs of three days holding and 49 SFAs of one-year, two-years, three-years, four-years holding and completing with one SFA of five years holding. The schematic arrangements of small and larger compartment are shown in Figure 3.

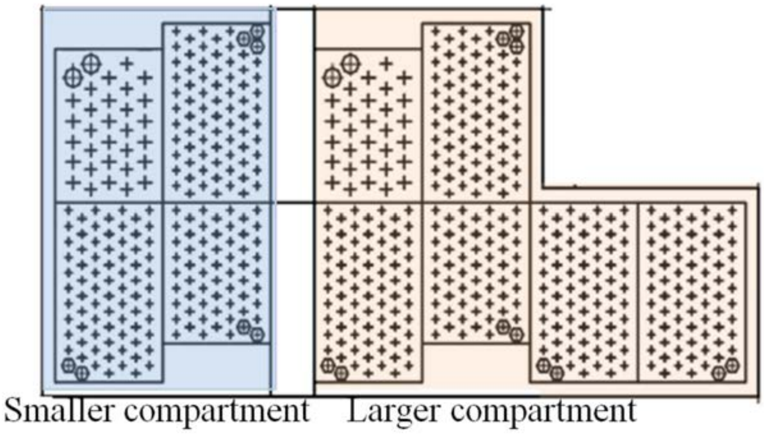

FIG. 3. Arrangement of FAs in smaller and larger compartments.

Case 2: Maximum filling of 'large' compartment (after planned refuelling) with SFAs is considered. 49 SFAs of three days holding and 49 SFAs of one-year, two-years, three-years, four- years, five-years, six-years, seven-years holding and completing with 8 SFAs of eight years holding.

The estimated decay heat with different shutdown duration of Spent FAs for the calculation is shown in the following table.

TABLE 1. SFP FUEL ASSEMBLIES DECAY HEAT VALUES

FAs types in SFP	Power of each FA in kW Power of FA × (f) × No of FAs
Three days holding	94.94
One-year holding	6.57
Two-year holding	3.22
Three-year holding	2.18
Four-year holding	1.64
Five-year holding	1.26
Six-year holding	1.08
Seven-year holding	0.98
Eight-year holding	0.91
	'f' is the power fraction [2]

4.1.2. Results

For Case 1, water inventory of 225 m^3 in the smaller compartment gets heated from the initial temperature of 50°C to 100°C during first 2.43 hr from the start of the initiating event. Thereafter water starts boiling and consequently inventory goes down. Out of total inventory of 225 m^3, boiling of 127.59 m^3 water, available above FAs takes 14.86 hours. Thus, total time for the start of fuel uncovering is 17.29 hours from the start of the initiating event. Also for compensation of level decrease during water evaporation it is required to provide water make up at the rate of not less than 2.52 kg/s. The inventory variation in this case is shown in Figure 4.

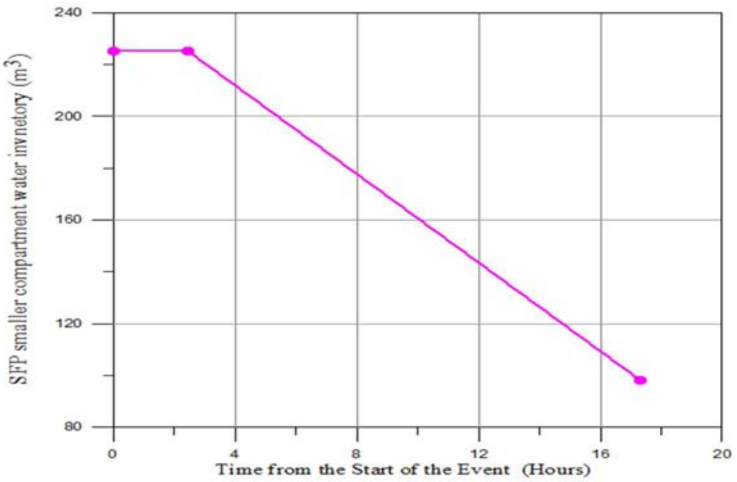

FIG. 4. SFP smaller compartment inventory variation with time.

For Case 2, water inventory of 342 m^3 in the larger compartment gets heated from 50°C to 100°C during first 3.58 h from the start of the initiating event. Thereafter water starts boiling and consequently inventory goes down.

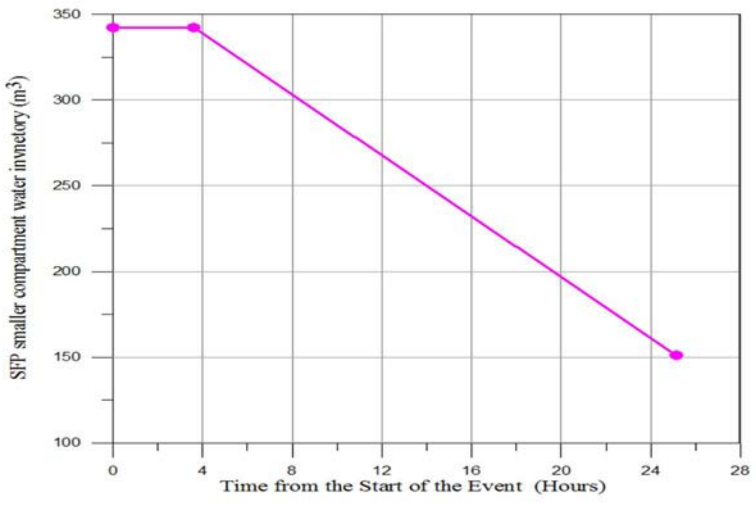

FIG. 5. SFP larger compartment inventory variation with time.

The time from the moment of stoppage of cooling water supply into the SFP (initial water level is 8.9 m above the SFP bottom) till the moment of beginning of the FA fuel part uncovering and SFP make-up water flow rate required for compensation of variation of water level in the SFP (SFP compartments) during boiling away are shown in the following Table.

TABLE 2: SUMMARY OF RESULTS (SFP LOSS OF COOLING)

Case No	Power of decay heat in SFP (MW)	Water flow rate for compensation of level (kg/s)	Time before beginning of uncovering from the initiation of event (h)
1	5.32	2.52	17.29
2	5.49	2.60	25.15

Thus, before 17.29 hours (from the initiating event) it is necessary to provide for connection of water make-up with flow rate not less than 2.60 kg/s for each SFP compartment to prevent fuel uncovery.

4.2. Loss of pool inventory (LOPI)

4.2.1. Causes and description of the event

An anticipated operational occurrence is considered namely a leak of the SFP facing at a rate equal to the rate of possible makeup to SFP (compensable leak) by the system of spent fuel pond water transfer for purification (FAL) system (50 m^3/h).

In case of SFP leak compensation, the water level in the SFP does not go down and a reliable heat removal from the spent fuel is provided. Operator's error is considered resulting from a failure to switch on the FAL system pumps for SFP make-up for leak compensation.

The purpose of the calculation for the considered condition of AOO is the determination of the time available before the fuel damage (beginning of uncovery) in the SFP. It is conservatively assumed that fuel damage in the SFP does not occur if there is no uncovery of the fuel part of the fuel assemblies placed in the SFP.

In the above scenario, the system for primary side emergency and scheduled cool down and SFPcooling (JNA) keeps functioning until water in the compartment (the leaking one) reaches the level for water withdrawal from the compartment. Following this, the supply of cooling water to the spent fuel pond terminates.

The thermal-hydraulic calculation is performed to determine the time before the FA active part uncovery starts in the SFP compartment, for the event of a leak through the bottom of the compartment facing at a rate equal to the flow rate of possible SFP feeding with water (compensable leak).

For the heat load, conservatively, an emergency refuelling a month after the beginning of scheduled refuelling: 163 FA of three-day holdup, 49 FA of one-month holdup and groups of 49 FAs ranging from one year — to eight year holdup have been assumed. Meanwhile, a complete fill-up of the "smaller" SFP compartment with FA (246 pcs.) is conservatively assumed, beginning with FA of three-day holdup (163 Nos) and 49 FAs of one-month holdup along with 34 FA of one-year holdup. The remaining FA (358 Nos) fill up the 'larger' compartment.

4.2.2. Results

For this scenario, the initial water volume of 878.1 m^3 and assuming leak rate of 50 m^3/hr, the time from the moment of initial event (leak initiation, t = 0) until the water level reaches the elevation mark of water withdrawal from the spent fuel pond compartment is 13.2 hours. During this time, cooling is intact and the water level goes down by leak only. Here onwards cooling stops and water temperature starts rising because of decay heat. Furthermore, water level goes down due to the leak and therefore mass of water present at any time varies with time. The time taken from this point to reach the saturation temperature is 0.4 hours. Thus after 13.6 hours from the start of the leak detection water reaches its saturation temperature.

Furthermore, water level goes down due to the leak as well as the evaporation of the water caused due to decay heat and therefore mass of water present at any time varies with time. The time taken from this point until the water level reaches the elevation mark at which fuel uncover starts is 1.25 hours. Thus time from event initiation (leak) until the water level reaches the elevation mark at which fuel uncover starts is 14.9 hours.

4.3 Extended station black out (ESBO)

Following the 2011 accident at the Fukushima Daiichi NPP, possible safety enhancement measures have been evaluated for all NPPs and several measures have been implemented. One of the measures related to make up water provision to SFP for handling extreme external events. For evaluating the makeup water requirements, extended station black out scenario has been evaluated.

During a Station Black Out (SBO), the initiation of continuous water addition to spent fuel pool (SFP) in case of full core unloaded to at the rate of 18 m^3/hr after 6 h of SBO. For the estimation, the decay heat load of 11.3 MW(th) considering full core having decay heat corresponding to sixth day (minimum time required to transfer FAs from Core to SFP) and decay heat load of 8 years spent FAs.

Analysis has also been extended to assess containment response during the postulated extended SBO considering mitigating provisions. This involves addition of water to SFP, (before the fuel rod gets exposed) and consequent assessment of containment pressurization with the boiling of water. Since the SFP is inside the containment, it is important to assess the containment pressurization due to the boiling of water and the time till its integrity can be maintained. Credit is given to only passive structural material for heat removal from containment atmosphere and no leakage from containment is considered.

It is seen that as soon as SBO occurs, cooling of SF pool is lost and the temperature of the pool water start rising. It may be seen that temperature of SF pool water reaches to saturation temperature (Corresponding to prevailing Pressure in the Containment) in 4.44 hours and start boiling. As the water addition into the SFP is started at 6 h, boiling rate reduces, which results in decrease in the rate of temperature rise of pool water as well as temperature & pressure in containment [3].

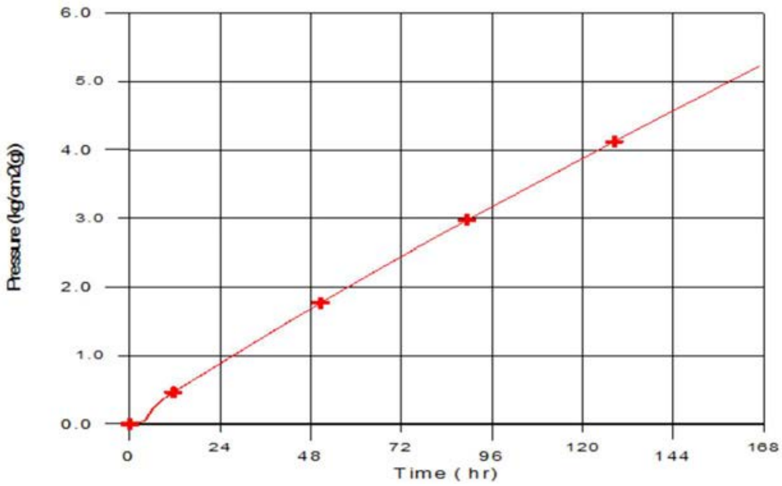

FIG. 6. Pressure in containment (Spent Fuel Pool compartment).

The analysis for the pressure and other thermal hydraulic parameter in the containment has been done for 7 days. It is seen in Figure 6 that the pressure in the containment rises and reaches the design pressure of 4.0 kg/cm^2(g) in approximately in 126 h from the initiation of accident. Further, containment pressure does reaches to 5.2 kg/cm^2(g) in 7 days from the initiation of postulated SBO.

5. USE OF COMPUTER CODE RELAP-5/ SCADAP MOD 3.2 FOR SFP EVENTS

For KKNPP, RELAP-5 is used as one of the safety analysis code for licensing requirements. RELAP-5/MOD 3.2 is a generic analysis code for thermal hydraulic analysis for all type of events which considers a fluid that may be a mixture of steam, water, non-condensable. Presently, the code is used for verification of calculations mentioned in section 3.0 for Spent Fuel Pool related events with the simple lumped modelling. The estimation of duration for mitigation measures have been evaluated with lumped modelling of SFP.

The severe accidents in Spent Fuel Pool are considered as a practically eliminated event and hence the detailed modelling of SFP along with various combinations of spent fuels for fuel melt progression related SFP have not been attempted. However, as part of SAMG evaluation, partial melt consequences and relevant phenomenon can be studied with RELAP-5/SCADAP code. But there are limitations in RELAP-5/SCADAP for capturing the severe accident phenomenon related to SFP. The limitations such as modelling for stratified flows in fully and partially drained pools, spray cooling scenarios, entrainment and detrainment of water droplets, simultaneous flow of air, steam or water droplets through FAs and consideration of air zirconium oxidation phenomenon [4].

6. POSITION OF SEVERE ACCIDENTS IN SFP

6.1. Preventive and mitigative provisions

As described in Section 3, the function of SFP cooling is performed by the emergency and planned cooling down of primary circuit and fuel pool cooling system (JNA). Availability of four independent train increases the availability of the systems and these systems are power by offsite and on-site power supply systems. Over and above, as part of post Fukushima safety enhancement, hook up water make up provisions have been implemented with adequate water supply for 7 days with the conservative Spent FAs heat load. Unlike the Reactor, SFP is a low pressure system and hence threat to containment due high pressure core melt etc also not exist for VVER (SFP is inside the containment). SFPs are low pressure systems and ample time is available for manual intervention to prevent fuel heat up for loss of cooling scenario. Moreover, in VVER, SFP is inside the containment, it adds the advantage of retaining radionuclides and hydrogen management provisions in the containment.

For VVER, containment spray will also act as SFP heat removal system through containment heat removal and SFP evaporation. So multiple means of obtaining power and water needed to fulfil the function of maintaining spent fuel pool cooling presently exist.

6.2. Spent fuel pool accident handling strategies

For SFP, preventive strategies will be the effective way for handling and terminating the accident progression. As mentioned in the previous sections, various provisions and ample operator time is available for the effective implementation of these measures. For SFP, there is no design provisions to handle severe accidents (like In Vessel retention /Core Catcher provision for reactor), so either prevent the fuel melt or early termination of event progression is the effective strategy which will eventually minimize releases of radioactive material from SFP.

In the SFP, badly damage core conditions will have potential challenges to the spent fuel pool structure and hence possibilities reaching preventing this plant damage condition are to be adopted as a good strategy.

7. IDENTIFICATION GAP AREAS FOR FURTHER IMPROVEMENT

It is required to identify additional research activities required to address gaps in the understanding of relevant phenomenological processes, where analytical tool deficiencies exist, and to reduce the uncertainties in this understanding. Events/Event sequences which could be the basis for implementation of improvements to minimize risk of fuel damage need to be further evaluated.

Guidance is needed for dealing multi-unit damage and estimation of leakage for liner crack or any non-compensable leaks.

Effectiveness of use of sprinkler systems as an alternative for cooling in the spent fuel pool, especially for situations with large losses of pool water inventory for PWR need to be studied.

The end state (severe accident safe state) considered for SFP severe accident event progression with fully drained pools need to be evolved.

Guidance is required on the level of detailed modelling to capture the phenomenon related to SFP accident progression, molten corium concrete interaction in SFP and mitigation measures along with modelling aspects. Experimental validation of partially drained pools and related phenomenon need to be studied.

CONCLUSIONS

The Fukushima Daiichi nuclear accident shows that it is necessary to study potential severe accidents and corresponding mitigation measures for the SFP of an NPP. From a spent fuel safety perspective, the low decay heat of FAs and large water inventory in the SFP may make the event progress slow compared to an accident in the core. So for the spent fuel pool, preventive measures are the effective strategy with various/alternate provisions.

Furthermore, as important mitigation measures, the effect of recovering the SFP cooling system and makeup water in SFP on the accident progressions have also been investigated respectively based on the events of pool water boiling and spent fuels uncovery.

The results showed that, severe accident might happen if SFP cooling system was not restored timely before the spent fuels started to become uncovered.

There are potential areas which require additional research activities and to address gaps in the understanding of relevant phenomenological processes and to reduce the uncertainties.

REFERENCES

[1] AGRAWAL, S.K., CHAUHAN, A., MISHRA, A., 'The VVERs at Kudankulam', Nuclear Engineering & Design **236** (2006) 812–835.

[2] AMERICAN NUCLEAR SOCIETY, Decay Heat Power in Light Water Reactors, ANSI/ANS-5.1-2005, ANS, La Grange Park, IL (2005).

[3] Design calculations on Containment pressurization during mitigated SBO due to evaporation of spent fuel pool water along with SAMG in KKNPP (2014).

[4] ZHANG, Z.W., DU, Y., LIANG, K.S. "Advanced modeling techniques of a spent fuel pool with both RELAP-5 and MELCORE and associated accident analysis, Annals of Nuclear Energy **100** (2017) 160–170.

CURRENT STATUS OF ANALYSIS TOOL FOR CANDU SPENT FUEL POOL ACCIDENT IN KOREA

J.Y. JUNG*, J.H. BAE, D.G. SON, J.Y. KANG, E.H. RYU, Y.M. SONG
Korea Atomic Energy Research Institute,
Daejeon
Korea

1. INTRODUCTION

In a CANDU reactor, spent fuel bundles are removed from the reactor core by refuelling machine everyday (typically two channels are refuelled with eight bundles each) and transferred from the fuelling machines into the discharge room through the spent fuel port, then they are transferred to the reception bay and spent fuel storage bay where there is wet storage of spent fuels. Reference [1] describes the overall process about the spent fuel treatment in CANDU reactor and what we have to consider from a safety perspective, as follows.

Spent fuel continues to produce power and emit radiation after it is discharged from the reactor. Therefore, we have to manage heat from the spent fuel and to monitor its activity to remain the safety of the spent fuel. Fortunately, since the power and radiation from the spent fuel decay with time, we can deal with the spent fuel through two phases of storage before final disposal like the following:

– Immediately after its discharge from the reactor, the spent fuel is stored for several years in deep cooling pools adjacent to the reactor.
– After several years of forced-circulation cooling in water, the spent fuel is transferred to concrete containers which are air-cooled by natural convection. The spent fuel can reside in these storage cylinders for up to 100 years before its final disposal.

During the spent fuel is stored in the water pool, we have to focus on some considerations to protect workers and public from radiological exposure from the spent fuels as follows:

– <u>Avoid overheating of irradiated fuel:</u> Even after discharge from the reactor, since spent fuel continues to produce power, the potential temperature increase caused by decay power should be controlled effectively to prevent overheating of both spent fuel and the materials used in the structures which have their respective temperature limits for safe operation.
– <u>Avoid mechanical damage to irradiated fuel bundles:</u> Irradiated fuel bundles are handled remotely by fuelling machines during their removal from the reactor into the irradiated fuel pool, and by operators using remotely operated tools for subsequent transfers. During this transfer of spent fuel, all procedure should be done safely so that the spent fuel bundles are not damaged.
– <u>Limit chemical and metallurgical damage to irradiated fuel bundles:</u> Damaged fuel can release highly radioactive substances into the irradiated fuel bay and also potentially into the air above. Such radiological contamination must be controlled to acceptably low levels to protect the workers and the general public. Therefore, degradation and damage to bundles must be limited to acceptably low levels.

In this paper, a transfer process of the CANDU spent fuel from reactor to wet storage and general aspects of the CANDU spent fuel pool (hereafter, called SFP) are described and a postulated severe accident for CANDU SFP and a former analysis experience regarding the loss of cooling accident of CANDU SFP are summarized. Finally, a current development plan for CANDU SFP severe accident analysis code including the SFP accident phenomena, major modelling issues, program logic and detailed calculation models are to be explained.

2. DESCRIPTION OF SPENT FUEL POOL IN CANDU

2.1. CANDU spent fuel transfer and storage

Fig. 1 shows the schematic process of CANDU fuel transfer from the charging and discharging of the fuel in reactor to the storage at the spent fuel pool. Spent fuel transfer and storage involves three bays filled with light water: the spent fuel discharge room, spent fuel reception bay and spent fuel storage bay (also referred to as the main storage bay or spent fuel pool).

The discharge equipment, which is located in the reactor building, receives irradiated fuel from the fuelling machine and lowers it into the discharge bay. It includes spent fuel ports that interface with the fuelling machine, and elevators to lower the fuel bundles into the water. It also includes the failed fuel canning equipment in the discharge bay, for handling and canning the small quantity of failed fuel.

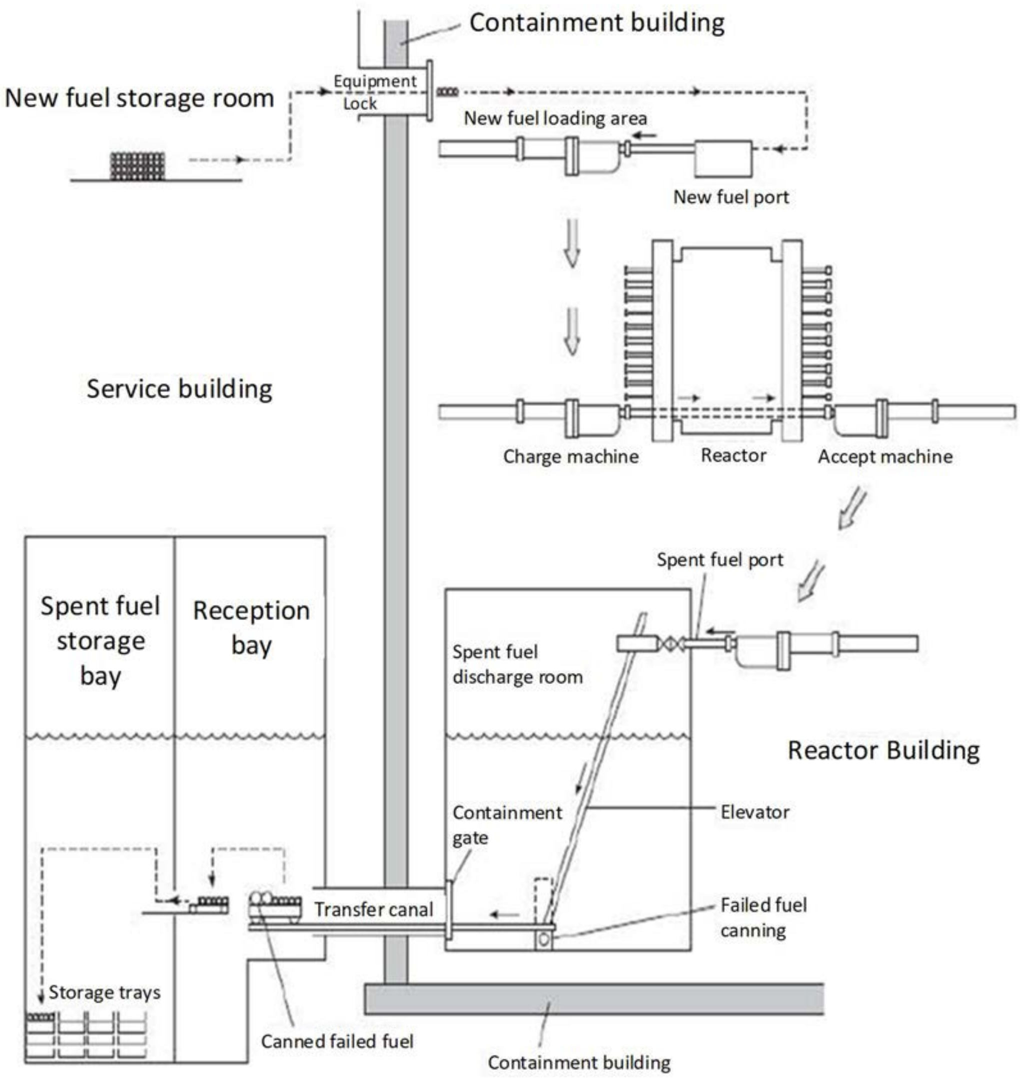

FIG. 1. Flow of fuel transfer in CANDU [1].

The spent fuel transfer equipment provides for the transportation of irradiated fuel from the discharge bay in the reactor building to the reception bay and the storage bay in the service building. It includes the discharge and transfer canal conveyors, the storage tray conveyor as well as tools and accessories for manipulating the fuel in the reception bay. The transfer of irradiated fuel between buildings is under water through a containment gate and a transfer canal, which connects the reception and storage bays under water. The reception bay is connected under water with the main storage bay by the penetration for the storage tray conveyor [1].

2.2. Spent fuel pool in CANDU

Spent fuels transferred from the reception bay are stored onto the storage tray that rests on storage rack. Each storage tray can hold 24 spent fuel bundles in two rows of 12 each. The trays are made of stainless-steel welded construction, with contoured cradle strips to support and separate the fuel bundles and are designed to be stackable. Storage tray supports consist of a diagonally braced, stainless-steel frame to support the stacks of trays.

Recently, considerations have been given to replace the storage trays or racks with storage baskets which are directly transferrable to dry storage containers. Both the trays or racks and the baskets are designed to ensure [1]:

- Adequate cooling of the bundles in the storage bay;
- Avoidance of damage to bundles during their residence in the pool;
- Compliance with safeguards monitoring requirements (e.g., bundle serial numbers are readily visible);
- Direct transfer of bundles (basket only) into dry storage containers;
- Use of the most compact arrangements of bundles in the pool.

FIG. 2. Typical SFP in CANDU [1].

The fuel bay is designed to accommodate spent fuel for 10 years and is designed to accommodate an additional full core discharge of fuel (4560 fuel bundles in CANDU 6). In practice, bundles could begin to be removed from the pool as early as seven years after their placement into the pool, reducing the risk that pool capacity would be reached anytime during reactor life. Spent fuel is received in the reception bay and stored there for one to two weeks. Then it is transferred to the spent fuel pool (long-term storage bay) for a few years. The spent fuel pool usually also has a fuel inspection station where fuel can be inspected underwater, for example to monitor and assess fuel performance. Fig. 2 illustrates a typical spent fuel pool [1]. It is filled with de-mineralized water and has a dedicated purification and cooling system. SFP is in a building that is outside the containment but adjacent to it.

The bottom of the SFP is below grade in service building which is a conventional reinforced concrete structure and a structural steel superstructure with metallic cladding and thermal insulation. A dedicated SFP cooling and purification system serves to keep the fuel covered with demineralized water and cools and maintains water chemistry and activity at acceptable levels. A ventilation system aides in maintaining air quality above the water level. The storage bay and the receiving bay are both provided with a glass fibre reinforced epoxy liner to prevent leakage. A sub drainage system intercepts any leakage and is drained to the sea. This drainage system is isolated from the surrounding water table and is non-nuclear grade, non-seismic qualified system. The base slab and side walls are 1.22 m thick reinforced concrete to satisfy the shielding requirements and the stringent control on crack development because of possible temperature differentials across the wall thicknesses.

Heat must be removed from the fuel bay to maintain water at a predetermined temperature and to continue to provide cooling to the fuel. Generally, SFP with 10 year storage is maintained at under 38°C and with 10 year storage plus one full core load, the pool is maintained at under 49°C. Major cooling systems are a pump, a heat exchanger, and a resin bed. In case of impaired heat removal capability, it is important for safety reasons to determine how much time may be allowed to elapse before auxiliary cooling must be provided.

The IAEA design guidelines for irradiated fuel storage and disposal include a need to assess conditions that could lead to criticality. There are no criticality-based restrictions on proximity of irradiated CANDU bundles in the pool because the remaining fissile content in spent fuel bundles is low enough. Bundles can be placed into the most compact configuration (based on heat transfer considerations only) and do not need to be re-racked during their residence in the pool.

The SFP is not covered by a leak-tight containment. Therefore, consequences of overheating and melting of fuel in the SFP can be very severe. However, due to low decay heat of fuel bundles, the heat-up processes in spent fuel bay are slow in comparison with processes in reactor core during a loss of coolant accident (LOCA) or due to a station blackout initiated loss of heat sinks.

3. ANALYSIS FOR POSTULATED SEVERE ACCIDENT IN CANDU SFP

3.1. General aspects of SFP accident [2]

Severe SFP accidents were originally regarded as highly improbable events, given the calculated time available for the operator to undertake corrective actions. However, the Fukushima Daiichi accident has led to a renewed interest in SFP safety during loss of cooling conditions for a prolonged time.

There are two principle means in which cooling of the spent fuel within the SFP can be lost:

- A malfunction of the SFP cooling system (loss of cooling accident);
- The loss of the SFP water inventory (loss of coolant accident).

While there are some similarities between reactors LOCAs and SFP incidents, it is important to note that SFP incidents tend to progress at a slower rate; this is due to the large water volumes and the relatively low power of the fuel compared to reactor conditions. In terms of potential consequence, it is also important to note that while fuel is in the reactor there are three containment barriers (fuel cladding, primary circuit (in CANDU the pressure tube), and containment building), whilst in the SFP there is usually only one (fuel cladding).

During the Fukushima accident, there was a concern that the SPFs could boil dry and ultimately lead to gross fuel failure. To prevent this, extraordinary measures were undertaken by the station staff to ensure sufficient cooling could be maintained until installation of the alternative cooling system. Such action likely mitigated more severe consequences.

3.2. SFP accident analysis for CANDU

No comprehensive analyses or methodologies exist for CANDU SFP accident analyses. The industry position on incredibility of such an accident and their blanket confidence in accident management capabilities, coupled with lower CANDU fuel decay powers has been the reason behind the publicly stated reasons for inaction on the issue.

The CANDU SFP is vulnerable to Zircaloy fires as they contain densely packed fuel bundles stacked in fish basket like trays and some of these bundles are at relatively high decay power. These geometries, while useful for cost effective under water storage of intact spent fuel are not conducive to their survival in absence of water as a heat sink and cannot effectively promote any air circulation for passive heat removal. Heat removal from within the fuel bundle can easily become a challenge.

3.3. Experience for the evaluation of spent fuel response after a loss of SFP cooling accident for CANDU [3]

3.3.1. Background and assumptions

After the Fukushima NPP accident at 2011, WENRA (Western European Nuclear Regulations Association) requested Cernavoda CANDU 6 plants (Romania) to assess the spent fuel response after a postulated loss of spent fuel bay cooling accident as a subtask of stress test. For this request, a loss of spent fuel bay cooling event was postulated with the following assumptions:

- No make-up water is supplied to the SFP after the initiation of event;
- The minimum shield water volume used is based on the design requirement of the safety marker;
- Each tray layer in the pool is completed filled with spent fuel bundles;
- Designed normal heat load (2 MW) in the SFP is assumed;
- Limited heat removal mechanisms are considered.

3.3.2. Assessment of results and conclusion

Onset of SFP water boiling: Based on the above assumptions, they obtained assessment results for onset of SFP water boiling and uncover time of top layer as shown in Table 1. For a minimum pool water volume and maximum operating temperature, onset of the SFP water boiling for the 2 MW was estimated at 60 h 23 min, or about 2.5 days, after a loss of the SFP cooling.

Onset of Spent Fuel Bundle Uncovering: Then, based on evaporation enthalpy and the heat load, it was calculated that it took an additional 13.3 days for the water to boil-off where the top row of fuel bundles started to get uncovered. At this point, 15.8 days after the event initiation, sufficient pool water cooling might not be available for the top spent fuel bundles.

Pool Water Boiling-Off: For the SFP water with 2 MW and 18 trays stack height upon the onset of uncovering, it took about 7.36 hours to have the top layer of water boiled-off. To have the top three layers of water boiled-off, it took about 23.5 hours. If the full power would continuously heat the remaining pool water, it would take about 5.37 days to have the low level layers uncovered.

TABLE 1. ESTIMATED UNCOVER TIME FOR TOP LAYER [3]

Case	2 MW	2 MW
Bay water surface area (m^2)	235.90	235.90
Shielding water depth (m)	4.50	4.64
Cover water volume (m^3)	1061.5	1093.8
Cover water evaporation time (days)	13.28	13.68
Onset of boiling (days) [a]	2.50	2.50
Minimum decay (days)[b]	15.8	16.2
Notes	19 trays, Unit 1	18 trays, Unit 2

[a] Onset boiling time 60 h 23 min (2.5 days).

[b] Minimum decay time accounting for normal discharge just out of the core upon loss of SFP cooling.

TABLE 2. PARAMETERS USED IN CALCULATION

Parameter	Value	Units
Safety marker	4.11	m
Shielding water for 19 trays	4.50	m
H evaporation[a]	2.26	MJ/kg
Density	958	kg/m^3
Tray height	136.35	Mm

[a] H evaporation = HG–HF = 2.675-0.149

Discussions on Potential Consequence and Mitigation Actions: Based on the assessment results, with a large amount of shield water in the CANDU SFP, as a passive inherent feature, it is expected that there would be no cliff-edge effects till onset of spent fuel uncovering, for a long period (15.8 days for 2 MW heat load) after the loss of the SFP cooling accident. However, if make-up continues to be unavailable with multi layers of spent fuel uncovered over days of weeks, there would be a potential for the consequence getting worse. For example, some parts of the tray would heat up beyond the material strength because of the high temperature of high power uncovered bundle, and experience a loss of integrity. Also, with prolonged high temperature and heavy oxidation, the fuel sheath might not be able to maintain its integrity to retain the fission product inventory inside. However, effective mitigation measures can be taken to prevent these consequences getting worse by restoring power or providing cooling water into the SFP, preferably prior to spent fuel uncovering such as supply of make-up water to the SFP, back-up fire water system or fire truck or mobile pump.

Conclusion: It is estimated that the onset-of uncovering took more than two weeks after a loss of the SFP cooling for the design load. Based on the estimated boil-off rate, a water make-up rate of about 1 kg/s is sufficient to maintain the pool water level for the SFP normal load (2 MW) for evaporative cooling. Hydrogen generation is insignificant as long as the spent fuel remains submerged. With the passive inherent feature of the CANDU SFP, there will be a significant amount of time to take corrective actions using a number of backup design provisions to prevent uncovering of the spent fuel bundles.

4. COMPUTER CODE FOR EVALUATION OF ACCIDENT PROGRESSION AND CONSEQUENCES FOR LOSS OF CANDU SFP WATER INVENTORY

4.1. Modelling and phenomenological issues for CANDU SFP

Once the loss of cooling function or loss of coolant occurs at the SFP, the water in the SFP should be heat-up and evaporated and spent fuel bundles might be uncovered from the coolant until the adequate corrective actions are taken. After the accident begins, we have to understand the following phenomenological issues which may occur in the CANDU SFP [4].

- **Pool Drain:** It estimates the rate of drain of the spent fuel pool as a function of the postulated break size and location and in doing so, incorporates the transient mitigating effect of any recovery pumps. Separate probabilistic analyses describe the range of credible events that can cause a pool drain. For a given break size and location, time of fuel tray uncovery and onset of heat-up are estimated by drain calculations. The results are used to demonstrate the range of times available to the operator to take action. Operator actions to add water to the pool at any time after the onset of break are also modelled.

- **Pool Water Evaporation:** The code calculates water evaporation as a function of spent fuel pool water temperature profile and building atmospheric conditions.

- **Fuel Bundle Heatup:** It estimates the heat-up of all uncovered fuel bundles following uncovery caused by drain. Separate analyses demonstrate that the fuel bundles cannot heat up while they are submerged in water (i.e. the heat removal by natural convection of water is sufficient as the heat flux is typically small). The fuel bundle heat-up calculations are therefore undertaken only after a fuel bundle is uncovered (i.e. water level drops below the top of the bundles). The calculations are undertaken separately for each representative fuel bundle and consider heat removal to the building atmosphere by natural convection. Loss of heat to the building structures by radiation is also considered, with special modelling for the outer fuel bundles that are exposed to the pool walls. The fuel bundles are fairly tightly packed in fuel trays and as such do not present opportunities for air ingress and are thus represented by a single transient temperature of a lumped mass. Surface areas available for oxidation and for heat removal are transiently changed.

- **Air Oxidation:** Early heat-up and thence air oxidation of Zirconium sheaths can start first at bundles freshly removed from the reactor. As a process that is more energetic than oxidation in steam, the exothermic heat can be transferred to adjacent bundles and initiate a runaway reaction that can propagate from one fuel tray to another. This is modelled in the code using several user specified propagation options. Hydrogen generated by air oxidation is coupled with hydrogen generation from other sources such as melt interaction with underlying water.

- **Fuel failure:** It incorporates a number of criteria for fuel failure based on various models including onset of runaway oxidation as a failure trigger. A fuel failure criterion is required to trigger release of gap inventory. Gap inventory releases are important for relatively fresh bundles where iodine have not decayed sufficiently. A coincidental release of ruthenium and fuel fines (aerosols) upon a loss of sheath integrity is also of concern. Creep ruptures are considered as additional failure mechanisms (e.g. 10 hours at 550 °C).

- **Debris Melt Relocation:** It calculates the onset of melting of those fuel bundles whose average temperature exceeds progressively the melting point of Zircaloy, eutectic or uranium. It also calculates the extent and superheating of the melt and its relocation to any underlying water. A range of melt propagation scenarios can be represented by choosing the melt superheat and initial relocation surface (water or underlying structures).

- **Melt quench and hydrogen generation:** It models quenching of melt and the consequential steam and hydrogen production. The thermal and chemical utilization of the melt can be specified externally. It calculates conditions necessary for the amount of steam produced by melt to cause building failure when a full conversion of melt energy to steam is postulated. The total amount of hydrogen that can be produced by a full oxidation of all melt during quench (and air oxidation) is compared to that required to cause a hydrogen burn in the building due to the large mixing volume available. Detailed modelling of individual bundle melt dispersion (e.g. droplet size dependence) and transient quenching is not undertaken within the code but in an external program (OXMELT) whose results are incorporated in the form of derived correlations and relatively simple models to capture the necessary phenomena. These are based on external analyses of quenching of droplets of a specified (e.g. normal) size distribution. Long term hydrogen generation by radiolysis is also modelled.

- **Fission Product Release:** It estimates the fission product release from the fuel bundles upon onset of deformation and upon melting. Up to 20 risk sensitive fission product species are tracked in the sample reference analysis. While these include various isotopes of the noble gases, the iodine and the caesium, other risk sensitive (high magnitude of inventory multiplied by dose conversion factors for ingestion and inhalation).

- **Fission Product concentration in the building:** It calculates the concentration of fission products in the SFP building and their release into the environment upon room pressurization. The computed concentration accounts for releases from the fuel, removal in the building and discharge from the building through leakage. Decay of fission product species is accounted for by using the known half lives in a simple model. Accumulation due to decay from other isotopes is currently neglected.

- **SFP building behaviour:** It calculates building response for the whole building modelled as one node with special considerations to enhanced heat transfer to air and structures in the upper part of the building. Average air temperature, pressure as well as humidity content are tracked. Temperature of concrete structures is also calculated. Discharge into the environment is calculated based on building leakage characteristics prior to the accident. Building failure due to over-pressurization can be modelled by specifying a failure pressure and increase in building leakage area. Building depressurization due to opening of a re-closable panel, if available, at elevated pressures can be modelled as well. Automatic or manual cessation of building ventilation can also be modelled.

- **Mitigating Actions and SFP Building:** It allows for various mitigating actions. The operator may isolate the SFP building at a given interval after an alarm indicating activity release through the ventilation ducts.

- **Fission product release into the environment:** Concentration of airborne fission products in the SFP building is used along with the building pressurization and leakage characteristics to evaluate the integrated discharge into the atmosphere. These data are used by a separate calculation to estimate doses to the public. The amount of fission products released into the atmosphere over specified periods is integrated for further independent dose calculations.

4.2. Structure of the analysis program for CANDU SFP accident

The computer program incorporates a methodology to characterize the thermal hydraulic phenomena and predict response of fuel bundles stored in CANDU SFP to an unmitigated loss of pool water inventory. Such an accident can cause the spent fuel bundles to potentially lose all significant heat sinks and heat-up to temperatures at which runaway oxidation with air can start and propagate. Ensuing deformations and thermo-chemical interactions with steam and air can cause significant releases of fission products if the spent fuel bundle temperatures get raised sufficiently. The special phenomena of interest is highly energetic and exothermic air oxidation and the generation and propagation of Zirconium fires. Given that a series of interdependent phenomena occur during heat-up of fuel bundles located over vast geometries, a dedicated approach to modelling of thousands of fuel bundles within hundreds of closely stacked fuel trays is required to predict accident consequences and mitigation action effectiveness.

A dedicated analytical methodology or even a dedicated computer code has been developing to evaluate spent fuel bundle heat-up transients once they uncovered due to liquid boil-off or draining. CANDU spent fuel bundle power is significantly lower than that of LWR fuel. However, heat-up of tightly packed horizontally placed CANDU fuel bundles with limited are access upon a fuel drain is inevitable. The decay heat is required only to bring the first rack of bundles to a temperature at which a self-sustaining exothermic oxidation process can take over. Thereafter, the bundles that are still relatively cold will also heat-up by association and the reaction can propagate into a Zirconium fire leading to large fission product releases into the atmosphere since the building in which the spent fuel is housed is not a containment.

Evaluation of thermal hydraulic response of the pool, its structures and fuel towers require a number of interdependent calculations including the followings.

– Decay heat distribution in the fuel stacked in the pool based on a specified history of fuel unloading from channels. Pool assumed full of its maximum inventory of fuel;
– Evaporation from pool under forced convection cooling of the room and under stagnant conditions if the ventilation system is lost;
– Draining of the pool due to evaporation, boiling and an accidental drain hole;
– Fuel bundle uncovery transients upon water drain;
– Air natural circulation potential within a stack (tower) in various placement configurations (near free edge, near a wall or enclosed by other stacks);
– Thermal response of individual fuel bundles and storage trays with underlying trays submerged;
– Thermal response of individual fuel bundles and storage trays in air only;
– Hydrogen production, transport and distribution;
– Fuel failure and relocation;
– Fission product release transients;
– Spent fuel bay room response;
– Effect and effectiveness of recovery actions.

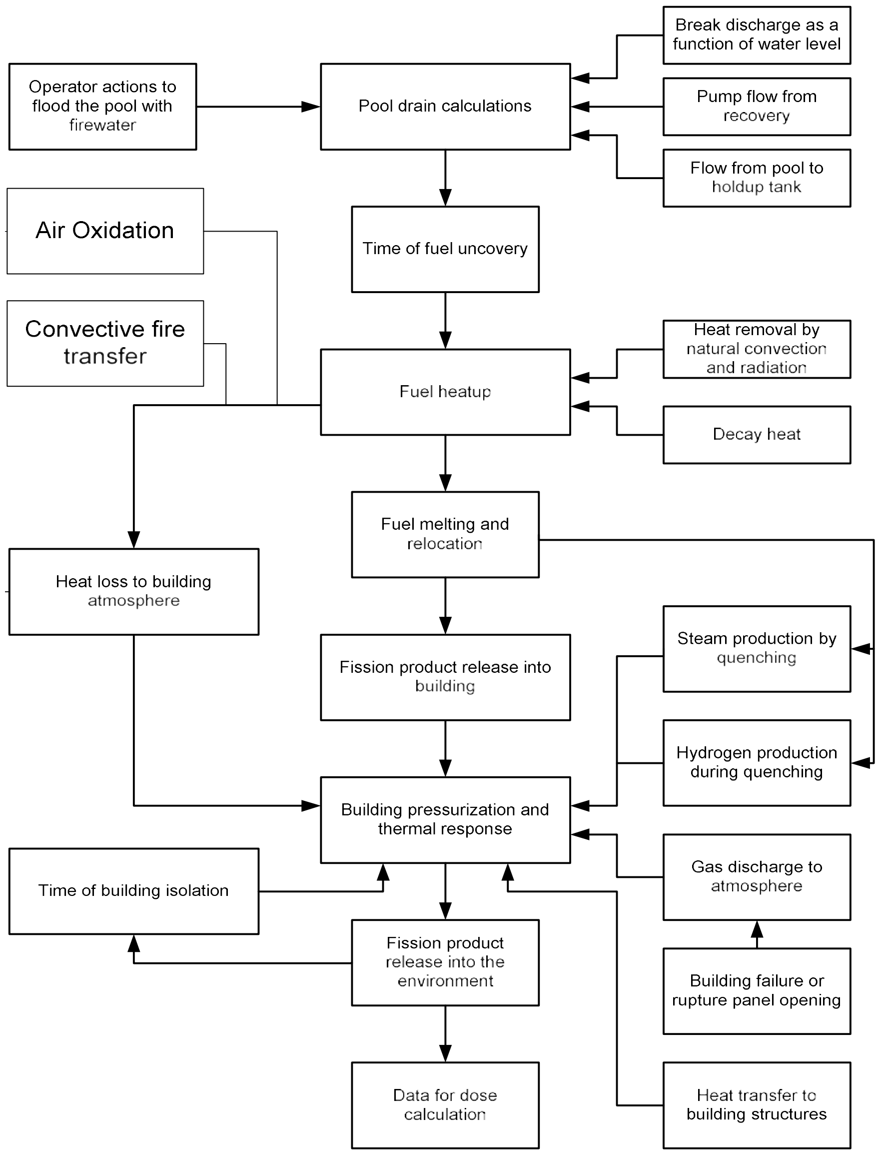

FIG. 3. Program logic for the calculation flow in the analysis code.

Fig. 3 shows the program logic for the calculation flow in the analysis code considering the above phenomena.

4.3. Detailed model of analysis program for each phenomena

Table 3 summarizes the detailed model adopted in the current analysis computer program for each phenomenon occurred during the CANDU SFP accident.

TABLE 3. DETAILED MODEL AND CALCULATION SUBJECTS

Module	Phenomenon	Detailed Calculation
POOL Model	Pool Drain	·Break discharge calculation ·Cooling system interactions ·Evaporation due to forced and natural convection ·Water loss due to boiling ·Bundle and rack uncovery
FUEL Model	Decay Heat	·Decay curve for CANDU fuel
	Fuel Heat-up	·Heat transfer to fluids and structures ·Interaction with underlying water ·Steam and air oxidation
DEBRIS Model	Fuel Melting & Relocation	·Debris interaction with air ·Heat transfer and oxidation kinetics ·Relocation of debris and melt ·Steam and hydrogen production by interaction of melt and debris with water
FISSION PRODUCT Model	FP Release	·FP release into room ·FP release from fuel and debris ·FP deposition in pool
CONTAINMENT Model	Building Pressurization and Thermal Response	·Thermal and mechanical response of walls, roof structure ·Steam and hydrogen production by quenching ·Pressure, temperature response of room air ·Building failure or rupture
CONSEQUENCE Model	FP Release & Dose Calculation	·Debris-concrete interactions ·Zirconium fires ·Recovery modes ·FP release into environment & dose calculation

ACKNOWLEDGEMENTS

This research was funded by the National Research Foundation of Korea (NRF) grant funded by the Korean Government (the Korean Ministry of Science and ICT) [No. NRF-2017M2A8A4017282].

REFERENCES

[1] TAYAL., M., GACESA., M., “Storage and Disposal of Irradiated Fuel”, The CANDU Essential (W.J. Garland, Ed), UNENE, Hamilton, ON, (2014) 16–20 www.unene.ca/education/candu-textbook.

[2] ORGANISATION FOR ECONOMIC CO-OPERATION AND DEVELOPMENT NUCLEAR ENERGY AGENCY, Status Report on Spent Fuel Pools under Loss-of-Cooling and Loss-of-Coolant Accident Conditions, CSNI/R (2015)2, OECD/NEA, Paris (2015).
[3] FAN H.Z., ABOUD R., CHOY E., ZHU W., LIU H., Spent Fuel Response after a Postulated Loss of Spent Fuel Bay Cooling Accident, CNS Bulletin **33** 3 (2012) 26–32.
[4] CANADIAN NUCLEAR LABORATORIES, Phenomena Identification and Ranking Table for a Severe Accident in a CANDU Irradiated Fuel Bay, CW-126800-REPT-001, CNL, Chalk River, ON (2017).

THE IMPORTANCE OF MODELLING FOR SEVERE ACCIDENTS IN PHWR SFPS

Y.M. SONG, J.H BAE, J.Y. JUNG
Korea Atomic Energy Research Institute,
Daejeon
Korea

S. NIJHAWAN
Prolet Inc,
Toronto
Canada

1. INTRODUCTION

A spent fuel pool and its storage racks serve the safety functions of cooling irradiated fuel bundles removed from the reactor, while maintaining them in a sub-critical configuration and providing a safe means of their reception, storage, and removal to a longer term storage solution. The potential for fuel heatup and subsequent Zircaloy fires in overheating fuel assemblies upon a sustained, accidental loss of cooling (and/or cooling water) from spent fuel storage pools is a safety concern [1] and has required special investigations [2] for all reactor designs since the Fukushima accident. CANDU fuel bundles are rather densely stored in stacked, 'fish-basket' like, relatively tightly packed, congested configurations that may severely limit the potential heat removal by the natural circulation of air after a loss of liquid water envelope. Potential exists for significant off site doses, should an accidental and sustained uncovery in air of spent fuel bundles cause energetic reactions leading to sheath failures and releases of radioactive fission products.

For PHWRs, related evaluations have largely been qualitative and primitive, citing the substantially lower than that for LWR decay heat owing to their substantially lower burnup. However, freshly discharged fuel bundles are added almost daily to the pool. Similarly to LWRs, their dense horizontal stacking in tightly packed vertically piled trays creates a potential for adverse consequences following an accidental, sustained fuel uncovery in air. This also makes the effectiveness of any recovery/mitigation measures likely to be very challenging. Thermo-chemically significant oxidation of zirconium in air starts early (at below 600 °C) and is about twice more energetic and appreciably faster than the zirconium oxidation in steam or even pure oxygen [3]. Early nitrogen reactions (also exothermic as with oxygen) produce porous sheath nitride layers, degrade the fuel cladding's 'protective' oxide layer, and accelerate the oxidation [4]. In addition, an energetic, runaway zirconium oxidation signifying a loss of protective layer will start within the 850 °C range in air as opposed to the 1150 °C range for steam. The resulting sharp increases in Zircaloy temperatures and accelerated exothermic oxidation are described as 'Zircaloy fires' that may propagate to adjacent fuel bundles by energy transfer through conduction, convection, and radiation. This may cause cascading fuel failures and large environmental releases of radioactivity, probably more severe than from a severe accident in the reactor itself.

2. ONSET OF ZIRCALOY FIRES FOLLOWING AN ADIABATIC HEATUP OF FUEL BUNDLES IN PHWR

It is estimated that an average fuel bundle that has been out of the reactor for a year will take about 15 hours to reach 1273 °C from their initial temperature of about 583 °C if it is heated adiabatically by its decay heat, and its further heatup is not dictated by its decay heat of about 60 W but an exothermic heat of oxidation of about 750 W for a bundled surface area of reaction of about 0.75 m^2, as enunciated below:

1. In CANDU-6 plants, the average power in a fuel bundle (mass ~22 kg) is about 440 kW (with the highest bundle power reaching 800 kW in a high power fuel channel).
2. According to PHWR decay curve [5], the decay heat at one year after discharge from the reactor is about 0.013%.
3. An average fuel bundle, one year out of reactor, will heatup at a rate of over 40°C/hour in absence of significant heat sinks [6].
4. Thermo-chemically significant oxidation of zirconium in air starts at below 600 °C which an average fuel bundle takes less than 15 hours to reach.
5. After oxidation starts, due to both decay and exothermic oxidation heats, the bundle temperature soon becomes 850 °C at which runaway zirconium oxidation signifying a loss of protective layer will start and an exothermic heat of oxidation becomes about 750 W (Fig. 1) for a bundle surface area of reaction of about 0.75 m^2 [7].
6. At 1250 °C and 1550 °C, air oxidation for a short period can produce up to 7500 and 75 000 watts, respectively, resulting in quick heatup of adjacent bundles and propagation of the fire to adjacent fuel bundles.

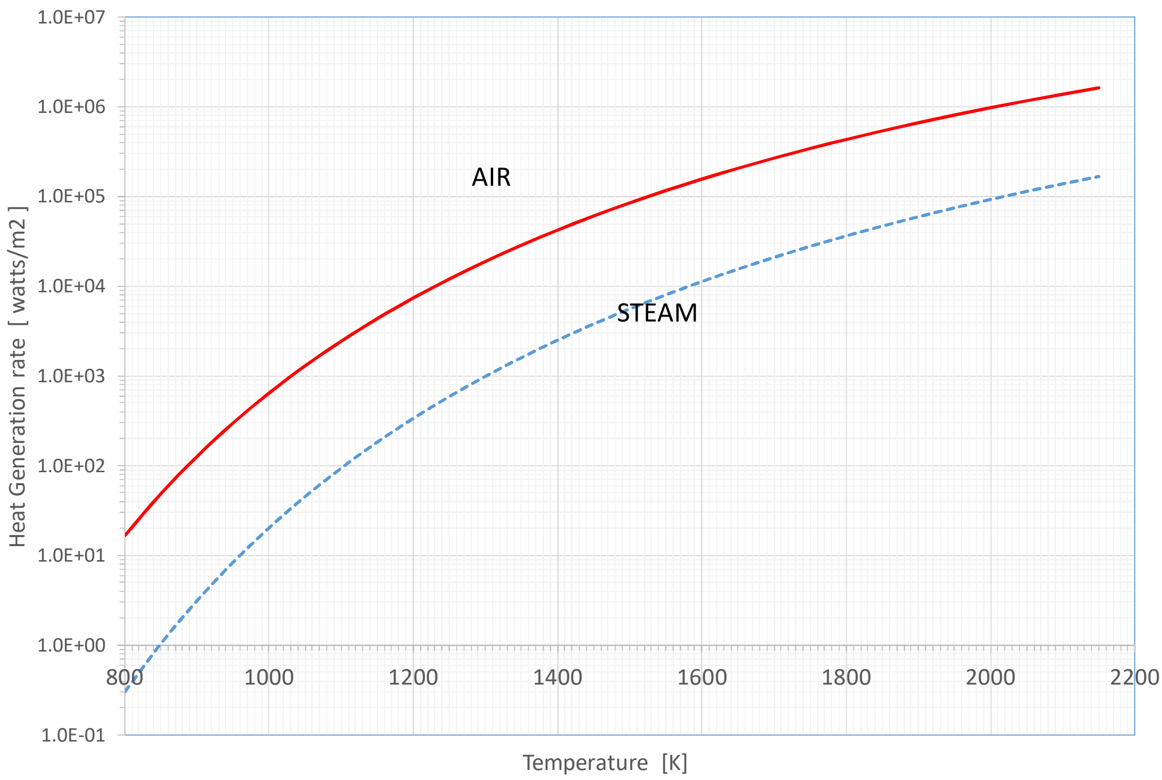

FIG. 1. Oxidation heat generation rates for 50 micron sheath oxide thickness.

The freshest bundles in the spent fuel bay may only be a week out of the reactor. Their decay heat of about 0.2 % for an 800 kW bundle corresponds to about 1600 W. If a half of the heat generated is assumed to be removed instead of adiabatic heatup, after less than 3 hours, the fuel bundle will reach a temperature of 1250°C at which the heat of oxidation (~7500 W) is about 5 times higher than that from the decay heat.

CONCLUSIONS

For an LWR assembly sitting vertically, there is a steam cool-off period after which a drained pool allows heat removal by natural air circulation. In PHWR, even very old (for example, one year old) bundles will get hot if there are not enough heat removal mechanisms for horizontal dense fish baskets. Zircaloy fires starting as earlier as several hours after drainage will propagate to adjacent bundles, as well as similarly overheating, and possibly cause a release of activity into the atmosphere. Furthermore, existing codes (MELCOR, MAAP5) used by LWR industry are not applicable as CANDU bundles stacked horizontally. In this sense, modelling of severe accidents including heat removal mechanisms in PHWR SFPs is very important.

ACKNOWLEDGMENTS

This research was funded by the National Research Foundation of Korea (NRF) grant funded by the Korean Government (the Korean Ministry of Science and ICT) (No. NRF-2017M2A8A4017283).

REFERENCES

[1] LEYSE, M., "Zirconium Fires in Pools of Spent Nuclear Fuel: High-Probability Scenarios and Phenomena", SNL, Atomic Safety Organization, New York, NY (2013).

[2] IRSN, "DENOPI project home page: https://www.irsn.fr/EN/Research/Research-organisation/Research-programmes/DENOPI-project/Pages/DENOPI-project.aspx" (2013–2019).

[3] COINDREAU, O., DURIEZ, C., EDERLI, S., Air Oxidation of Zircaloy-4 in the 600-1000°C Temperature Range: Modelling for ASTEC Code Application, Journal of Nuclear Materials **405** (2010) 208.

[4] DURIEZ, C., Et Al., Zircaloy-4 and M5® high temperature oxidation and nitriding in air, Journal of Nuclear Materials **380** 1–3 (2008) 30–45.

[5] TAYAL., M., GACESA., M., "Storage and Disposal of Irradiated Fuel", The CANDU Essential (W.J. Garland, Ed), UNENE, Hamilton, ON, (2014) 16–20, www.unene.ca/education/candu-textbook.

[6] CHOI, J.W., WHANG, J.H., KIM, K.S., PARK, H.S., Estimation of Decay Heat Generation from Long-Term Management of Spent Fuel, Journal of Korean Nuclear Society **21** 1 (1989).

[7] SONG, Y., JUNG, J., NIJHAWAN, S., Assessment of Spent CANDU Fuel Bundle Behaviour Following a Pool Loss Of Coolant and Consideration of Potential Zircaloy Fires Using KAERI's Dedicated CANDU Spent Fuel Bay Computer Code FUELPOOL, Proc. 2017 Water Reactor Fuel Performance Meeting, Jeju Island (2017).

LITHUANIAN ENERGY INSTITUTE EXPERIENCE ON MODELLING SPENT FUEL POOLS DURING SEVERE ACCIDENT CONDITIONS

T. KALIATKA, V. VILEINISKIS, A. KALIATKA, E. USPURAS
Laboratory of Nuclear Installations Safety,
Lithuanian Energy Institute,
Kaunas,
Lithuania

1. INTRODUCTION

The tsunami that followed the earthquake at the Fukushima Daiichi nuclear plants in Japan [1] showed that a loss of heat removal in the spent fuel pools (SFPs) may lead to very serious consequences. The consequences of such an accident can be very serious creating a possibility of significant amount of radioactive material release to the environment and can possibly be equivalent to the Chernobyl accident, which has been rated at 7 on the International Nuclear Event Scale. This is because SFPs are in general not housed in a containment with the same integrity as the containment around the reactor core and primary pressure boundary. Thus, the loss of water, which leads to the loss of heat removal in SFP may lead to very serious consequences.

In this article the Lithuanian Energy Institute experience and main conclusions on the modelling of SFPs during severe accident conditions are shortly presented. This experience is based on the modelling provided for the Ignalina NPP (RBMK-1500) SFP. In this article 2 cases of the modelling of loss of water in the SFPs are presented related to the Ignalina NPP (RBMK-1500):

- The evaluation of the worst possible consequences, assuming the maximal amount of Spent Fuel Assemblies (SFA) in the pools and the maximal possible residual heat of nuclear fuel. This case with the theoretically maximal possible residual heat in SFP is related to the moment before the shutdown of Unit 2 of the Ignalina NPP for the decommissioning (i.e. at the end of 2009).
- The second analysis was performed for situation - three years after the permanent shutdown of Unit 2 reactor of Ignalina NPP.

2. LOCA ACCIDENT IN THE SPENT FUEL POOLS OF RBMK-1500 TYPE REACTOR

At the Ignalina NPP (Lithuania) two Russian design channel-type graphite-moderated boiling water reactors (RBMK-1500) are shut down for decommissioning (in 2004 and 2009). The RBMK fuel assembly consists of two fuel bundles 3.5 m long, placed one above the other (the core height of RBMK-1500 reactor is 7 m) [2]. The reloaded from the RBMK-1500 reactor fuel assemblies remain in the pool for at least a year, after which they may be removed to be cut in a hot cell. During this procedure the two fuel bundles are separated and placed into the special shipping casks. The shipping casks with spent fuel assemblies are stored in the storage pools until they are loaded into the protective casks CASTOR or CONSTOR to be further transported to the dry spent fuel storage facility.

Each reactor unit at Ignalina NPP is equipped with a system of spent fuel pools. All process of operations related to the handling of the spent fuel are performed in the central hall or in the spent storage pools hall. The spent fuel assemblies, prepared to be cut in the hot cell, are accumulated in a separate pool (compartment ‘234’). After cutting, the Spent Fuel Assemblies (SFAs) are stored in shipping casks in shallow compartments of the storage pool (compartments ‘336’, ‘337/1’, ‘337/2’, ‘339/1’, and ‘339/2’). The non-cut SFAs are stored in deep compartments of storage pool (compartments ‘236/1’ and ‘236/2’). The loading of the shipping casks is performed in two pools (compartments ‘338/1’ and ‘338/2’). Also, there is a transport corridor (compartment ‘235’) for the transportation of SFAs and shipping casks between the pools and the transport corridor (compartment ‘157’) for transportation of fuel assemblies between the spent fuel hall and reactor hall. The fuel assemblies with fuel rods, which lose whey leak-tightness, are placed in a special individual sheaths (for single assembly — two fuel bundles) and stored together with other non-cut fuel assemblies [3]. The whole complex of storage pools of the spent fuel storage and handling system comprises 12 pools. The detailed description of spent fuel pools in Ignalina NPP is presented in Refs. [3] and [4].

The heat removal from the SFAs can be lost due to failure of heat removal system, which uses the pumps and heat exchangers. Such failure can be due to loss of electric power supply (station blackout case). The removal of decay heat from spent fuel also may be disturbed in the case of uncompensated leakage of water from SFPs. The possible consequences of loss of heat removal in the spent fuel pools are analysed in this paper. The analysis was performed using RELAP/SCDAPSIM and ASTEC computer codes. These codes are developed for the analysis of accidents with fuel rods degradation and release and transport of fission product and aerosols.

2.1. Analysis of loss of water accidents at maximal possible residual heat level

Analysis of loss of heat removal accident in the SFPs of Ignalina NPP was performed using the codes for severe accident analysis ASTEC [5] and RELAP/SCDAPSIM [6]. The model developed using ICARE module of ASTEC V2.0R2 code is single pool model with 4 different fuel rod groups. The SFP model for RELAP/SCDAPSIM code is very similar to ASTEC code model, only one difference exists in fuel modelling – all fuel assemblies in RELAP/SCDAPSIM were modelled by one equivalent fuel rod ‘Fuel rod 1’, which represents 7901 SFAs with total decay heat of SFP (4253 kW). The removal of the heat from the SFAs to the outside air through concrete walls of spent fuel pools was evaluated in all models. Total volume of water in the SFP is 5070 m^3. Detail description of the developed models presented in the article [7].

During the analysis of loss of water in SFP it was assumed the initial temperature of water in SFP equal 50°C. The water leakage from SFPs was assumed equal to maximal possible (21.11 kg/s) [8]. The leakage of water leads to water level decrease in the pool (see Fig. 1). The sequence of analysed accident will be the following:

- t= 0 s – initiation of water leakage in the SFP;
- t= 16.67 h – water level decreases down to the top of SFA (fuel uncovering and heat up in air starts);
- t= 59.72 h – water level decreases down to the bottom of SFA (all SFAs are fully uncovered);
- t= 65.28 h – water level decreases down to the bottom of SFP (stop of water leakage from SFP);
- t= 83.33 h – water injection starts;
- t=87.50 h – water level increases up to the bottom part of SFA;

- t=116.67 h – water level increases up to the top of SFA (all SFAs and molten material are cooled down).

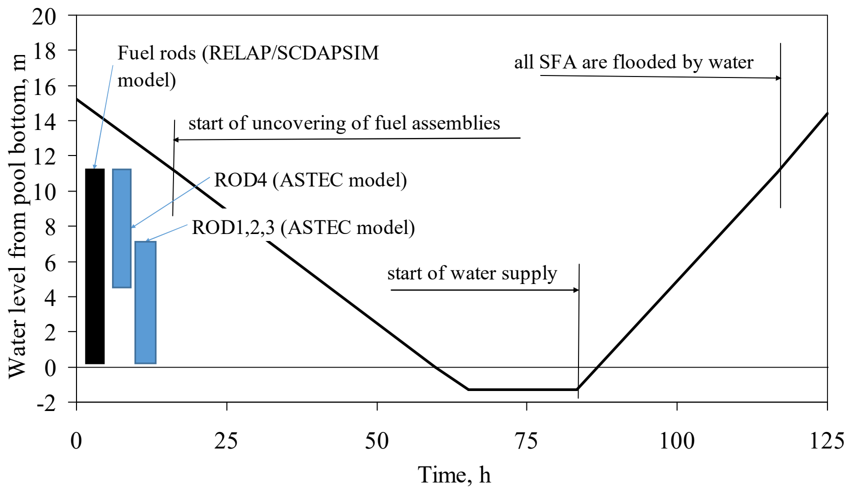

FIG. 1. Behaviour of water level in SFPs (RELAP/SCDAPSIM and ASTEC analysis).

The behaviour of the fuel pellet centre temperatures, and the generated amount of hydrogen, calculated using ASTEC and RELAP/SCDAPSIM codes, are presented in Fig. 2 and 3. The results of calculation show that after the beginning of fuel assembly uncovering (t = 16.67 h), the fuel heat up process starts. The calculated by RELAP/SCDAPSIM fuel temperatures are bounding the temperatures in different groups of fuel assemblies, modelled by ASTEC. The simplified single pool models, developed using ASTEC and RELAP/SCDAPSIM, do not allow to model the natural circulation of air in the spent fuel pools compartments.

The first fuel cladding rupture occurs at ~ 67 h. Maximal temperatures in the upper part of SFAs reached about 2200°C. Fast increase of temperature at t=87.50 h (Fig. 2) occurs due to intensive steam – zirconium reaction after increase of amount of available steam for oxidation. Steam in SFP starts to generate intensively at about 87.50 h when water level increases up to the bottom part of SFA (Fig. 1) and contact with hot SFAs (temperature of the bottom part of SFAs is about 500°C) occurs. The generated steam cools down the SFAs in the very bottom part, because the amount of generated heat there is relatively low.

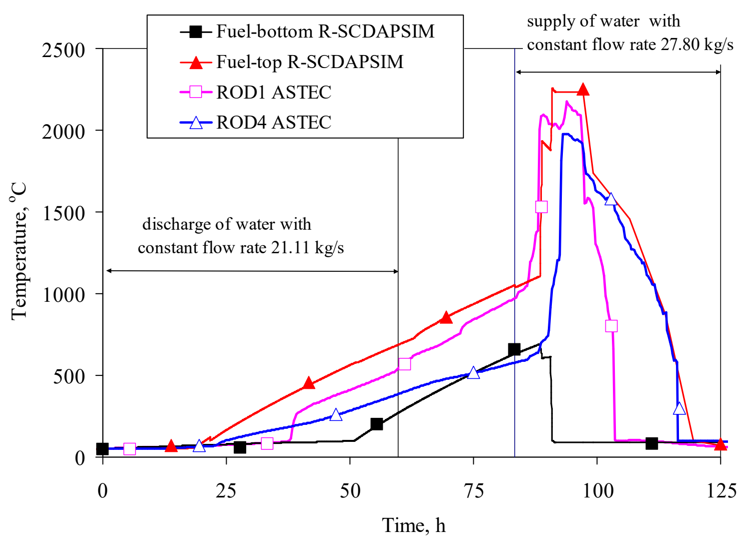

FIG. 2. Fuel temperature in SFAs (ASTEC and RELAP/SCDAPSIM analysis).

In Fig. 3, the comparison of generated hydrogen calculated by different codes is presented. In the ASTEC calculations total amount of hydrogen generated due to Zr oxidation after late supply of water in the SFP is higher as 7200 kg. The maximal amount of generated hydrogen calculated by RELAP5 [9] (assuming the ideal contact of water with the zirconium) is higher – 9100 kg of hydrogen. Both results are overestimated — in RELAP5 calculation the total hydrogen mass generated by the metal-water reaction is calculated by multiplying the mass of zirconium reacted by the ratio of the molecular weight of 4 hydrogen atoms to 1 zirconium atom [9]. Regarding the ASTEC code –it is shown in Ref. [10], that the hydrogen generation in ASTEC code during fuel cladding oxidation at temperature range over 2000°C is overestimated from 10–30%.

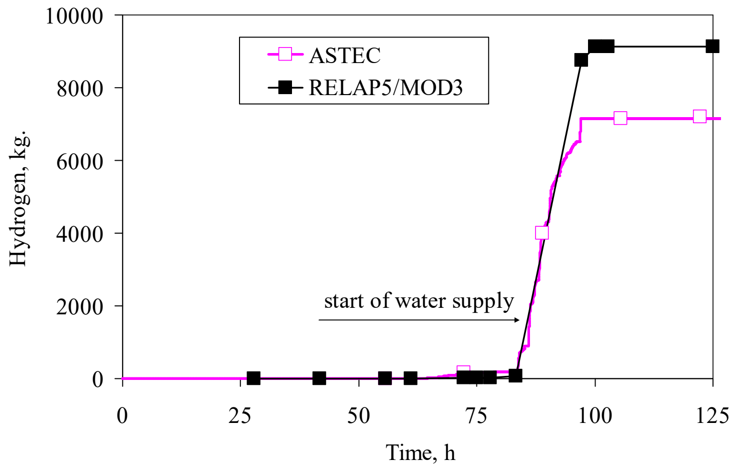

FIG. 3. Hydrogen generation due to Zr and water reaction (ASTEC and RELAP5 analysis).

2.2. Analysis of loss of water accidents in SFP three years after the shutdown of reactor

In this chapter the analysis of loss of water in the SFP of second unit of Ignalina NPP is performed, simulating the situation which was three years after permanent shutdown of reactor. According Ignalina NPP data, the total decay heat in the SFP of Unit 2 in year 2012 was 810 kW. The maximal uncompensated water leak from spent fuel pool (21.1 kg/s) was analysed.

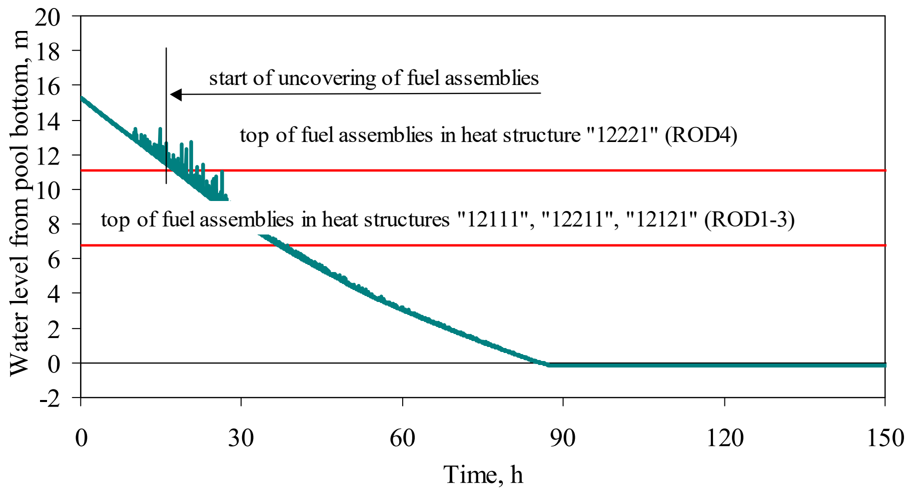

FIG. 4. Water level in SFP in case loss of cooling water (ASTEC).

All parameters, used in calculation: assumed geometry of SFPs, initial level and temperature of water in SFPs, accident scenario and etc. were assumed the same as in the theoretically maximal possible decay heat of spent fuel in SFPs case. It is assumed that operators do not intervene. The analysis was performed using ASTEC code. Because the water is not injected into the SFP, the spent fuel assemblies are cooled by air after pools are empty. The behaviour of water level in the pool and maximal fuel temperatures are presented in Fig. 4 and Fig. 5. As it is visible from Fig. 5, the temperature of fuel in SFAs after the loss of water is increasing, but it is stabilising at the level of approximately 400°C. This indicated that decay heat from the spent nuclear fuel is removed by air and by conduction through walls of SFP building is transferred to outside air.

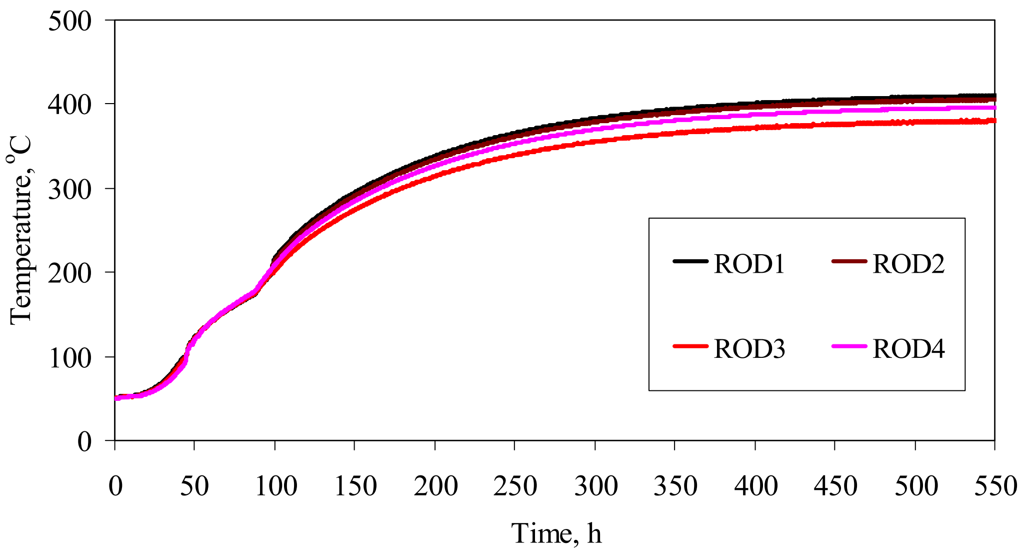

FIG. 5. Behaviour of fuel temperatures in case loss of cooling water in SFP (ASTEC)

CONCLUSIONS

1. This article presents the calculation results of the hypothetical beyond design basis accident in spent fuel pools at RBMK-1500 (Ignalina NPP) type reactor — loss of cooling water, which leads to the loss of heat removal. For the analysis the SFPs models were developed using the RELAP5, RELAP/SCDAPSIM and ASTEC codes. The developed models allowed to model different phenomena: uncovering and heat-up of fuel rods, steam–zirconium reaction, quenching of hot fuel rods by water, etc.
2. The results of the RBMK-1500 analysis showed that:
   - Assuming theoretically maximal possible residual heat of fuel assemblies in SFP (4253 kW), the late operator action can lead to the generation of huge amount of hydrogen, failure of fuel claddings and release of radioactive isotopes to the environment.
   - For the situation – more as three years after the permanent shutdown of Unit 2 reactor of Ignalina NPP. The total decay heat of spent nuclear fuel in SFP of Unit 2 decreased down to 810 kW. In the case of total loss of water, the increase of fuel temperature is very slow. The preliminary analysis using ASTEC code showed that SFAs can be cooled by the air circulation.
3. The performed analysis is useful for the evaluation of different accident mitigation measures.

REFERENCES

[1] http://www.nei.org.

[2] ALMENAS, K., KALIATKA, A., UŠPURAS, E. Ignalina RBMK-1500, A Source Book. Extended and Updated Version, Lithuanian Energy Institute, Kaunas (1998).

[3] KALIATKA, A., OGNERUBOV, V., VILEINISKIS, V., Analysis of the processes in spent fuel pools of Ignalina NPP in case of loss of heat removal, Nucl. Eng. Des. **240** (2010) 1073–1082, ISSN 0029-5493.

[4] ALL RUSSIAN RESEARCH AND DESIGNING INSTITUTE OF COMPLEX ENGINEERING TECHNOLOGY 'VNIPIET', Additional to Ignalina NPP design – safe storage of uranium-erbium fuel with enrichment of 2.8%, No. 03-02499. TASpd-1299-70796, VNIPIET, St. Petersburg (2003) (in Russian).

[5] VAN DORSSELAERE, J.P., SEROPIAN, C., CHATELARD, P., JACQ, F., FLEUROT, J., et. al., The ASTEC integral code for severe accident simulation, Nucl. Technol. **165** (2009) 293–307.

[6] ALLISON, C.M., HOHORST, J.K., Project Report: Role of RELAP/SCDAPSIM in Nuclear Safety, Sci. Technol. Nucl. Install. **2010** (2010) Article ID 425658.

[7] KALIATKA, A., VILEINIŠKIS, V., UŠPURAS, E., Analysis of heat removal accidents during the wet storage phase in Ignalina nuclear power plant, Presented at 26th Int. Symp. on transport phenomena (ISTP26), Leoben, Austria, 27 September – 1 October 2015.

[8] KALIATKA, A., OGNERUBOV, V., VAISNORAS, M., USPURAS, E., TRAMBAUER, K. Analysis of beyond design basis accidents in spent fuel pools of the Ignalina NPP. Proceedings of ICAPP '08, 2008 International Congress on Advances in Nuclear Power Plants, Anaheim, CA June 8–12, Curran Associates, Red Hook, NY, (2008) 1–10, ISBN: 0-89448-061-8.

[9] FLETCHER, C.D., et al., "RELAP5/MOD3 Code Manual User's Guidelines". NUREG/CR-5535, Idaho National Engineering Lab, Idaho Falls, ID. (1992).

[10] KALIATKA, A., VILEINISKIS, V., Best estimate analysis of PHEBUS FPT1 experiment bundle phase using ASTEC code ICARE module, Kerntechnik **76** 4 (2011) 254–260.

SOURCE TERM CALCULATIONS FOR LOSS OF COOLING ACCIDENT AT CANDU SPENT FUEL POOL

M. CONSTANTIN
Institute for Nuclear Research, RATEN ICN,
Pitesti
Romania
Email: marin.constantin@nuclear.ro

Abstract

An investigation of the loss of cooling accident at a CANDU type spent fuel pool is presented. The analysis is intended to understand the potential of the accident to evolve towards a severe accident. The daily refuelling together with the relatively low burnup of the CANDU fuel ensure a large grace time for the intervention (around 2 weeks). Adding make-up water at a flow rate of 1.25 kg/s is sufficient to keep a constant level of water in the pool. However, in case of the refurbishment process (replacement of fuel channels to extend the plant life) a full core is discharged. The potential of a loss of cooling accident to evolve towards a severe accident was detailed investigated by numerical simulation using some of the modules of the ASTEC code. The main results consist of the transfer fraction for the most important elements of the source term.

1. INTRODUCTION

One of the peculiarities of CANDU type reactors is the use of the natural uranium. Due to the low reactivity reserve, heavy water is used both as coolant and moderator, instead of light water. On the other hand, in order to keep the required level of core reactivity a quasi-continuous refuelling is necessary. Due to practical considerations of the work scheduling and equipment maintenance the replacing of some fuel bundles and a reshuffling is daily performed. In CANDU the fuel is structured in short fuel bundles (approximately 50 cm long).

The core is structured in horizontal fuel channels cooled by high-pressure heavy water. The fuel bundles reside inside the channels. During refuelling, the fresh fuel bundles are inserted usually in the same direction as the coolant flow, and the spent fuel bundles are extracted from the same fuel channel.

Typically, 12 to 16 fuel bundles are extracted from the core and replaced, each day [1]. As a routine refuelling, for a fuel channel 4 or 8 bundles are unloaded and replaced by new fuel, therefore some fuel channels are involved daily in refuelling operations.

Two fuelling machines operating in tandem are used to load (the ‘charge’ machine), respectively unload (the ‘accept’ machine) the fuel bundles. Due to the bidirectional flow in two adjacent channels the machines have to reverse their charge/accept roles. After the unloading of the spent fuel bundles the “accept” machine delivers the irradiated bundles to the irradiated fuel port.

It has to be noted the horizontal orientation of the fuel bundles during the operation is maintained also for all the movements and finally for the wet storage since this is the design orientation.

Due to the relative low burnup, and also due to the daily refuelling the inventory in the spent fuel pool of CANDU type plants, and consequently the residual power, is reduced in comparison with a plant using enriched uranium. However, in some circumstances, such as the discharging of a full core during refurbishment process, the evolution of the spent fuel pool

(SFP) should be detailed investigated. The paper presents simulation results based on the use of some of the modules of ASTEC [2] source term code.

2. DESCRIPTION OF CANDU TYPE SPENT FUEL POOL

The design, layout, and dimensions of the spent fuel pool of CANDU differs from one to another plants, but almost all are structured in three sections: (1) the reception, (2) the main storage, (3) the transfer bay. A schematic view is presented in Figure 1. The spent fuel bundles unloaded from a channel will be transferred from the refuelling machine, which contains heavy water, to the spent fuel port, and through an air-cooled interlock and elevator at atmospheric pressure, to the spent fuel discharge room. The movement of bundles through the atmosphere is strictly timed to prevent the overheating. Accidents in relation with the fuel bundle handling is defined (for example. End Fitting Fuel Failure or fuel transfer accident).

The spent fuel bundles are transferred through the transfer channel outside the containment in the reception of the SFP, and after that to the main storage. Here, the bundles are horizontally stored in storage trays which rest on the storage racks. The racks are immersed deeply in a pool with light water. Usually there are 6 to 8 m height of water in the pool in order to ensure the radiological shielding.

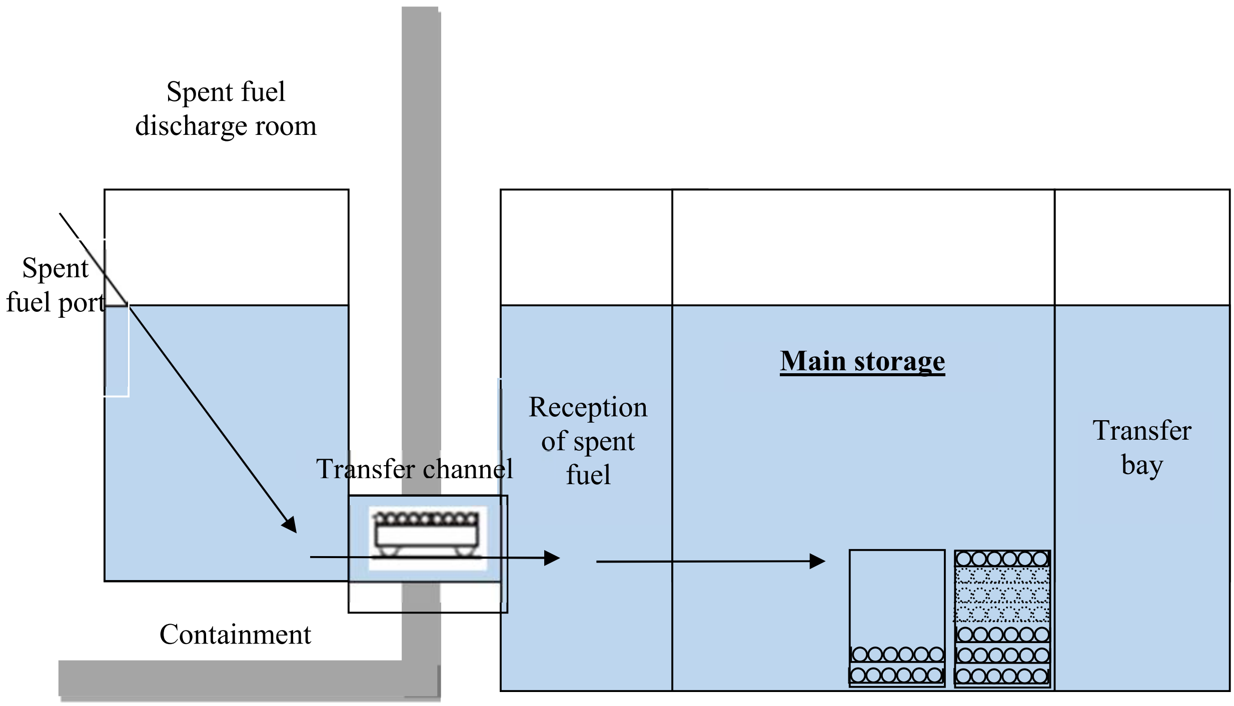

FIG. 1. Simplified scheme of the spent fuel wet storage arrangement.

For CANDU plants there are different sizes of SFP, from small ones (20 × 12 m) to the large ones (34 × 17 m) [3]. The structure of the pool consists of a double-walled reinforced concrete. Usually the reception bay has a volume of around 700 m^3, and the main storage a volume of around 2000 m^3 [1].

Generally, the dimensions of the SFP are chosen to accommodate around 50 000 spent fuel bundles (equivalent of 10 years of planned operation) and, additionally, a full core (4560 bundles) for the refurbishment operation (aimed to extent the plant life).

The residence time of the spent fuel bundles in the main storage is 7 to 10 years, depending on the unit design and the strategy adopted for the intermediate dry storage. After this period the bundles are transferred to a dedicated dry storage where they reside around 50 years before the transfer to the final disposal.

The decay heat produced by the spent fuel bundles is removed by a dedicated cooling system. The residual power decreases systematically. For example, the residual power per bundle at the reception in the SFP represents around 5.8% of the power, 1.3% after 1h and 0.3% after a week. The low burnup (7000–8000 MWd/tU) of CANDU fuel bundles together with the daily refuelling reduces the risk of accidentally fuel bundles into the atmosphere by water pool evaporation. Moreover, the storage procedures are developed to minimize this risk by storing the most recent unloaded bundles at the bottom of the racks.

From the point of view of the SFP inventory it should be noted that the spent fuel bundles are progressively accumulated in the first 7–10 years of operation of the plant. After this period, the transfer of spent fuel to the dry storage is performed, and the inventory reaches a stagnant state, denoted as the equilibrium inventory of SFP.

In CANDU type reactors the fuel channels located into the core are affected by irradiation and after around 30 years of operation (more exactly after 210 000 hours of operation at rated output, the limit is referred as effective full power hours, EFPH) have to be replaced by re-tubing operations in order to extend the plant life with another 30 years period. This refurbishment is made after unloading a full core. This large batch of spent fuel will be stored in the SFP and will lead to a case with larger potential to evolve to a severe accident in case of the loss of cooling.

3. THE ACCIDENT AND THE ASSUMPTIONS

The paper investigates an accident of total loss of cooling at a generic SFP of a CANDU type plant. The purpose of the investigation is to estimate the potential of release of the fission products (FPs) at the level of SFP room atmosphere, and later (filtered or not) into the environment.

In case of a partial or total loss of cooling a progressive heating of the water will occur. Further after the boiling, the water level in the pool will decrease continuously and after a time the fuel bundles placed on the top trays will be uncovered. An increase of the fuel cladding temperature will occur, with a rate dependent on the irradiation history and the residence time in the SFP. A failure of the cladding may follow and consequently a release of fission products (FPs) in the SFP room, starting with the volatile content of the gap and continued, later, after enough heat up, with other radioisotopes contained in the fuel pellets.

At the same time a deformation of the fuel racks may occur under the temperature effect and also changing in the load structure causing mechanical failure. The collapsing of the racks structures could temporarily re-submerge the fuel bundles.

The released FPs will be transported in the atmosphere of the SFP room suffering different phenomena and after that may arrive into the environmental atmosphere if a path (filtered or not) is open.

The following assumptions are used in order to produce the model of the accident and to generate the source term:

(1) A total loss of cooling occurs;

(2) The SFP inventory is at equilibrium and, additionally, a full core was unloaded and transferred in the main storage, as a consequence of the refurbishment operation;

(3) All the unloaded fuels were considered having an average discharge burnup of 7400 MWd/tU;

(4) The pool was represented in cylindrical coordinates with an equivalent radius of 17.34 m; the water deep was considered as h=7.57 m; the fuel bundles are stored on trays at elevations $z \in [0.0, 2.0]$ m;

(5) Accidentally some recent unloaded fuel bundles were placed at the top of the tracks;

(6) The initial temperature of pool is 400°C, and the initial temperature of the atmosphere of the SFP room is considered as 380°C;

(7) The connection of the SFP room with the environment may be filtered with efficiency depending on the isotope, and defined as input parameters;

(8) In order to investigate the mitigation of the accident, a make-up water adding option was considered, for some circumstances;

(9) The following cases were investigated:

(C1) – reference case: equilibrium inventory (after first 7 y of operation), no make-up water;

(C2) – reference case, but with adding make-up water after the water level in the pool decrease at an elevation of 5.00 m;

(C3) – refurbishment reference case (A): equilibrium inventory (after 30 y of operation) and additionally a full core was discharged with a rate of 10 channels (120 fuel bundles) per day;

(C4) – refurbishment case B: same as A but with 15 channels/day;

(C5) - refurbishment case C: same as A but with 20 channels/day.

The three cases for the refurbishment was chosen based on technical constraint of the discharging (timing of the refuelling machines) and the needs to reduce the refurbishment duration (for better economics).

4. THE METHODOLOGY

This investigation is based on some modules of the source term integral code for severe accident simulation, ASTEC [2]. The code was developed by IRSN and GRS and was originally developed for PWR type reactors. Later it was extended to all the plants existing in Europe Union (PWR, VVER, BWR, CANDU) [4, 5] in the frame of SARNET [6] and SARNET2 [7] Euratom projects.

Additionally, the ORIGEN code [8] was used to calculate the inventory in the spent fuel bundles and the corresponding residual power per bundle and its time evolution.

ASTEC code is developed in a modular manner. Each module may be used in stand-alone option or the user can select a set of modules to work in a coupled calculation. The coupling is achieved through a database (DB) where the parameters are stored at each macro time step. The modules exchange data regularly with the DB. A simplified scheme of the methodology is presented in Figure 2.

For the investigation presented in this paper the following modules of the ASTEC code were selected:

(1) ICARE [9] module. In the ASTEC code, ICARE is the module responsible with in-vessel core degradation simulating the behaviour of in-vessel structures as well as the chemical interactions. In the present paper ICARE is used is used to simulate the degradation of fuel bundles accidentally exposed in air and the release of different radioactive elements.

(2) CESAR [10] module. In the ASTEC code, CESAR is the module in charge of the thermal hydraulics for the primary and secondary circuits. The module is based on a set of conservation equations for the mass, energy for the liquid and gas phases, and momentum for the two-phase mixture. The mechanical non-equilibrium is simulated by a set of drift correlations and it is represented by interfacial heat transfer models. In the paper, CESAR is used to simulate the thermal hydraulics of the pool, including the addition of make-up water in order to mitigate the accident.

(3) SOPHAEROS [11] module. In the ASTEC code, SOPHAEROS models the fission product and, also, the structural material transport and deposition. The involved models include vapour-phase phenomena, vapour interactions with structures (condensation, sorption) as well as numerous aerosol deposition and agglomeration mechanisms. In the paper SOPHAEROS is used to simulate the transport of FPs in the SFP room and through the junctions to the environment.

(4) CPA [12] module. In the ASTEC code, CPA has the role to simulate all relevant thermal hydraulic processes and plant states during severe accidents in the containment. The code considers the different interactions between the relevant phenomena necessary for best estimate integral code calculations. The results include the gas distribution, pressure built up, hydrogen combustion, behaviour of safety systems, chemistry in the containment, etc. In the present paper CPA is used to simulate the evolution of the thermal hydraulic conditions in the room of the SFP.

(5) IODE [13] module. In the ASTEC code, IODE is devoted to simulate all the phenomena of iodine and ruthenium chemistry in the reactor containment during a severe accident. For the present paper, it is used for the chemistry of iodine in the SFP.

(6) ISODOP [14] module. In the ASTEC code, ISODOP computes the isotopic masses based on the fission products release estimated by other modules and the solution of the

decay equations. Also it provides power and activity of each element. For the present paper, it is used to estimate the isotopic structure of the source term in the environment.

(7) DOSE [15] module. In the ASTEC code, DOSE calculates the dose rate in bulk gas phase for each zone of the containment, as well as the inner wall dose rate. The dose rates include β and γ radiation contributions relative to each isotope. In the present paper it is used to calculate the doses in the SFP room.

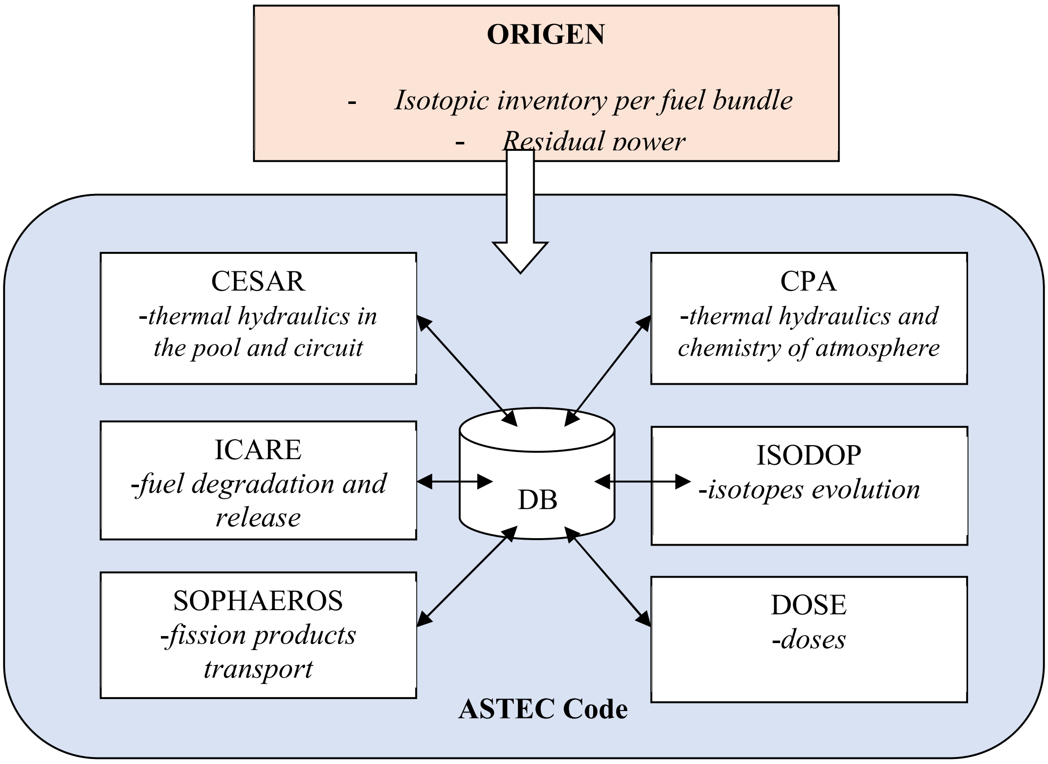

FIG. 2. The codes and modules used in the methodology.

5. RESULTS AND DISCUSSIONS

The evolution of the residual power and inventory for was calculated by ORIGEN code considering the fuel bundles unloaded at the same average burnup of 7400 MWd/tU. The daily refuelling of CANDU type reactors increase the complexity of the fuel bundle inventory types in the pool. In order to obtain an acceptable approximation for the residual power and for the inventory, the interval (0, 7) years was divided into non-uniform steps, with very short intervals for the first days, and after that with a progressive relaxing of the interval size.

For the sake of simplicity, the residual power values are represented as fractions from the normal operational power. Briefly the residual power represents: (1) 10.3% at discharge, (2) 5.8% (at reception in SFP), (3) 1.3% (after 1 h), (4) 0.6% (after 1 day), (5) 0.3% (after 1 week), (6) 0.15% (after 1 month), (7) 0.015% (after 1 year), (8) 0.002% (after 6 years), (9) 0.001% (after 10 years).

TABLE 1. RESIDUAL POWER ADDED BY A FULL CORE DISCHARGED DURING THE REFURBISHMENT PROCESS

Case	Discharge	Added residual power due to the core discharge at a specific time after the complete unloading	
		T [days]	P_res [W]
C1	10 fuel channels/day (120 fuel bundles/day)	0	4.38E+06
		1	4.12E+06
		2	3.89E+06
		3	3.75E+06
		4	3.64E+06
C2	15 fuel channels/day (180 fuel bundles/day)	0	5.05E+06
		1	4.67E+06
		2	4.33E+06
		3	4.14E+06
		4	3.98E+06
C3	20 fuel channels/day (240 fuel bundles/day)	0	5.66E+06
		1	5.16E+06
		2	4.70E+06
		3	4.45E+06
		4	4.25E+06

The most important parameter for the first phase of the SFP accident (the progressive heating of the water in the pool) is the total residual power due to the isotopic inventory. It was estimated for the reference case at 3.3 MW and is only slightly dependent on the time after the accident start. This is valid for the cases C1 and C2 defined in a previous section. For the cases C3, C4, and C5 additionally to the 3.3 MW, the residual power of the last core discharged for the purpose of the refurbishment have to be added. This part is more dependent on the time. Exemplificative results are presented in Table 1, limited to the variation during the first 4 days after the end of the completely discharge of the last core.

In the absence of the cooling, the residual power will increase the temperature of the water. The evolution of the temperature of water from the SFP, obtained by ASTEC simulation (CESAR module) is presented in Fig. 3. The saturation temperature is reached after around 8 days from the start of the loss of cooling accident at the SFP.

The next critical point is the reaching of the state with uncovered fuel bundles due to the evaporation and boiling of the water. In case C1 the result of the simulation presents an interval time of 13.5 days to decrease the water level until the elevation of 2.00 m, where the uppermost fuel bundles are stored. In Ref. [16] this interval time is estimated at 15 days. On the other hand, the reaching of the threshold for radiological alarm (1.7 mSv/h) is estimated at 9 days [16] after the start of the accident. Both the interval times are appreciated as enough large to manage the accident based on the APOP (Abnormal Plant Operating Procedure).

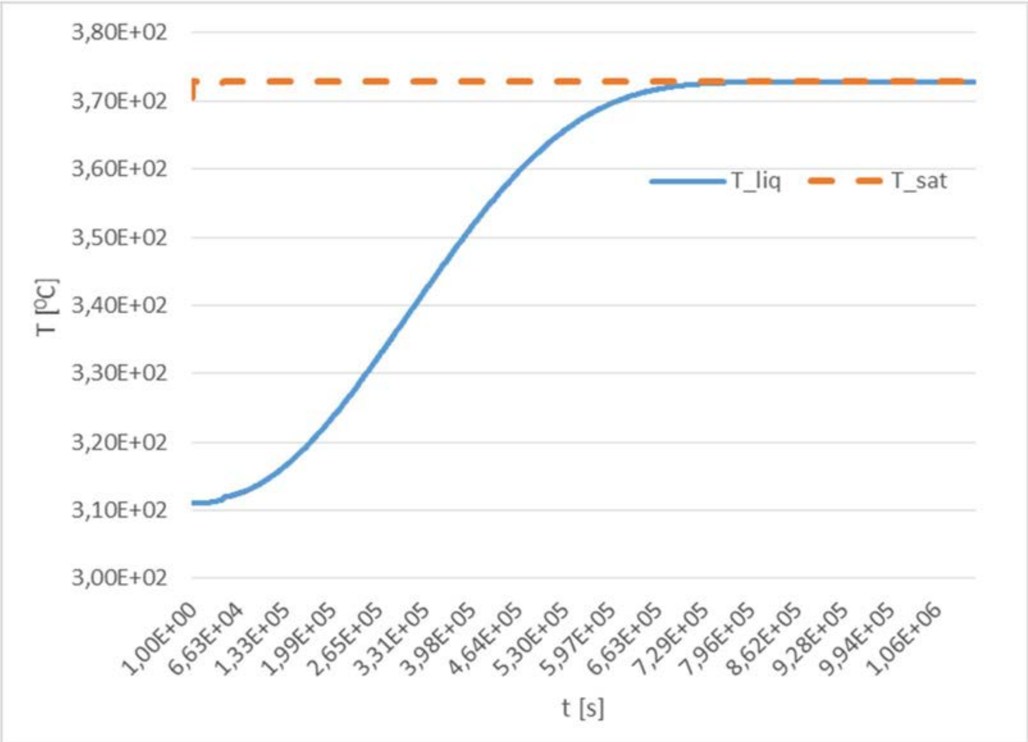

FIG. 3. The evolution of the temperature of water in the pool, case C1 (reference).

As a consequence, no fuel failure and no radioisotope release are credited for the loss of cooling at the SFP. Also the hydrogen production is not considered based on the estimated evolution of the temperature. Moreover, by adding make-up water the accident may be stopped preventing the appearing of a radiological alarm and the release of radioisotopes in the room. In Ref. [16] it is appreciated that a flow rate of 1.0 kg/s of make-up water is needed.

In the present paper the initiation of the adding make-up water was considered (case C2) at the moment when the level decrease below the elevation of 5.00 m (after 6.8 days after the start of the accident). The estimations by CESAR show that a flow rate of around 1.25 kg/s is needed to keep a level constant (at 5.00 m). In Figure 4 the evolution of the water level until reaching the 5.00 m elevation and after that, by adding different flow rate of make-up water, is presented.

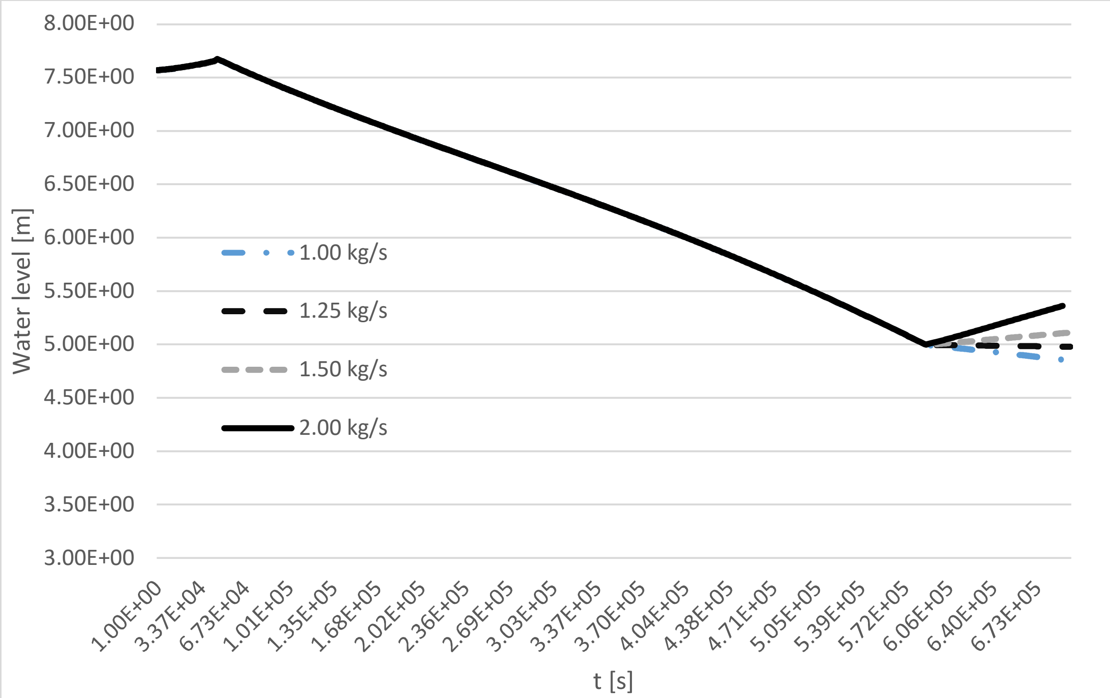

FIG. 4. The evolution of water level in the SFP, case C2.

For the refurbishment cases (C3, C4, and C5) the duration until the uncovering of the highest plane of fuel bundles is shorter than the reference case (C1). The results are presented in Table 2. However, even in the worst case (C3) there are around 5 days until the uppermost fuel bundles will be exposed in air. By adding make-up water, the accident may be stopped. CESAR calculations show that a flow rate of 2.7 kg/s is enough to keep the level at 5.00 m (the supposed intervention level).

TABLE 2. DURATION FROM THE START OF LOSS OF COOLING UNTIL THE WATER LEVEL DECREASE AT 2.00 M

Case	Duration [days]
C3	5.49
C4	5.15
C5	4.88

In Figure 5 the evolution of the temperature of water in the pool, cases C3, C4, and C5 is presented.

Supposing the lack of make-up water the investigation continued with the behaviour of the spent fuel bundles exposed in the air. The ICARE module of ASTEC was used to estimate the time for the cladding failure and the evolution of the release. The influence of different parameters on the release fraction was investigated in Ref. [17]. The critical parameters are: (1) the residence time in the SFP (interval time from the unloading from the core to the accidentally entering in the atmosphere), (2) the flowrate of the convection on the cladding surface.

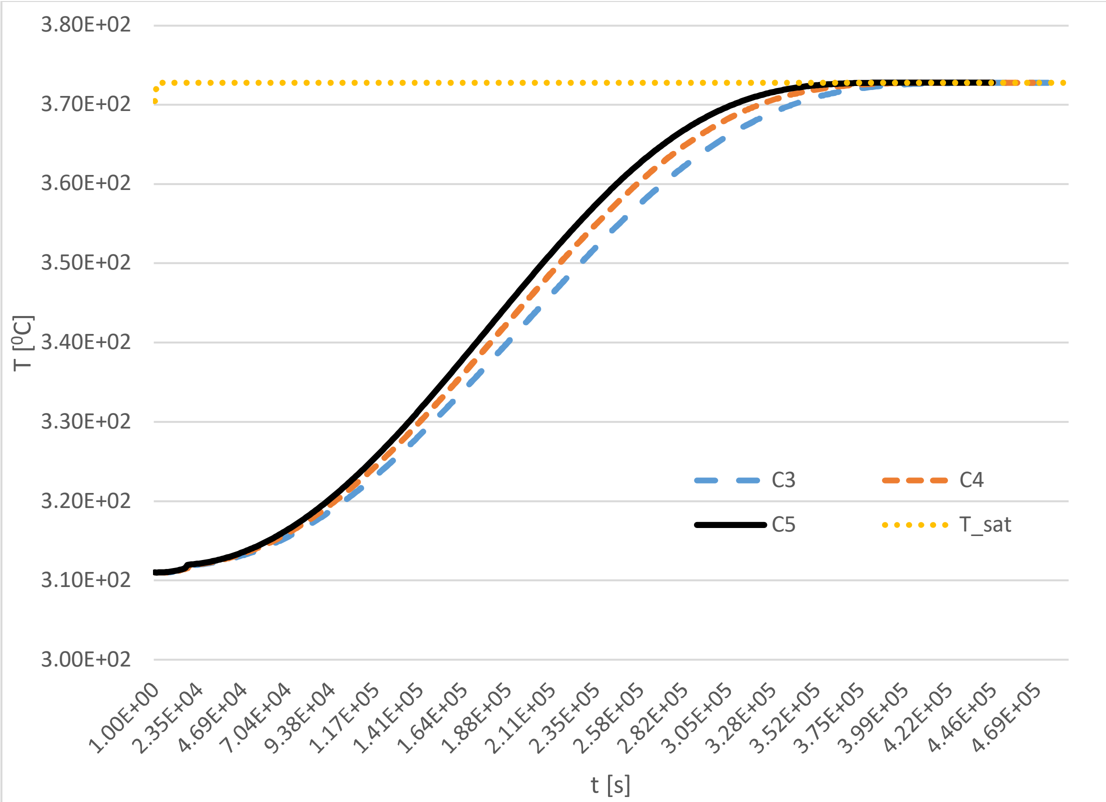

FIG. 5. The evolution of the temperature of water in the pool, cases C3, C4, and C5.

In Figure 6 the release fractions of Cs element are represented for different spent fuel bundles accidentally in the atmosphere. The typology of the bundles was reduced, based on the time intervals spent from the discharge until the accidentally entering into the atmosphere, to the followings: (F1) 7 days, (F2) 1 month, (F3) 1 year, (F4) 3 years.

In order to present the influence of the residence time the convection was supressed, and only radiation is the mechanism of heat evacuation. The main result consists of the interval time needed for the cladding failure: 1.7 h for F1, 3.6 h for F2, 1.5 d for F3. In case of F4 no cladding failure occurs in the first 5 days. In fact, the residual power of a F3 bundle is around 20 W. In this case it seems the radiation transfer is enough to keep the temperature under the threshold failure value. Another important result presented in Figure 6 is the maximum release for the Cs (around 80%), in the condition of overheating of the fuel elements in the absence of cooling by convection.

The influence of the convection (considering natural or forced ventilation in the SFP room) is illustratively presented for fuel bundles F2, in Figure 7. For such a fuel having a residual power of approximately 700 W a velocity of the convection larger than 0.22 m/s is sufficient to keep an intact cladding. Even for recent unloaded fuel bundles (F1, 7 days) a velocity of the convection greater than 0.48 m/s [17] ensures enough cooling and no release occurs.

The released radioisotopes will suffer transport phenomena in the SFP room and if a communication with the environment is opened, a fraction of them will be transferred to the environment. In the present paper it was supposed that the convection is not able to stop the fuel cladding failure.

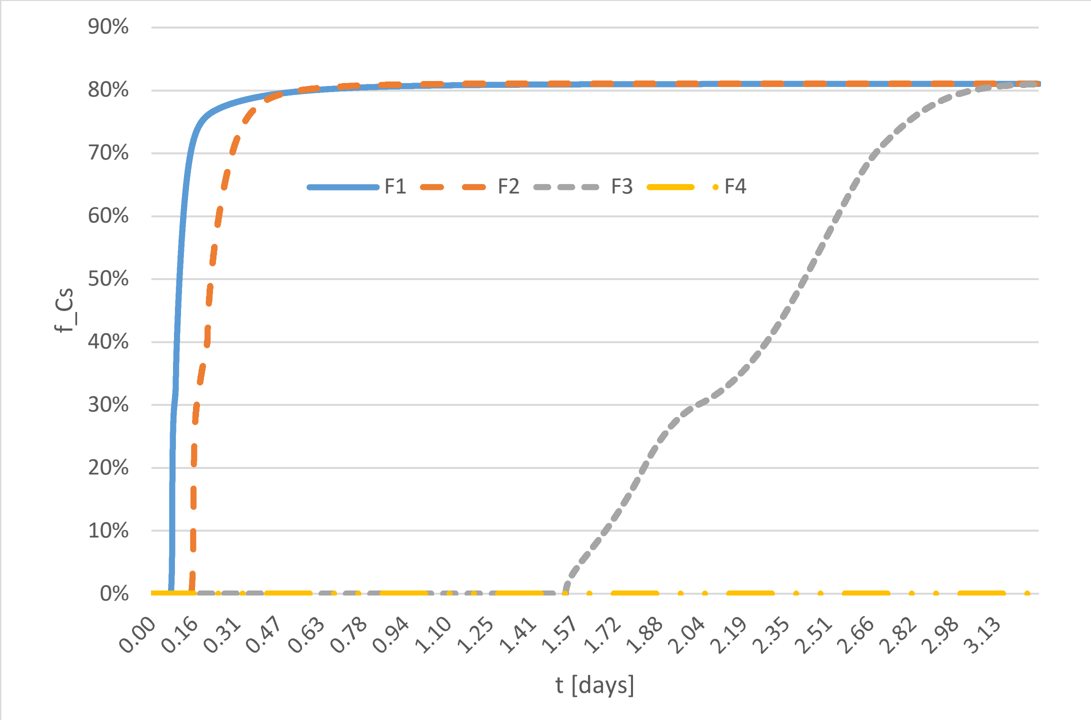

FIG. 6. Release fraction of Cs element, for fuel bundles (accidentally in air, no convection, only radiation) with different residence time (7d (F1), 1m (F2), 1y (F3), 3y (F4).

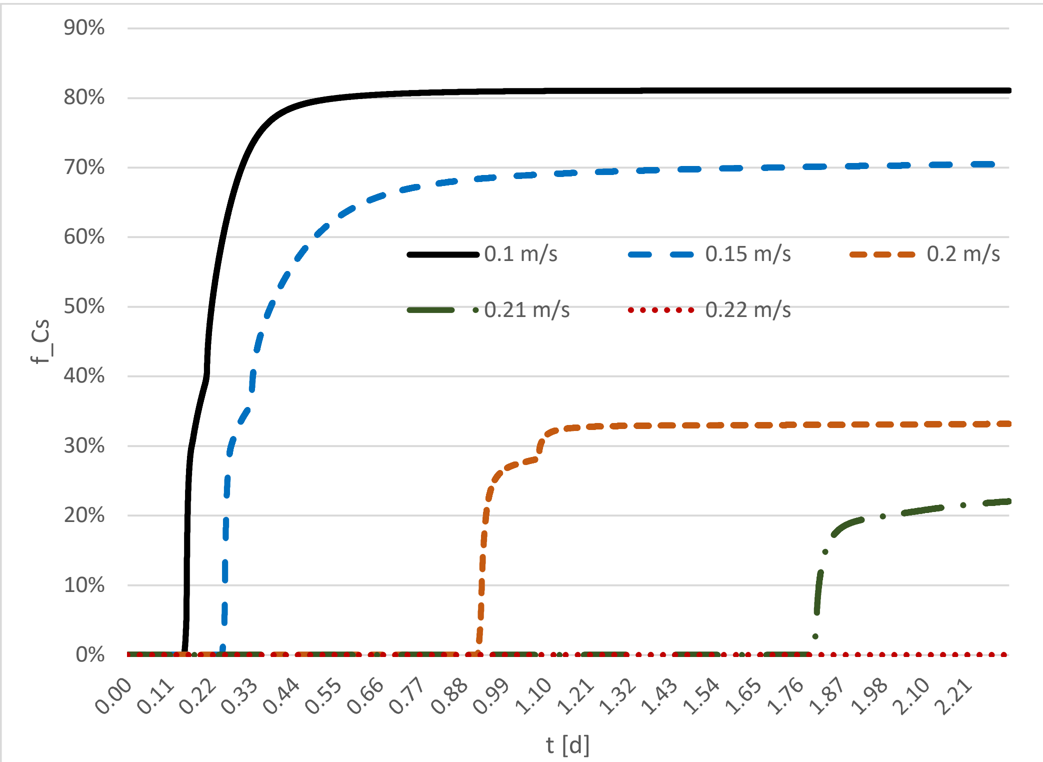

FIG. 7. The influence of the speed of the natural or forced ventilation on the release fraction of Cs element, for fuel bundles F2 (1 m).

Coupled calculations SOPHAEROS-CPA-CESAR-ISODOP-DOSE were performed to investigate the releases to the environment. For simplicity only the results for Cs and I elements are presented.

For the synthesis of the results, the fractions of release (mass ratio between the mass of the isotope in the environment and the mass released into SFP room) are calculated. For Iodine the fraction is 2.52%. The mass in the environment tends to reach the saturation after 2 days from the start of the release. For Caesium the fraction is 1.15% and the saturation effect is similar with the case of Iodine.

Iodine and Caesium forms some chemical species that are present in the environment: CsI, CH_3I, I_2O_5, Cs_2O, Cs_2I_2. The evolution of the masses of the species was calculated by the proposed methodology. For simplicity in the masses (in kg), I the environment, at t= 14 days after the start of fuel bundles exposed in air are: 2.06E-06 (CsI),9.32E-03 (CH_3I), 7.50E-04 (I_2O_5), 5.93E-20 (Cs_2O), 6.74E-07 (Cs_2I_2), The values are expressed per 1 kg of Iodine and 1 kg of Cs injected into the atmosphere.

At the same time ISODOP offers the isotopic profile for each element. The methodology may treat all the fission products in a single calculation. Since the details are important only for the further calculation of the propagation in the environment they are not presented in this paper.

Finally, it should be noted that the used assumptions are based on physical considerations and intended to reduce the complexity. However experimental data are needed to obtain better models for the evacuation of heat from the fuel bundles exposed in air. At the same time the multitude of fuel bundles arranged on the trays and the interactions with the racks needs supplementary investigation, especially for heat transfer by conduction and radiation in such a complex structure. It should be noted the present evaluation is conservative since systematically reduce or neglect the extraction of heat by interaction with the rack structure, trays and other fuel bundles.

CONCLUSIONS

(C1) Due to the relatively low burnup of CANDU fuel and due to the daily refuelling, the potential of loss of cooling at the spent fuel pool is reduced in comparison with the technologies based on the enriched uranium. Around 2 weeks are needed from the start of the accident until de discovering of the highest plane of fuel bundles. At the same time by introducing make-up water at a flow rate of 1.25 kg/s is enough to keep a constant level at an elevation of 5.00 m.

(C2) The complexity of the SFP inventory is generated by the daily refuelling. It may be reduced by an adequate grouping of the spent fuel bundles in categories of similar residual power and isotopic inventory, based on physical considerations and by using ORIGEN calculations.

(C3) After around 30 years of operation at nominal power of CANDU units, the replacement of horizontal fuel channels affected by the irradiation is needed. In this case, a full core is discharged and added to the SFP. This situation reduces the interval time for the evaporation of water, until the free level reaches the first fuel bundles, to approximately 5 days. The case was investigated in the paper to understand the potential of the accident to produce the release of the radioisotopes.

(C4) Even for the fuel with low residence time in the spent fuel pool (around 7 days) the presence of the convection of the air (by natural or forced ventilation) drastically reduce the potential of the accident. A speed of 0.22 m/s is sufficient to keep intact the cladding of the fuel bundles with a residence time of around 1 month.

(C5) In order to have a complete view on the potential for the release of radioactivity form the SFP to the environment, the convection was artificially suppressed in the numerical simulation and the transfer fractions to the environment was calculated for different isotopes. Also the chemical species structure of the source term was simulated. In summary the transfer fraction (from the SFP room to the environment) for Iodine, in the absence of filtration, is 2.5%, and for the Caesium is 1.2%.

(C6) Some experimental data are needed to refine the assumptions and the models, especially at the level of the behaviour of the fuel bundles accidentally placed in the atmosphere. This knowledge has to be incorporated in the future versions of ASTEC code.

REFERENCES

[1] TAYAL., M., GACESA., M., "Storage and Disposal of Irradiated Fuel", The CANDU Essential (W.J. Garland, Ed), UNENE, Hamilton, ON, (2014) 16–20, www.unene.ca/education/candu-textbook

[2] VAN DORSSELAERE, J.P., et al., The ASTEC integral code for severe accident simulation, Nucl. Technol. **165** (2009) 293–307.

[3] ORGANISATION FOR ECONOMIC CO-OPERATION AND DEVELOPMENT NUCLEAR ENERGY AGENCY, Status Report on Spent Fuel Pools under Loss-of-Cooling and Loss-of-Coolant Accident Conditions, Nuclear Energy Agency, Report NEA/CSNI/R(2015)2, OECD-NEA, Paris (2015).

[4] VAN DORSSELAERE, J.P., ET AL., ASTEC Extension to other Reactor Types than Generation II PWR, Presented at 3rd European Review Meeting on Severe Accident Research (ERMSAR-2008), Nesseber, 23–25 September 2008 (2008).

[5] CHATELARD, P., et al., Synthesis of the ASTEC Integral Code Activities in SARNET – Focus on ASTEC V2 Plant Applications, Ann. Nucl. Energy **74** (2014) 224–242.

[6] EUROPEAN COMMISSION, "SARNET: Network of Excellence for a Sustainable Integration of European research on Severe Accident Phenomenology and Management – Phase 2; Annex I", 7th Framework Programme, Grant agreement 231747, EC, Brussels (2008).

[7] CHATELARD, P., et al., Synthesis of the SARNET2 activities on ASTEC topic, Presented at 6th European Review meeting on Severe Accident Research (ERMSAR-2013), Avignon 2–4 October 2013.

[8] GAULD, I.C., et al., ORIGEN-S. NUREG/CR-0200, Rev7, Volume 2, Section F7, ORNL/NUREG/CSD-2/V2/R7, ORNL, Oak Ridge, TN (2002).

[9] COINDREAU, O., ASTEC V2.1 Physical modelling of the ICARE module, SN-RES/SAG/2016-00422 IRSN, Fontenay-aux-Roses (2016).

[10] PIAR, L., ASTEC V2.1 CESAR Physical and Numerical Modelling, PSN-RES/SAG/2015-00332, IRSN, Fontenay-aux-Roses (2015).

[11] COUSIN, F., BOSLAND L., ASTEC V2.1.1, SOPHAEROS Module, PSN-RES/SAG/2017-00215, IRSN, Fontenay-aux-Roses (2017).

[12] WEBER, G., ASTEC V0 Description of Aerosol Models in the Containment Part of ASTEC (CPA), GRS, Cologne (1999).

[13] BOSLAND, L., ASTEC V2.0 rev2 code IODE module: iodine and ruthenium behaviour in the containment, DPAM-SEMIC-2011-345, IRSN, Fontenay-aux-Roses (2011).

[14] COUSIN, F., JACQ, F., ASTEC V2.1, ISODOP Module", PSN-RES/SAG/2015-00366, IRSN, Fontenay-aux-Roses (2015).
[15] CANTREL, L., Description of the DOSE module of ASTEC V2, DPAM/SEMIC 2009-357, IRSN, Fontenay-aux-Roses (2009).
[16] NUCLEARELECTRICA, Safety Features of CANDU6 Design and Stress Test Summary Report, Nuclearelectrica Bucharest (2015).
[17] CONSTANTIN, M., et al., Analysis of the Releases Produced by CANDU Type Irradiated Fuel Bundles Accidentally Remained in the Air", Prog. Nucl Energy **108** (2018) 351–357.

SIMULATION OF CANDU FUEL THERMAL-HYDRAULIC BEHAVIOUR DURING SPENT FUEL BAY LOSS OF COOLING EVENTS

C. ZĂLOG
Reactor Physics and Safety Analyses Group,
Cernavoda NPP,
Romania

Abstract

After the Fukushima accident, one of the highest priorities for CERNAVODA NPP was to investigate events that can lead to Spent Fuel Bay (SFB) loss of cooling and loss of coolant inventory. In CANDU plants, fuelling is performed on-power. Daily, fresh fuel bundles are loaded in core and spent fuel bundles are discharged from the core, transferred and stored in SFB. Due to the SFB limited storage capacity, bundles having 6 years or more of cooling time are transferred to the Dry Storage Facility. Thus, as per design, a maximum number of around 38 000 fuel bundles can be stored, at any time, in SFB. Following a loss of class III and class IV power sources (e.g. Station Blackout), the cooling and purification systems for SFB water become unavailable. Consequently, the bay water temperature increases up to the boiling conditions and, due to boiling and vaporization, the water inventory and level will decrease in time. The decrease of coolant level can leave uncovered a number of fuel bundles, degrading their cooling. The present paper reviews the analysis methodology and results for a typical event of Spent Fuel Bay loss of cooling. Methodologies used in the analysis and results presented are focused upon the CANDU fuel thermal-hydraulic behaviour during the event and upon its potential radiological hazard.

1. INTRODUCTION

Following a loss of class III and class IV power sources (e.g. Station Blackout), the cooling and purification systems for the Spent Fuel Bay (SFB) water become unavailable. Consequently, the bay water temperature increases up to the boiling conditions and, due to subsequent vaporization, the water inventory and level will decrease in time. The decrease of coolant level can lead to uncovering of a number of fuel bundles, degrading their cooling.

Regardless the initiation condition, a certain sequence of events develops for an SFB loss of cooling accident:

(a) The cooling system of the SFB water becomes unavailable;

(b) Because the stored fuel decay power cannot be removed, the water temperature increases up to the boiling point;

(c) If SFB cooling remains unavailable, in the boiling conditions, the bay water vaporizes and its level decreases in time;

(d) If SFB cooling still remains unavailable, water must be added to maintain the level above fuel, keeping its normal cooling conditions;

(e) If SFB cooling and water addition remain unavailable, the water level decreases continuously until the top fuel bundles remain uncovered, entering in a degraded cooling conditions (natural convection in air).

At any time, actions must be taken to restore the SFB coolant inventory and cooling capacity, in order to return to the normal cooling conditions for the stored fuel.

Two distinct domains are considered for the analysis of fuel thermal-hydraulic behaviour:

– Normal cooling conditions (fuel bundle is covered by the bay cooling water, in normal operating conditions);

– Degraded cooling conditions (fuel bundle is covered by boiling water or remains uncovered).

To evaluate the potential radiological hazard, an estimate of the radioactive inventory of the spent fuel stored in the bay was performed. As the heat load of the stored fuel is generated by the radioactive decay, a decay power calculation was, also, performed.

2. HEAT LOAD AND RADIOACTIVE INVENTORY OF THE SPENT BAY

2.1. Introduction

After discharge from reactor core, spent fuel bundles are transferred, for cooling and storage, to the SFB. Following Fukushima accident, the problem of assessing the consequences of a Loss of Cooling event at the SFB was raised. In order to estimate the event impact, two types of calculation were performed:

– for determining time evolution of the decay power generated by the spent fuel bundles in the bay, from first bundles discharged from core, up to bay maximum storage capacity and

– for estimating the fission products inventory of the spent fuel bundles stored in the bay filled up to its maximum storage capacity.

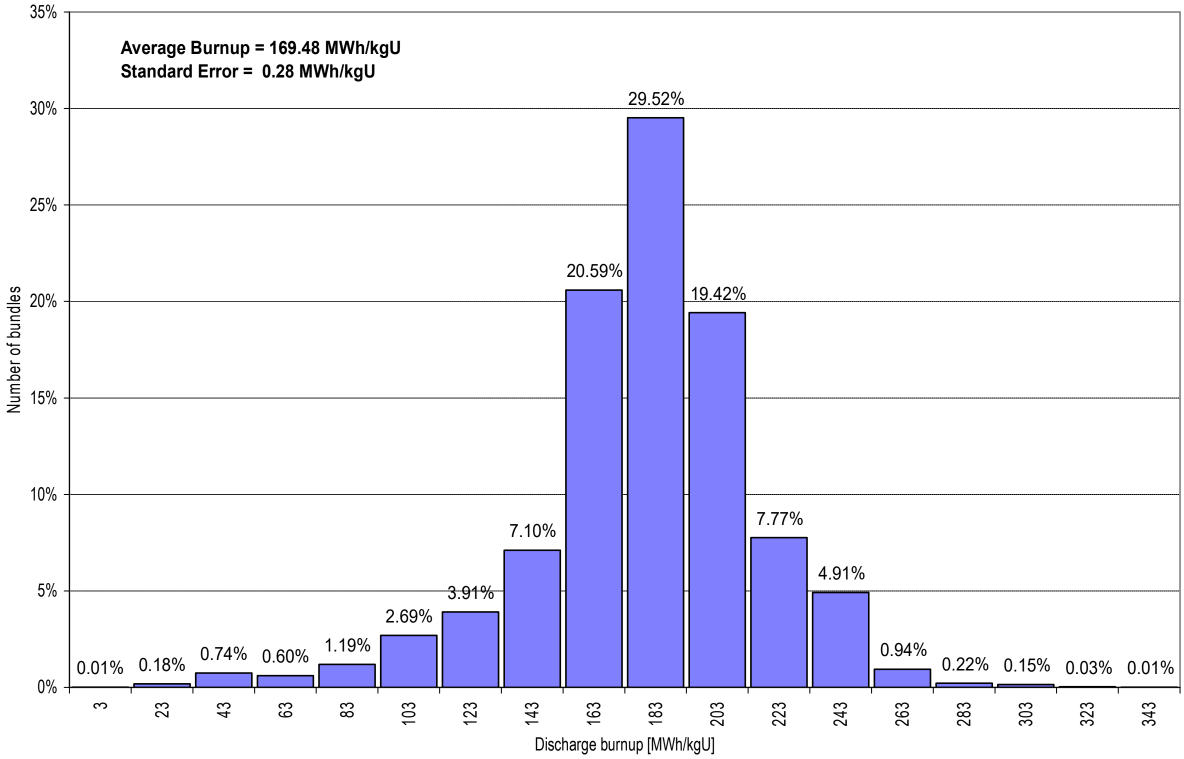

FIG. 1. Statistics on discharged spent fuel bundles.

2.2. Methodology

2.2.1. Calculation assumptions

Burnup and in-core irradiation power are the key parameters in obtaining fission products inventory and decay power for a fuel bundle. Because spent fuel bundles discharged in the bay have different exit burnups and were irradiated at different powers, it is unreasonable to perform inventory decay power calculation for each bundle. Consequently, prior calculations, the *typical spent fuel bundle (exit burnup and irradiation power)* is defined, assuming that all fuel bundles stored in the Spent Fuel Bay are identical with it.

- *Typical bundle exit burnup (**170 MWh/kgU**)* is obtained from a statistical analysis on the spent fuel bundles discharged during the first five years of operation at full power, as upper limit, with 95% level of confidence (Figure 1).

- In-core *typical irradiation power* is, conservatively, assumed to be the nominal design power peak of ***800 kW/bundle***.

2.2.2. Computer codes

Calculations, both for radioactive inventory and for decay power, were performed with the ORIGEN-S computer code [1], using a proprieties library specific for CANDU fuel [2].

For the *typical spent fuel bundle*, evolution of the decay power, up to 6 years cooling time, is given in Figure 2 and, as an example, time evolution of I-131 inventory is given in Figure 3. It can be seen that, after 600 days of cooling time, I-131 inventory is negligible.

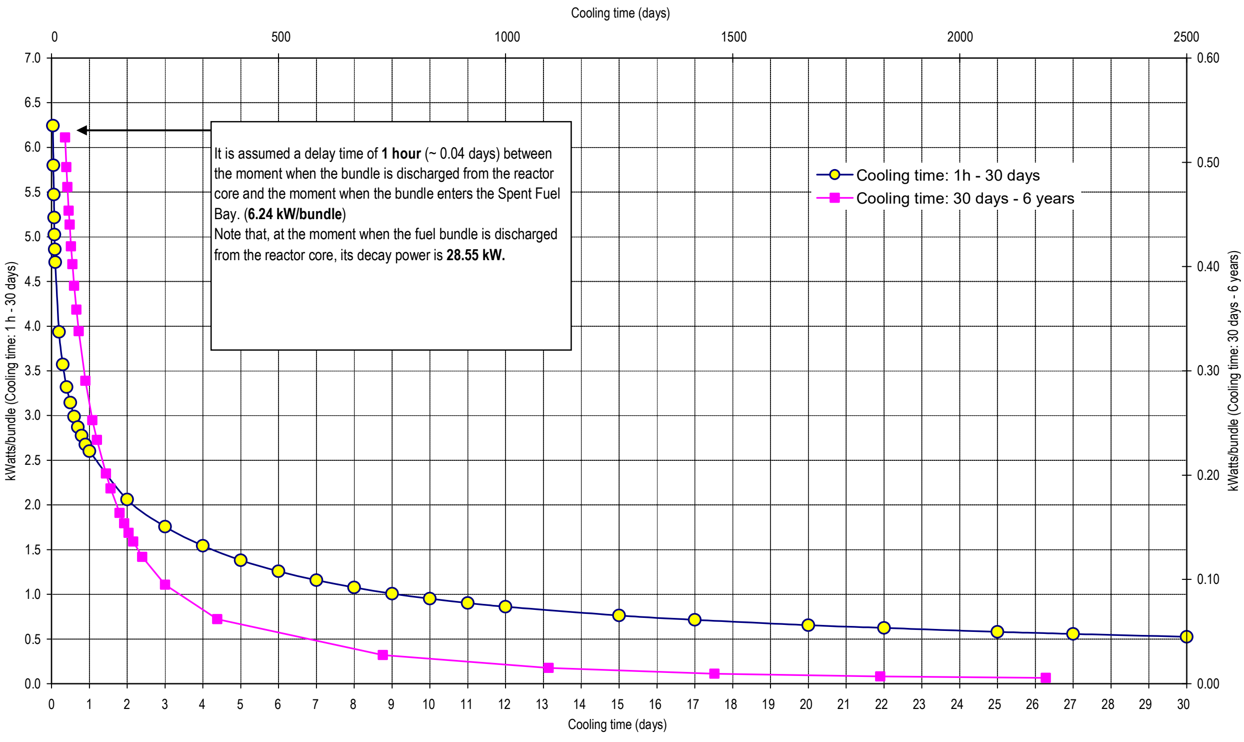

FIG. 2. Decay heat for the typical spent fuel bundle.

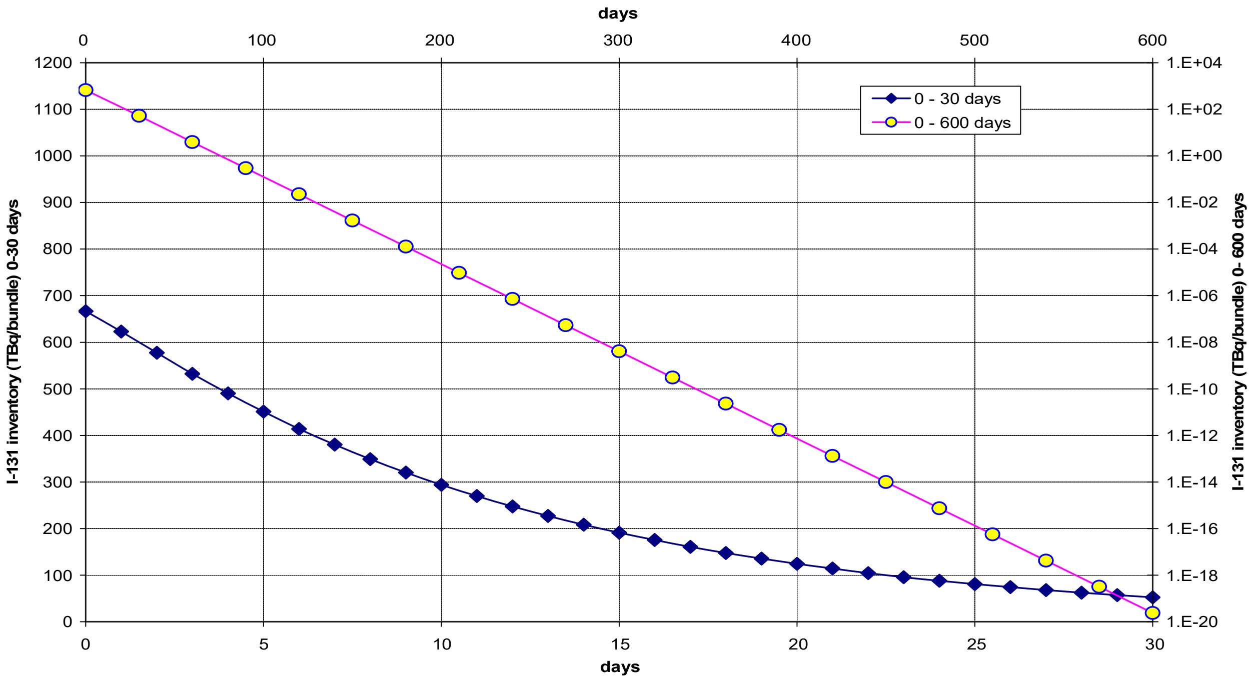

FIG. 3. I-131 inventory for the typical spent fuel bundle.

2.3. Results and conclusions

2.3.1. Spent fuel bay decay power

Decay power evolution in the Spent Fuel Bay is obtained by summing the contribution of all discharged spent fuel bundles, from the first bundles discharged, up to the total filling of the bay (Figure 4).

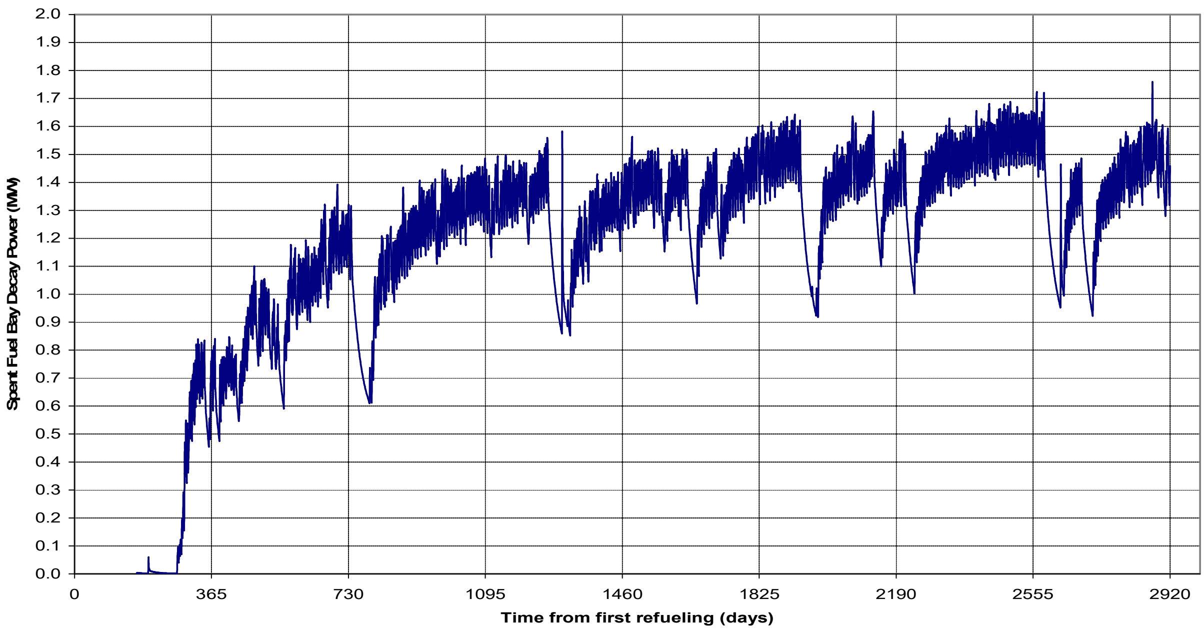

FIG. 4. Spent fuel bay decay power.

All bundles in the bay are considered to be identical with the *typical spent fuel bundle*. It was assumed the actual refuelling program from operation, close to a rate of 2 channels/FPD (16 bundles/FPD). Thus, at any time, while new bundles, with high decay powers, enter the bay, decay power from bundles already stored decreases. Even the Spent Fuel Bay was designed with a storage capacity for 8 years of reactor operation at 80% FP, after 6 years of cooling in the bay, spent fuel bundles are transferred to a dry storage facility, in annually campaigns. In our calculations, for bundles with more than 6 years of cooling time, the decay power was, conservatively, assumed to be constant, equal with the decay power reached after 6 years of cooling. These bundles were considered to remain stored in the pool. Figure 4 shows that, even with these conservative assumptions, the Spent Fuel Bay maximum heat load would be, with a large margin, below the design heat exchangers capacity (2 MW). Also, it is noticeable that the heat load has a consistent decrease during shut-down periods.

2.3.2. Spent fuel bay fission products inventory

Fission products inventory in the Spent Fuel Bay is obtained by summing the contribution of all discharged spent fuel bundles, from the first bundles discharged, up to the total filling of the bay (Figure 5). All bundles in the bay are considered to be identical with the *typical spent fuel bundle*. It was assumed a continuous refuelling rate of 2 channels/FPD (16 bundles/FPD), close to the value obtained in operation. Figure 5 shows that short-lived isotopes (like I-131) levels out in the early stage of bay filling, while total inventory (with prevalent contribution from long-lived isotopes) has a continuous increase, yet with a decreasing slope.

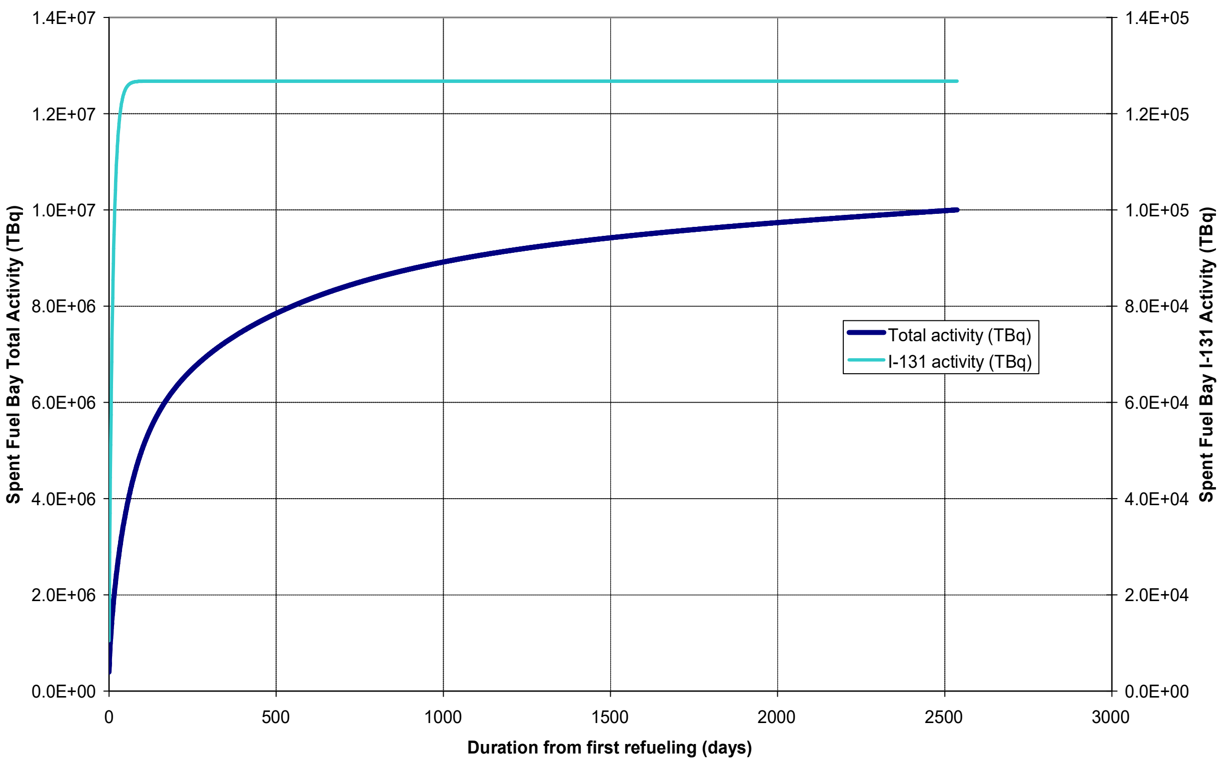

FIG. 5. Spent fuel bay activity.

3. SPENT FUEL BAY COOLANT BEHAVIOUR

3.1. Introduction

Regardless the initiation event for an SFB loss of cooling accident, a certain sequence of events develops:

a) The cooling system of the SFB water becomes unavailable;

b) Because the stored fuel decay power cannot be removed, the water temperature increases up to the boiling point;

c) If SFB cooling remains unavailable, in the boiling conditions, the bay water vaporizes and its level decreases in time.

3.2. Methodology

3.2.1. Calculation assumptions

(a) When SFB cooling is lost, the reactor is shutdown, no more fuel bundles from the core are transferred to the bay and SFB overall power source decreases due to decay.

(b) In SFB, fuel bundles are stored on steel trays, in stacks of 19 trays each. The total volume of fuel (37 392 bundles as per design) and trays stored in the bay is of 110 m^3.

(c) The total bay water volume is of 1620 m^3.

(d) Above bay water level, it is the normal atmospheric pressure.

(e) Initial temperature of the air above water is 30 °C, initial bay water temperature is 38°C and earth temperature is 12°C.

(f) The decay power generated by the fuel stored in SFB is assumed to be transferred to the:

- Metallic structure of the fuel bundles;
- Storage trays;
- Water in the bay;
- Air above water;
- Bay walls.

3.2.2. Computer codes

No computer codes were used. Simply, assuming the fuel stored in the bay as the unique heat source, heat transport equations were used, considering:

- Homogeneous, calorimetric heat transfer to the bay water and metal structure of fuel bundles;
- Homogeneous, bulk convection and conduction with the bay surrounding environment.

3.2.3. Sequence of events

The events simulated are:

- Heat transfer from fuel to the surrounding elements (water, metal, air, walls) up to the bay water boiling point;
- Heat transfer from fuel to the surrounding elements (water, metal, air, walls) during bay water evaporation (conservatively, it was assumed that all heat from fuel is used for water evaporation).

3.3. Results and conclusions

3.3.1. Bay water temperature increase

Using the methodology and assumptions given in section 3.2, it was obtained a rate of water average temperature increase of **0.83°C/h**. Thus, the SFB water average temperature will increase from its initial value of **38°C** to the boiling point of **100°C** in about **75 hours**.

3.3.2. Bay water level decrease

At boiling temperature, if cooling is not restored, due to vaporization, the bay water level decreases in time with a rate of about **24.2 cm/day**. After about **16 days** from the loss of cooling, the bay water is with 1 meter above fuel and, at about **20 days**, the water level reaches the top surface of the fuel bundles. From this moment on, if water level is not restored by water addition, fuel bundles will begin to lose water coverage, entering in a degraded cooling conditions (natural convection in air). As a matter of fact, the fuel bundles from the top trays are fully uncovered in about **2 days**.

3.3.3. Water addition flow to maintain the SFB water level above fuel

After reaching the boiling point, due to boiling and vaporization, the bay water inventory decreases with a rate of **0.84 kg/s**. Thus, at any time before the water level reaches the fuel top surface, in order to keep water level constant above fuel, water must be added to the bay at a rate at least equal with the vaporization rate.

3.3.4. Conclusions

The analysis shows that, if SFB cooling is lost, water temperature increases with about 1 degree/h, reaching boiling in about 2.5 days. If cooling is still not restored, the pool water evaporates and, in about two weeks, its level reaches one meter above fuel stack. As, with one meter of water above fuel, staff access is not restricted in the area for radiological hazard reasons, it was concluded that, in case of loss of cooling at the Spent Fuel Bay, **enough time (*more than two weeks*) remains for compensatory measures, i.e. to supply alternative cooling sources**.

4. FUEL THERMAL-HYDRAULIC BEHAVIOUR IN THE SPENT FUEL BAY

4.1. CANDU fuel description

The CANDU fuel is designed as a bundle of 37 fuel elements distributed in a cylindrical geometry. The main characteristics of the CANDU fuel are given in Table 1, while its geometry is presented in Figure 6.

TABLE 1. SUMMARY OF CANDU FUEL BUNDLE CHARACTERISTICS

Parameter	Best-Estimate	Standard Error	Distribution
Pellet			
Number of pellets in a fuel element	30 + 1	N/A	N/A
Pellet diameter (mm)	12.222	0.0262	Normal
Pellet density (g/cm^3)	10.59	0.0024	Normal
^{235}U enrichment (wt%) / (atom %)	0.711 / 0.72	N/A	N/A
^{234}U (atom %)	0.0055	N/A	N/A
^{238}U (atom %)	99.2745	N/A	N/A
Pellets stack length in fuel element (mm)	481.71	0.433	Uniform
Fuel element and bundle			
Number of fuel elements in a bundle	37	N/A	N/A
Sheath outside diameter (mm)	13.095	0.014	Uniform
Sheath inside diameter (mm)	12.31	0.014	Uniform
Filling gas pressure (atm)	1.0	N/A	N/A
He content in the filling gas (volumetric fraction)	0.9001	-	-
Bundle U mass (kg)	19.3286	0.0005	Normal
Bundle UO_2 mass (kg)	21.927	0.0005	Normal
Bundle Zy mass (kg)	2.1524	0.00005	Normal
Bundle length (mm)	495.896	0.001	Normal
Bundle outer diameter (mm)	< 102.77	0.003	Uniform
Volume displaced by the fuel bundle (cm^3)	2459.826	5.50	Normal

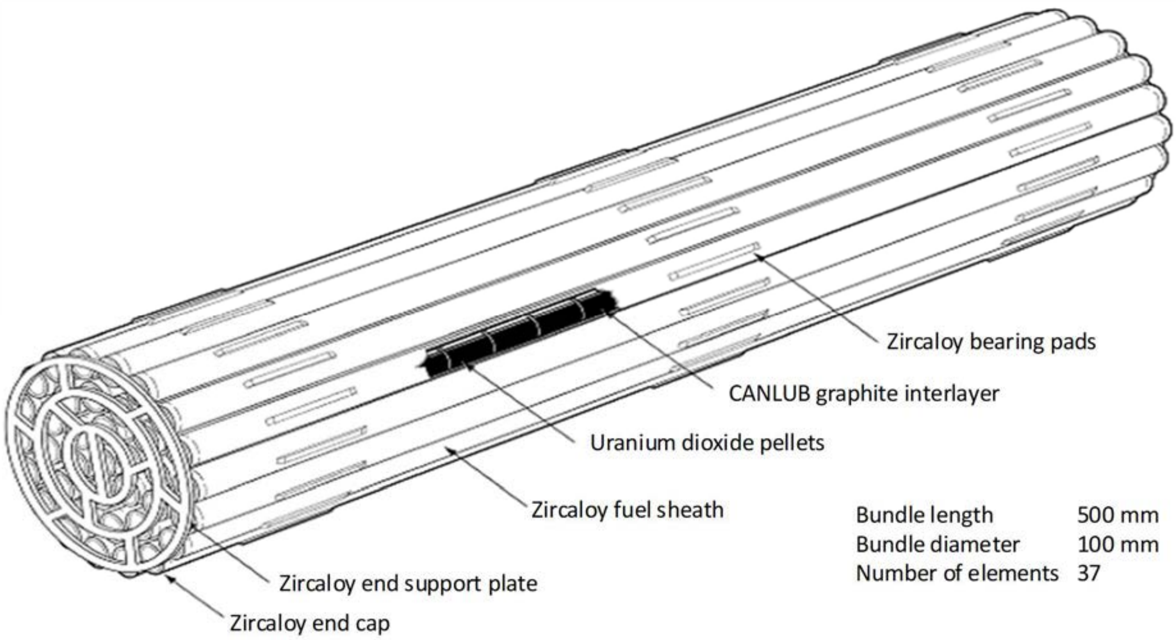

FIG. 6. CANDU fuel bundle.

4.2. Computer codes

For CANDU fuel safety analyses, a set of computer codes, developed in CANADA, are used to simulate the behaviour of the nuclear fuel: ELESTRES [3], for Normal Operating Conditions (NOC), and ELOCA [4], for Transient Conditions (TC).

ELESTRES is a fuel-performance computer code. It is used to predict the on-power behaviour of a CANDU fuel element, for a given geometry and power-burnup history, under in-core NOC. The code performs the following major calculations:

– Pellet and sheath temperatures;
– Fission-gas release;
– Internal pressure;
– Sheath strain.

Data produced by the code are used for design and assessments and to provide information on initial conditions for the analysis of a postulated transient event with the transient code ELOCA.

The ELOCA code assesses the thermal-mechanical response of a CANDU fuel element under TC. As part of its input, ELOCA requires, via a transfer file, the initial physical conditions of the fuel, as calculated by the NOC code ELESTRES, the power generation history and the boundary conditions history (i.e. coolant temperature, coolant pressure and sheath-to-coolant heat transfer coefficient). The code performs its major calculations for:

– Expansion, contraction, cracking and melting of the fuel;
– Variations in the fuel element internal pressure;
– Changes in the fuel-to-sheath heat transfer;
– Deformation of the sheath;
– Chemical reaction of Zr with H_2O and UO_2;
– Beryllium-assisted cracking of the sheath.

4.3. Fuel failure mechanisms

Seven fuel failure mechanisms were identified to be of relevance to the Design Basis Accidents [5] and to be, also, used as failure mechanisms in Spent Fuel Bay loss of cooling events:

a) Sheath failure by overstrain;
b) Low ductility sheath failure;
c) Beryllium-assisted crack penetration;
d) Oxygen embrittlement;
e) Fuel melting;
f) Sheath melting;
g) Failure due to oxidation and overstrain under oxide cracks, including oxidation in a mixed air/steam environment following bundle ejection.

4.3.1. Sheath failure by overstrain

4.3.1.1. Mechanism

Sheath failure by overstrain can be considered the most important failure mechanism, as it is the most frequently invoked in design basis accidents. Even the details of the mechanisms leading to sheath failure by overstrain are complex, a brief description can make the failure mechanics seem sufficient simple.

The fuel-to-sheath gap inside a fuel element contains a mixture of filling gas added during manufacture and fission gas generated during the normal operation of the fuel. In most accident scenarios, the fuel element is subject to high temperatures. As temperature increases, the gas pressure inside the fuel-to-sheath gap rises and the yield stress of the Zircaloy sheath decreases. If the fuel element internal gas pressure exceeds the coolant pressure such that the hoop stress exceeds the yield stress, the sheath will undergo plastic strain. If the straining continues unrestricted, the sheath will, eventually, fail.

4.3.1.2. Failure criterion

The approach used in the CANDU industry is to base the failure criterion on the concept of “limit of plastic stability”. Materials that work-harden (Zircaloy sheath is among them) exhibit uniform strain (i.e. resist necking) below a critical strain limit [6]. A consequence of this phenomenon is that, when thin walled tubes are subject to internal pressure, they exhibit uniform hoop strain, along their length, up to a critical strain. Once the critical strain is reached, the tube will undergo localized ballooning, which will, generally, lead to failure.

In the early 1970s, it was determined the minimum value of hoop strain at which ballooning may be initiated as 7±1.5% plastic strain [7]. To accommodate the uncertainty in measurements, a value of 5% hoop strain, averaged along the length of the fuel element, is used as the overstrain criterion for CANDU fuel safety analyses [8].

4.3.2. Low ductility sheath failure

4.3.2.1. Mechanism

At low temperatures (<700 K), Zircaloy fuel cladding has exhibited low ductility due to work hardening, during the manufacturing process, followed by irradiation hardening while in use [9]. At temperatures typical for Normal Operating Conditions (NOC), the dislocations, formed by the irradiation damage, anneal out continuously until a steady-state is reached and the rate of dislocations formation matches the annealing rate. This equilibrium state is reached within the first few hours of NOC irradiation.

For most accident transients, the sheath temperature rises and ductility is restored before significant loads are imposed on the sheath. However, if fuel experience a rapid power pulse, the fuel pellet may heat-up and expand thermally before the sheath temperature has risen sufficiently for ductility restore to occur. Under these circumstances, the strain rate, imposed on the sheath by the expanding fuel, results in a stress beyond the yield point. The dominant deformation mechanism is dislocation, also known as athermal glide [10]. As the sheath was embrittled by irradiation hardening, it is unable to withstand any significant deformation induced by the process and, as observed in tests [9], fails at strains much lower than the criterion for overstrain failure specified in section 4.3.1.2.

4.3.2.2. Failure criterion

Experimental data on sheath failure due to low ductility show a considerable spread in the values of failure strains, making it difficult to determine a practical failure criterion. At present, it is assumed that the sheath will fail, due to the mechanism induced by low ductility, if the strain, due to athermal glide, exceeds 0.4% before 95% of the sheath microstructure has annealed. This failure criterion is embodied in the ELOCA code [11], the code used for fuel behaviour during transients. The code includes models for determining strain due to the athermal glide and for the annealing process.

4.3.3. Sheath failure by Beryllium-assisted crack penetration

4.3.3.1. Mechanism

Zircaloy appendages (bearing pads and spacers) are beryllium-brazed to the outer surface of the fuel element Zircaloy sheath. The process involves coating the appendages with beryllium, tack welding the appendages to the sheath and, finally, induction heating of the assembly. During induction heating, beryllium alloys and the zirconium from Zircaloy form a braze alloy.

The brazing technique has been found to be a reliable and efficient technique for attaching appendages to the CANDU fuel cladding. It has been proved to be durable under NOC, with both adequate strength and corrosion resistance. However, at high temperature and high hoop stress, fuel element sheath with beryllium-brazed appendages have exhibited failures in the brazing regions. These failures have been attributed to a mechanism known as “liquid metal embrittlement”. The net result of this failure mechanism is that, once a crack is initiated on the sheath surface, in the brazed regions, the presence of beryllium can cause the crack to propagate through the sheath, causing failure.

4.3.3.2. Failure criterion

Current fuel safety analyses use the model developed by Kohn and Clendening [12] to predict the timing of sheath failure by beryllium-assisted crack penetration. Because the processes of beryllium-assisted crack formation and crack propagation are probabilistic, the model assesses failure by assigning a probability distribution to the crack propagation rate. The model is embodied in the ELOCA code [11]. The code gives, in the output file, the time evolution for the probability of failure by beryllium-brazed crack penetration.

4.3.4. Sheath failure by oxygen embrittlement

4.3.4.1. Mechanism

In the steam environment and at the elevated temperatures typical for Loss of Coolant Accidents (LOCA), the oxide layer on the Zircaloy sheath surface can grow rapidly. In addition, at these high temperatures, oxygen diffuses into the metallic fuel sheath and has a significant impact on the material properties of Zircaloy. As long as temperature remains high and there is sufficient supply of oxygen, the ZrO_2 and oxygen-stabilized alpha layers will grow at the expense of the beta layer. The ZrO_2 layer is, inherently, brittle, while ductility of the alpha and beta Zircaloy layers is negatively influenced by the presence of dissolved oxygen.

At the high temperatures reached during LOCA accidents, sheath maintains enough ductility to preserve its structural integrity. Upon injection of Emergency Core Cooling (ECC), sheath temperature falls rapidly and, due to thermal shock, the combination of reduced ductility and increased mechanical load may cause sheath failure and, possibly, fragmentation. An additional concern is that, once cooled, sheath is further embrittled by the precipitation of hydrides in the Zircaloy beta layer. Thus, if sheath may survive the thermal shock of ECC, the subsequent embrittlement will cause failure.

4.3.4.2. Failure criterion

Current CANDU fuel safety analyses use the oxygen embrittlement sheath failure criterion suggested by Sawatzky [13]. This criterion is based on measurements of the Ultimate Tensile Strength (UTS) of Zircaloy sheath samples, after being subject to elevated temperatures, in a steam environment. Based on experimental data, Sawatzky confirmed that Zircaloy containing more than 0.7 wt% of oxygen should be considered brittle at room temperature. He also observed that, at room temperature and at 800ºC, the UTS of Zircaloy with an oxygen concentration of 0.7 wt% is about twice that of as-received material at 800ºC and is greater at all intermediate temperatures (between room temperature and 800ºC).

Based on the mentioned observations, Sawatzky proposed in the Ref. [13] the following failure criterion:

> '*If the cladding remains intact at temperatures above 800ºC then, provided the oxygen concentration remains less than 0.7 wt% through at least half the wall thickness, its load bearing ability at lower temperatures will be enough to keep it intact'*.

Thus, if the calculated oxygen concentration exceeds 0.7 wt% for more than half of the sheath thickness, then sheath may fail upon rewet.

4.3.5. Sheath failure by fuel melting

4.3.5.1. Mechanism

In several accident scenarios there is a potential for the fuel temperatures to approach melting point. This may occur due to degraded cooling of the fuel element before reactor trip or due to power excursions associated to Large Break LOCA or Loss of Regulation accidents. If fuel temperature approaches melting point, then melting would occur at the fuel centre line and most of the melt material would be expected to be contained by the cooler portion of the pellet. However, there are chances for the melt to reach fuel sheath via pellet cracks and the pellet-to-pellet interfaces, causing sheath failure.

4.3.5.2. Failure criterion

For the purposes of CANDU fuel safety analyses, the melting temperature of stoichiometric UO_2 fuel is considered to be 2840ºC, consistent with the value provided by the MATPRO handbook [14].

4.3.6. Sheath failure by fuel sheath melting

4.3.6.1. Mechanism

Under conditions of degraded cooling, fuel sheath may heat-up to the melting point, losing its capability of effective barrier to fission product release. In practice, the sheath will fail due to one of the other failure mechanisms, before melting occurs.

4.3.6.2. Failure criterion

The presence of dissolved oxygen in the fuel sheath has the effect of increasing its melting point. Based on experimental measurements [15], IAEA recommends, for the melting point, a set of correlations as function of oxygen content [16]. Conservatively, in CANDU fuel safety analyses, melting temperatures for sheath are considered to be 1760 ºC (without oxide) and 1850 ºC (with oxide).

4.3.7. Sheath failure by oxidation and overstrain under oxide cracks

4.3.7.1. Mechanism

At the high temperatures reached during most of the accident scenarios, the Zircaloy fuel sheath will undergo an exothermic oxidation reaction with the heavy water coolant:

$$Zr + 2D_2O \rightarrow ZrO_2 + 2D_2 \tag{1}$$

and a layer of ZrO_2 will grow on the outer surface of the sheath. The reaction rate is temperature dependent, starts at around 1200 ºC and increases rapidly above 1500ºC. If the heat released by oxidation exceeds the rate of cooling from sheath surface, the sheath temperature may escalate, resulting in a 'runaway' oxidation.

Although through-wall sheath oxidation is a concern, the sheath is likely to undergo mechanical failure before complete oxidation occurs. The oxide layer on the outside of the sheath is brittle and cannot withstand any significant tensile load. Hence, most of the hoop stress in the sheath must be carried by the declining thickness of the metallic substrate.

An additional factor leading to strain localization and instability is cracking of the oxide layer. The oxide layer formed on the outside sheath surface is brittle and cracks develop at low levels of sheath strain (around 2%). The reduced sheath thickness under the crack results in localized stresses higher than the average over sheath, leading to failure.

4.3.7.2. Failure criterion

For sheath temperatures below 1000ºC, there is no metal/water reaction because oxidation starts at about 1200ºC. For sheath temperatures over 1000ºC, in conditions of sheath oxidation, if uniform sheath strain exceeds 2%, the sheath is likely to undergo mechanical failure before complete oxidation occurs.

4.4. Fuel behaviour during normal cooling conditions

It was simulated the behaviour of a fuel element from the outer ring of a typical fuel bundle discharged from core and transferred to the Spent fuel Bay operating in normal conditions.

4.4.1. Methodology

For NOC simulation with the ELESTRES code, it was selected the typical configuration of a fuel discharged to the Spent Fuel Bay, as described in section 2.2.1.:

- Exit burnup of 170 MWh/kgU;
- In-core irradiation at 800 kW/bundle.

For TC simulation with the ELOCA code:

- Power was assumed to be given by the fuel decay curve after discharging from core (see section 2.2.1. and Figure 2), while

– Coolant properties were assumed to be those of the bay water, in normal operating conditions:
    - Pressure = 1 atm (equals the atmospheric pressure above the water surface);
    - Temperature of 40 °C (conservatively, higher than the operating setpoint of 38 °C);
    - Heat transfer coefficient sheath-to-coolant corresponding to free convection in liquids (conservatively, was selected the lowest value of the domain: 50 W/m^2K).

4.4.2. Results and conclusions

The results of the simulation with ELOCA code show that no failure occurs, and fuel element integrity is preserved. See Figure 7 that checks the overstrain mechanism (criteria 1 and 7).

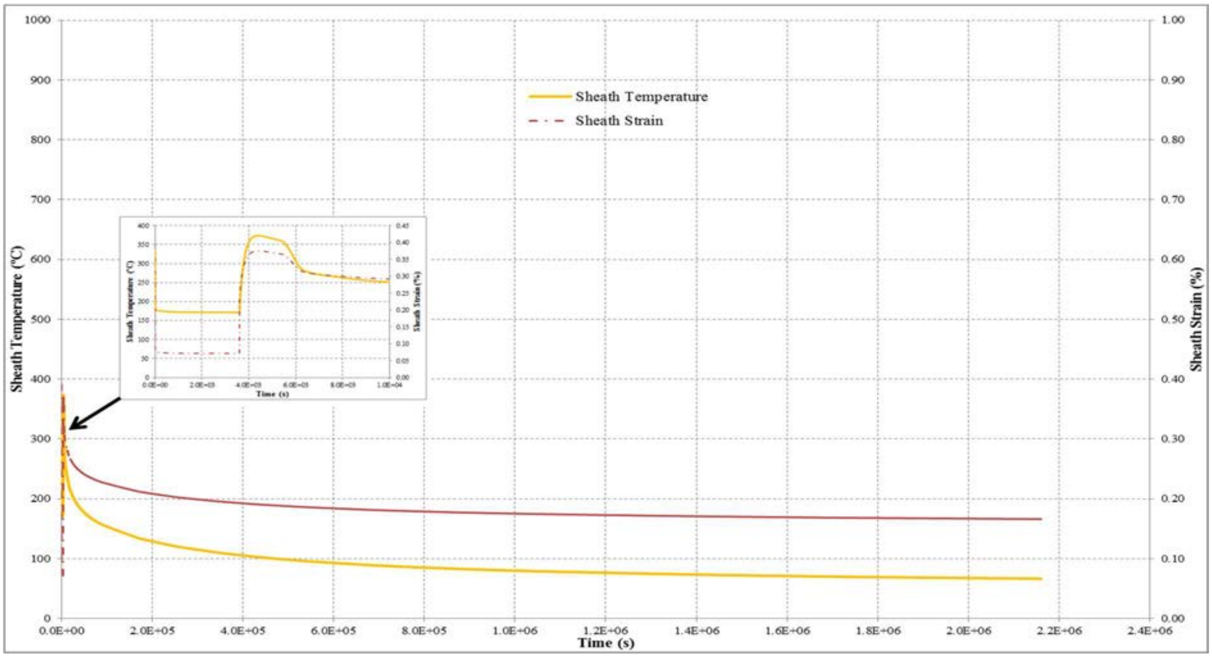

FIG. 7. CANDU fuel behaviour during normal cooling conditions (in cold water).

4.5. Fuel behaviour during degraded cooling conditions

It was simulated the behaviour of a typical fuel bundle discharged from core and transferred to the Spent Fuel Bay, following a loss of cooling event. Two types of degraded cooling were considered:

– Cooling in hot water (if the bundle is still covered by water);
– Cooling in air (if the bundle becomes totally uncovered by the water).

4.5.1. Methodology

For NOC simulation with the ELESTRES code, it was selected the typical configuration of a fuel discharged to the Spent Fuel Bay, as described in section 2.2.1.

For TC simulation with the ELOCA code, the power transient was assumed the be the fuel decay curve (section 2.2.1 and Figure 2) while coolant was assumed to operate during a loss of pool cooling:

(a) Cooling in boiling water

– Pressure = 1 atm (equals the atmospheric pressure above the water surface);
– Temperature of 100°C (boiling conditions);
– Heat transfer coefficient sheath-to-coolant corresponding to free convection in liquids (conservatively, was selected the lowest value of the domain: 50 W/m^2K).

(b) Cooling in air

– Pressure = 1 atm (equals the atmospheric pressure above the water surface);
– Temperature of 100°C (air above boiling water);
– Heat transfer coefficient sheath-to-coolant corresponding to free convection in gases (conservatively, was selected the lowest value of the domain: 2 W/m^2K).

4.5.2. Results and conclusions

(a) Cooling in boiling water

Results of the simulation show that, if cooling in boiling water, **no failure occurs,** and fuel integrity is preserved. See Figure 8 that checks the overstrain mechanism (criteria 1 and 7).

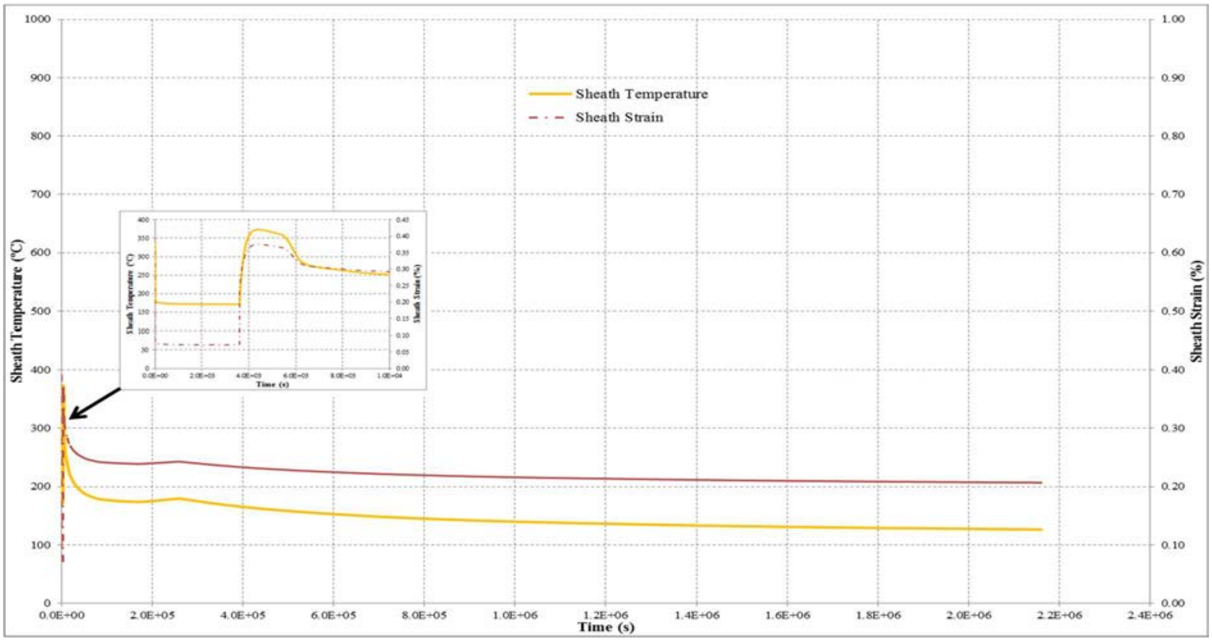

FIG. 8. CANDU fuel behaviour during degraded cooling conditions (in boiling water).

(b) Cooling in air

The results of the simulation with ELOCA code show that (Figure 9), in conditions of cooling in air, **failure occurs due to the overstrain mechanism** (criterion 1).

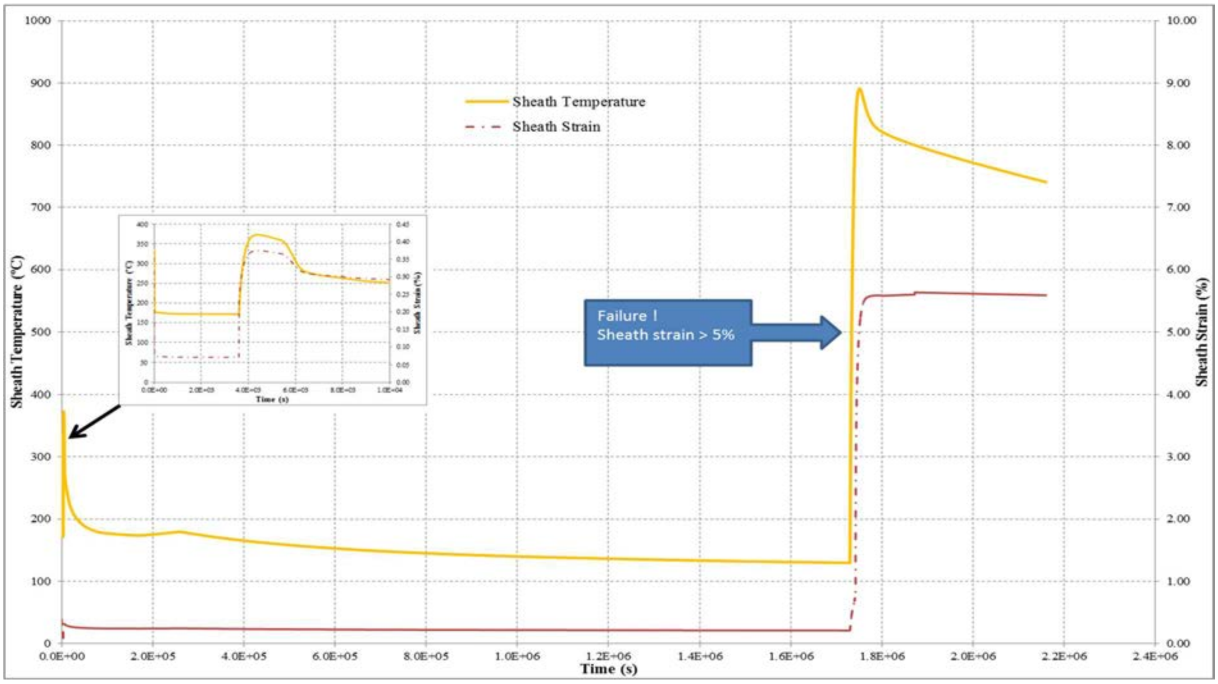

FIG. 9. CANDU fuel behaviour during degraded cooling conditions (in air).

CONCLUSIONS

The analyses showed that if, at all times, spent fuel is kept entirely covered by the pool water, even at boiling, no failure occurs.

Consequently, in case of a Spent Fuel Bay Loss of Cooling accident, all efforts must be made to keep constant the pool water level (i.e. inventory) above fuel.

At Cernavoda NPP enough time (about two weeks) is available for adequate compensatory action to be taken.

REFERENCES

[1] OAK RIDGE NATIONAL LABORATORY, Origen-S: Scale Module System to Calculate Fuel Depletion, Actinide Transmutation, Fission Product Build-up and Decay, and Associated Radiation Source Term, NUREG/CR-0200, rev. 6, vol. 2, section F7, ORNL, Oak Ridge, TN (2000).
[2] GAULD, I. C., CARLSON, P. A., LITWIN, K. A., Production and Validation of Origen-S Cross-section Libraries for CANDU Reactor Fuel Studies, Rep. RC-1442, COG-I-95-200, Atomic Energy of Canada Limited, Mississauga, ON (1995).
[3] CHASSIE, G. G., ELESTRES-IST 1.0 User’s Manual, TTR-733, rev. 1, Atomic Energy of Canada Limited, Mississauga, ON (2002).
[4] CASWELL, D. J., WILLIAMS, A. F., RICHMOND, W. R., ELOCA 2.2 User’s Manual, Rep. 153-113400-UM-001, rev. 0, Chalk River Laboratories, Chalk River, ON (2005).
[5] WILLIAMS, A. F., State of The Art Report on Fuel Sheath Failure Mechanisms for Design Basis Accidents, COG-09-2068, Chalk River Laboratories, Chalk River, ON (2011).
[6] SACHS, G., LUBAHN, J. D., Failure of Ductile Metals in Tension, Trans. ASME **68** (1946) 271.

[7] HARDY, D. G., High Temperature Expansion and Rupture Behavior of Zircaloy Tubing, Proc. National Topical Meeting on Water Reactor Safety, Salt Lake City, Utah 1973, ANS CONF-730304 (Freund, G.A. Ed.), ANS, La Grange Park, IL (1973) 254–273.
[8] HUNT, C. E. L., The Limit of Uniform Strain or Onset of Ballooning in Fuel Sheath Ballooning Tests, Rep. CRNL-1187, Chalk River Laboratories, Chalk River, ON (1974).
[9] HARDY, D. G., The Effect of Neutron Irradiation on the Mechanical Properties of Zirconium Fuel Cladding Alloys in Uniaxial and Biaxial Tests, Rep. CRNL-537, Chalk River Laboratories, Chalk River, ON (1970).
[10] ASHBY, M. F., A First Report on Deformation-Mechanisms Map, Acta Mettalurgica **20** (1972) 887–897.
[11] RICHMOND, W. R. et al., ELOCA 2.2: Theory Manual, Rep. 153-113400-COG-012, rev. 0, Chalk River Laboratories, Chalk River, ON (2007).
[12] KOHN, E., CLENDENING, W. R., A Model for Predicting the Behavior of Zircaloy-4 Fuel Sheath Ruptures at Brazed Appendages, Rep. CWAPD-313, CANDEV 78-06, Westinghouse Canada Limited, Toronto, ON (1978).
[13] SAWATZKY, A., A proposed Criterion for the Oxygen Embrittlement of Zircaloy-4 Fuel Cladding, Zirconium in the Nuclear Industry, ASTM International Conference, 1979 (Schemel, J., Papazoglou, T., Eds), ASTM, West Conshohocken, PA (1979) 497–496.
[14] LEE, R. Y., MATPRO, a Library of Material Properties for Light-Water-Reactor Accident Analysis, U. S. Government Printing Office, Washington DC (1998).
[15] HAYWARD, P. J., GEORGE, I. M., Determination of Melting Points of Zircaloy-4/oxygen alloys, Rep. COG-98-159, Candu Owners Group, Toronto, ON (1998).
[16] INTERNATIONAL ATOMIC ENERGY AGENCY, Thermo physical properties database of materials for light water reactors and heavy water reactors, IAEA-TECDOC-1496, IAEA, Vienna (2006).

ASSESSMENT OF THERMAL BEHAVIOUR OF SPENT NUCLEAR FUEL STORAGE POOL IN THE EXSICCATION ACCIDENT

A.V. KURYNDIN, A.M. KIRKIN, S.V. SINEGRIBOV, M.Y. KARYAKIN
SEC NRS,
Moscow
Russian Federation

1. INTRODUCTION

The accident at the Japanese nuclear power plant (NPP) Fukushima-1 in March 2011 showed that possibility of accidents with potentially serious radiation consequences couldn't be excluded with large-scale measures for improvement of safety level. For spent nuclear fuel storage facilities, one of such accidents may be the interruption of heat removal from spent nuclear fuel (SNF) due to the failure of the cooling system as a result of disruption of the power supply system with the failure of backup power sources or rapid full dehydration of the wet SNF storage as a result of the destruction of building structures and its depressurization. The decision to take preventive measures in advance to minimize exposure to personnel and the public is based on conservative estimates of possible radioactive discharges. To perform such assessments, the operating organizations carry out a calculated justification of the thermal and hydraulic characteristics of the SNF system in the accident scenarios with long-term blackout and a violation of heat removal.

APROS is one of the software tools that are used in SEC NRS for calculating the thermal-hydraulic characteristics of systems in transient modes by solving the equations of heat and mass transfer in a steam-water mixture [1]. For more detailed calculations of the structural elements of spent fuel assemblies (SFA) temperature, the ANSYS software is used, which implements the finite element method [2]. The results obtained with the help of the above simulation tools are used by specialists of SEC NRS to assess the protective measures developed by operating organizations.

In the present report for representative scenarios of occurrence of accidents involving loss of decay heat removal from the SNF the description used in SEC NRS assumptions and approximations to create computational models of wet SNF storage is given. Taking the example of the computational models are shown implemented in the SEC NRS approaches to independent evaluation of the thermohydraulics characteristics of the SNF storage and time intervals, describing the different stages of occurrence of an accident.

2. SIMULATION OF AN ACCIDENT UNDER PROLONGED LOSS OF EXTERNAL AND BACKUP POWER SUPPLY FAILURE

2.1. Input data

The considered scenario is characterized by a long-term loss of external power supply to a fully loaded SNF storage facility with the inability to start emergency diesel generator substation. As a result of the considered failure, all active systems, including cooling and ventilation systems, are shut down. Residual heat generation of SNF leads to heating of the coolant, subsequent excess of the operational limits and conditions on the water temperature and the beginning of the developed bulk boiling in the compartments of the SNF storage. The steam formed on the water surface is removed due to the pressure difference from under the overlap of the compartments into the high-rise pipe of the ventilation system.

The subsequent boiling of the water to the upper part of fuel rods and below leads to heating of the exposed sections of the fuel rods up to a temperature of +600°C, at which the complete depressurization of the fuel cladding is postulated. At the same time, a decrease in the heat exchange area of water with the surface of the fuel rod shells leads to a significant heating of the latter. The result of the reduction of the water when passing through the design of the cover also reduces the heat and mass transfer, which leads to acceleration of heating of fuel elements, reducing water levels and intensification of evaporation of water in the compartment of the SNF storage. At the same time, a decrease in the water level leads to a decrease in the volume of boiling and, as a consequence, to a decrease in the pressure of saturated vapours under the overlap.

2.2. Computational model

The estimated model of wet SNF storage facility for the considered initial events developed with the use of APROS software 6, designed to determine the thermal-hydraulic characteristics of systems in transient operating conditions by solving the equations of heat and mass transfer in steam-water mixture in the nodal approximation. It is assumed that the SNF storage facility consists of monolithic reinforced concrete storage compartments filled with water and interconnected by a transport corridor. In the upper part of compartments there is a metal overlap, modelled in the form of holes above each fuel assembly, through which the supply air is evenly distributed throughout the surface space of the compartment model [3].

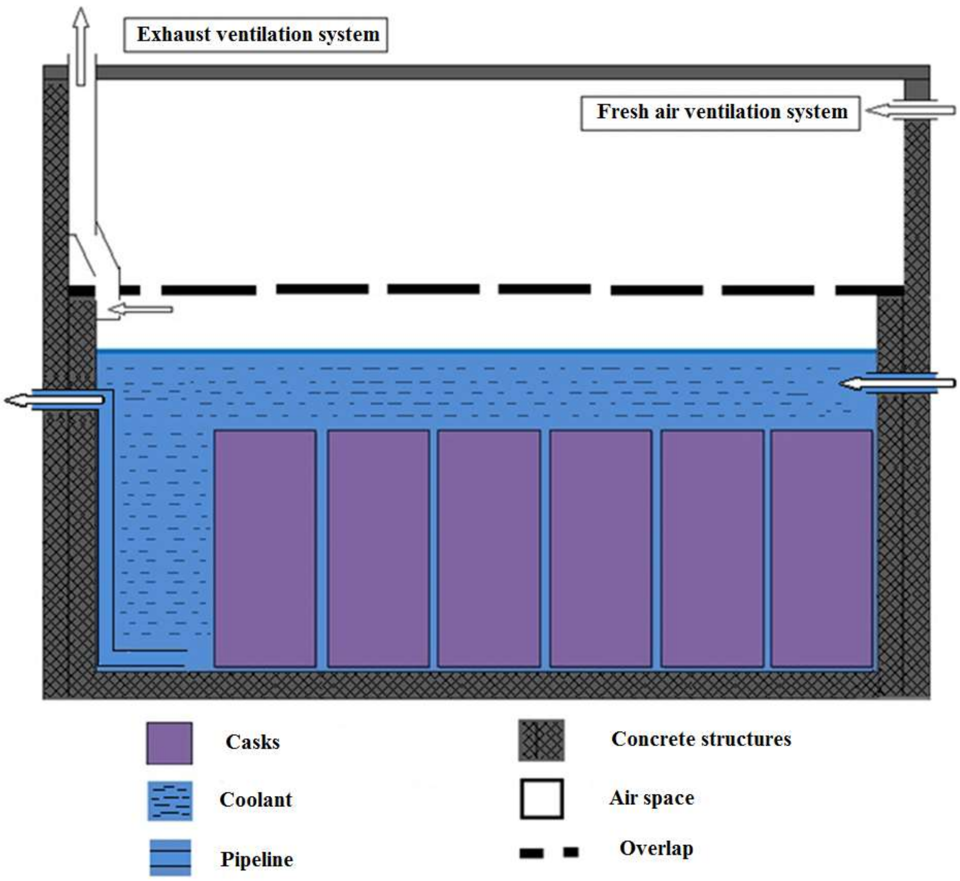

FIG. 1. Compartment of SNF storage facility.

The normal operation of the SNF storage facility is provided by heat-removal system, water supply system and draining of compartments system, as well as the supply and exhaust ventilation system. It is assumed that the SNF storage is loaded with SFA of VVER-1000 reactors with initial enrichment up to 4.95% ^{235}U, burnup up to 58 GWd/tU and a holding time of 5 years, placed in casks with a capacity of 16 SFA each [4]. The simulated schemes of SNF storage compartment and cask are shown in Figures 1 and 2.

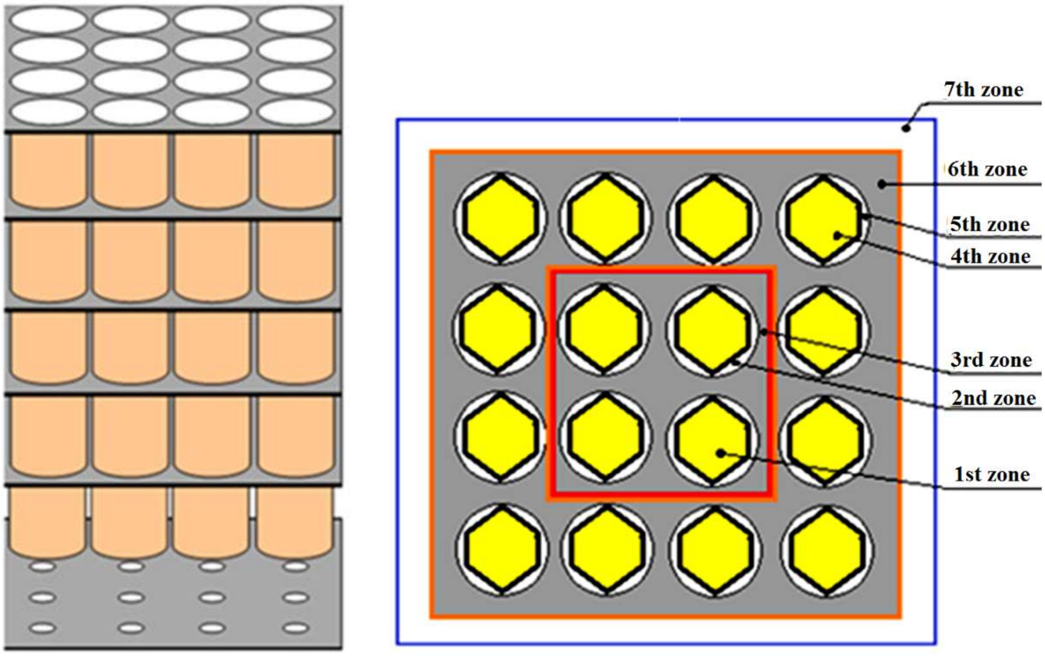

FIG. 2. Cask diagram.

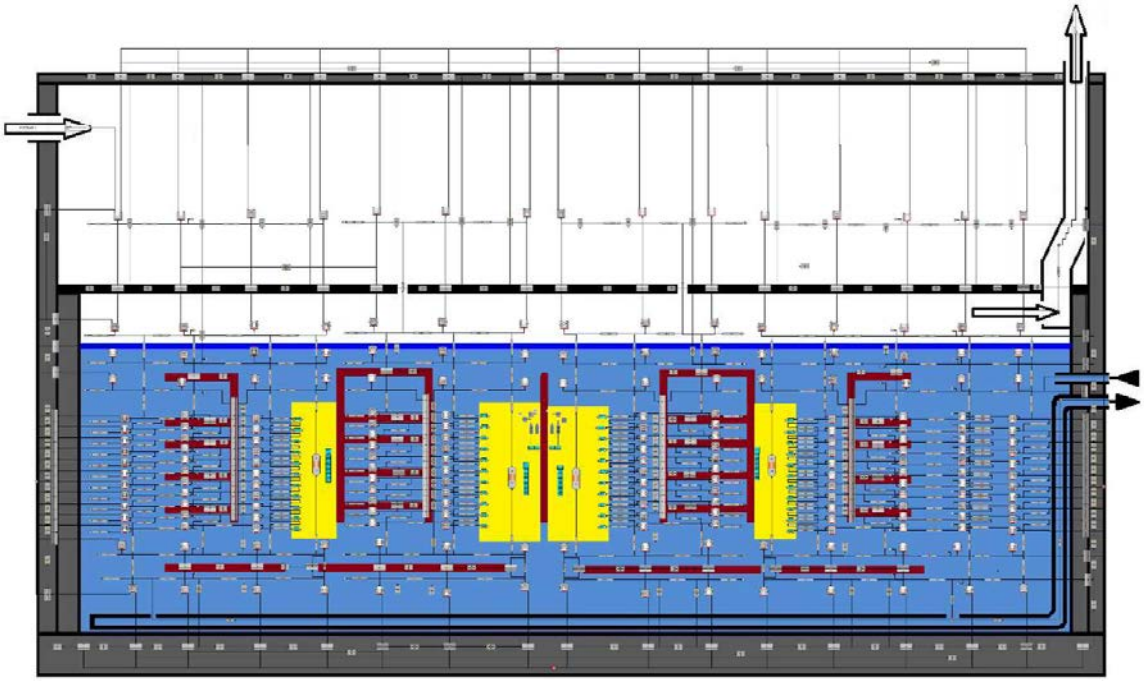

FIG. 3. Computational model of storage compartment.

The diagram shown in Figure 2 shows that the design of the cells in which the SFA is placed is a downcomer pipe and excluding lateral transfer of the coolant during cooling of SNF, thus creating the most stressed zone in the centre of the cover. In order to consider this structural feature and correct flow calculations, calculational model of the cask is divided in two parts and 6 computational zones. The first part of the cask includes distancing grids, 4 central covering tubes with SFA and coolant. The second part includes a distancing grids, 12 peripheral covering tubes with SFA and coolant. Calculated zones include SFA (1st and 4th zones), the space between SFA and pipe (2nd and 5th zones), the inter-tube space (3rd and 6th zones) and inter-casks space (7th zone). Developed using the APROS software, the design model of the storage compartment filled with SNF of the VVER-1000 reactor includes the main systems and elements, including cleaning, filling and draining systems and is shown in Figure 3.

2.3. Results

As a result of the calculation, it was found that the excess of the safe operation limit for the water temperature in the compartment (+90°C) occurs 41 hours after the failure of the power supply system. Heating the compartment leads to a significant increase in the rate of evaporation of water. The steam produced on the surface of the water is removed by natural ventilation from under the metal plates of the compartments into the high-altitude pipe.

The process of bulk boiling in the area of the covering tubes begins 68 hours after the failure of the power supply system. Figure 4 provide dependence of operating parameters of ventilation system on time. “Negative” rate in supply ventilation system shows that natural air circulation through ventilation system is maintained up to boiling-up of coolant in the SNF storage facility. At first flow through input of supply ventilation system decreases, saturated vapor pressure under metal plates of storage compartment increases and evaporation rate of the water increases. After boiling water in the compartment, the vapor pressure under the overlap exceeds atmospheric pressure at the entrance to the system of ventilation in the result of saturated steam penetrates through the overlap, preventing the flow of supply air into the compartment of the SNF storage. Further, fresh air does not enter through ventilation system. Reduction of the mixture flow rate after boiling-up to the level of spent nuclear fuel assemblies caused by decreasing of water volume in the storage compartment.

After the beginning of the process of developed boiling, the water in the storage compartment is boiled up to the level of SFA, accompanied by decrease in the mass of water in the storage compartment (Figure 5). This stage is characterized by a stable temperature distribution field, and its duration is about 130 hours. At the same time, the temperature of the shell of the most heated fuel rod in the storage compartment does not exceed +102°C.

Further heating of nuclear fuel in SFA takes place in the absence of water cooling of the fuel cladding and lasts about 140 hours. Decreasing of water level and heat removal of fuel rod cladding surface leads to their considerable heating. In addition, when water level passing through the structure of the cask, then water mirror area, heat transfer and mass transfer decreases. This leads to a nonlinear change in the water level and rate of evaporation of water in the storage compartment.

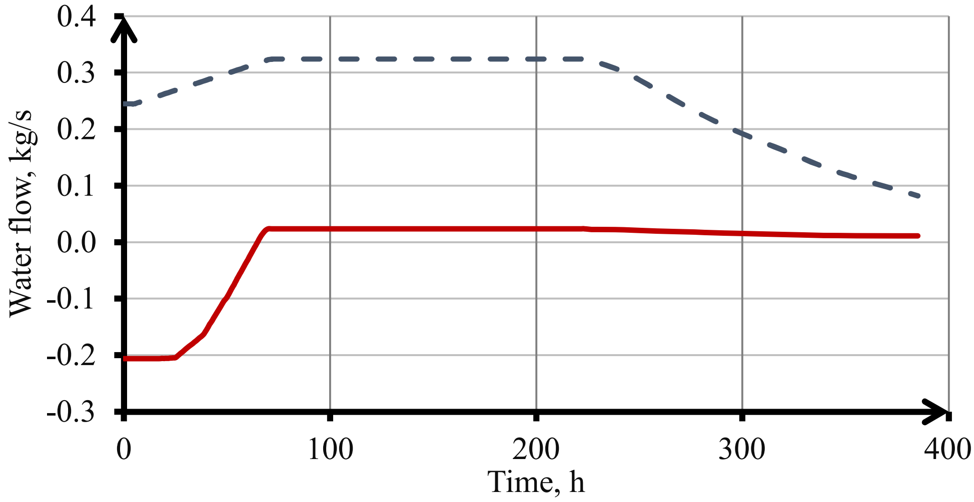

FIG. 4. Mixture of air and aerosol flow rate in supply (blue) and exhaust (red) ventilation systems dependence on time.

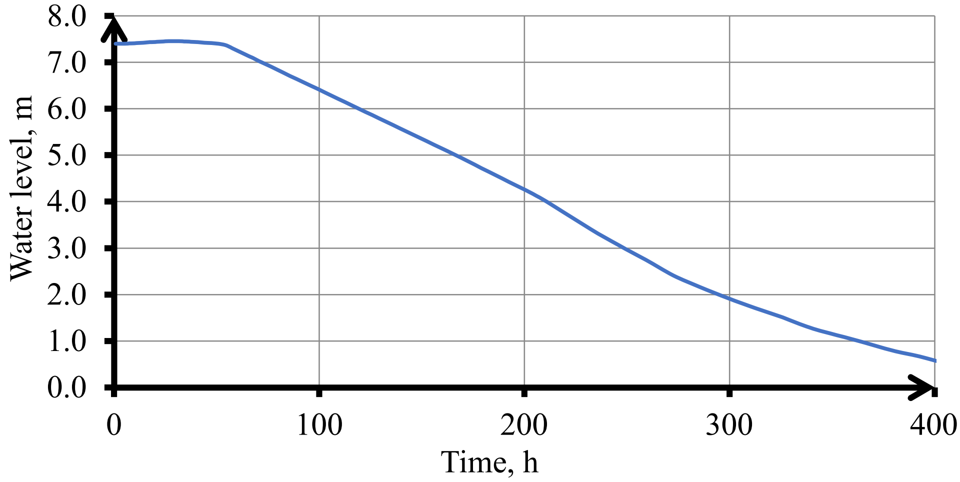

FIG. 5. Water level dependence on time.

Figure 6 provides a dependence of the temperature of maximum stressed section of fuel cladding and covering tube on time. Dependence shows that the temperature of all elements of the SNF storage starts to increase only after coolant dry-up, and before that, temperature of non-fuel elements is equal to the boiling point of water (~+100°C).

Figure 7 provides a distribution of temperature of the fuel cladding over the height for various times of accident evolution. The chart shows that the graph of the temperature increase has non-linear dependence on height, which associated with the design features of the cask (distancing grids contribute to the heat transfer in certain areas of the cask in height). The maximum temperature of fuel rod is at the upper part of the fuel rod (at level of 3.68 m). The temperature drops at highest point of the fuel element due to presence of gas gap instead of a fuel column.

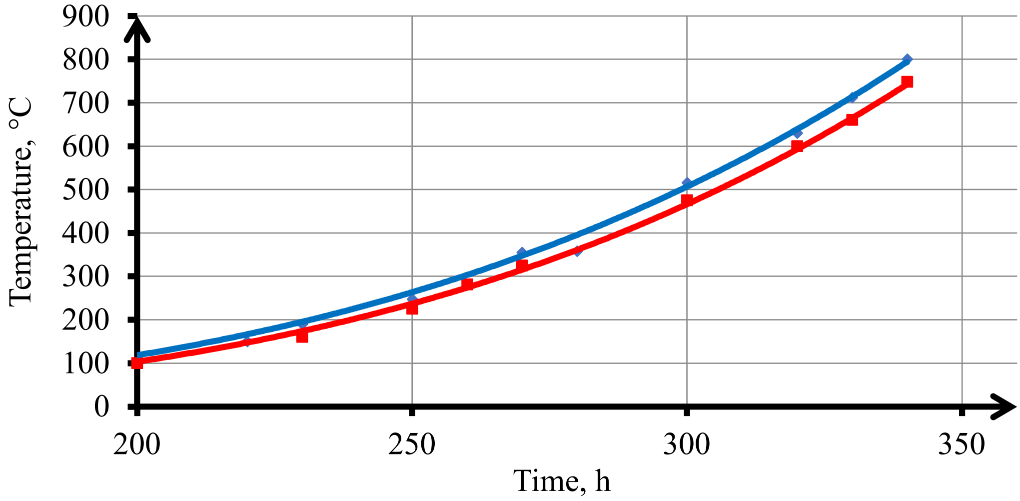

FIG. 6. Temperature of the maximum stressed section of fuel rod cladding (blue) and covering tube (red) dependence on time.

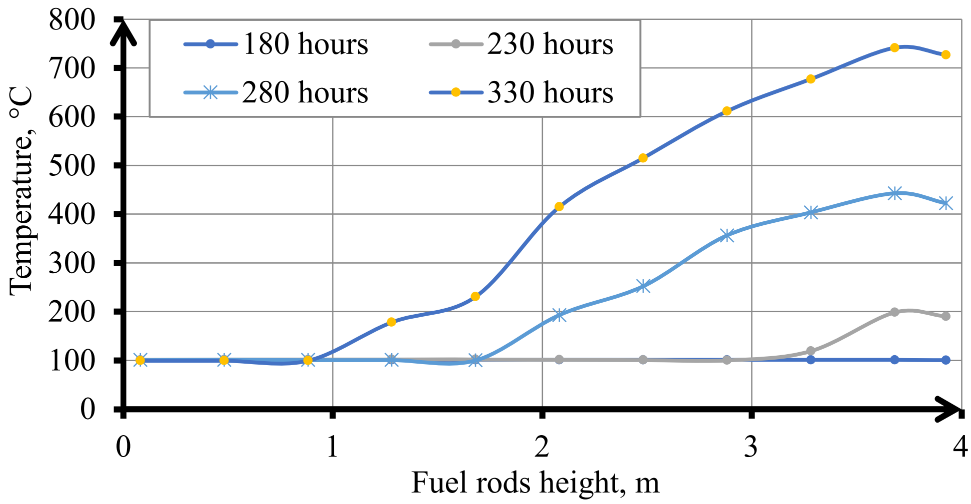

FIG. 7. The temperature distribution in the cladding height for different development times of the accident.

The initial stage of development of accident is characterized by yield of activity from the emergency compartment of the storage facility along with the vapor. With the further evolution of this accident and the achievement of fuel cladding temperature 600°C, depressurization of 100% fuel rods in the emergency compartment is postulated, with the release of activity accumulated in the gap between the shell and nuclear fuel into the atmospheric air without purification. 340 hours after the failure of the power supply system, as a result of boiling water level drops to 1.3 meters, and the maximum temperature of the fuel rods (at the top) reaches 800 °C. Further progress of the heating process is accompanied by chemical reaction between zirconium clad and water vapor (steam-zirconium reaction) and release of heat which exceed residual heat from SFA, which leads to additional heating of the SNF and the output part of the accumulated activity in the air.

The data obtained using APROS, after this time point is not used in further calculations due to high-level of error. However, it should be noted that APROS at the initial stage of the steam-zirconium reaction correctly demonstrates a sharp increase in the temperature of the fuel cladding to its melting point.

3. SIMULATION OF AN ACCIDENT WITH COMPLETE DEHYDRATION OF THE SPENT NUCLEAR FUEL STORAGE FACILITY

3.1. Input data

This emergency scenario refers to beyond design basis accidents and is characterized by the destruction of the building structures of the SNF storage, accompanied by a violation in the operation of the recharge system. In the presence of an uncompensated leak, a pressure drop is formed in the compartment, which is recorded by the control systems. The cooling system in the damaged compartment is switched off by the operator or after a while fails due to the lack of water flow. Additionally, in this scenario, due to damage of pipeline have a fault-feeding system SNF storage facility. All other systems of normal operation and systems important for safety function normally. The conditions of occurrence of this accident completely eliminate oxidation of zirconium of the fuel cladding of the fuel assemblies, since the loss of coolant in the emergency compartment. In this regard, the yield of radionuclides from SFA fuel can be due to the depressurization of fuel cladding due to thermal effects, which occurs when the temperature reaches +600°C. In addition, it is postulated that at +1000°C the destruction of the fuel matrix begins, which leads to an additional output of gaseous fission products into the environment.

3.2. Computational model

The calculations were carried out using the ANSYS Fluent software, which is designed to simulate and solve the finite volume problems of hydrodynamics, acoustics, heat transfer with the possibility of accounting for phase transitions, radiation heat transfer, chemical reactions in complex bodies and systems of bodies, and also allows you to simulate multiphase flows [2].

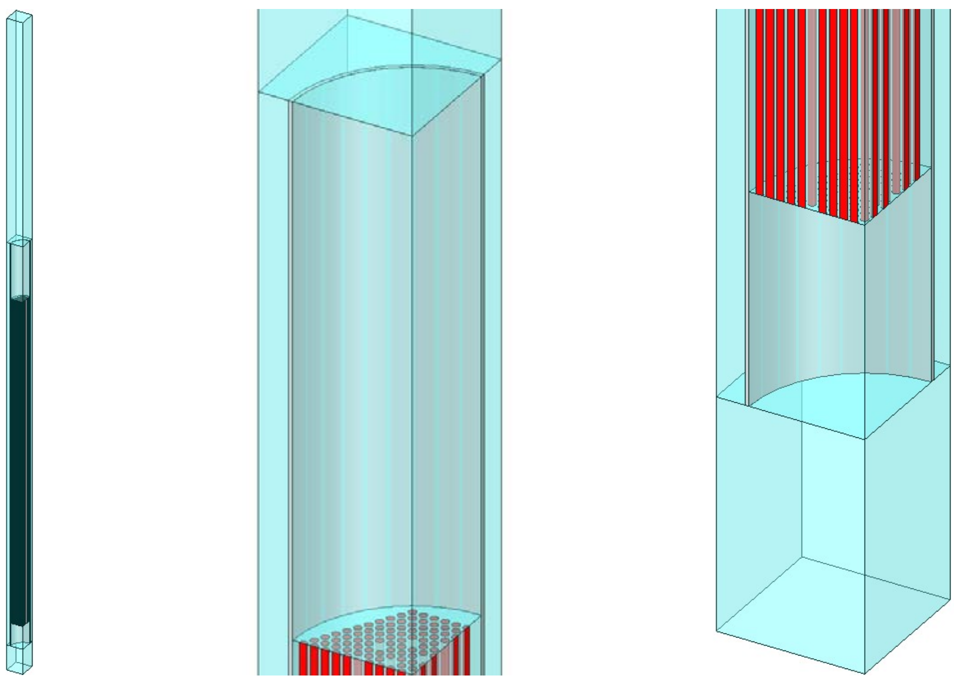

FIG. 8. Computational model of accident with storage compartment dehydration.

The design model is a 1/64 part of the cover in the form of a parallelepiped placed in the SNF storage, which includes a part of the bottom of the emergency compartment made of concrete and 1/4 part of the stainless steel cover pipe with the VVER-1000 fuel rods in it. Figure 8 shows the design model performed in the graphical module SpaceClaim of ANSYS software.

The following approximations and assumptions are accepted in the development of the computational model. It is considered that due to the rapid complete dehydration, the storage volume occupied before by water is replaced with air. A small part of the water vapor is removed from under the overlap by the ventilation system pipe into the environment. The chosen geometry allows to accept adiabatic boundary conditions on the side surfaces of the computational model. The heated air may flow and the return air current from the environment through the open upper boundary of the design model. The air flow regime was calculated using the ANSYS k-ε models implemented in the Fluent PS module and the Boussinesq approximation in the gravity field.

3.3. Results

According to the estimated values obtained as a result of the assessment (Figure 9), it was found that the time of reaching the temperature of +600°C by fuel cladding, at which the depressurization of all fuel rods stored in the emergency compartment of the SNF storage is postulated, will be about 2 days. In addition, the results of the calculation show that the beginning of the final stage of the accident occurs after 5.5 days (reaching the temperature of +1000°C by the fuel cladding), and it will take about 8 days to achieve the quasi-stationary temperature of the fuel rods. The steady-state value of the temperature does not exceed 1200°C.

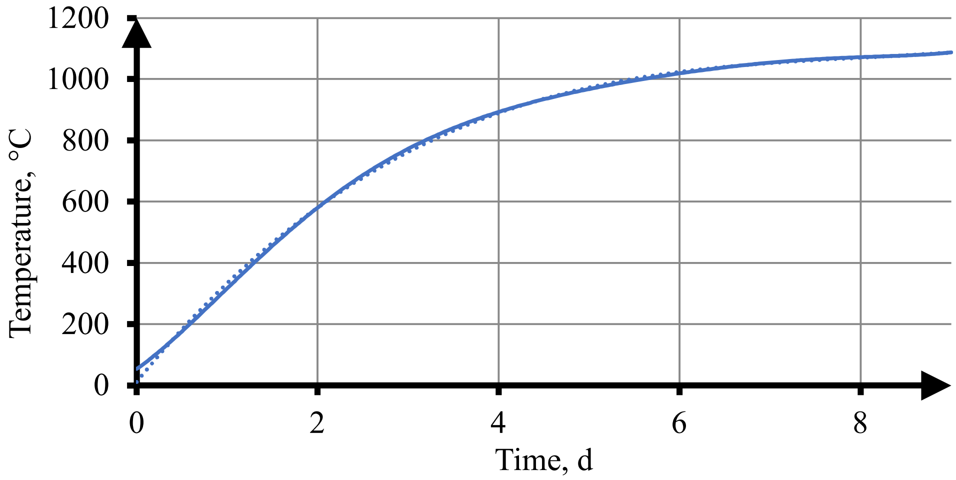

FIG. 9. The temperature dependence in the fuel rods cladding at time.

CONCLUSIONS

At present, much attention is paid to the analysis of severe accidents not only at nuclear power plants but also at the enterprises of the nuclear fuel cycle. The presented qualitative analysis of the possibility of radiation consequences of the accident with the complete loss of power supply in the SNF storage indicates the need for a more detailed consideration of possible severe accidents at nuclear fuel cycle enterprises. It is shown that for the early adoption of preventive measures for the organization of additional recharge emergency storage compartment at the initial stage of the accident, it is important to determine as accurately as possible the available time for their implementation.

REFERENCES

[1] VTT TECHNICAL RESEARCH CENTRE OF FINLAND, HELSINKI, APROS 6 Feature Tutorial. Release: APROS 6.06, Fortum, Helsinki, (2016).

[2] ANSYS, INC., Release Notes. Release: ANSYS 18.1, Canonsburg, (2017).

[3] MERKULOV I.A., MATSELYA V.I., SEYELEV I.N., KORNEYEV M.I., SKURYDINA YE.S., "Extending the lifetime of a water-cooled VVER-1000 SNF storage facility (HOT-1) at FGUP "MCC", Russian Phys. J. **60** (2013) 54–59.

[4] OKB "GIDROPRESS", Nuclear fuel assemblies second generation. TVS-2M (2014), http://www.gidropress.podolsk.ru/files/booklets/ru/TVS_rus.pdf.

MODELLING OF PARAMETER-SF4 EXPERIMENT WITH SOCRAT/V1 CODE

K.S. DOLGANOV, A.E. KISELEV, D.Y. TOMASHCHIK, T.A. YUDINA
Nuclear Safety Institute of Russian Academy of Sciences (IBRAE),
Bolshaya Tulskaya str. 52, Moscow
Russian Federation

Abstract

The PARAMETER-SF4 experiment was performed at the PARAMETER test facility at FSUE SRI SIA "LUCH" on 21 July 2009 to study the behaviour of a pre-oxidized fuel bundle under conditions of air ingress with a small flowrate and subsequent bottom quenching. Fundamentally the same phenomena are expected during severe accidents at spent fuel pools (SFPs), therefore the data can be used for validation of codes that can be applied for the SFP analysis. The main purpose of the simulation PARAMETER SF4 experiment with the SOCRAT code was to check the consistency of the code models to solve the thermal problem and to simulate the bundle degradation and relocation of the materials as well as the effect of the bundle quenching.

1. INTRODUCTION

The experiment PARAMETER-SF4 [1] was the fourth test in PARAMETER-SF series performed within the ISTC (International Scientific and Technical Centre) project. The PARAMETER-SF4 test was planned as a counterpart of QUENCH-10 test [2] initially dedicated to study air ingress with subsequent water flooding during a severe accident in a spent fuel pool [3]. The PARAMETER-SF4 scenario followed the common test sequence defined for PARAMETER-SF test series (PARAMETER-SF1, -SF2, -SF3, -SF4 [1,4] that included preheating, pre-oxidation, transient and flooding phases. The PARAMETER-SF bundles are prototypical to the geometry and materials of the fuel assemblies (FAs) used in VVER-1000 reactor. The bundle heating to target temperatures is carried out electrically using tantalum heating elements installed in the centre of the rods and surrounded by annular UO_2 pellets.

The experiment SF4 was conducted with the aim to study the model of VVER-1000 FA under simulated conditions of a severe accident including the stages of air ingress and further quenching by the bottom flooding with water, namely:

– Study of the behaviour of FA structural components (fuel pellets and claddings, spacer grids);
– Study of the oxidation degree of FA structural components;
– Study of interaction and structural-phase changes in the materials of FA model (fuel pellets and claddings);
– Study of the hydrogen release.

The SF4 test was successfully conducted at the FSUE SRI SIA "LUCH", Podolsk, Russia [1]. It covers the initial phase of fuel rod claddings pre-oxidation in steam, as long as fuel uncovery occurs, and further substitution of steam into air atmosphere, once the water level decreases below bottom of active fuel and convection loops assure the ingress of air to fuel rods.

2. PARAMETER TEST FACILITY

Detailed description of the PARAMETER SF4 test section is given in Ref. [5]. The investigated test bundle consisted of 19 fuel rods with E110 claddings and UO_2 pellets, surrounded by 12 peripheral solid rods and shroud (Fig. 1). The electrical heating of 18 fuel rods was provided by central tantalum heaters (length 1275 mm, diameter 4 mm). One unheated fuel rod was located in the centre of the test bundle.

The measurement system of facility included the following components:

- 52 thermocouples of three types with external and internal mounting (in the test bundle);
- 3 pressure pick-ups (in the test bundle);
- Electronic flow meters for steam, argon, air and water;
- SOV-3 detector for hydrogen concentration;
- OLCT-20D detector for oxygen concentration;
- State of the valves.

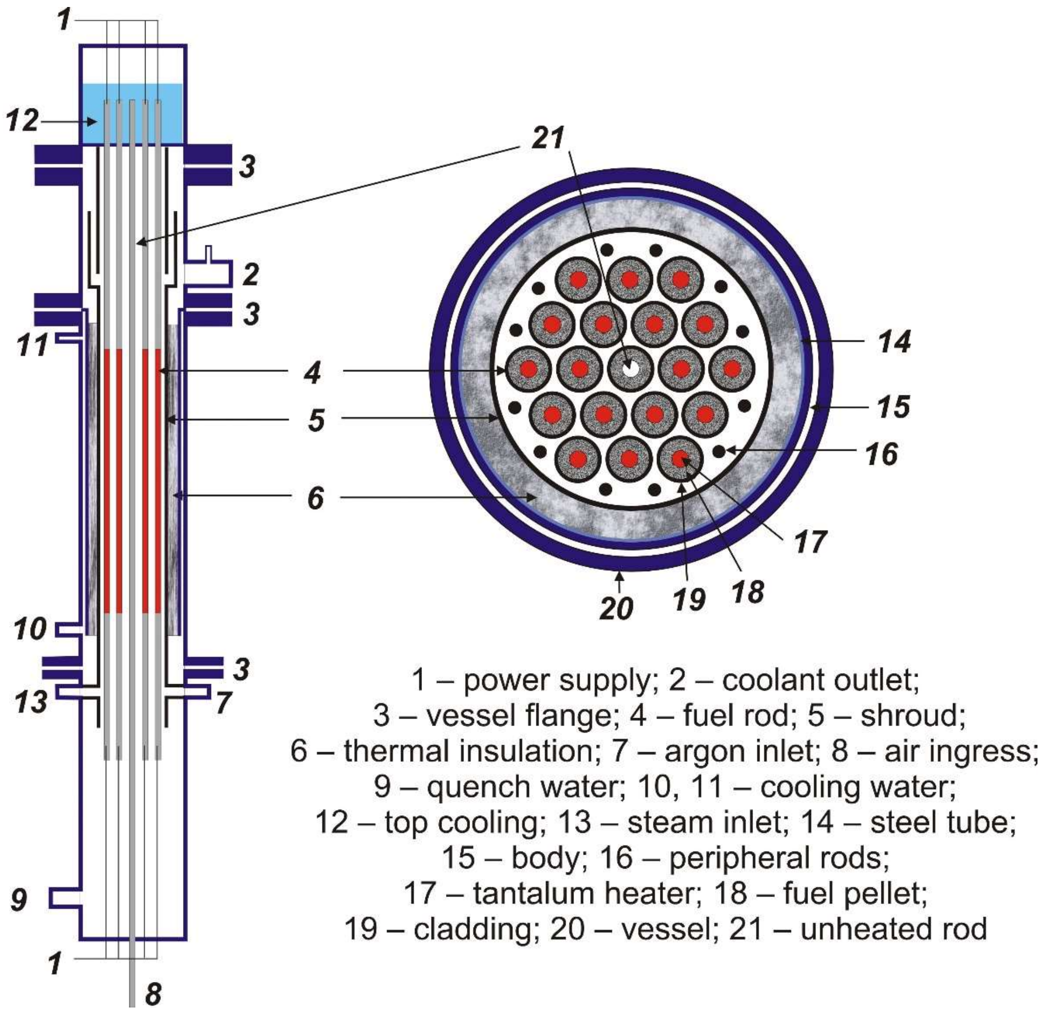

FIG. 1. PARAMETER SF4 test bundle.

3. EXPERIMENTAL SCENARIO

Description of the PARAMETER SF4 test scenario is given in Ref. [5]. The experiment consisted of five main stages (Fig. 2):

- *Preparation and heating up stage* (0–8000 s) — stabilization of coolant parameters: argon flow rate (~ 2 g/s, inlet temperature ~ 530°C), steam flow rate (~ 3.5 g/s, inlet temperature ~ 280°C), pressure (~ 0.48 MPa at 1475 mm);
- *Pre-oxidation stage* (8000–13 886 s) — FA holdup at temperature of ~ 1200°C in the hottest zone (1250 -1300 mm) for ~ 6000 s. Electrical power was 7500 to ~ 8500 W
- *Cool down stage* (13 886–16 035 s) — maximal FA temperature at the end of the stage ~ 600°C. Electrical power was ~ 4000 W;
- *Air ingress stage* (16 035– 17 500 s) with subsequent (from 16 355 s to 17 434 s) assembly heating-up to FA maximum temperature of ~ 1750°C in the hottest zone;
- *Bottom flooding stage* (~17 500–17 900 s) — flooding of the bundle from bottom.

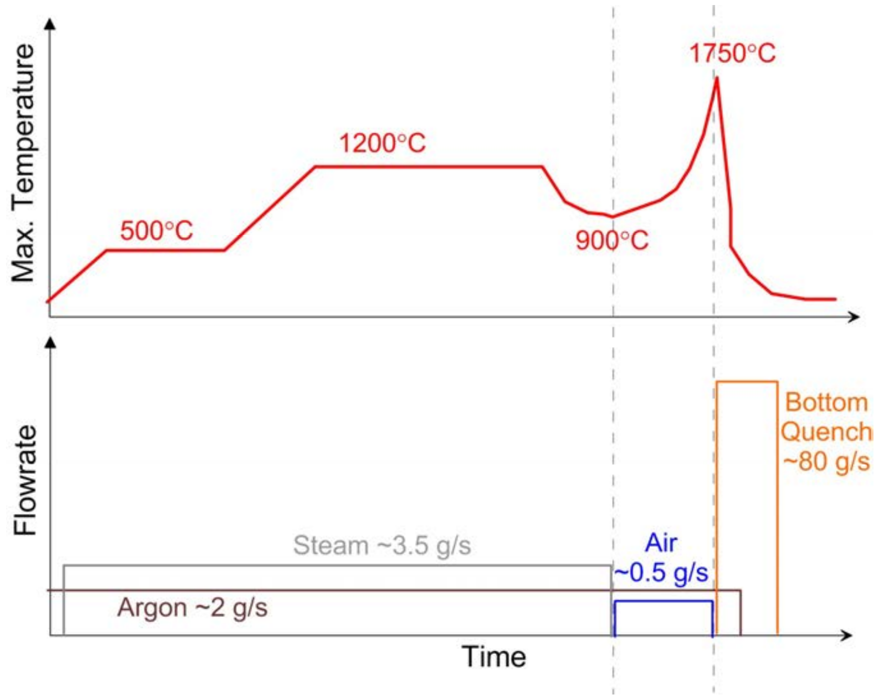

FIG. 2. PARAMETER SF4 scenario [6].

4. SOCRAT CODE DESCRIPTION AND TEST FACILITY MODELLING

SOCRAT/V1 (System Of Codes for Realistic Assessment of severe accidents) is an integral computer code intended for a coupled modelling of a wide range of thermohydraulic, physicochemical and thermomechanical processes at all stages of accident progression at VVER reactors, starting from initial event and ending with full corium release following the reactor vessel failure. The code is essentially developed to model VVER NPPs, but it was also applied to simulate the severe accidents at integral-type light water reactors, BWRs (Fukushima Daiichi) and PWR reactors (TMI-2). SOCRAT is widely validated on experimental data got from Integral and Separate effect tests, including International standard problems and benchmarks and national experiments [7].

The main areas of SOCRAT/V1 application include the estimates of hydrogen source to the containment, and source of corium (mass, energy and composition) from reactor pressure vessel after its melt-through. These data were also used as initial data for the design of safety systems (number and positioning of hydrogen recombiners, core catcher).

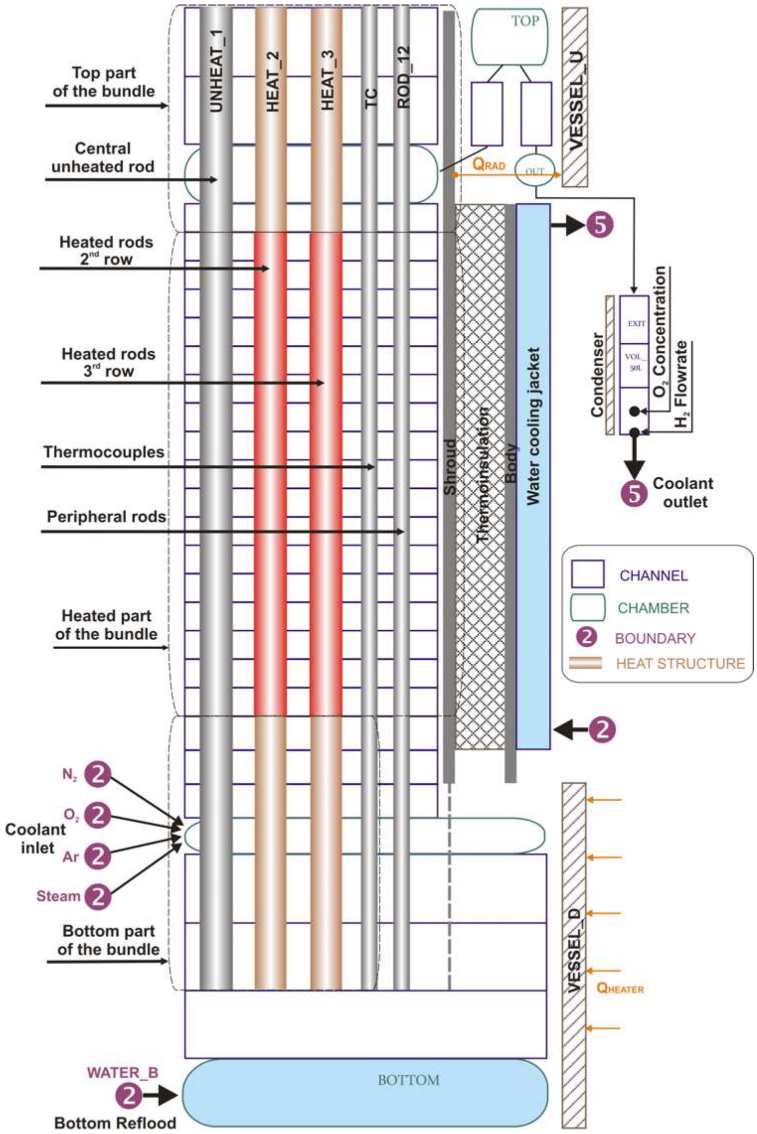

FIG. 3. SOCRAT nodalization scheme for PARAMETER SF4 test bundle.

FIG. 4. SOCRAT nodalization scheme for fuel rod simulator heaters.

SOCRAT/V1 has a modular structure. Each module contains the realistic models of a separate set of physical processes, and interaction between different processes is assured by coupling of modules through the common interface standards. SOCRAT/V1 contains the data base of thermo-physical properties of different materials.

The nodalization scheme of PARAMETER test facility for the SOCRAT/V1 code is presented in Fig. 3. It has five radial zones (central rod, heated rods of the 2nd and the 3rd row, peripheral rods, and shroud) and 27 axial cells. Thermocouples are modelled as a separate element "TC". Zirconium mass in spacer grids is added to fuel rods and shroud at 6 elevations.

Electric heating nodalization (Fig. 4) includes tantalum heater (marked in red) and current leads. Resistance of wires R_{add} is accounted to match experimental current and power for groups of heaters.

Steam condenser and line to SOV-3 detector are modelled to compare calculated hydrogen concentration with experimental data. Inertia of SOV-3 is also taken into account using simple memory average (SMA) method.

To model air ingress stage a correction to SOCRAT/V1 oxidation model was applied. Heat of reaction depends on steam-oxygen volumetric concentration.

5. RESULTS OF PARAMETER SF4 TEST MODELLING

5.1. Initial and boundary conditions

Calculation starts at time 0 s with initial test section temperature 300 K. Electrical power matches exactly the measured data (Fig. 5). The mass flow rates of steam, argon, air, and bottom quench water at bundle inlet are averaged based on experimental data [2]. Coolant pressure mainly depends on outlet noncondensable gas volumetric flow rates and is also presented in Fig. 5.

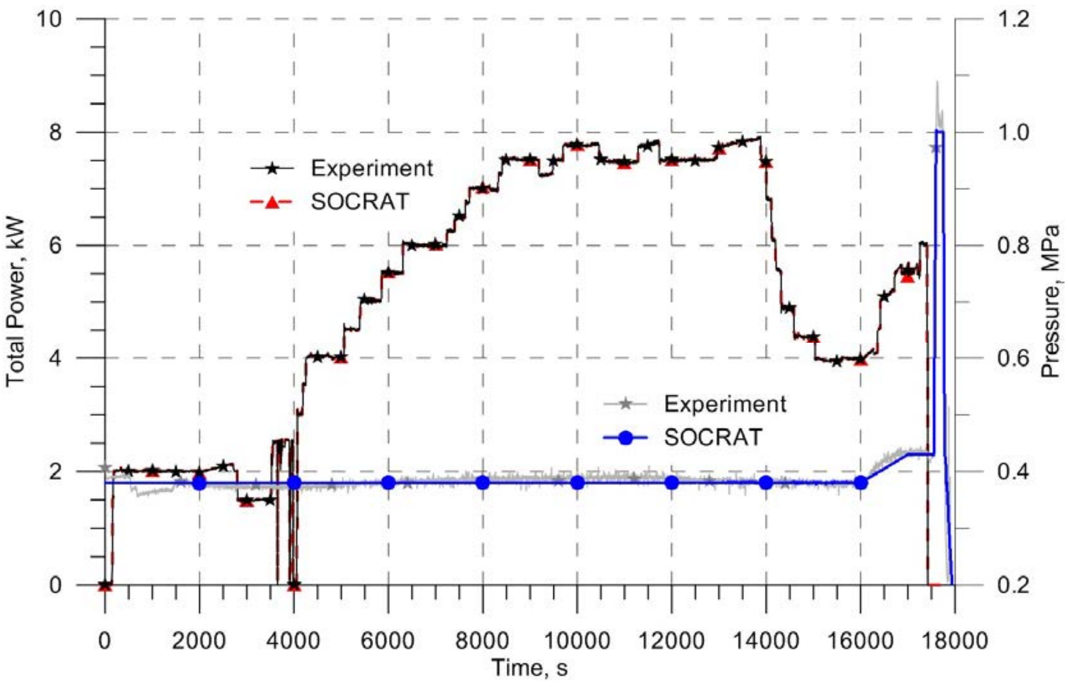

FIG. 5. Total electrical power history and coolant pressure in test bundle.

5.2. Bundle thermal response before flooding stage

Thermocouple (TC) data at elevation 200 mm (Fig. 6a) show practically uniform radial distribution of temperature across the bundle. There is no temperature escalation (oxidation or melt propagation) at this elevation. The claddings at elevations from 300 to 400 (Fig. 6b) mm are also not pre-oxidized due to low temperature. One can notice that the measured temperature of a heated rod at 400 mm is slightly lower than that at 300 mm. This is due to a failure of two heaters during pre-oxidation stage. Fast temperature increase in the beginning of flooding stage corresponds to melt relocation from upper part of the bundle.

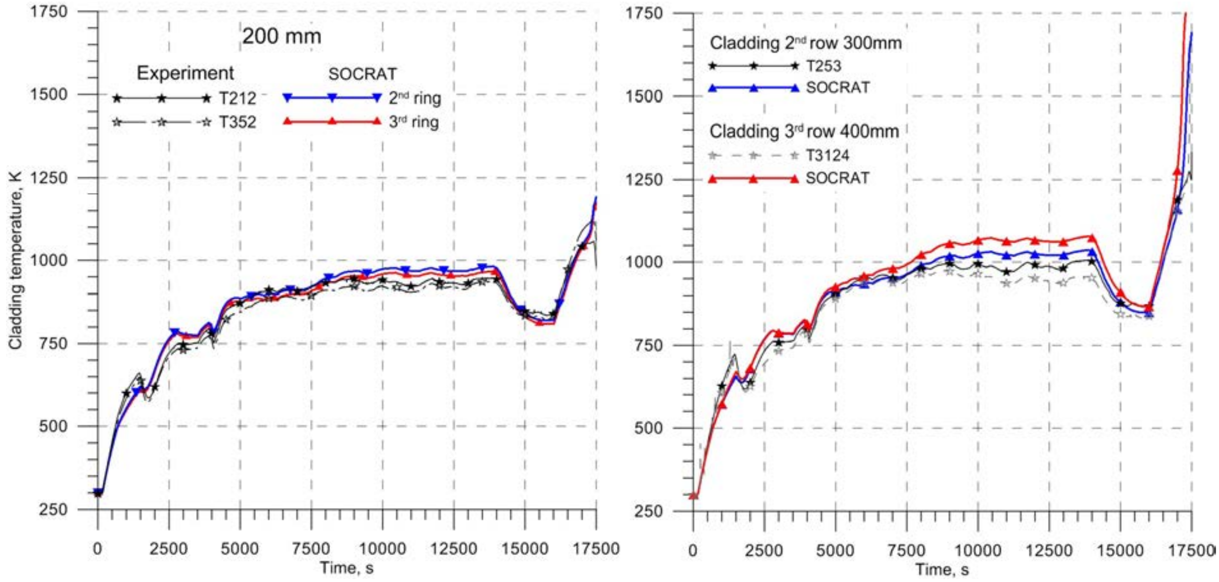

a) b)

FIG. 6. Rod temperature at elevations (a) 200 mm and (b) 300 & 400 mm.

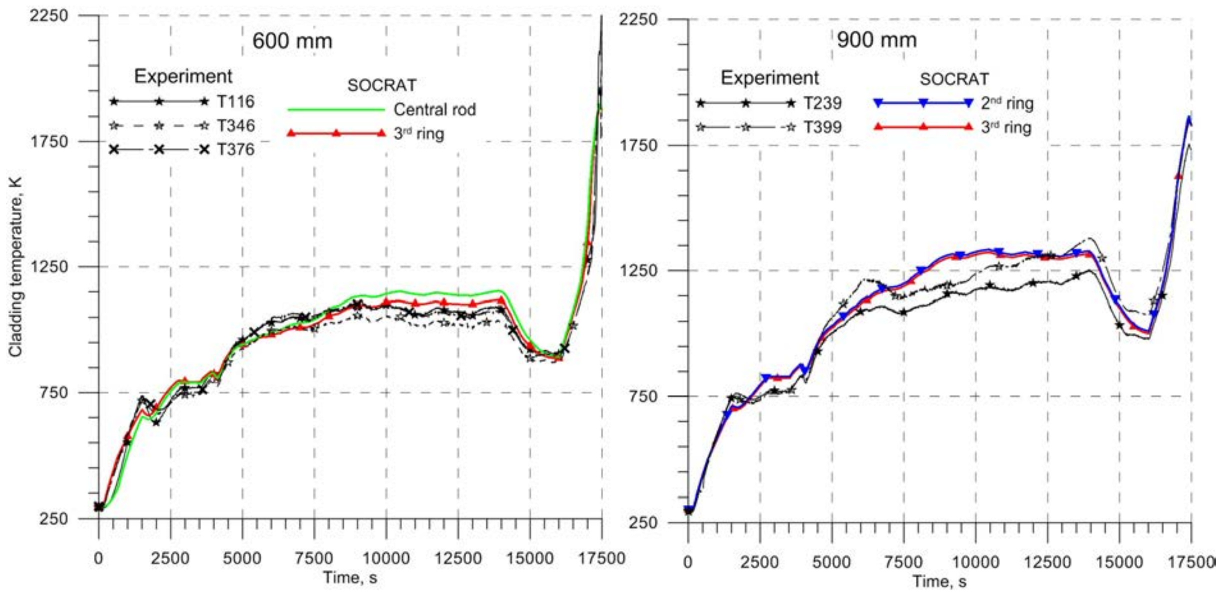

a) b)

FIG. 7. Rod temperature at elevations (a) 600 mm and (b) 900 mm.

Midplane of the heated part of the bundle (600 mm, Fig. 7a) was the hottest part at the end of air ingress stage. Melting of claddings is very likely to occur in this region before the flooding onset but this is not reliably recorded due to TC failure. SOCRAT/V1 predicts the melting of cladding at this elevation at the beginning of flooding stage. Upper half of the bundle (700 to 1300 mm) was equipped with high temperature W-Re TC. According to Fig. 7b, SOCRAT/V1 correctly reproduces the temperature history at the elevation 900 mm.

As it follows from Fig. 8a, the surface temperature of rod 3.4 (TC T3411 means rod 3.4 elevation 1100 mm) at elevation 1100 mm corresponds to that of unheated surfaces (peripheral rods and shroud). This means that the heater of this rod failed. Temperatures near the outlet of the bundle heated part (1250 mm, FIG 8b) are slightly underestimated by SOCRAT/V1 code at pre-oxidation stage. This results in a faster temperature escalation at air ingress stage until starvation conditions occur.

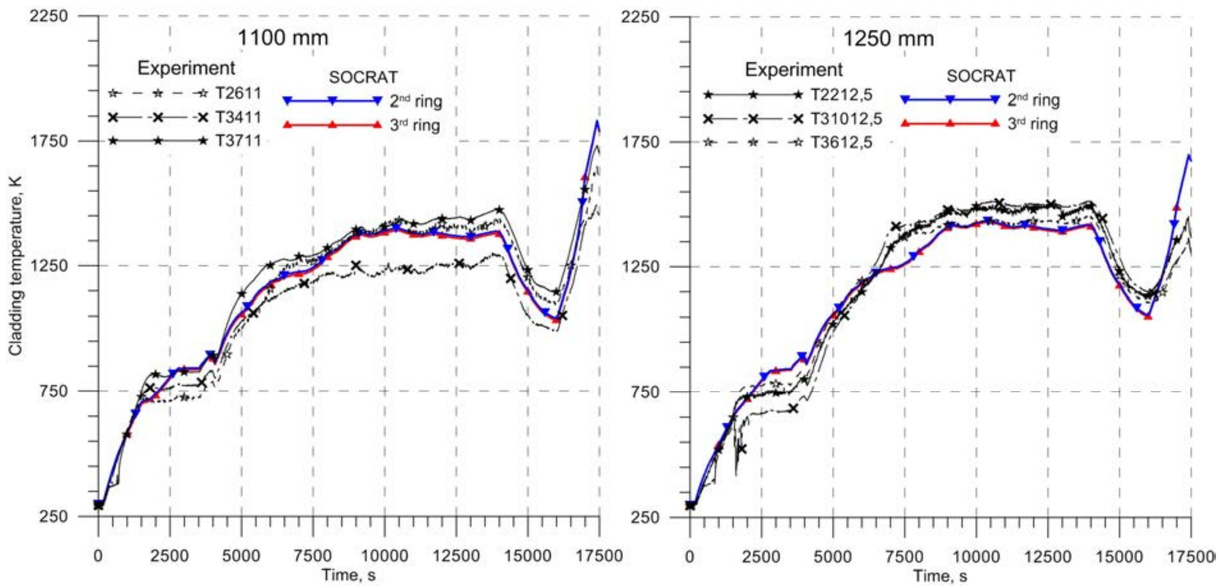

a) b)

FIG. 8. Rod temperature at elevations (a) 1100 mm and (b) 1250 mm.

5.3. Bundle degradation and hydrogen production

Figure 9 presents the measurements of volumetric concentration of oxygen at bundle outlet from the OLCT-20D detector. Indications of OLCT20 were provided in the on-line mode. Significant oxygen consumption starts at 16 700 s when bundle temperature reaches ~1400 K (Fig. 10). Starvation conditions (~0% oxygen concentration) lasts from ~17 100 s to 17 500 s. Time shift in SOCRAT/V1 calculation is due to gas transport time to OLCT-20D location. Figure 10 shows that SOCRAT/V1 predicts a peak of temperature moving in the bundle from elevation 1250 mm down to 1100 mm in 700 s (before starvation), and from 1100 mm down to 700 mm in 500 s without production significant amount of melt. SOCRAT/V1 reproduce these temperature histories at air ingress stage.

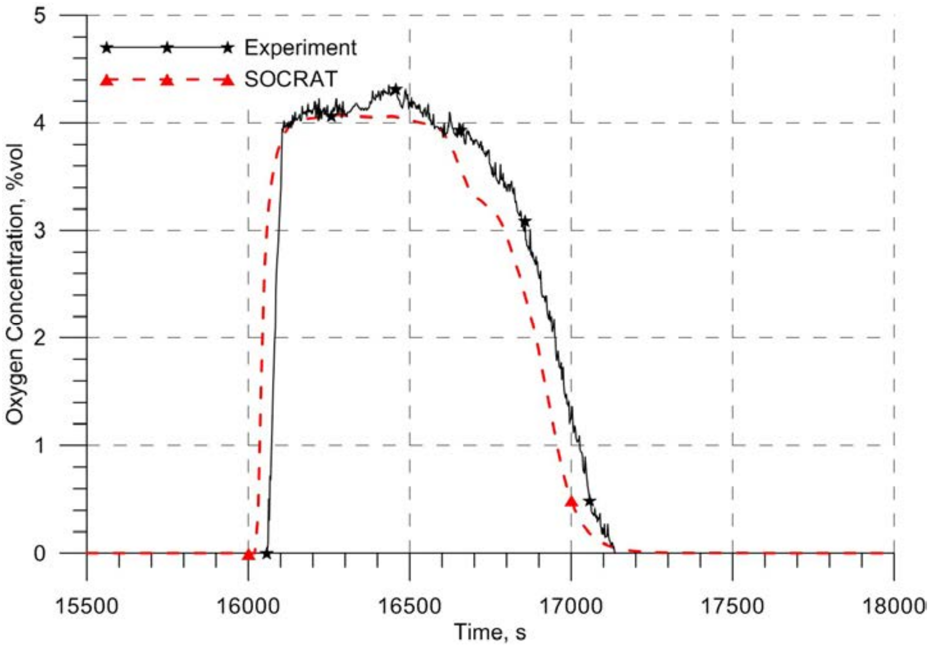

FIG. 9. Oxygen concentration at bundle outlet.

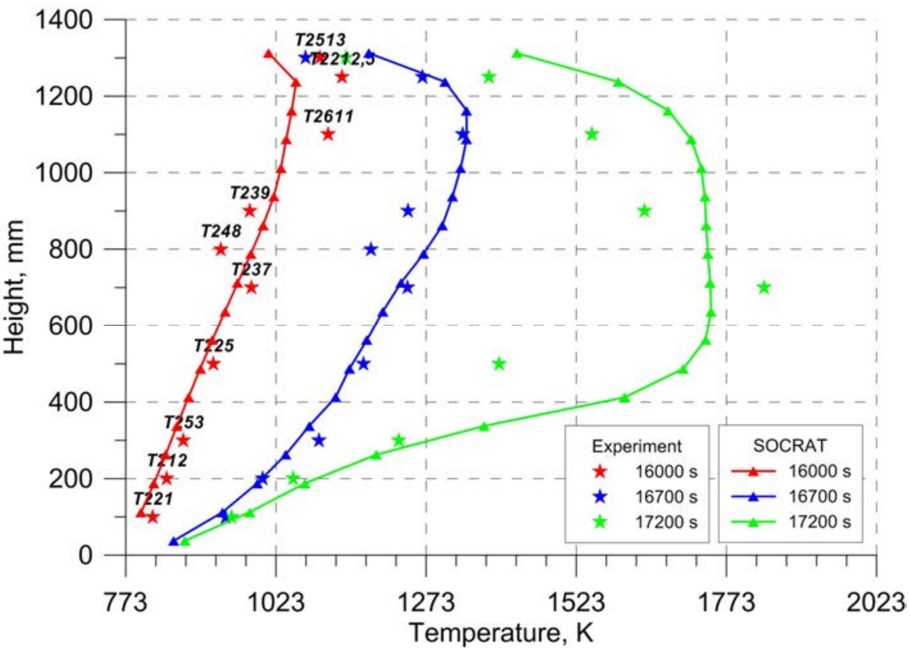

FIG. 10. Temperature profile in the second row rods.

The bottom water supply system started at 17 434 s and was supposed to provide an average flow rate of ~80 g/s. Immediately after the water supply was initiated, TC began to show a decrease of the surface temperature of fuel rods at elevations 0–200 mm (Fig. 11a). At elevations from 400 mm (Fig. 11b), temperature escalation continued, so that after about a few seconds TC reached the upper limit of measured temperatures (1650 K). At elevations above 800 mm, a rather slow but stable cooling of the rods was observed up to ~17 550 s. But after this time their reheating began (Fig. 12). At the same time, a sharp increase of pressure in the test assembly was registered (up to ~1 MPa, Fig. 5.). The pressure jump during water filling together with high temperature of the test assembly resulted in a short-term reduction of water injection, and then due to the intensive gas formation - destruction of the locally superheated shroud.

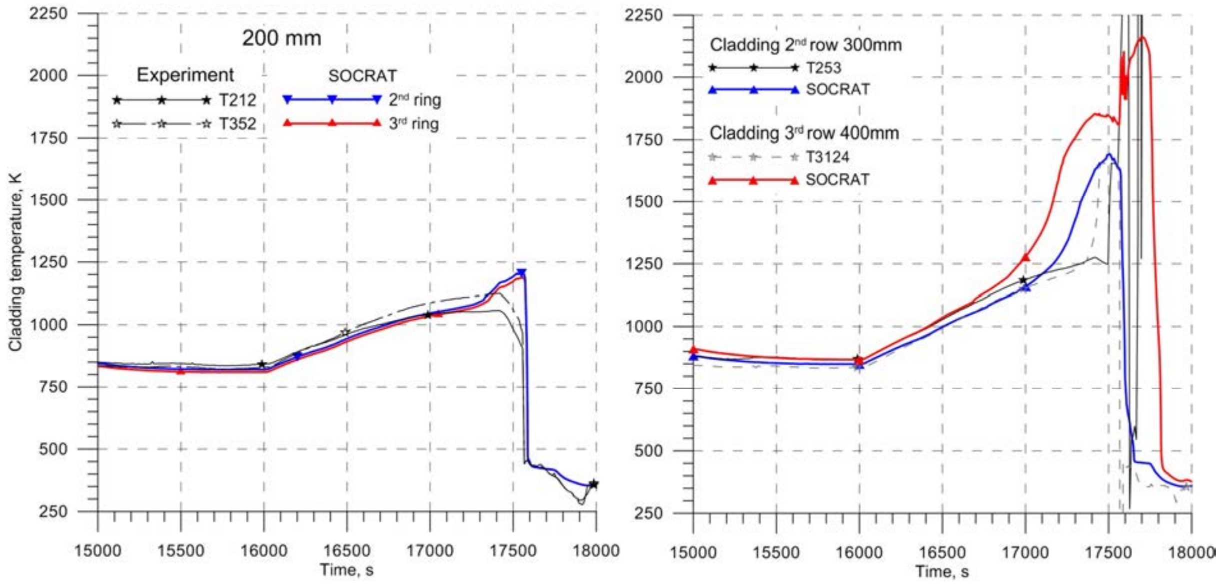

a) b)

FIG. 11. Rod temperature at elevations (a) 200 mm and (b) 300 & 400 mm (bundle degradation stage).

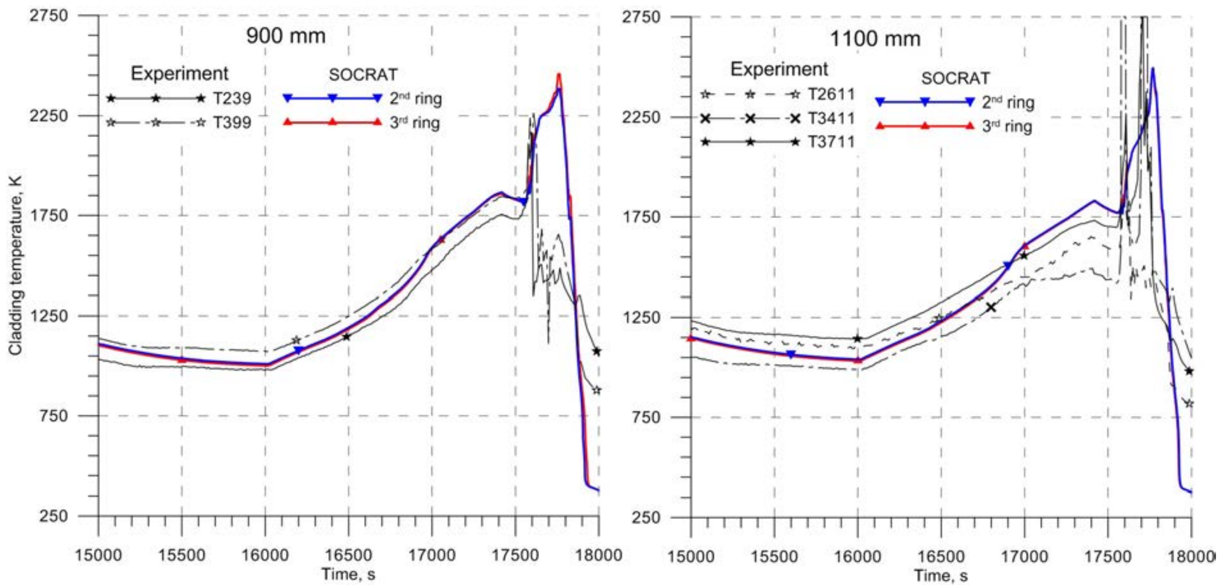

a) b)

FIG. 12. Rod temperature at elevations (a) 900 and (b) 1100 mm (bundle degradation stage).

Analysis of the results of hydrogen measurement by SOV-3 system has shown that at the pre-oxidation stage ~21 g of hydrogen was generated, and at the flooding stage the generation was ~86 g. (Fig. 13) [5]. Results of SOCRAT/V1 calculation are in a good agreement with the measurement data for hydrogen generation dynamics. This evidences of a correct modelling not only of the oxidation of intact bundle, but also of the processes of melt relocation and oxidation, formation of local blockages.

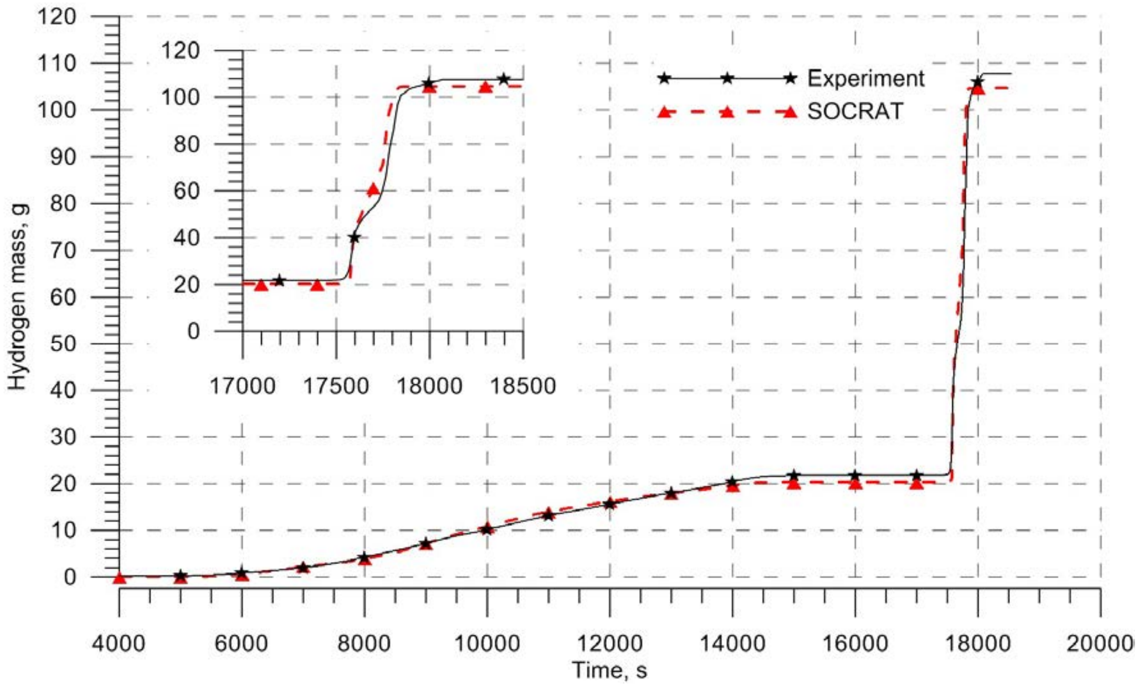

FIG. 13. Total hydrogen production.

Post-test bundle examination [8] demonstrates that at the elevation 130 mm the assembly does not have any visible damages (all fuel rod claddings and periphery rods kept their integrity). The oxide scale on fuel rod claddings is thin and well attached to metal; the measured thickness of zirconium oxide scale varies within 4–9 μm. SOCRAT/V1 code predicts the thickness of zirconia to be 6–7 μm in heated rods at this elevation.

CONCLUSIONS

The air ingress test PARAMETER-SF4 was performed in July 2009 with the aim to investigate the behaviour of a VVER fuel assembly during water flooding after air ingress phase. The scenario and conditions of the experiment are prototypical for a severe accident with fuel rod uncovery and degradation in a spent fuel pool. SF4 experiment has been simulated with the severe accident code SOCRAT/V1. The results of the simulations show a reasonable agreement of calculations with measurements of temperature histories, outlet oxygen concentration and hydrogen production. Insignificant differences were found in melt progression and maximal temperatures in the bundle.

REFERENCES

[1] DEGTYAREVA, L.S., ET AL., Final Report on Scientific Work under ISTC Project No. 3690. Studies of Fuel Assemblies under Severe Accident Top Quenching Conditions in the PARAMETER-SF Test Series (2009).

[2] SCHANZ, G., ET AL., Results of the QUENCH-10 Experiment on Air Ingress, FZKA 7087 (2006).

[3] HOMANN, CH., HERING, W., BIRCHLEY, J., HASTE, T., Analytical Support for the Preparation of Bundle Test QUENCH-10 on Air Ingress, FZKA 7086 (2005).

[4] FSUE SRI SIA "LUCH", Fuel assembly tests under severe accident conditions (PARAMETER-SF test series), Scientific and Research Final Report on the work of ISTC Project No. 3194 (2007).

[5] FSUE SRI SIA "LUCH", Protocol of PARAMETER-SF4 Experiment Results, ISTC Project #3690 "Study of fuel assemblies under severe accident top quenching conditions in the PARAMETER-SF test series" (2009).

[6] YUDINA, T., Comparison results of pretest PARAMETER-SF4 test numerical modeling. In: Proc. .15th Int. QUENCH Workshop, 3–5 November 2009, Karlsruhe, Germany. ISBN 978-3-923704-71-2.

[7] BOLSHOV, L.A., DOLGANOV, K.S., KISELEV A.E., STRIZHOV V.F., Results of SOCRAT code development, validation and applications for NPP safety assessment under severe accidents, Nuclear Engineering and Design **341** (2019) 326–345.

[8] IGNATIEV, D., Post-test examination of the PARAMETER-SF4 fuel assembly. In: Proceedings Proc. of .15th International Int. QUENCH Workshop, 3–5 November 2009, Karlsruhe, Germany. ISBN 978-3-923704-71-2 (2009).

LOSS OF COOLING ACCIDENTS MODELLING IN AT-REACTOR SPENT FUEL POOL OF VVER-1200

Y.A. ZVONAREV, V. V. MERKULOV
National Research Centre 'Kurchatov Institute',
Moscow
Russian Federation
Email: Zvonarev_YA@nrcki.ru

Abstract

This paper presents the results of the modelling of the loss of cooling accident in at-reactor spent fuel pool of VVER-1200. The calculations of the accident were performed with 3 Russian codes: best-estimate severe accident code SOCRAT/V1 (processes in the spent fuel pool), containment lumped-parameters code ANGAR (parameters of the containment atmosphere during the accident) and calculation code GEFEST-ULR (molten corium-concrete interaction). Such combination of codes allowed to perform complex evaluation of the severe accident: from the initial event (loss of cooling) to the melt-through of the spent fuel pool concrete bottom, taking into account change of the containment atmosphere during the accident.

1. INTRODUCTION

Nuclear power units with the VVER-1200 reactor type (AES-2006 project) belong to generation 3+, which uses the latest achievements and developments that meet the post Fukushima requirements. The main feature of the power unit with VVER-1200 reactor type is the unique combination of active and passive safety systems making NPPs maximum resistant to external and internal hazards. To achieve high competitiveness NPP with VVER-1200 reactor type must provide safety even in the case of severe accidents (SA) with fuel melting. NRC 'Kurchatov Institute' caries out the scientific support of new NPP projects development, including issues of ensuring nuclear and radiation safety, as well as the management of SA. In accordance with the IAEA recommendations, NPPs safety in all modes of operation and in the case of accidents is ensured due to the progressive implementation of the defence-in-depth principle that is based on the application of the system of physical barriers at the path of ionizing radiation and radioactive materials propagation into the environment.

2. BRIEF DESCRIPTION OF THE SPENT FUEL POOL OF THE VVER REACTOR

Spent fuel pool (SFP) of the VVER reactors belong to at-reactor pools type, since placed near the reactor pressure vessel inside the containment — the 4th physical barrier of the safety. Safety ensuring of the nuclear fuel storage is an important task in the design, construction and operation of the nuclear power plant (NPP). Analysis of the accident at the Fukushima NPP showed [1–2], that under considering possible accident scenarios it's necessary to analyze even unlikely scenarios, including scenario with long-time full station blackout. During the accident full station blackout with launch failure of back-up diesel generators transition of the beyond design basis accident to the severe accident (SA) is possible not only in the reactor pressure vessel (RPV), but in the SFP too. In the case of absence of the operator actions water will evaporate from SFP until complete draining, fuel assemblies (FA) in the SFP will heat up and melt. The number of the FAs in the SFP significantly exceeds the number of the FAs in the RPV; therefore, the severe accident in the SFP can potentially lead to more severe consequences from the points of view of hydrogen explosion and radiological hazards.

The design and size of the SFP may vary slightly depending on specific NPP project, nuclear fuel cycle and customer requirements. In this paper the single section SFP of the NPP with VVER-1200 reactor type is considered — concrete compartment with metal stainless steel liner. On the SFP walls there are pipelines of the cooling system intake. The total water volume during the fuel storage in the SFP is about 1200 m^3. SFP is equipped with fuel close packed storage rack (FCSR). Total capacity of the SFP is 732 cells for FAs. FA cells in the SFP are the hexagonal shrouds of borated steel with a thickness of 6 mm, in which FAs are placed.

3. GENERAL DESCRIPTION OF THE PHENOMENA DURING THE SEVERE ACCIDENT THE SPENT FUEL POOL

When analysing the SA in the SFP, two types of accidents can be identified – loss of cooling, for example, due to station blackout, and loss of coolant, for example, due to leakage through the SFP liner, break of sampling pipelines, etc. Scenarios of both accident types are similar and differed mainly by the process velocity and chronology of main events [3].

The phenomenology of the SA in the SFP is generally the same as for the accident in RPV. One considers the SA in the SFP; the following processes should be analyzed:

– Initial thermohydraulic stage of the accident;
– Convective heat transfer;
– Coolant heating and boiling;
– Uncover and heating of FAs;
– Oxidation of fuel claddings and structural elements;
– Eutectic interaction of materials (uranium dioxide, zirconium, steel);
– Radiation heat transfer;
– FAs melting;
– The formation of porous debris and melt, relocation/collapse of FAs components, melt oxidation;
– Interaction of the melt with FAs elements, steel structures, concrete walls and floor of the SFP;
– Etc.

At the same time, the occurrence of the accident in the SFP will differ from analogous accident in the RPV for several key parameters, affecting the speed of the accident and the consequences:

– In the SFP there is much more water than in the RPV;
– In the SFP there are more FAs with significantly varying distribution of the decay heat per FA (from 150 to less than 1 kW per FA) than in the RPV;
– Total power of the decay heat may be less than in the RPV;
– Turing the uncover and following oxidation of the rods cladding it is necessary to consider the presence of air, which can significantly accelerate the oxidation of the cladding (breakaway);
– The presence of air also accelerates the degradation of nuclear fuel and may increase the release of ruthenium and other less volatile fission products;
– Radiation heat transfer takes place in a more complex geometry than in the RPV (each FA is placed into borated steel shroud);
– Accident occurs under low pressure of atmosphere;
– In case of the SA in the SFP, it is necessary to consider the erosion of concrete and its melting (molten corium concrete interaction).

4. ACCIDENT SCENARIO DESCRIPTION AND INITIAL DATA

In this paper, is considered the severe accident in the SFP with full station blackout of the NPP with VVER-1200 reactor type. It is postulated the launch failure of back-up diesel generators transition, which excludes water supply to the SFP by basis safety systems. It is assumed that at the start of the accident in the SFP there are 163 FAs with 3 days storage time (full core unloading), 42 FAs with 30 days storage time and 42 FAs with 1–10 years storage time. Total decay heat of all FAs in the SFP is 14.18 MW (Table 1). Such approach is conservative (max number of FAs in the SFP and max decay heat) and corresponds emergency full core unloading to the SFP after 30 days NPP operation (12 months fuel cycle).

Initial water level in the SFP corresponds to the water level during the core unloading; it is 16.3 m above the SFP bottom. Initial water temperature in the SFP is 333 K (60 °C). The atmosphere pressure in the containment is 10^5 Pa.

TABLE 1. DECAY HEAT AND NUMBER OF FAS IN THE SFP

Storage time	FAs number	Decay heat of the FAs group (kW)
3 days	163	12 425
30 days	42	884
1 year	42	254
2 years	42	147
3 years	42	99.5
4 years	42	75.3
5 years	42	62.1
6 years	42	54.2
7 years	42	49.2
8 years	42	45.8
9 years	42	43.3
10 years	42	41.3

5. CALCULATION SCHEMES FOR SOCRAT, ANGAR AND GEFEST-ULR CODES

Nowadays there are no specific calculation software codes for SA analysis in the SFP, thus existing integral severe accident codes (ASTEC, MELCOR, etc.) are used for SA analysis in the SFP. Originally, these codes were designed for the SA analysis in the RPVs. In this paper for the SA analysis in the SFP the Russian best-estimate integral severe accident SOCRAT/V1 code is used [4]. First calculations of the severe accident in the SFP of NPP with VVER-1000 reactor type were performed in the NRC ‘Kurchatov institute’ in 2013 [5]. Calculation scheme of the SFP for SOCRAT code is represented on the Figure 1. The scheme contains hydraulic channels and heat elements for modelling of the FAs and borated steel shrouds of the FCSR.

The hydrodynamic elements ‘Channel_left’ and ‘Channel_right’ simulate the space between pipes of the SFP. The separation of main volume of SFP on two parallel channels allows more realistic description of the spatial inhomogeneity of the temperature field in the system in comparison with the model of one large channel. There are heat elements inside these volumes. Those heat elements simulate the shrouds of borated steel, which contain FAs. The channels

'Channel-1', 'Channel-2', etc. describe the free volume inside the pipes. These channels are connected with channels, modelling interpipe free volume, by lower and upper mixing chambers ('BottomGap', 'Up3pool' and 'Up3pool_2'). Channels 'Pool' and 'Pool_2' simulate the water volumes above the FAs. Side channels 'Downcomer_a' and 'Downcomer_b' are modelled too. These channels make possible the simulation of the elevating and descending convective flows in the SFP both at the stage of water-filled SFP and at the stage of full uncovering of the FAs. The channel 'Dome' simulates the air above the spent fuel pool. Side walls and upper structures of the spent fuel pool are simulated by the heat elements 'sidewall_a', 'sidewall_b' and 'roof', respectively. These heat elements take part in convective and radiative heat transfer.

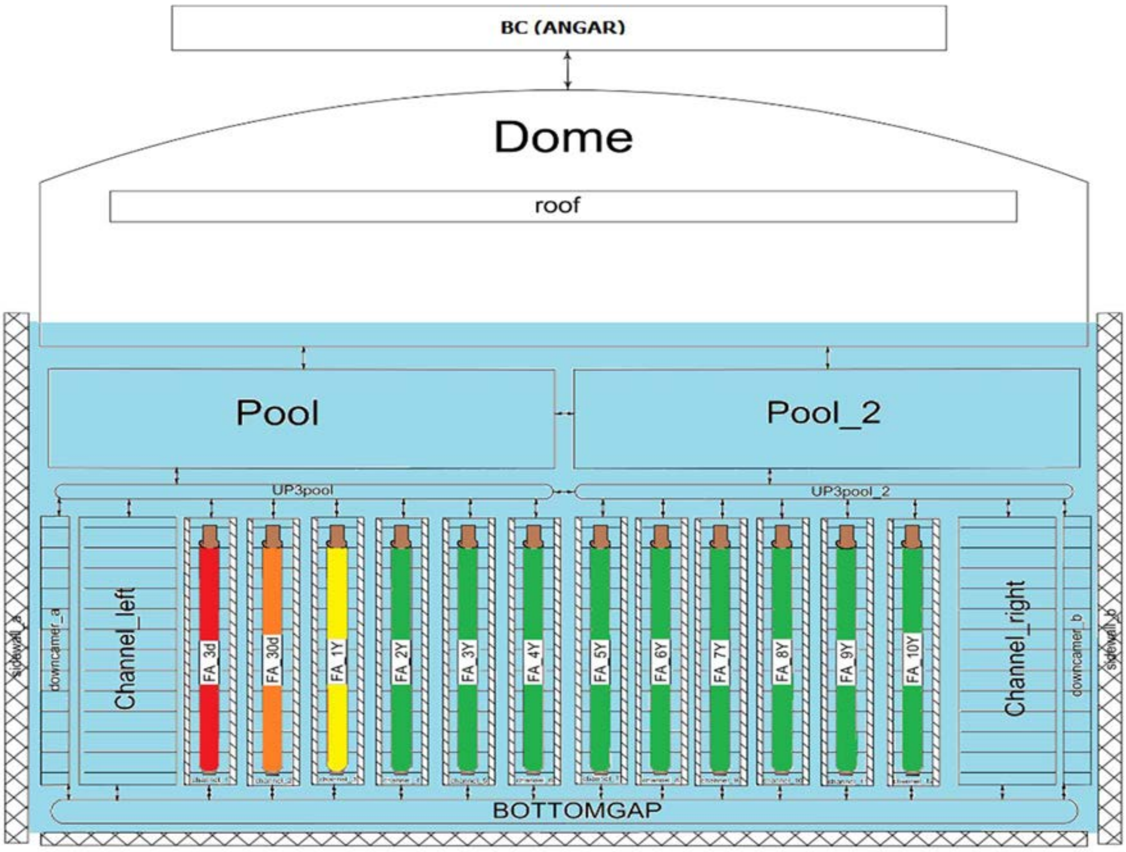

FIG. 1. Calculation scheme of the SFP for the SOCRAT/V1 code.

All FAs presented in SFP are separated into 12 groups which differ from each other by storage time. The approach is presented in the Table 2.

TABLE 2. NUMBER OF FAS IN THE SFP AND STORAGE TIME

Element	Number of FAs	Storage time
FA_3d	163	3 days
FA_30d	42	30 days
FA_1	42	1 year
FA_2	42	2 years
FA_3	42	3 years
FA_4	42	4 years
FA_5	42	5 years
FA_6	42	6 years
FA_7	42	7 years
FA_8	42	8 years
FA_9	42	9 years
FA_10	42	10 years

Axial nodding of heat elements corresponds to the nodalization of adjacent hydraulic element. Every FA consists of rods group, which is simulated by one representative rod. This rod is simulated as cylindrical object with layer structure. FA is divided into 13 cells along height. The heat generation is set in the layers with nuclear fuel (10 cells).

Calculation of the SA in the SFP is performed in conjunction with the calculation of the parameters of the atmosphere in the containment. For the calculation of the parameters of the atmosphere in the containment it is used the containment lumped-parameters ANGAR code. The ANGAR code is designed for computational modelling of changes of the thermophysical parameters and fractional composition of the vapour-gas mixture, the temperature state of construction structures and technological equipment in a system of interconnected compartments inside the containment of the NPP under various operating conditions, including accident conditions.

The calculation scheme of the containment for the ANGAR code is represented in Figure 2. The containment is modelled by several separated compartments, which contain heat structures (construction structures and technological equipment). Connections between the compartments allow vapor-gas mixture to circulate inside the containment. The developed calculation scheme for ANGAR code allow to simulate active and passive safety systems, including the passive heat removal system (PHRS) of the containment. Experimental research of the containment PHRS proved that for the any BDBA, including core damage, loss of coolant of the primary circuit, failure of the active safety systems or full station blackout, long-term heat removal from the containment will be fully ensured. Pressure inside the containment will remain within the limits of the NPP basis design. Thus integrity of the containment, as last barrier of the NPP, will be guaranteed. It will eliminate the fission products release into the environment.

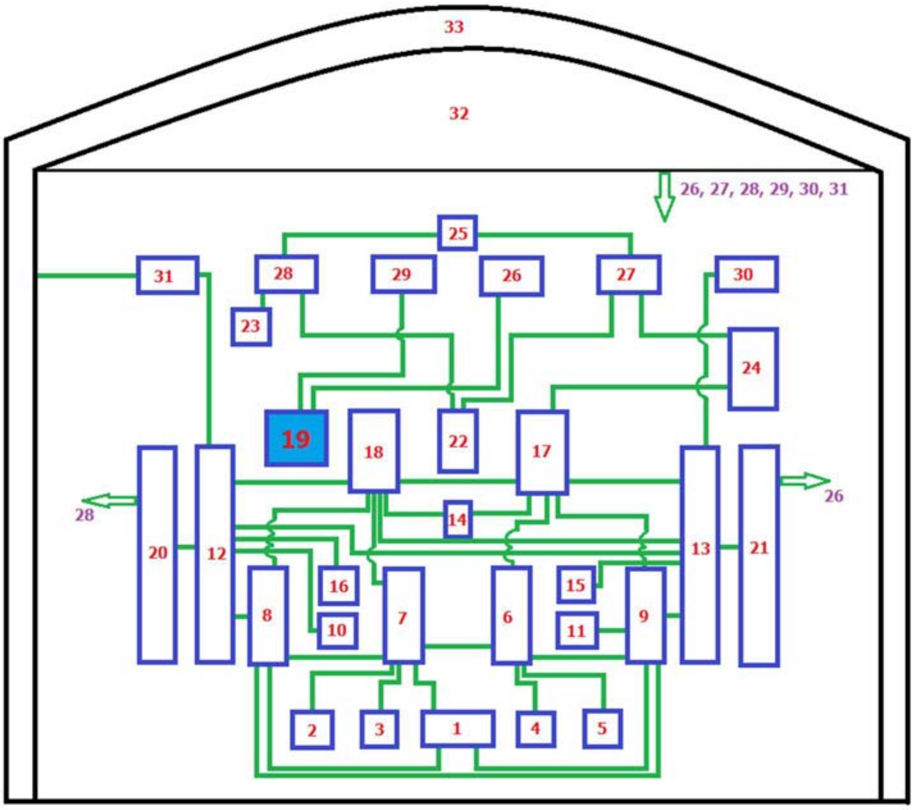

FIG. 2. Calculation scheme of the containment for ANGAR code.

For the evaluation of the metal corium-concrete interaction (MCCI) it is used the calculation software GEFEST-ULR code [6]. The GEFEST-ULR calculation code is designed to simulate the interaction of the melt with structures, accompanied by its movement, spreading of the melting region, and changing of the composition. The application area of the code is the in-vessel and ex-vessel stages of the SA. The calculation scheme is based on a numerical solution of the heat equation in the two-dimensional axisymmetric region by the finite element method.

To simulate the interaction of the corium with concrete of the SFP's bottom, it is necessary to describe the geometry of the SFP's bottom and to create corresponding mesh for calculation. The SFP's bottom is simulated as hollow cylinder with height of 3 m, base radius of 5.7 m, sidewalls and base thickness of 0.7 m (Figure 3). The calculation mesh has spatial step of 0.025 m. The geometry of the model is axisymmetric. Total amount of the elements is equal to 27 360. On the upper surfaces the boundary conditions for the radiation heat transfer are given. The upper boundary is tied to the subregion, occupied by the material, and moves as the empty layers fill with incoming materials (FAs' components). For the MCCI it is assumed that the melt has a uniform composition (i.e. stratification into the oxide and metal components doesn't occur).

Preliminary analysis of the results of the SA stage calculation showed that only FAs with 3 days storage time are melted due to heat up and relocate to the SFP's bottom. Other groups of FAs are damaged and melted partially. HEFEST-ULR calculation code does not have possibility to simulate corium spreading along the concrete surface. Therefore, for MCCI calculations it was considered that FAs' relocation to the SFP's bottom occurs locally and the melt does not spread along the concrete bottom. Under these conditions, it was assumed that the area of melt corium spot is corresponding to the area of relocated FAs (FAs with 3 days storage time). This area is proportional to the FAs quantity and equal ~18 m^2. Thus, the radius of the melt's spot will be equal to ~2.5 m. (Figure 4).

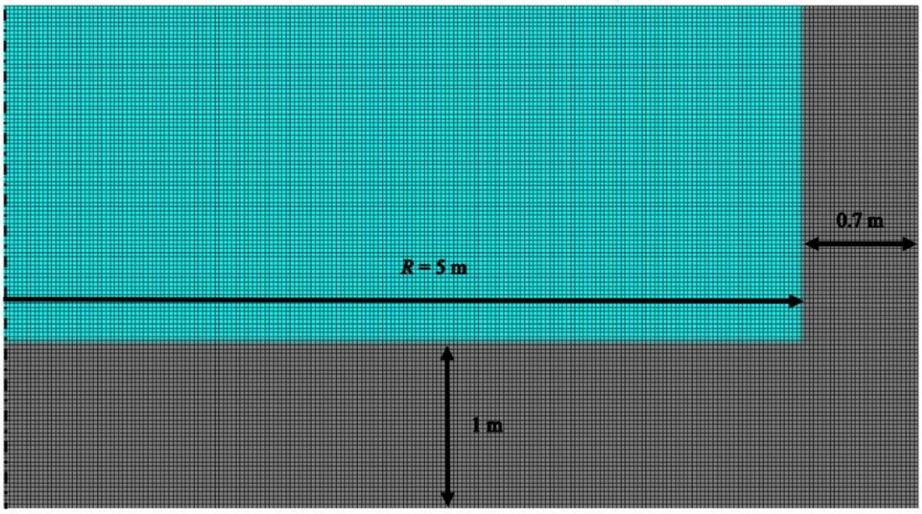

FIG. 3. Calculation scheme of the SFP lower plenum for HEFEST-ULR code.

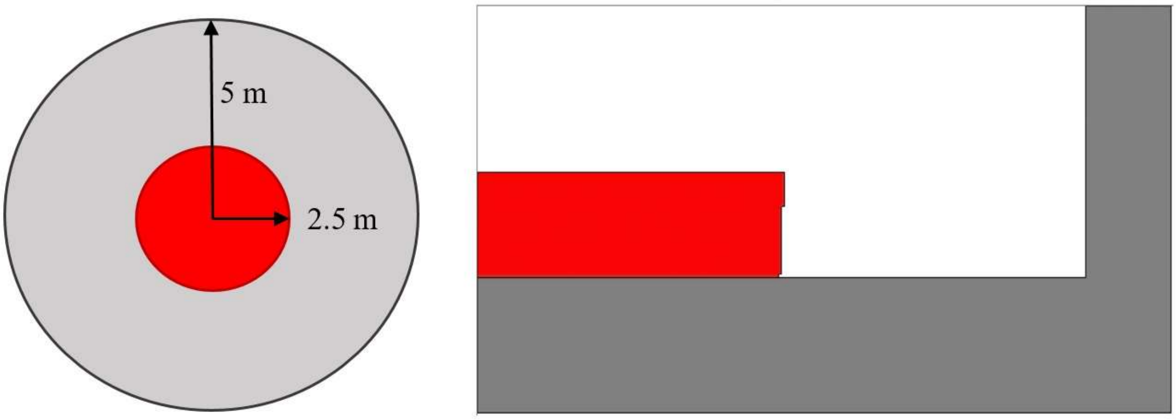

FIG. 4. Melt corium on the SFP concrete bottom.

6. CALCULATION RESULTS

The results of the calculations of the SA in the SFP are given below. The chronology of main events during the accident is presented in Table 3.

TABLE 3. CHRONOLOGY OF MAIN EVENTS DURING THE SA IN THE SFP (STATION BLACKOUT)

Event	Time (h)
Station blackout, accident start	0
Water boiling start	4.8
Water level in SFP reduces to the upper edge of FAs	45
Fuel part uncovering for the FAs with 2-10 years storage time	49.1
Fuel part uncovering for the FAs with 1 year storage time	49.9
Fuel part uncovering for the FAs with 30 days storage time	50.4
Fuel part uncovering for the FAs with 3 days storage time	51.6
Start of the hydrogen generation because of zirconium-steam reaction	51.5
Depressurization of the fuel rods of the FAs with 3 days storage time	54.7
Maximum temperature of rods claddings reaches 1473 K	55
Start of the melting of the FAs with 3 days storage time	57.3
Maximum temperature of the fuel reaches 2550 K	58.9
FAs collapse, materials of the FAs relocate to the SFP bottom	64.2
Melt-through of the SFP concrete bottom	73.3
End of the calculation	73.3

The heating of water in the SFP starts immediately after the beginning of the accident due to FAs decay heat. Heating of water is accompanied by the thermal expansion and the water level in SFP increases at first time (Figure 5a). After 4.8 h after the beginning of the accident the temperature of upper layer of water in SFP reaches the saturation temperature, evaporation from the water surface starts. The water level decreases. Mass of water in SFP decreases too, mass of released steam increases (Figure 5b).

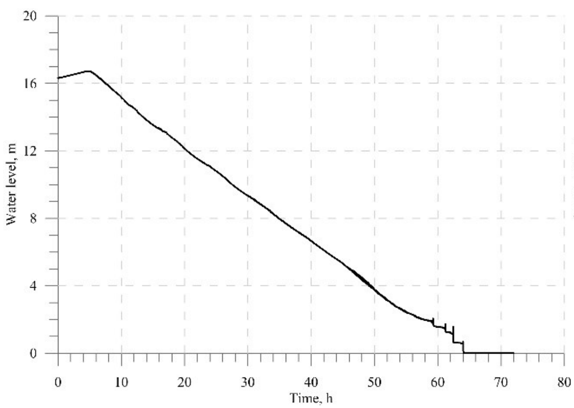

(a)

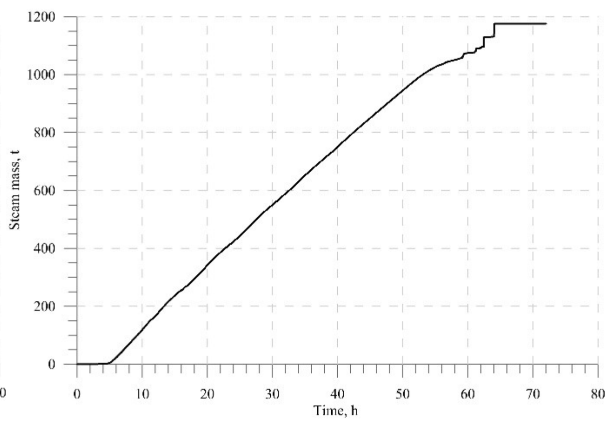

(b)

FIG. 5. a) Water level time dependence in the SFP; b) Released from SFP steam mass.

In 45 h after the beginning of the accident the water level in SFP decreases to the upper edge of FAs (5.31 m from the SFP floor) and the uncovering of FAs starts. Analysis of the results showed that the fuel part of FAs with 3 days storage time uncovers later than the fuel part of FAs of other groups. For FAs with 3 days storage time fuel part becomes uncovered in 51.6 h, for FAs with 30 days storage time – in 50.4 h, for FAs with 1 year storage time – after 49.9 h, for other groups of FAs with 2–10 years storage time the uncovering of fuel part begins in 49.1 h. Time difference for uncovering of FAs fuel parts occurs because of the fact that in the FCSR pipe with FAs with 3 days storage time the steam void in the coolant will be the greatest due to the maximum decay heat. Therefore, the average density of the coolant will be minimal. Condition of the equal pressures of coolant heights in the pipes with FAs leads to the fact, that the level of coolant in the pipes with FAs with 3 days storage time will be higher (due to the lower density). The difference in the levels of the coolant is reduced over time, since the decay heat transfer to the coolant decreases with uncovering of fuel part and, consequently, steam void decreases and the average density of coolant increases.

Figure 6 presents the temperatures of the all fuel axial layers for FAs with 3 days storage time and maximum temperature through all layers for each FAs group. Analysis of the results showed that, despite the fact that the fuel part of FAs with 3 days storage time uncovers after the fuel part of other FAs groups, the temperature of fuel and rod claddings of FAs with 3 days storage time grows much faster than temperatures of the FAs with other storage times. For FAs with 3 days storage time the maximum temperature of the fuel rod cladding reaches 1473 K after 55 h, the melting of FAs begins at 57.3 h, and the maximum fuel temperature reaches 2550 K over 58.9 h after beginning of the accident.

Generation of hydrogen by zirconium-steam reaction starts in 51.5 h after beginning of the accident (Figure 7). Analysis of the calculation results showed that the total amount of hydrogen during the accident is 1154 kg, while 990 kg produced due to the oxidation of the zirconium fuel cladding and 164 kg produced due to the oxidation of steel structures. The maximum hydrogen generation rate is 4.5 kg/s, the average rate is 0.038 kg/s.

During the accident, only the collapse of FAs with 3 days storage time occurs in the SFP. The rest of FAs groups are melted partially. The components of FAs with 3 days storage time start to relocate to the bottom of the SFP in 64.2 h. At the same time, at the collapse moment for FAs with 3 days storage time there is some water in the SFP (~0.6 m water level, or ~50 t of water). Collapse of the FAs components with high temperatures causes significantly rise of evaporation, the rest mass of water evaporates, and relocated components of FAs partially cooled: average temperature decreases from 2550 K to ~1500 K.

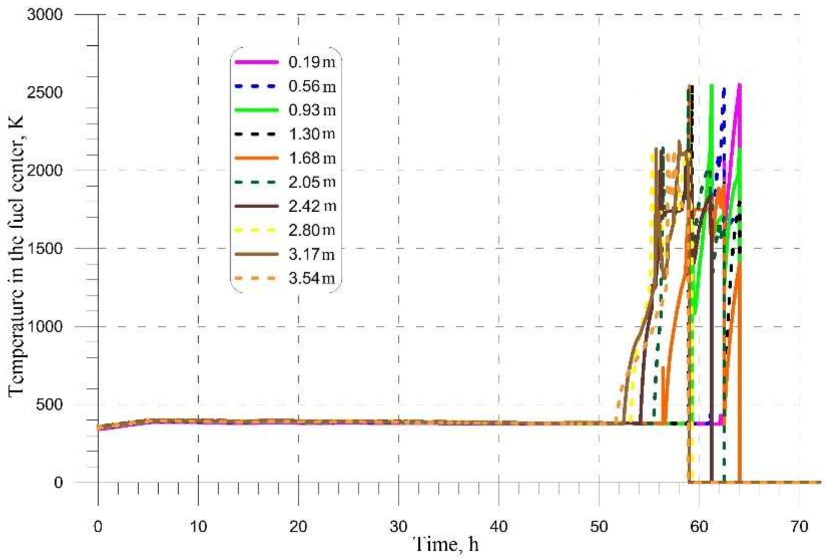

(a)

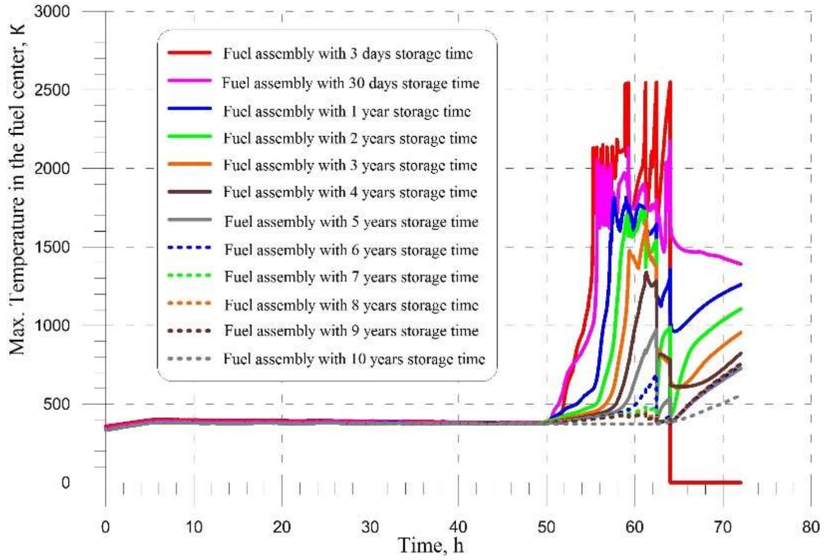

(b)

FIG. 6. a) Fuel centre temperature time dependence for fuel assemblies with 3 days storage time; b) Maximum fuel temperature for all FAs groups with different storage time.

Figure 8 presents the results of the calculation of the containment atmosphere parameters. Approximately in 20 h after the beginning of the accident the containment pressure stabilizes at ~1.8 atm value and the containment temperature stabilizes at 375 K value (due to the operation of the PHRS system). Figure 9 shows the state of the SFP concrete bottom for different moments of time. Melt-through of the SFP concrete bottom occurs in 73.3 h after the beginning of the accident (almost 19 h later after the FAs collapse). By this time, 192 kg of hydrogen and 485 kg of carbon monoxide is released due to the MCCI (Figure 10). Figure 11 shows the results of the calculation of the corium density and corium temperature.

The density of the melt is reduced due to the dilution of corium with concrete. The average temperature of corium, which increased at the initial moment of time due to the heating of corium to the melting temperature, also rapidly decreases after the beginning of the MCCI and reaches almost constant value of 2050 K.

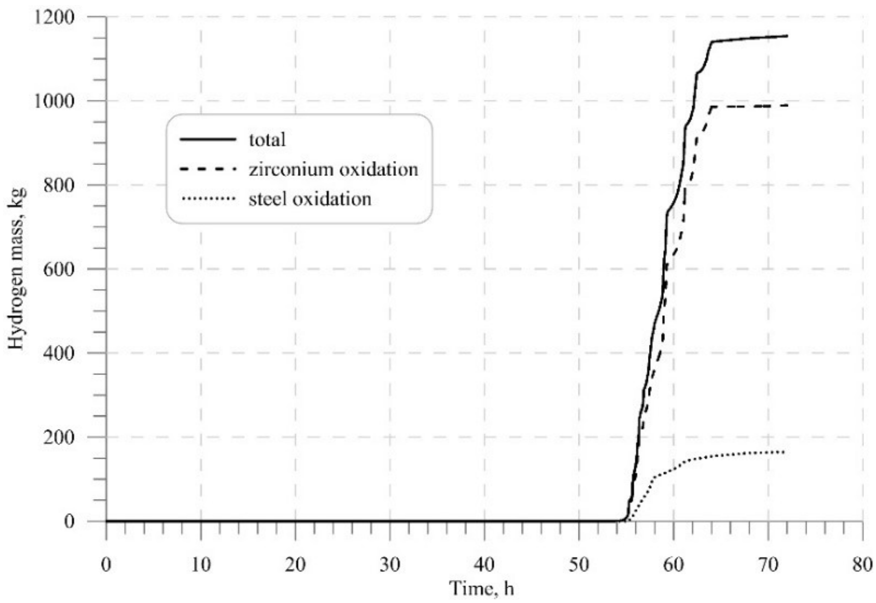

FIG. 7. Hydrogen production during the accident.

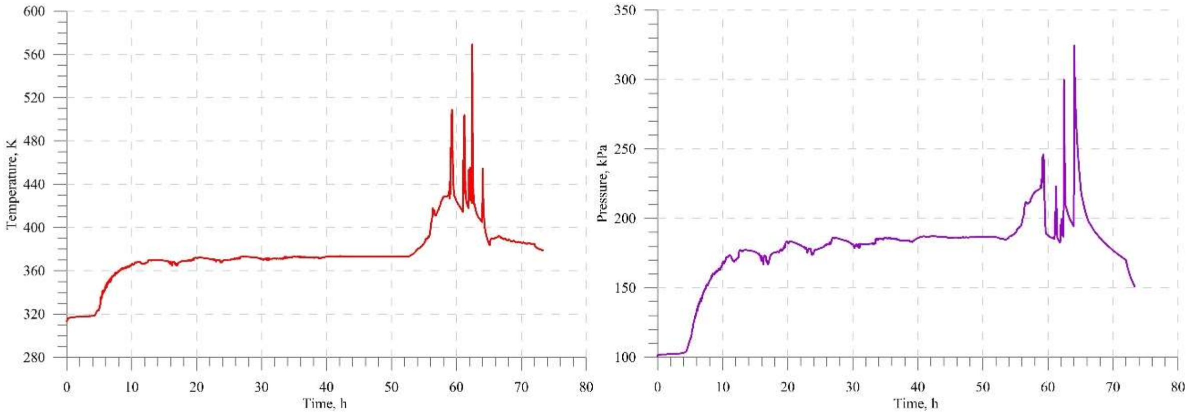

(a) (b)

FIG. 8. a) Temperature of atmosphere in the central hall of the reactor building; b) Pressure of atmosphere in the central hall of the reactor building.

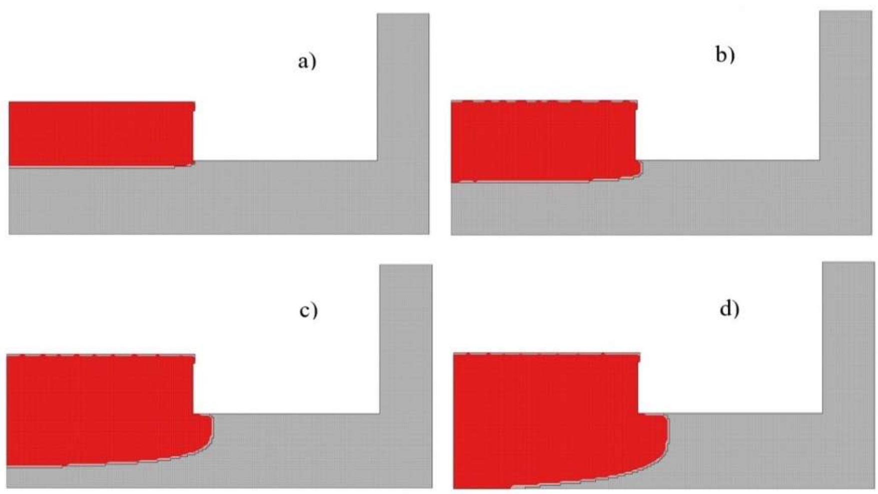

FIG. 9. The results of the calculation of MCCI at different moments of time: a) 66.1 h; b) 67.5 h; c) 70.8 h; d) 73.3 h.

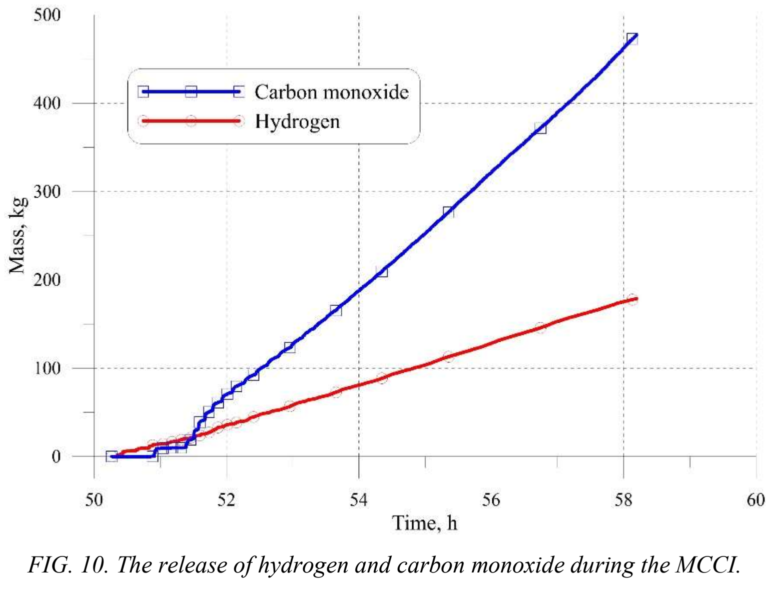

FIG. 10. The release of hydrogen and carbon monoxide during the MCCI.

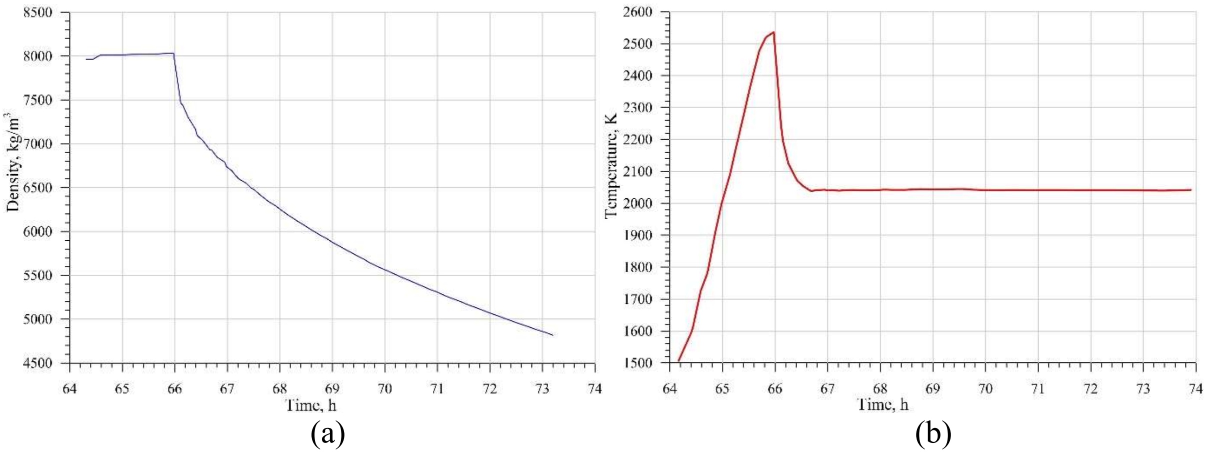

FIG. 11. The time dependence of the density (a) and temperature (b) of the melt on the concrete bottom of the SFP.

Various water sources as well as the ability to supply water in several ways are reliable accident management measures, which can prevent getting beyond design-basis accident шт the SFP into severe stage. NPP with VVER-1200 reactor type (AES-2006 project) has the following additional water sources inside the containment:

- Borated water storage tanks for the stock of borated water with a concentration of 16 g N_3BO_3/kg H_2O with a total capacity of 2000 m^3;
- 2 storage tanks of desalinated water with 700 m^3 of water each.

The following possible measures for supplying water to the SFP can be used:

- Filling the SFP with a sprinkler pump along the line: storage tank of borated water, sprinkler pump, sprinkler piping system, piping and fittings for the cooling system of SFP, piping system, wells of the reactor internals revision shaft;
- Filling the SFP with SFP cooling system pump along the line: tank-pit, pipelines of the tank-pit, SFP cooling system pump, heat exchanger, SFP;
- Filling the SFP with a pump for feeding borated water to the filters from the sump tanks;
- SFP supply from the secondary circuit make-up water system from desalinated water tanks with pump.

In addition to this measures its possible to supply water from outside the containment, using reserve diesel generator and corresponding pipelines.

CONCLUSIONS

Existing calculation software codes allow performing complex evaluation of the severe accident in the spent fuel pool – from the initial event to the melt-through of the concrete SFP bottom, considering change of the containment atmosphere. Nevertheless, the following lacks and unsolved problems of the SA simulation in the SFP can be noticed:

- Integral severe accident SOCRAT/V1 code was not developed for the modelling of the SA in the SFP. It's necessary to revise it related to modelling of rods cladding oxidation, taking into account the composition of the containment atmosphere: the oxidation of the zirconium claddings of in the SFP will take place in atmosphere, consisting of oxygen, nitrogen and steam, while the claddings oxidation in the RPV occurs in the steam. The density of oxygen is higher than the density of steam — this fact improves the access of oxygen to the claddings surface. Under these conditions, zirconium claddings are oxidized by oxygen first, and then by steam.

- It is necessary to revise the SOCRAT/V1 code in terms of modelling radiation heat transfer, taking into account the characteristics of SFP — the rectangular geometry of the SFP (currently calculations are performed in an axisymmetric cylindrical geometry). It is also necessary to more thoroughly model the radiation and re-radiation between the elements of the SFP (FAs and borated steel shrouds of the FCSR).
- The HEFEST-ULR code doesn't allow simulating the corium spreading on the concrete bottom of the SFP. The development of an appropriate model and its implementation in the calculation code is necessary.

REFERENCES

[1] GOVERNMENT OF JAPAN, Report of Japanese Government presented to the IAEA Ministerial Conference on Nuclear Safety, "The Accident at TEPCO's Fukushima Nuclear Power Stations", Vienna, June 2011, Government of Japan Nuclear Emergency Response Headquarters, (2011).

[2] FUKASAWA, M., "Overview of Fukushima-Accident Analysis", Proc. 2012 SARNET International Meeting (SARNET 2012), Cologne, Germany, March 21–23, 2012.

[3] Status report on spent fuel pools under loss-of-cooling and loss-of-coolant accident conditions, Nuclear safety NEA/CSNI/R(2015)2, May 2015.

[4] BEZLEPKIN, V.V., KUCHTEVICH, V.O., VASILIEV, A.D., et al. "The status of development of code RATEG/SVECHA/HEFEST for modeling of core degradation processes at severe accidents", Proc. 2nd ISTC "Safety Assurance of NPP's with VVER", Podolsk, Russia, November 19–23, 2001.

[5] MERKULOV, V.V., BUDAEV. M.A., ZVONAREV, Yu.A., "Hydrogen generation during unwatering of the spent fuel pool during an accident with complete blackout", Proc. 8th ISTC "Safety Assurance of NPP's with VVER", Podolsk, Russia, 28–31 May, 2013.

[6] ZVONAREV, Yu.A., KOBZAR, V.L., MELNIKOV, I.A., PHILIPPOV, A.S., "Verification of HEFEST-ULR code for Substantiation of Core Catcher Efficiency", Proc. 8th ISTC "Safety Assurance of NPP's with VVER", Podolsk, Russia, 28–31 May, 2013.

MELCOR ANALYSIS OF SEVERE ACCIDENT RISK IN THE SPENT FUEL POOL OF A NORDIC BOILING WATER REACTOR

Y. CHEN[1], Z. HUANG[1], P. ISAKSSON[2], W. MA[1]

[1]Royal Institute of Technology (KTH)
Stockholm

[2]Swedish Radiation Safety Authority (SSM)
Stockholm

Sweden

Abstract

The Fukushima accident raised a concern on severe accident risk of a spent fuel pool (SFP), since the earthquake may breach the pool boundary and/or stop cooling the pool due to loss of AC power. Since then, a substantial effort has been made to analyse severe accidents which may occur in SFPs. In this context, the present study was intended to assess the severe accident risk of the SFP in a Nordic boiling water reactor (BWR). Two accident scenarios of risk importance, namely loss of cooling flow accident (LOF) and loss of coolant accident (LOCA) due to 0.01 m^2 breach at the bottom of the pool, were simulated by two different MELCOR versions 1.8.6 and 2.2. The results show that the fuel degradation occurs at ~55 h and ~3 h for the LOF scenario and the LOCA scenario, respectively. Larger amount of H_2 generation was predicted in the LOF (c.a. 1500 kg) than the LOCA (c.a. 400~450 kg). A sensitivity study on the breach size showed that a larger breach size led to earlier fuel degradation but less H_2 generation. The comparison of the simulation results from the two MELCOR versions indicated that the transients of water level in the pool were similar, but the fuel degradation began earlier and more H_2 was produced in MELCOR 2.2 simulation.

1. INTRODUCTION

Spent fuel pools (SFPs) are constructed to temporarily store the irradiated fuels, which are removed from the reactor because of regular refueling or maintenance. Before Fukushima severe accident, the severe accident of SFP is considered to be highly improbable because of the low decay heat and the slowly accident progression compared with reactor core, which provides enough time for the action of mitigation measurements to prevent from loss of cooling of the pool [1]. However, the energetic explosion occurred in the building which accommodated the spent fuel pool of the Unit 4 in the Fukushima accident has raised up extensive concern about the safety of SFP worldwide. Although later investigation proves that the source of hydrogen which resulted in the explosion came from the Unit 3 through leakage path of the shared ventilation duct, rather than from the cladding-steam reaction of the spent fuel as a result of loss of cooling, this event warns the nuclear industry and regulatory bodies of the possible damage to the cooling system or the integrity of SFP in a severe accident of a nuclear power plant.

The cooling for the spent fuel stored in the SFP could be lost either by malfunction of the pool cooling system or by the loss of the pool inventory. The first type, loss of cooling flow (LOF) accident, is mostly caused by inoperable cooling pump, inadvertent diversion of coolant flow and loss of ultimate heat sink. While the other type, loss of coolant accident (LOCA), is initiated through improper line-up or breaks in connected pipes and system, etc. [2] In Fukushima severe accident, the loss of cooling flow accident was occurred at the Unit 1 to Unit 4 SFPs due to station blackout (SBO), which was both loss of offsite AC power and loss of emergency diesel generators caused by the flooding of tsunami. The emergency injection was implemented by helicopters and trucks to prevent the escalation of the SFP accident, and alternative cooling system for SFP was put in use eventually.

Motivated by the Fukushima severe accident, much research isconducted regarding the safety analysis of SFP for different types of reactor power plants [3–5]. The phenomena during SFP accident include fuel uncovery and heat-up, degradation of fuel and racks, melt-concrete interaction and possible release of the fission products. The computation codes, which are developed originally for reactor accident analysis, can be also used for SFP accident analysis since the major phenomena are similar. MELCOR, developed by Sandia National Laboratories under the auspice of the U.S. NRC, is one of severe accident analysis codes that is capable to perform the severe accident simulation of SFP. Furthermore, some model improvement has been made to MELCOR to facilitate the SFP analysis since version 1.8.6 including the modelling for SFP racks and an enhanced air oxidation kinetics model [6].

In this paper, the safety analysis of the SFP of Nordic BWR is performed with MELCOR regarding two accident scenarios: LOF and LOCA. The responses of the pool and the spent fuel assemblies during accident are simulated for better understanding of key severe accident phenomena and acquiring the safety margin of existing SFP design. Besides, two versions of MELCOR (1.8.6 and 2.2) are both utilized and compared, in order to evaluate the effect of models in different versions of MELCOR regarding the severe accident phenomena in an SFP.

2. SPENT FUEL POOL OF BWR

For BWRs, the SFPs are generally located within the reactor building. The pools, which are constructed of reinforced concrete with a stainless steel liner to prevent leakage and maintain water quality, are designed to survive seismic events. The fuel assemblies are stored in stainless racks with water above the top, which provides cooling and radiological shielding.

The coolant in an SFP is cooled by a cooling system consisting of pump, heat exchanger, intermediate cooling system and pipe. In normal operation, the coolant is pumped through the heat exchanger, where the sensible heat generated by fuel is transferred to the intermediate cooling system and finally to the plant's ultimate heat sink. Then the coolant returns back to the pool through the piping lines that either locate near the top of pool or at the bottom. While inside the pool, the fuel assemblies are cooled by means of natural circulation. In the event that the normal cooling system is unavailable, for many advanced plants, some kind of passive cooling systems are actuated to maintain the flow and remove residual heat from the SFP, in order to control the temperature of the pool water.

3. MELCOR MODEL

The SFP-BWR type of core is used in the MELCOR COR package definition. The fuel assemblies stored in the SFP of Nordic BWR are divided into 5 radial rings and 10 axial levels for the MELCOR core nodalization. A flat type of lower head is used. The thermal-hydraulic control volume (CV) nodalization is shown in Fig. 1. CV101 is for modelling the bottom of the SFP, associated with the flat lower head of the COR nodalization. Control volume CVi02 (i=1~5) is associated with the radial Ring #i of fuel assemblies, providing thermal-hydraulic boundary conditions for fuel rods. CV200 represents the bypass flow, whereas CV300 is the space of pool above racks. CV400 models the environment by a time-independent volume. The cross flow between fuel rings is not considered since there is no connection between the canisters of BWR fuel assemblies.

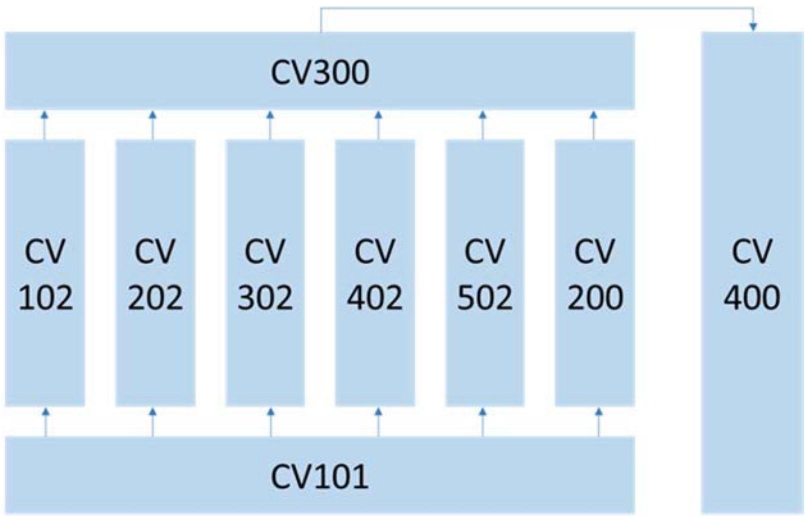

FIG. 1. Thermal-hydraulic nodalization of the SFP.

4. RESULTS AND DISCUSSION

In the present study, two categories of accident scenarios are analysed: a) loss of cooling flow; and b) loss of coolant accident, with two MELCOR versions: 1.8.6 and 2.2.

If the cooling system of the SFP fails due to the mechanical malfunction of the components or the loss of power, the cooling ability is lost. Consequently, the cooling water in the pool starts to heat up and evaporate into the atmosphere, leading to the exposure of the fuel assemblies to the environment eventually, if there are no other measures to remove the decay heat.

If the concrete wall of the pool is breached or a break occurs at the penetration pipe, the coolant will leak, also leading to the uncovery of the fuel in the end. Compared with the loss of cooling accident, if the break size is large, the water level usually drops faster, which means an earlier exposure of the fuel rods.

4.1 Loss of cooling flow

The LOF accident is assumed to occur at 0 s in the simulation and the time for main events of the accident progression is listed in Table 1, with the comparison between two MELCOR versions. With the absence of the cooling system, it takes around 40 h for the water pool to boil off to the fuel level. After the uncovery of fuel by water, fuel temperature increases rapidly and cladding material start to oxidize at around 55 h, as a result H_2 start to generate. With further oxidation, cladding material fails to hold its shape and the radioactive fission products located in the gap between fuel and cladding begin to release. Due to the power difference among fuel rings, the time of gap release in fuel rings is different, with around maximum 10 h difference. In general, the accident progression obtained in version 2.2 is earlier than version 1.8.6, however, the difference between two versions is small. The maximum difference is 1.6 h for the gap release time in Ring #5.

Fig. 2 shows the collapsed water level with time. At the first 10 h, the water level goes up a little because the water swells when heated by spent fuels. Then fast decrease of water level can be observed at around 9 h, when the water pool achieves the saturated temperature and the effect of evaporation becomes predominant. The water level keeps decreasing afterwards to the pool bottom afterwards. The water level transients from two MELCOR versions show little difference.

TABLE 1. TIME FOR MAIN EVENTS IN LOSS OF COOLING

Event of loss of cooling	MELCOR 1.8.6	MELCOR 2.2
Start of fuel uncovery	41.0 h	40.2 h
Start of H_2 generation	54.8 h	54.5 h
Start of radioactive release	55.6 h	54.9 h
Gap release in Ring #2	55.6 h	54.9 h
Gap release in Ring #1	56.5 h	56.5 h
Gap release in Ring #3	58.8 h	58.0 h
Gap release in Ring #4	61.4 h	60.3 h
Gap release in Ring #5	64.9 h	63.3 h

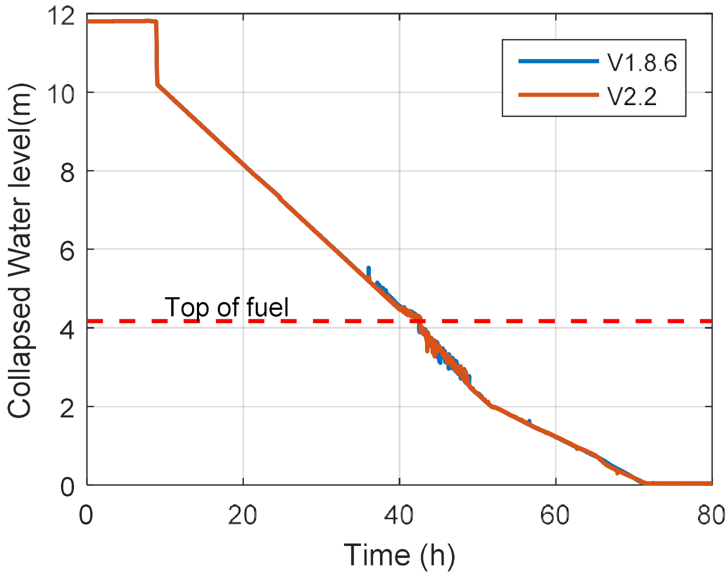

FIG. 2. Collapsed water level in LOF.

The variation of cladding temperature of Ring #1 is depicted in Fig. 3. At the early stage of the accident, the cladding temperature increases slightly to the saturated temperature of water coolant. With the decreasing of water level, spent fuel assemblies start to expose to the air from 41 h. Without sufficient cooling, fuel cladding temperature begins to increase significantly from the top core cell to the bottom. The decrease of temperature to 0 means the collapse of cladding material in that core cell into particle debris, therefore, cladding does not exist.

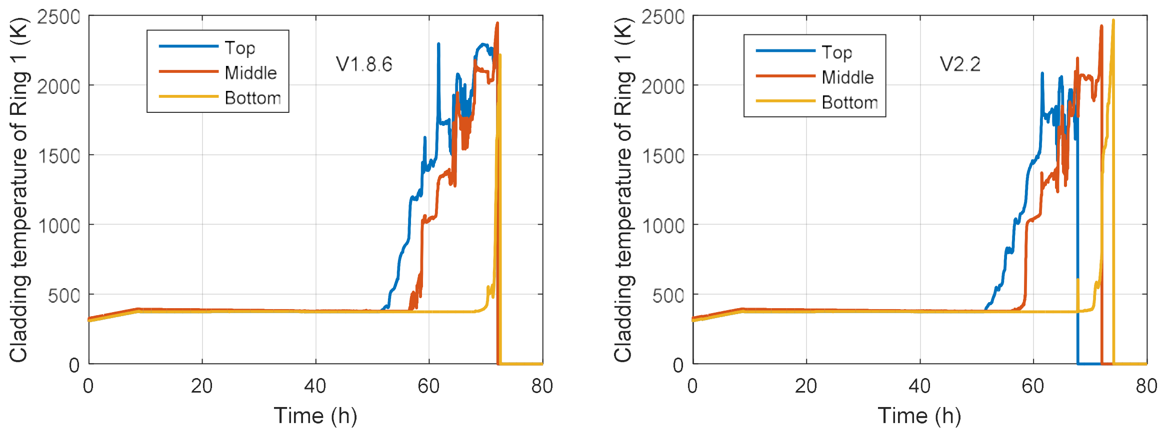

(a) 1.8.6 (b) 2.2

FIG. 3. Cladding temperature of Ring #1 in LOF.

The result from version 1.8.6 shows that the failure of cladding Ring #1 occurs simultaneously, while from version 2.2 it shows that cladding in the top cells fails earlier than the bottom. In the model of MELCOR, once the thickness of unoxidized Zircaloy in one core cell is thinner than the minimum thickness (0.1 mm by default for both versions), the cladding in that cell is assumed to fail. The difference of cladding failure time is possibly due to the change of default Zircaloy oxidation rate constant coefficients between two MELCOR versions. Specifically, the Zircaloy oxidation rate by O_2 is calculated by:

Version 1.8.6:

$$K(T) = 50.4exp(-14630.0/T) \tag{1}$$

Version 2.2:

$$K(T) = 26.7exp(-17490.0/T) \tag{2}$$

where K is the Zircaloy oxidation rate (unit: $kg^2{\cdot}m^{-4}s$) as a function of temperature T of Zircaloy (unit: K) [6, 7].

The comparison of cladding temperature at different time with two MELCOR versions is shown in Table 2. The cells filled in white represent that the cladding has collasped in that cell or dose not exit. The fuel degradation starts from the upper part of the central ring. Compared two code versions, the failure of caldding occurs earlier in version 2.2 than version 1.8.6, while it takes longer time for version 2.2 to reach the failure of all cladding. However, the difference is quite small since that all cladding fails at 75.0 h and 74.5 h for version 2.2 and 1.8.6, separately.

The generation of H_2 is also affected by the change of oxidation model, since the oxidation of Zircaloy contributes the most of the H_2 generation. Fig. 4 shows the total H_2 generation in the SFP in LOF, calculated from two MELCOR versions. The final generation of H_2 is 1556.16 kg from version 1.8.6, and 1582.52 kg from version 2.2, with around 1.7% difference. The H_2 generation stops at around 75 h for both cases, due to the collapsed of all cladding materials.

TABLE 2. CLADDING TEMPERATURE COMPARISON IN LOF

	MELCOR 1.8.6	MELCOR 2.2	Temperature (K)
60h	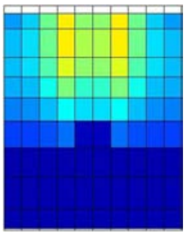	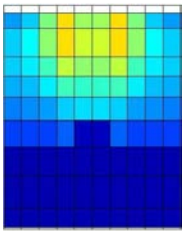	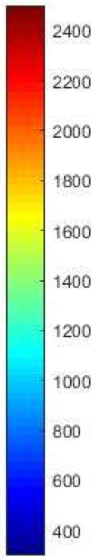
65h	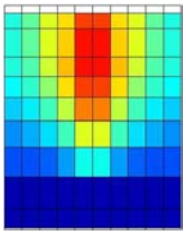	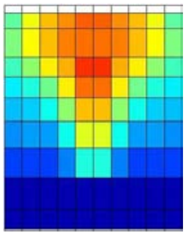	
70h	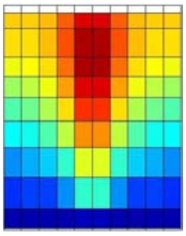	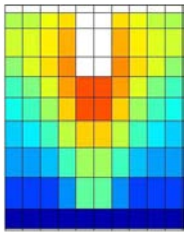	
72h	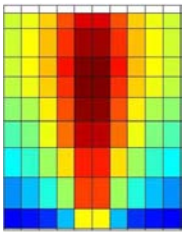	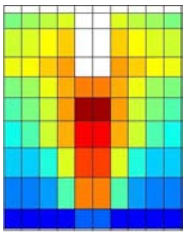	
73h	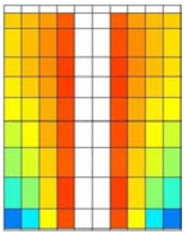	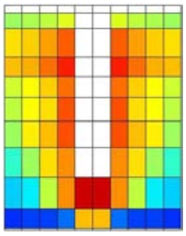	
74h	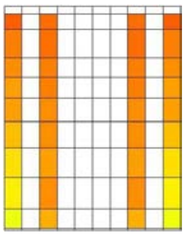	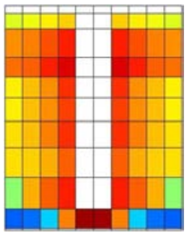	
74.5h	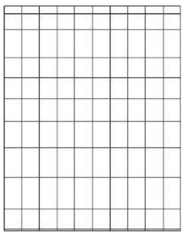	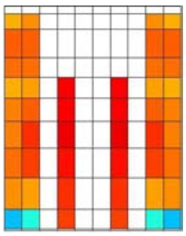	

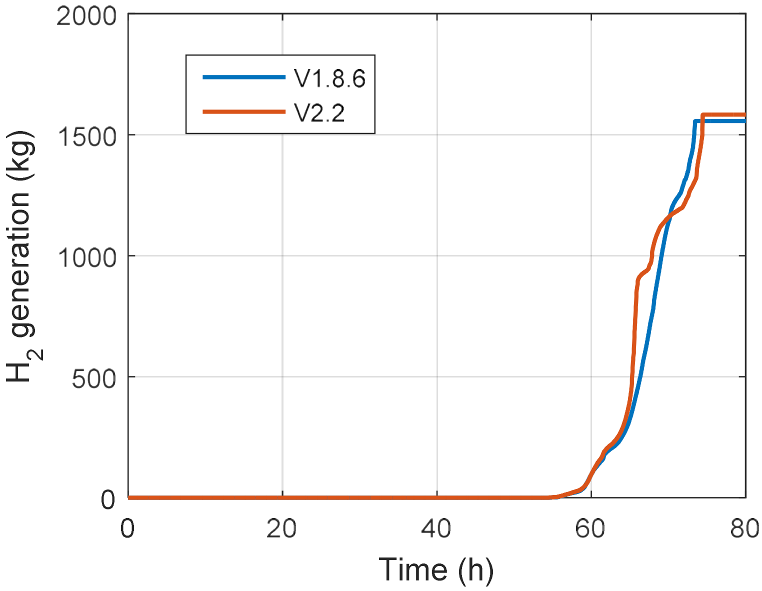

FIG. 4. H_2 generation in LOF.

4.2. Loss of coolant

A breach size of 0.01 m^2 is assumed to appear at the bottom of the spent fuel pool at 0 s, for the simulation of LOCA. The time of main events is listed in TABLE 3, as a comparison of two MELCOR versions. Compared with LOF accident, the LOCA scenario proceeds much faster. Similarly, the results from version 2.2 predict an earlier occurrence regarding the gap release in ring #3–5, although the difference is quite small.

TABLE 3. TIME FOR MAIN EVENTS IN LOSS OF COOLANT

Event of loss of coolant	MELCOR 1.8.6	MELCOR 2.2
Start of fuel uncovery	2.0 h	2.0 h
Start of H_2 generation	2.8 h	2.8 h
Start of radioactive release	2.8 h	2.8 h
Gap release in Ring #1	2.8 h	2.8 h
Gap release in Ring #2	3.0 h	3.0 h
Gap release in Ring #3	4.0 h	3.8 h
Gap release in Ring #4	5.1 h	4.8 h
Gap release in Ring #5	6.3 h	5.9 h

The collapsed water level of the pool during loss of coolant accident is shown in Fig. 5. The decreasing rate of the water level is much faster due to the leakage, resulting in the earlier exposure and damage of the fuel rods. There is barely no difference for the water level transient between two versions.

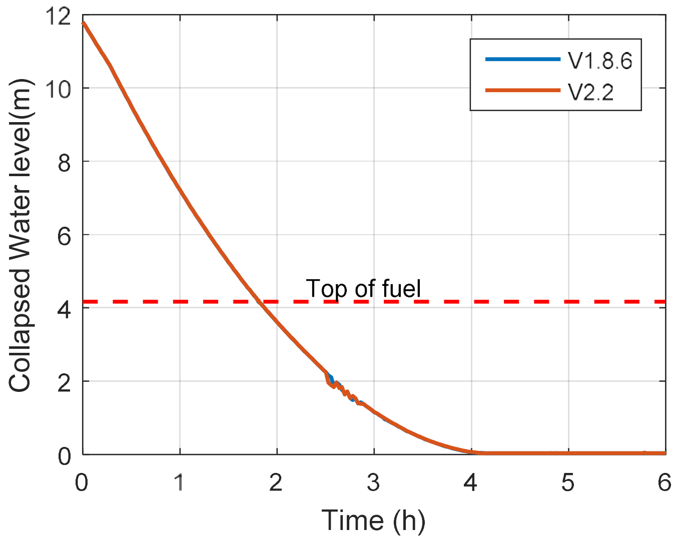

FIG. 5. Collapsed water level in LOCA.

The rapid loss of coolant leads to earlier damage to the cladding, as the cladding temperature shown in Fig. 6. Similar to the result of LOF scenario, an earlier failure of cladding is predicted in version 2.2 at top core cells.

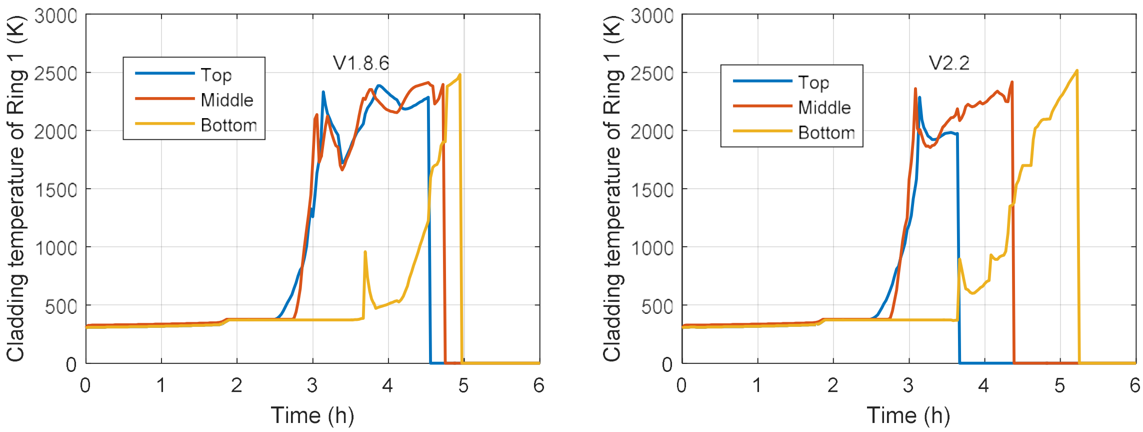

(a) 1.8.6 (b) 2.2

FIG. 6. Cladding temperature of Ring #1 in LOCA.

The cladding temperature is also compared at different time point, as listed in Table 4. Similarly, with LOF scenario, the fuel degradation starts from upper part of central ring and then extends to the outer rings. The fuel degradation develops very fast due to the rapid coolant loss. All cladding fails at 10.0 h and 9.8 h, as predicted from version 1.8.6 and version 2.2, separately.

Fig. 7 show the H_2 generation in LOCA scenario, from two MELCOR versions. Due to the rapid loss of water, less H_2 is generated in LOCA scenario, compared with LOF scenario, which is only one third. The total H_2 generation from version 2.2 is higher than version 1.8.6, with 458.76 kg from version 2.2, and 411.89 kg from version 1.8.6. The difference is 11.4%, which is higher than the difference in LOF scenario (1.7%).

TABLE 4. CLADDING TEMPERATURE COMPARISON IN LOCA

	MELCOR 1.8.6	MELCOR 2.2	
3h	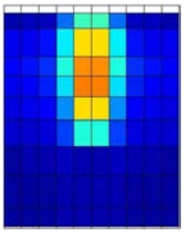	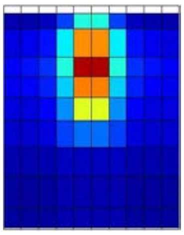	Temperature (K) 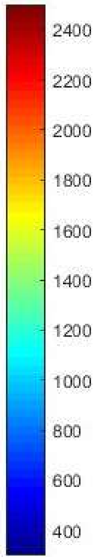
4h	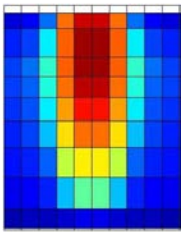	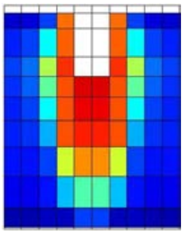	
5h	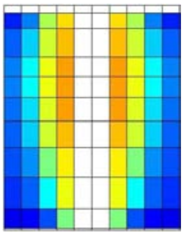	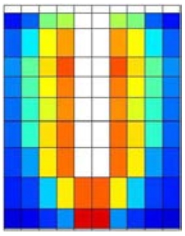	
6h	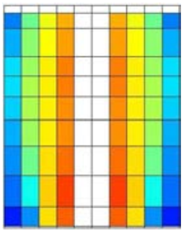	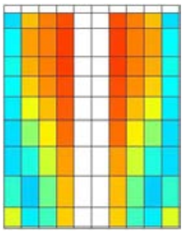	
7h	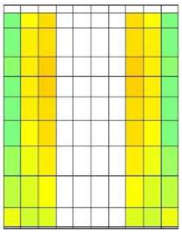	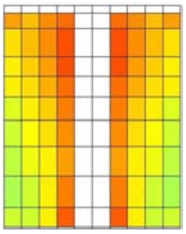	
8h	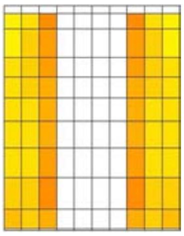	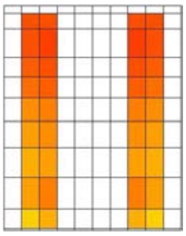	
9h	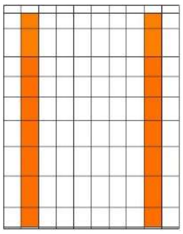	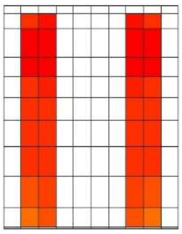	

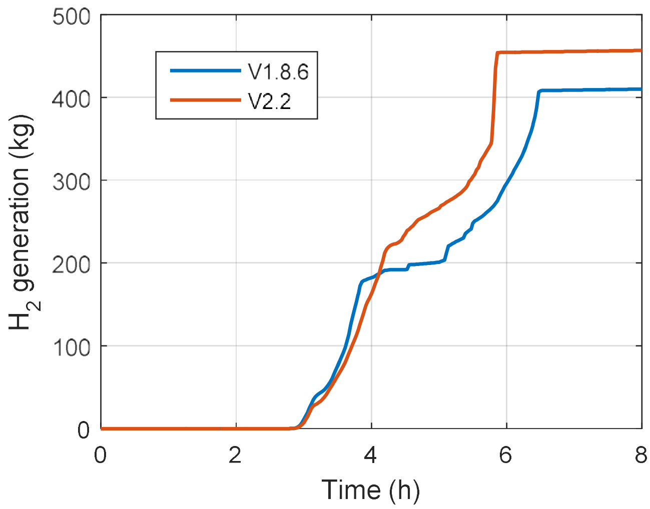

FIG. 7. H_2 generation in LOCA.

4.3. Sensitivity study on breach size

To analyse and demonstrate the effect of breach size to the accident progression of LOCA, a sensitivity study is conducted with accidents initiated by different breach sizes. Four breach sizes (0.1 m^2, 0.04 m^2, 0.01 m^2, and 0.005 m^2) are assumed to open at 0 s. The evolution of collapsed water level in four cases are shown in Fig. 8. It can be observed that the larger breach size leads to the larger leakage flow, which results in the earlier exposure of the core. The results from two MELCOR versions are identical.

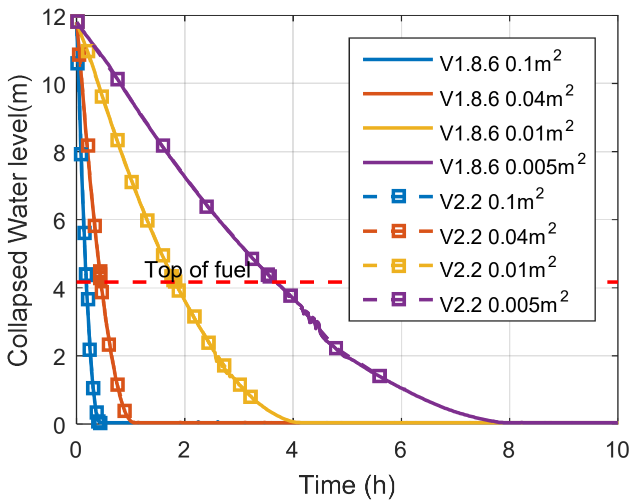

FIG. 8. Collapsed water level with different breach size.

The H_2 generation results are shown in Fig. 9. The production of H_2 decreases as the breach size increases, because of the starvation of steam. Difference can be observed regarding the total generation of H_2 from two code versions. In general, the total amount of H_2 generation predicted from version 2.2 is higher than version 1.8.6, except the largest breach size case, as compared in TABLE 5. The maximum difference appears in the smallest breach size case, with 176 kg difference (28.6%).

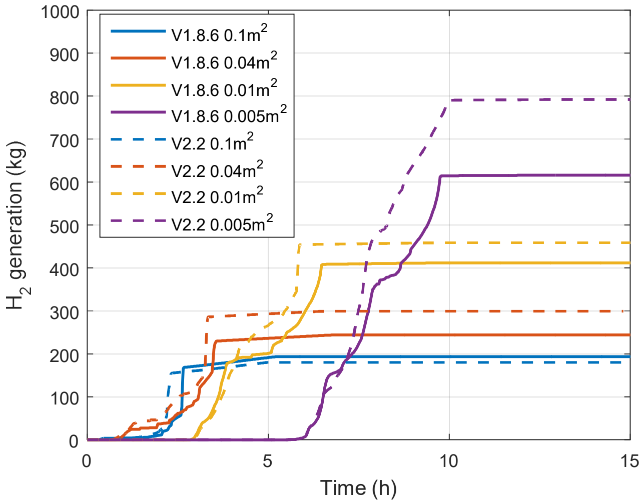

FIG. 9. H_2 generation with different breach size.

TABLE 5. TOTAL AMOUNT OF H_2 GENERATION

Breach size	MELCOR 1.8.6	MELCOR 2.2
0.1 m^2	193.38 kg	180.00 kg
0.04 m^2	244.23 kg	299.08 kg
0.01 m^2	411.89 kg	458.76 kg
0.005 m^2	616.02 kg	791.97 kg

CONCLUSIONS

Motivated by assessment of severe accident risk in a spent fuel pool (SFP), MELCOR 1.8.6 and MELCOR 2.2 models were developed to simulate postulated severe accidents of the SFP of a reference Nordic BWR. For two accident scenarios chosen, i.e., loss of cooling flow accident and loss of coolant accident, the simulation results were presented in terms of H_2 generation mass, fuel cladding temperature and water level, with a focus on the comparison between the two MELCOR versions.

The trends of accident evolution were similar for the loss of cooling flow accident and the loss of coolant accident. However, the decreasing rate of the water level in the LOCA was much faster, resulting in earlier exposure and damage of the fuel rods. As a result, the consequence of LOCA was much more severe in radioactive release, but less pronounced in H_2 generation. A sensitivity study indicated that the breach size of LOCA had a significant impact on accident progression, and a larger breach led to earlier and severer fuel degradation but less H_2 production.

Two MELCOR versions predicted similar results regarding the water level evolution in the SFP. The difference appeared in fuel degradation and H_2 generation, since updates of some models (e.g., Zircaloy oxidation model) were implemented in the newer version of MELCOR. Generally speaking, MELCOR 2.2 predicted earlier fuel degradation and more H_2 generation.

REFERENCES

[1] COINDREAU, O., et al., Severe Accident Code-to-Code Comparison for Two Accident Scenarios in a Spent Fuel Pool, Ann. Nucl. Energy, **120** (2018) 880–887.

[2] ORGANISATION FOR ECONOMIC CO-OPERATION AND DEVELOPMENT NUCLEAR ENERGY AGENCY, Status Report on Spent Fuel Pools under Loss-of-Coolant Accident Conditions, NEA/CSNI/R(2015)2, OECD/NEA, Paris (2015)

[3] KOTOUC, M., Analyses of Severe Accident Sequences in the Spent Fuel Pool of the VVER-1000 Type of Reactor with MELCOR 1.8.6, Proceedings of the 2014 22nd International Conference on Nuclear Engineering (ICONE22), American Society of Mechanical Engineers, New York, NY (2014).

[4] KÖNÖNEN, N. E., Spent Fuel Pool Accidents in a Nordic BWR, Proceedings of the 2013 21st International Conference on Nuclear Engineering (ICONE21), Elsevier, Amsterdam (2013).

[5] ZHANG, Z.W., DU, Y., LIANG, K.S., Advanced Modeling Techniques of a Spent Fuel Pool with Both RELAP5 And MELCOR and Associated Accident Analysis, Ann. Nucl. Energy, **110** (2017) 160–170.

[6] HUMPHRIES, L.L., BEENY, B. A., GELBARD, F., LOUIE, D. L., PHILLIPS, J., MELCOR Computer Code Manuals Vol.1: Primer and Users' Guide, SAND2017-0455 O, Albuquerque (2017) NM 87185-0748.

[7] GAUNTT, R. O., et al., MELCOR Computer Code Manuals Vol.1: Primer and Users' Guide, SAND2005-5713, Albuquerque (2005) NM 87185-0739.

APPLICATION OF MODIFIED ART MOD 2 CODE TO FISSION PRODUCT BEHAVIOUR ANALYSIS FOR SPENT FUEL POOL OF NUCLEAR POWER PLANT

W. VECHGAMA*, K. SILVA
Thailand Institute of Nuclear Technology
(Public Organization)
*Corresponding author
Email: wasin@tint.or.th (wasinvechgama@gmail.com)

C. KITTASIN, S. RASSAME
Chulalongkorn University

Thailand

Abstract

It is well-known that Loss of Coolant Accident (LOCA) has a significant contribution to fuel damage. Not only LOCA in the reactor cooling system but also LOCA in the spent fuel pool (SFP) need to be evaluated since it stores a lot of spent fuels which contain significant amount of radionuclide. In our previous studies, ART Mod 2 were modified and validated to ensure accurate calculation of fission product behaviour. The objective of this study is to assess fission product behaviour in the SFP during LOCA (or complete draining) using ART Mod 2. The geometry and conditions of the Robert Emmett Ginna Nuclear Power Plant is used as the reference. Caesium iodide (CsI) in gas form and caesium hydroxide (CsOH) in aerosol form are used to represent caesium compounds. It is found that modified ART Mod 2 code can capture the trend of CsI gas release into environment, but not that of CsOH aerosols. Total caesium compounds release and retention in all forms can be more accurately estimated if source term ratio of gas and aerosol, difference between wall and ambient temperatures, and chemical reactions are appropriately considered.

1. INTRODUCTION

Nuclear energy is a clean base load power. It supports zero emission which contributes to Sustainable Development Goal (SDG) 7, affordable and clean energy [1]. Researchers in ASEAN region realize the importance of ensuring safe use of nuclear power, and established ASEAN Network on Nuclear Power Safety Research (ASEAN NPSR) in 2017 [2]. ASEAN NPSR is driven by seven ASEAN countries, including Laos, Malaysia, Myanmar, the Philippines, Singapore, Thailand and Vietnam. ASEAN NPSR’s goal is to reinforce nuclear power safety in ASEAN through research and development (R&D), human resource development and regional cooperation, in order to support the preparation of the regional strategy for accident management corresponding to the IAEA Safety Standards and lessons learned from the Fukushima Nuclear Accident.

Fission product behaviour analysis is one of the R&D activities of the ASEAN NPSR. The main cause of fuel damage in the reactor core is Loss of Coolant Accident (LOCA) which significantly contributes to radioactive release [3, 4]. LOCA is also the main cause of fuel damage in spent fuel pool (SFP) [5, 6]. To thoroughly understand the fission product behaviour during LOCA, all possible source terms (i.e. releases from fuel damage in both reactor and SFP) need to be considered.

Thailand Institute of Nuclear Technology (TINT) and Chulalongkorn University (CU) have studied fission product behaviour during a severe accident in nuclear power plants since 2012 [7]. This study supports ASEAN NPSR in determining source term release data which contributes to the understanding of the consequences of a radioactive release from neighbouring nuclear power plants. In our previous studies, fission product behaviour was studied by ART Mod 2 of Japan Atomic Energy Agency (JAEA) [8]. It has been modified and validated by TINT and CU in 2019 [9]. Modified ART Mod 2 was used to assess fission product behaviour in reactor pressure vessel [7] and containment vessel [9] during severe accident. However, modified ART Mod 2 has never been used to study fission product behaviour in the SFP.

In the past, the main focus of the research was on the management of spent fuel for the extended storage of spent fuels [10] and the protection design of the SFP to reduce the hazards from stored spent fuels [11]. Yet there are certain researchers paying efforts on the SFP accident analysis. Sailor V. L., et al. [5] found that the LOCA (or complete draining) of the SFP is the main cause of fuel damage and fission product release in the SFP of a Light Water Reactor (LWR) such as the Robert Emmett Ginna Nuclear Power Plant (R.E. Ginna NPP) and the Millstone Nuclear Power Plant. Throm E. D. [6] found that risk of the Beyond Design Basis Accident (BDBA) in the SFP of LWR was dominated by earthquake causing a LOCA in the SFP. Although there are the studies of hazards of spent fuels in the SFP [11], and causes and consequences during a severe accident of the SFP [5, 6], transportation and deposition phenomena of radioactive releases in the SFP were not studied as much as releases in the reactor core [12] and containment vessel [9, 13].

To fulfil the abovementioned gap, TINT and CU decided to apply modified ART Mod 2 code to assess of fission product behaviour in the SFP in order to help understand the overall consequences of fission product deposition and release during severe accident of nuclear power plants. The objective of this study is to assess fission product behaviour in the SFP using the geometry and conditions of the R.E. Ginna NPP. This is because it is Pressurized Water Reactor (PWR) type which is the same type of the neighbouring nuclear power plants [14], and reports on postulated accidents in this SFP are publicly available [5, 6]. This study focuses on fission product behaviour of release of compounds of caesium-137 (Cs-137) in forms of gas and aerosol because caesium compounds are known to have long term effects after a severe accident [15].

This research is divided to five parts. This part is the introduction. The second part is the information of modified ART Mod 2 code including related deposition models in this assessment. The third part is the simulation conditions. The fourth part is the results and discussions of caesium compounds release in forms of gas and aerosol in the SFP. The fifth part is the conclusions.

2. MODIFIED ART MOD 2 CODE

Modified ART Mod 2 code is a tool for studying fission product behaviour in gas and aerosol forms. The characteristics of deposition phenomena of gas and aerosol forms of modified ART Mod 2 code are shown in Fig. 1 [8]. Aerosol deposition models of ART Mod 2 code were modified and validated in 2019 including models of gravitational settling, Brownian diffusion, diffusiophoresis and thermophoresis [9]. The details of each deposition velocity calculation models of both gas and aerosol forms are shown in this section below.

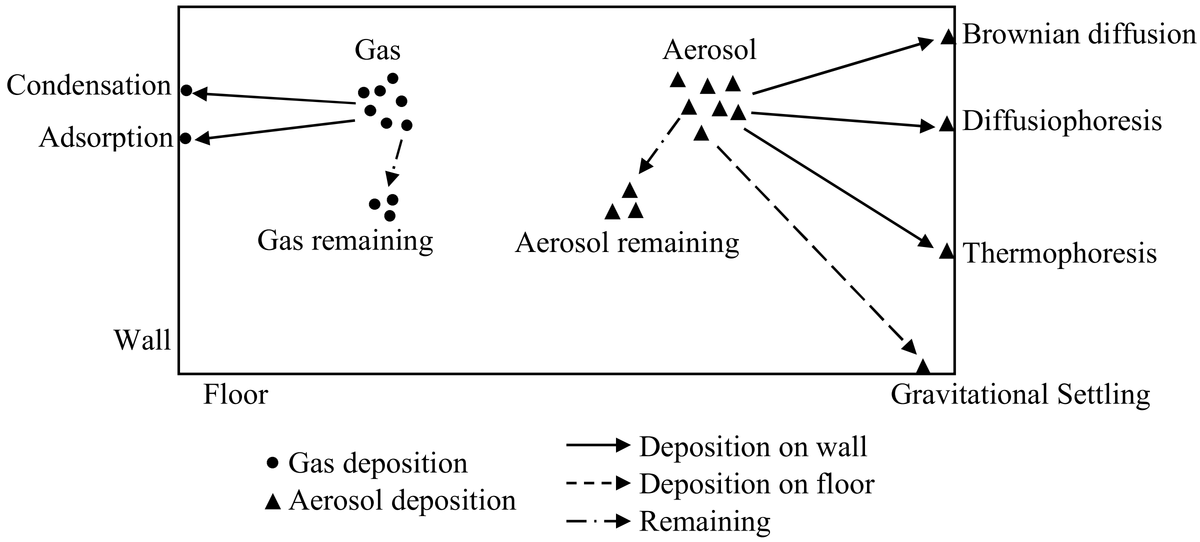

FIG. 1. The characteristic of deposition phenomena of gas and aerosol forms of modified ART Mod 2 code [8].

2.1. Deposition models of gas [8]

Phenomena of condensation and adsorption in modified ART Mod 2 code affect deposition at wall surface in Fig. 1. Deposition velocity models of two phenomena are shown below.

2.1.1. Condensation

Condensation velocity, v_{cond} [cm/s], of fission product in gas form occurs from differences between partial pressure and saturated vapor pressure in the system. The equation of condensation velocity used for the calculation is as follows:

$$v_{cond} = \frac{D_g^k}{(1-\gamma_g)\delta_D}\left(1 - \frac{\gamma_g^{k(s)}}{\gamma_g^k}\right) \tag{1}$$

where
D_g^k is the diffusion coefficient of the radionuclides k, (cm^2/s);
δ_D is the thickness of the boundary layer, (cm);
γ_g is the ratio of partial pressure without the radionuclides k;
γ_g^k is the ratio of partial pressure without the radionuclides k of the total pressure;
$\gamma_g^{k(s)}$ is the ratio of saturated pressure without the radionuclides k of the total pressure.

2.1.2. Adsorption

Adsorption velocity, v_{ads} (cm/s), of fission product in gas form occurs from reaction of radionuclides and surface of material in high temperature condition. The equation of adsorption velocity used for the calculation is as follows:

$$v_{ads} = A_o exp\left(-\frac{\varepsilon_a^k}{k_B T_{surf}}\right) \tag{2}$$

where
A_o is the velocity constant of the radionuclides k (cm/s);
ε_a^k is the activation energy of reaction of the radionuclide k (erg);
k_B is the Boltzmann constant, (erg/(K·g);
T_{surf} is the temperature of surface (K).

2.2. Deposition models of aerosol [9]

Deposition velocity models of aerosol in modified ART Mod 2 code is divided into two main regions, including floor region and wall region. The region of floor is attributed to gravitational settling while region of wall is attributed to three phenomena, namely Brownian diffusion, diffusiophoresis and thermophoresis.

2.2.1. Gravitational settling

Deposition velocity from gravitational settling, $v_{gra}(r)$ (cm/s], is the parameter used to determine the deposition characteristics on floor due to the gravitational settling. It is derived from drag force of aerosol surface which depends on Reynolds number, Re. In the case of small Reynolds number (Re < 1), settling velocity of aerosols is calculated by the Stoke's approximation. On the other hand, if Reynolds number is larger than 1 (Re > 1), settling velocity of aerosols is calculated by the Newton's approximation. The equations used for the calculation are as follows;

$$v_{gra}(r) = \begin{cases} \frac{2r^2 g(\rho_p - \rho_g)}{9\mu_g} Cu(r), & \mathrm{Re} < 1 \\ \frac{\mu_g \mathrm{Re}}{2r\rho_p}, & \mathrm{Re} > 1, \end{cases} \tag{3}$$

where
r is the radius of aerosol (cm);,
g is the gravitational acceleration (cm/s^2);
ρ_p is the density of aerosol (g/cm^3);
ρ_g is the density of gas(g/cm^3);
$Cu(r)$ is the Cunningham factor;
μ_g is the viscosity of gas (dyn·s/cm^2).

2.2.2. Brownian diffusion

Deposition velocity from Brownian diffusion, v_{diff} (cm/s), is based on an empirically derived model that consider upward flow direction in vertical duct, particle size of around 2–4 µm and volumetric flow rate of around 6.2×10^{-4}–5×10^{-3} m^3/s in order to study particle deposition on wall, as follows;

$$v_{diff} = \begin{cases} 0.0899\ \mathrm{Sc}^{-0.704} u_\tau & ; \tau^+ < 0.2 \\ 3.25 \times 10^{-4} {\tau^+}^2 u_\tau & ; 0.2 < \tau^+ < 22.9 \\ 0.17 u_\tau & ; \tau^+ > 22.9 \end{cases} \tag{4}$$

where
τ^+ is the dimensionless particle relaxation time;

Sc is the Schmidt number;
u_τ is the friction velocity(cm/s).

2.2.3. Diffusiophoresis

Deposition velocity from diffusiophoresis, $v_{diffp}\ (r)$ (cm/s), is controlled by the flow of the condensing steam and partial pressures of non-condensable gas near the structure surface. The model of diffusiophoresis considers both velocity of Stephan flow and gas momentum transfer. The model is as follows;

$$v_{diffph}(r) = \left[U_c + \frac{Cu(r)}{\chi}\frac{\sqrt{m_s}}{\gamma_s\sqrt{m_s}+\gamma_a\sqrt{m_a}}\gamma_a U_c\right] \tag{5}$$

where
m_s is the molecule weight of steam (g);
m_a is the molecule weight of noncondensible gas (g);
γ_s is the pressure fraction of steam;
γ_a is the pressure fraction of noncondensible gas;
U_c is the velocity of condensing steam (cm/s).

2.2.4. Thermophoresis

Deposition velocity from thermophoresis, $v_{ther}(r)$ [cm/s] is used to determine the deposition characteristics on wall due to thermophoresis. As is in the case of diffusiophoresis, since it is a system of large volume, it is affected by convective diffusion of aerosol same as in actual power plants. The aerosol deposition velocity from thermophoresis is derived using Monte-Carlo type numerical modelling, as follows;

$$v_{ther}(r) = \frac{2v_g Cu(r)\left(\lambda_g + C_t \mathrm{Kn}(r)\lambda_p\right)\left(1+\frac{9\mathrm{Kn}}{\left(4+\frac{\pi}{2}\right)}\right)}{T_g\left(1+3C_m \mathrm{Kn}(r)\right)\left(2\lambda_g+\lambda_p+2C_t \mathrm{Kn}(r)\lambda_p\right)} \nabla T_g \tag{6}$$

where
v_g is the dynamic viscosity of gas (cm^2/s];
λ_g is the conductivity of mixed gas (erg/(K·cm·s));
λ_p is the conductivity of aerosol (erg/(K·cm·s);
C_t is the coefficients of the energy exchanges between the aerosol and gas;
C_m is the coefficients of the momentum exchanges between the aerosol and gas;
α_m is the accommodation factor for momentum exchange;
α_t is the accommodation factor for energy exchange;
∇T_g is the gradient of temperature of gas (K).

3. SIMULATION CONDITION

LOCA (or complete draining of the SFP) of The SFP of the R.E. Ginna NPP is selected as a representative accident in this simulation. The SFP is located at Ontario, New York, USA [16]. The first operation was in June 1, 1970 at capacity of 490 MW(e) [17]. Geometry parameters of the SFP of the R.E. Ginna NPP [6] are used to determine nodalization in modified ART Mod 2 code. Its thermal hydraulic parameters and amount of caesium inventory [5] is used to study caesium compounds behaviour in modified ART Mod 2 code. Two types of caesium compounds are studied. One is the caesium iodide (CsI) in gas form; another is the caesium hydroxide (CsOH) in aerosol form. CsI and CsOH are selected because they are dominant caesium compounds in the SFP analysis [18]. Geometry parameters, source term parameters, and thermal hydraulic parameters for the simulation of the two cases are shown in Table 1, Table 2 and Table 3, respectively [5, 6, 19]. The two cases assumed that the SFP is open to the environment.

Nodalization of the SFP of the R.E. Ginna NPP for modified ART Mod 2 code is shown in Fig. 2. There are SFP volume and environment volume. In the SFP volume, the authors adopt the temperature from heat decay and oxidation reaction in Fig. 3 as the temperatures of source term, gas and wall. In Fig. 3, before points of complete draining of the SFP at 18 000 seconds and self-sustaining oxidation reaction at 18 760 seconds, the temperatures were calculated based on conditions of temperature rate from the boiling experiment from [5]. From the calculation, point of complete draining of the SFP at 18 000 seconds in Fig. 3 is the starting point of caesium compounds release. After point of self-sustaining oxidation reaction point at 18 760 seconds in Fig. 3, condition of temperature was reproduced based on measurement of temperature increases due to heat decay and self-sustaining oxidation reaction of cladding from [5]. For the environment volume, the temperatures are set at room temperature (25°C at 1 atm) based on open pool assumption [20]. Volumetric flow rate of source term to environment is designed based on boil off rate of vapor at 13 ft^3/hr.

TABLE 1. GEOMETRY PARAMETERS OF THE SFP OF THE ROBERT EMMETT GINNA NUCLEAR POWER PLANT [6]

Geometry parameters	Data
Length (ft)	43.0
Width (ft)	22.2
Hight (ft)	41.7
Volume (ft^3)	3.98×10^4

TABLE 2. SOURCE TERM PARAMETERS OF THE SFP OF THE ROBERT EMMETT GINNA NUCLEAR POWER PLANT [5, 19]

Source term parameters	Case 1	Case 2
Source term type	CsI	CsOH
Form	Gas	Aerosol
Size (µm)	-	50-70
Amount (Ci)	1.48×10^7	1.48×10^7

TABLE 3. THERMAL HYDRAULIC PARAMETERS OF THE SFP OF THE ROBERT EMMETT GINNA NUCLEAR POWER PLANT [5]

Thermal hydraulic parameters	Data
Rate of temperature Increase during boiling (°C/hr)	~7
Self-sustaining oxidation temperature (°C)	~900
Cut-off oxidation temperature (°C)	~1900
Pressure (MPa)	0.101
Boil off rate (ft^3/hr)	13

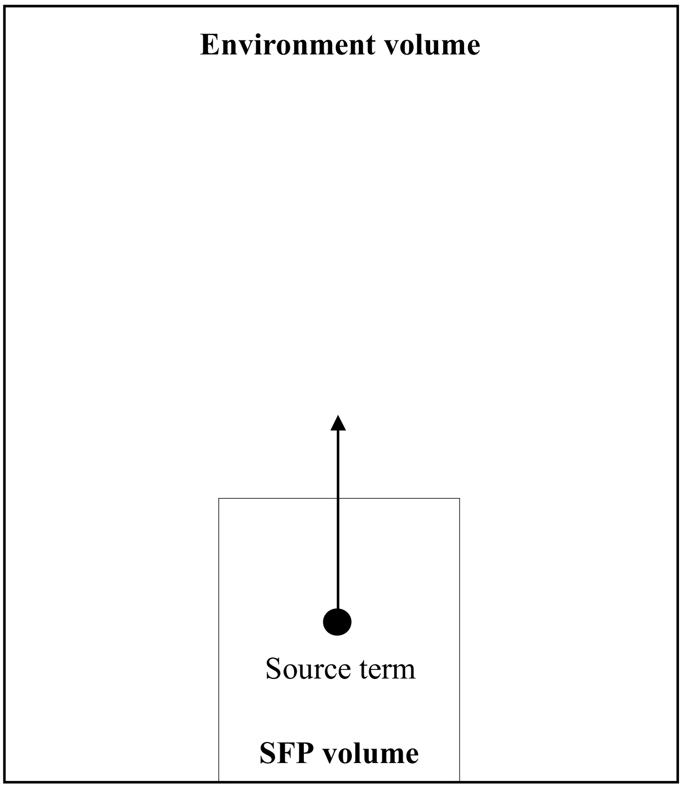

FIG. 2. Nodalization of the SFP of the R.E. Ginna NPP for modified ART Mod 2 code.

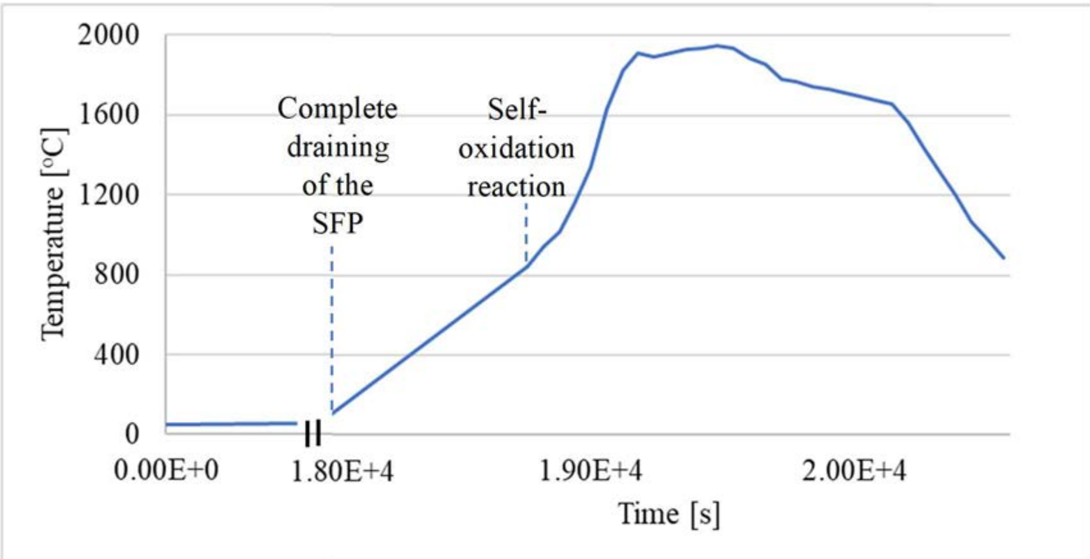

FIG. 3. Temperature of heat decay and oxidation reaction of the SFP of the R.E. Ginna NPP for modified ART Mod 2 code.

4. RESULTS AND DISCUSSIONS

The first case is the study of caesium compound behaviour using CsI in gas form. The authors started to study CsI behaviour at 18 760 seconds in Fig. 4 which is the starting point of caesium compounds release from the fuel cladding. The amount of CsI deposit on wall of the SFP due to adsorption phenomenon is very small. Most suspended CsI release into environment at 1 500 000 seconds or approximately 17 days. In the case of CsOH in aerosol form, it is found that CsOH mostly deposit on wall of the SFP from Brownian diffusion, and slightly on floor of the SFP from gravitational settling phenomenon as depicted in Fig. 5. Brownian diffusion is dominant because CsOH aerosol was simulated at high temperature. This increases turbulence flow which is sensitive to Brownian diffusion [21].

From the results, it is found that most CsI is released into environment. The CsI release is consistence to measurement data set of caesium and iodide during the Fukushima Nuclear Accident: the major part of the release is estimated to be within 19 days after the accident starts [22]. As for the CsOH deposition, there are no wall depositions from diffusiophoresis and thermophoresis because of assuming no difference of wall temperature and gas temperature due to the lack of data. CsOH can also exist in form gas because of reaction between CsI and steam [23]. Therefore, there is a potential of a larger release of CsOH into environment when compared to the simulation results. Accuracy of the results can be further increased by considering the ratio between gas and aerosol of the source term, and chemical reactions. Our previous study noted the possibility of having different caesium compounds due to chemical reactions, such as caesium molybdate (Cs_2MoO_4), caesium telluride (Cs_2Te); and iodine compounds, such as iodine (I_2), methyl iodide (CH_3I), iodine pentoxide (I_2O_5) [24].

It can be concluded that modified ART Mod 2 code can capture the trend of CsI gas release but not that of CsOH aerosols. Total caesium compounds release and retention in all forms can be more accurately estimated if source term ratio of gas and aerosol, difference between wall and ambient temperatures, and chemical reactions are appropriately considered.

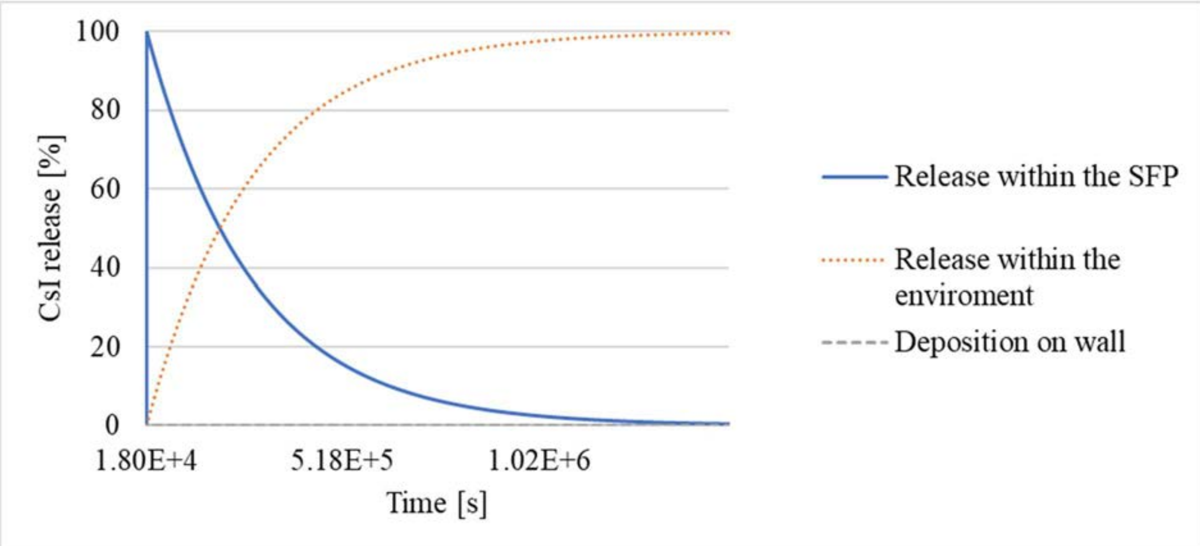

FIG. 4. CsI release in the SFP of the R.E. Ginna NPP using modified ART Mod 2 code.

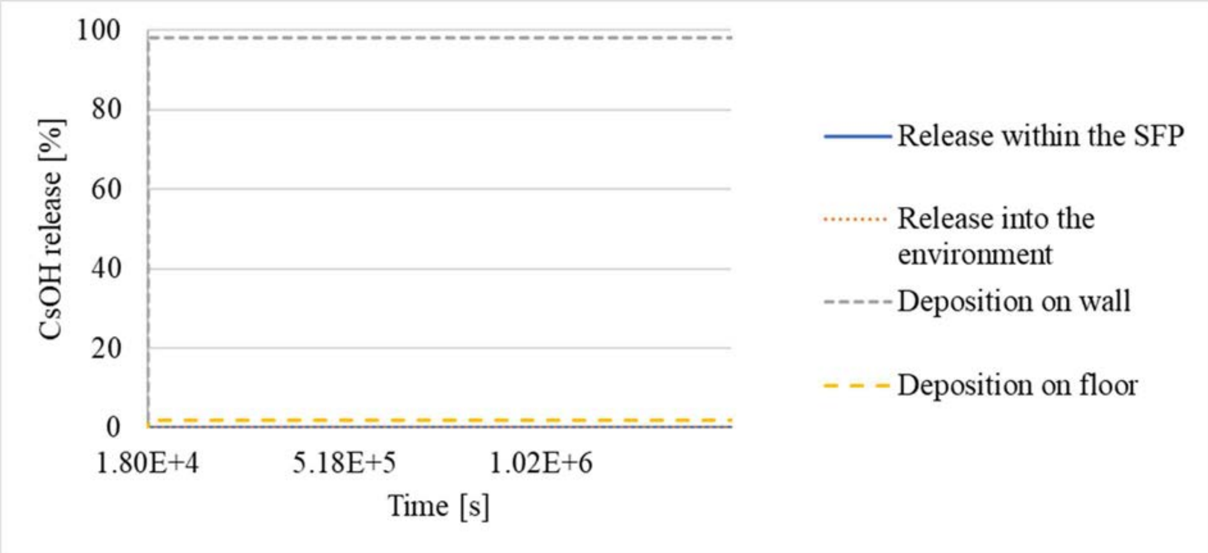

FIG. 5. CsOH release in the SFP of the R.E. Ginna NPP using modified ART Mod 2 code.

CONCLUSIONS

Modified ART Mod 2 code was used to assess caesium compounds behaviour of the LOCA (or complete draining) in SFP using the geometry and conditions of the R.E. Ginna NPP.

- Most suspended CsI tend to be released into environment within 17 days which resembles the release of caesium and iodine from the Fukushima Nuclear Accident in early period. The amount of CsI deposit on wall of the SFP due to adsorption phenomenon is very small.
- Brownian diffusion phenomenon is dominating CsOH aerosol deposition because CsOH aerosol at high temperature increases turbulence flow which is sensitive to Brownian diffusion.
- Modified ART Mod 2 code can capture the trend of release of CsI gas into environment but not CsOH aerosols because of assuming no difference of wall temperature and gas temperature.
- Total caesium compounds release and retention in all forms can be more accurately estimated if source term ratio of gas and aerosol, difference between wall and ambient temperatures, and chemical reactions are appropriately considered

As for the future plan, the authors view as proper that modified ART Mod 2 code be adjusted to accurately evaluate caesium aerosols and to enable studies of other caesium compounds. Then the combination of radioactive releases from the reactor and the SFP should be considered to identify mass balance in the systems and calculate amount of fission product into environment.

REFERENCES

[1] UNITED NATIONS, Transforming our World: The 2030 Agenda for Sustainable Development, A/RES/70/1, UN, New York, NY (2015).
[2] ASEAN NETWORK ON NUCLEAR POWER SAFETY RESEARCH, Joint Communique on the Establishment of ASEAN Network on Nuclear Power Safety Research, Bangkok (2017).

[3] INTERNATIONAL ATOMIC ENERGY AGENCY, The Fukushima Daiichi Accident: Report by the Director General, IAEA, Vienna (2014).
[4] TOKYO ELECTRIC POWER COMPANY, Fukushima Nuclear Accident Analysis Report, TEPCO, Tokyo (2012).
[5] UNITED STATES NUCLEAR REGULATORY COMMISSION, Severe Accidents in Spent Fuel Pools in Support of Generic Safety Issue 82, USNRC, Washington DC (1987).
[6] UNITED STATES NUCLEAR REGULATORY COMMISSION, Regulatory Analysis for the Resolution of Generic Issue 82, “Beyond Design Basis Accidents in Spent Fuel Pools”, USNRC, Washington DC (1989).
[7] VECHGAMA, W., SILVA, K., RASSAME, S., “Investigation and Modification of Aerosol Deposition Model of ART Mod 2 using Experimental Data from NSPP-502 and Phébus FPT1”, Presented at 11th Int. Topical Mtg on Nuclear Reactor Thermal-Hydraulics, Operation and Safety ‘NUTHOS-11’, Gyeongju, Korea, 2016.
[8] KAJIMOTO, M., HIDAKA, A., MURAMATSU, K., SUGIMOTO, J., “A Computer Code for the Analysis of Radionuclide Transport and Deposition under Severe Accident Conditions: Model Description and User’s Manual”, Japan Atomic Energy Research Institute, Tokyo (1988).
[9] VECHGAMA, W., SILVA, K., RASSAME, S., Validation of Modified ART Mod 2 Code through Comparison with Aerosol Deposition of Cesium Compound in Phébus FPT3 Containment Vessel, Sci Technol Nucl Ins., **2019** (2019) 16.
[10] INTERNATIONAL ATOMIC ENERGY AGENCY, Further analysis of extended storage of spent fuel, IAEA-TECDOC-944, IAEA, Vienna (1997).
[11] Alvarez, R., Beyea, J., Janberg, K., Kang, J., Lyman, E., Macfarlane, A., Thompson, G., Hippe, F.N.V., Reducing the Hazards from Stored Spent Power-Reactor Fuel in the United States., Sci Glob Secur, **11** (2003) 1–51.
[12] HIDAKA, A., HASHIMOTO, K., SUGIMOTO J., “Experiment Analysis with ART Code FP Behavior under severe accident conditions: Validation of Systems Transients Analysis Codes. 223” Japan Atomic Energy Research Institute, Tokyo (1995).
[13] LAURIE, M., MARCH, P., SIMONDI-TEISSEIRE, B., PAYOT, F., Reprint of containment behaviour in Phébus FP, Ann. Nucl. Energy., **61** (2013) 122–134.
[14] KHUNSRIMEK, N., VECHGAMA, W., SILVA, K., RASSAME, S., “Effects of radionuclide atmosphere dispersion from a hypothetical severe accident at Fangchenggang and Ninh Thuan Nuclear Power Stations to Thailand”, Asian Symposium on Risk Assessment and Management 2017 ‘ASRAM2017’, Atomic Energy Society of Japan, Tokyo (2017).
[15] INTERNATIONAL COMMISSION ON RADIOLOGICAL PROTECTION, Occupational Intakes of Radionuclides: ICRP Publication 103, Ontario, Canada (2007).
[16] LORENZ, H., Design of The Concrete Containment Vessel for R.E.Ginna Nuclear Power Plant, Nucl Eng Des., **6** (1967) 360–366.
[17] CONSTELLATION ENERGY, R.E. Ginna Nuclear Power Plant (2007), http://www.constellation.com/portal/site/constellation/menuitem.385c7a188817d1908d84ff10025166a0/
[18] DE LA ROSA BLUL, C.J., MC MINN, P., GRAH, A., Analysis of the Inherent Response of Nuclear Spent Fuel Pools, Ann Nucl Energy. **124** (2019) 295–326.
[19] FYNBO, P., HAGGBLOM, H., JOKINIEMI, J., Aerosol Transport in Severe Reactor Accidents, Nordic Liaison Committee for Atomic Energy, Nyköping (1990).
[20] SEPPÄNEN, O., FISK, W.J., LEI, Q.H., Effect of Temperature on Task Performance in Office Environment, LBNL-60946, Lawrence Berkeley National Laboratory, Berkley, CA (2006).

[21] XU, P., MUJUMDAR, A.S., POH, H.J., YU, B., Heat transfer under a pulsed slot turbulent impinging jet at large temperature differences., Therm Sci., **14** 1 (2010) 271–281.
[22] KATATA, G., CHINO, M., KOBAYASHI, T., TERADA, H., OTA, M., et al., Detailed source term estimation of the atmospheric release for the Fukushima Daiichi Nuclear Power Station accident by coupling simulations of an atmospheric dispersion model with an improved deposition scheme and oceanic dispersion mode, Atmos. Chem. Phys **15** (2015) 1029–1070.
[23] SULKOVA, K., CANTREL, L., LOUIS, F., Gas-Phase Reactivity of Cesium-Containing Species by Quantum Chemistry., J Phys Chem A., **119** 35 (2015) 9373–9384.
[24] VECHGAMA, W., SILVA, K., "Study of Fission Product Behavior in Containment Vessel using Modified ART Mod 2: Update of Cesium and Iodine Compound Models", Proc., 26th Int. Conf. Nuclear Engineering 'ICONE26', ASME, New York, NY (2018).

SIMULATION SEVERE ACCIDENT IN THE SPENT FUEL POOL WITH VIOLATION OF THE HEAT SINK IN THE POWER UNIT NO.1 OF SOUTH UKRAINIAN NPP

O. BALASHEVSKYI
Department of Scientific and Technical Support
SS “Scientific and Technical Centre” of SE NNEGC “Energoatom”
Kyiv, Ukraine
Email: o.balashevsky@ntc.atom.gov.ua

Abstract

A simulation model of the spent fuel pool of power unit No.1 of the south Ukrainian NPP was developed for MELCOR 1.8.5. The initial event was analyzed in case of loss of heat removal. The consequences and the time of fuel damage, the amount of generated hydrogen and the moment of the beginning of the interaction of the melt with concrete were determined.

1. INTRODUCTION

The reason for the increased attention of simulation of a severe accident in the spent fuel pool (SFP) related to the violation of the heat removal as the initial event (IS) is that something similar took place on March 11, 2011 at the Fukushima Japanese NPP. As events have shown [1], the threat of loss of cooling of the SFP becomes very acute when the power unit is de-energized, without timely restoration of the backup power supply. It is necessary to evaluate the time, conditions and consequences of a severe accident that will determine the vulnerability of the power unit to this type of IS and to take the necessary measures to prevent or mitigate the development of this accident.

A simulation model of power unit No. 1 of the SUNPP (V302) for the analysis of beyond design basis accidents for the MELCOR [2] and calculation data [3–5] were used.

Under the conducted calculation, the analysis of a severe accident under conditions of complete loss of heat removal from SFP using the developed model was carried out, and the time of the processes, the amount of hydrogen formed, qualitative and quantitative parameters of processes and its features were determined.

The applicability of this conducted simulation model can be expanded by carrying out an analysis of SA in SFP for all nuclear power plants of Ukraine with VVER with the use of strategy of SFP replenishing and assessing the SA radiation consequences.

2. SHORT DESCRIPTION OF THE SPENT FUEL POOL

The SFP is used for temporary storage of spent nuclear fuel assembles (SFAs) for at least three years during a three year refuelling interval up to achieving residual energy emissions that allow their unloading and transportation. The SFP is located in the reactor containment and consists of a spent fuel assemblies compartment designed specifically for storing SFAs and container compartment with a stationary rack for fresh fuel and a universal loading /unloading zone - for spent and fresh fuel assembles containers (Fig. 1, [3]). The racks of SFP have a metal structure consisting of an absorption part, a base plate, extendable support part and other small parts used to install the rack.

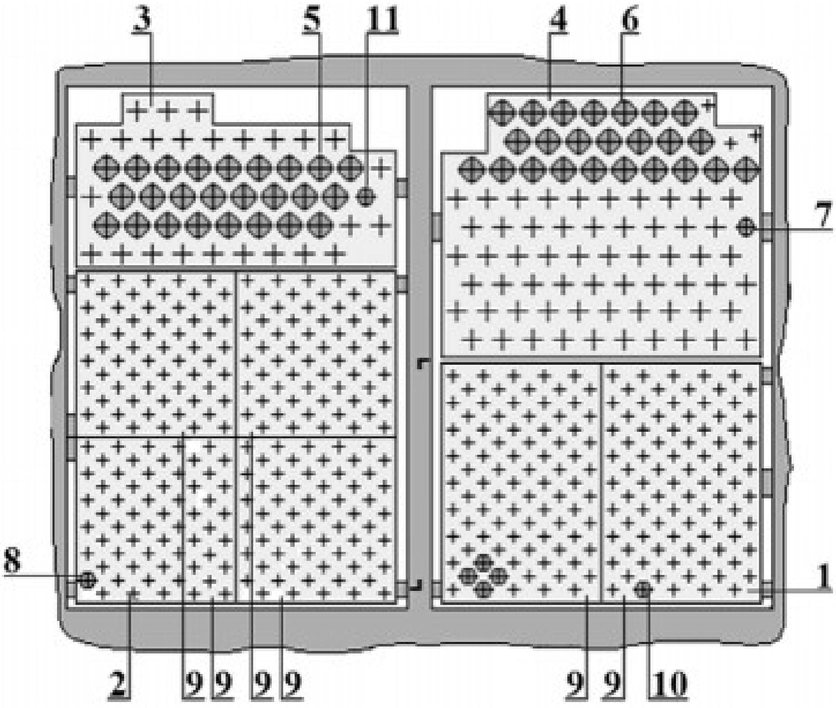

FIG. 1. Scheme of the racks of the storage pool (top view): 1 - Racks of compacted fuel storage of the container compartment; 2 - Racks of compacted fuel storage of the assembly compartment; 3 - Uncompressed rack; 4 - Removable (emergency) rack; 5 - Cells for SFA covers 25 pcs; 6 - Cells for SFA covers 24 pcs; 7 - Cells for assemblies 61 pcs; 8 - Cells for assemblies 192 pcs; 9 - Blocks of covers; 10 - Cells for assemblies 136 pcs; 11 - Cells for assemblies 27 pcs.

The absorption part is a welded metal structure, consisting of three plates (lower, middle and upper) with hexagonal holes, into which are welded 221 (a rack for installing SFAs in container compartment) and 244 (a rack for installing SFAs in assembly compartment) of hexagonal absorption pipes with length of 4350 mm that are made of 5 mm thick boron corrosion-resistant steel for installing spent fuel assemblies for storage in SFP. The base plate is supported by extendable support structure and support posts. Racks are welded to the floor of SFP at elevation + 21.9 m. The base plate is made of stainless steel and has openings for supplying cooling water to the SFAs and canisters.

3. DESCRIPTION OF THE SIMULATION MODEL OF SFP

The simulation model of SFP for the MELCOR 1.8.5 is the model of the assembly and container compartments of power unit No. 1 of the South Ukrainian NPP, in which racks for storing SFAs are installed.

The main changes affected the following components of the simulation model.

1. Instead of a pre-existing simplified model of SFP, a detailed model of SFP is developed with spent fuel storage racks, including assembly and container compartments.
2. Nodalization of SFP with installed racks of compacted fuel storage (RCFS) is adapted for MELCOR 1.8.5. These changes in the complex allowed us to simulate all processes occurring in SFP, including evaporation, heating, damage and destruction of the spent fuel assemblies and RCFS, the formation of melt and hydrogen, the relocation of the melt and its interaction with the lining of the bottom of SFP (penetration) and concrete.

3. Nodalization of supporting structures is developed. This made it possible to simulate the accumulation of the melt and the progressive interaction of the melt with the concrete structure.

The model includes 14 control volumes and 23 connection paths (Fig. 2).

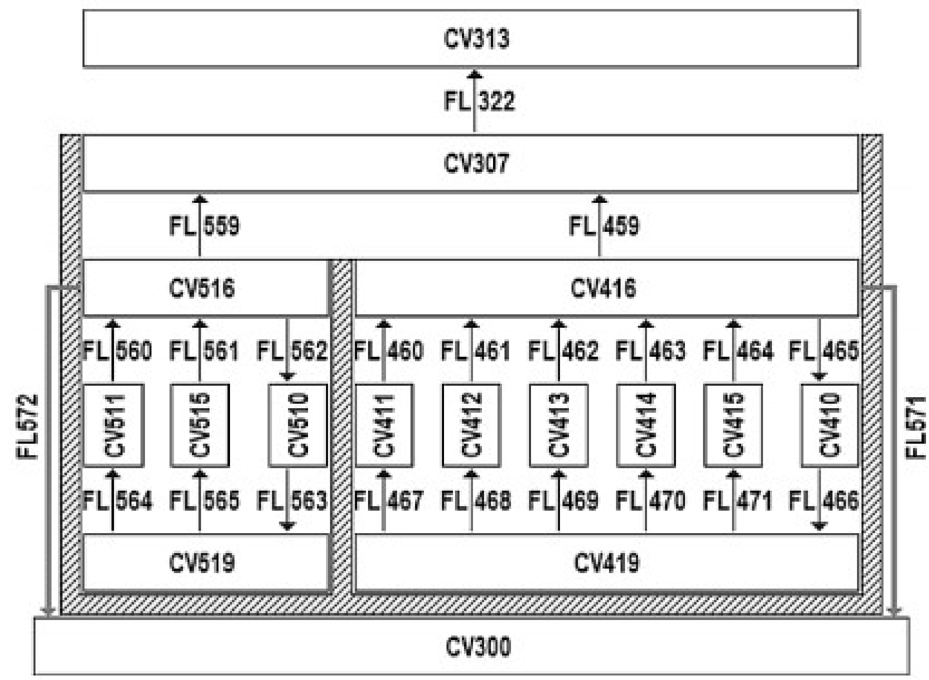

FIG. 2. Nodalization scheme of the SFP of the first unit of the South Ukrainian NPP.

The numbers of the control volumes of the more heat-stressed assembly compartment have format 'CV4xx', less heat-stressed container compartment 'CV5xx'.

The control volumes CV419 and CV519 simulate the lower volumes of the pool compartments from the lower floor elevation of 21.9 m to the lower border of the lower base plate of SFA storage racks.

The control volumes CV411–415, CV511 and CV515 are the volumes in which the SFAs are located inside the jacketed hex pipes, from the shanks of the SFAs in lower base plate to the top part of the metal structures of the racks.

The control volumes CV410 and CV510 simulate a bypass between the outer side surface of the peripheral rows of absorption tubes and the side surface of SFP compartments. Control volumes CV416 and CV516 simulate sections of assembly and container compartments from metal structures of racks to the top of the wall separating compartments.

The control volume CV307 simulates the total volume for the two compartments located above the separating wall to the upper elevation of concrete structures 38.1 m. The flow paths FL571 and FL572 simulate overflows at 30.03 m elevation (normally open when RU is operating at the rated power).

According to the current loading of the nuclear reactor at the SUNPP [5], there are 222 SFAs in the assembly compartment and 48 in the container compartment, i.e. it is necessary to simulate the two compartments. The MELCOR 1.8.5 does not have the ability to simulate two spatially separated cores in one model. Based on the fact that the biggest part of SFAs is located in the cassette compartment, a decision was made to model it in the COR package. The container compartment is modelled using a package of thermal structures HS with a given level of energy release.

According to the current loading of the nuclear unit of the SUNPP [5], there are 222 SFAs in the assembly compartment and 48 SFA in the container compartment, i.e. it is necessary to simulate two SFA locations. The MELCOR does not have the ability to simulate two spatially separated active zones in one model. Based on the fact that the main part of the SFA is located in the assembly compartment, a decision was made to model it in the COR package. The container compartment is modelled using a package of thermal structures HS with a given level of energy release.

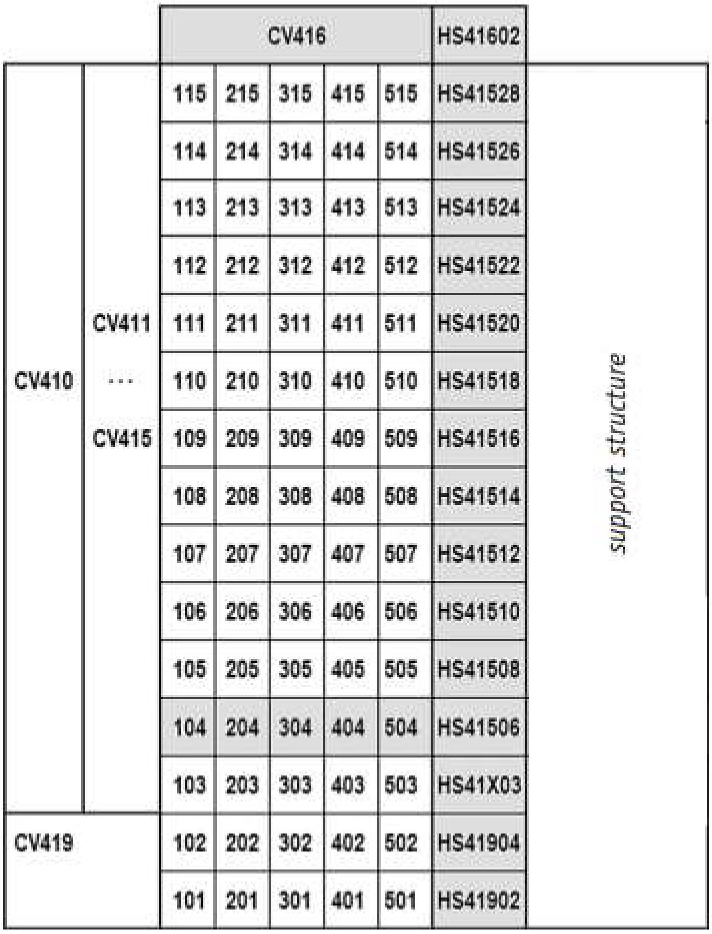

FIG. 3. Assembly compartment levels of the SFP in COR package.

The COR package breaks down the simulated assembly compartment of SFP into sections in elevation (Fig. 3). In height, the model contains 15 elements, including the lower, middle and upper base plates as a supporting structure.

The processes inside the fuel grid are modelled by the COR package for which a core model is being constructed within the framework of the SFP assembly compartment.

When developing the model of the assembly compartment, the presence of water filled the gaps between the pipes and the material of the casing pipe of the racks is taken into account. The model considered also the masses of all structural materials used in the SFP and SFA and their distribution along the height. The lining of the SFP floor plays the role of a bottom, the violation of the bearing capacity of which occurs when the temperature exceeds 1000°C (this value is defied by default in the MELCOR 1.8.5). Further, after the destruction of the flooring, the melt will interact with concrete.

In the radial direction the SFA assembly compartment (244 pieces) consists of zones (Fig. 4). The first zone (central) contains 29 SFAs, the second 50, the third 74, the fourth 69 and the fifth zone (peripheral) contains 22 free cells for installing the SFA.

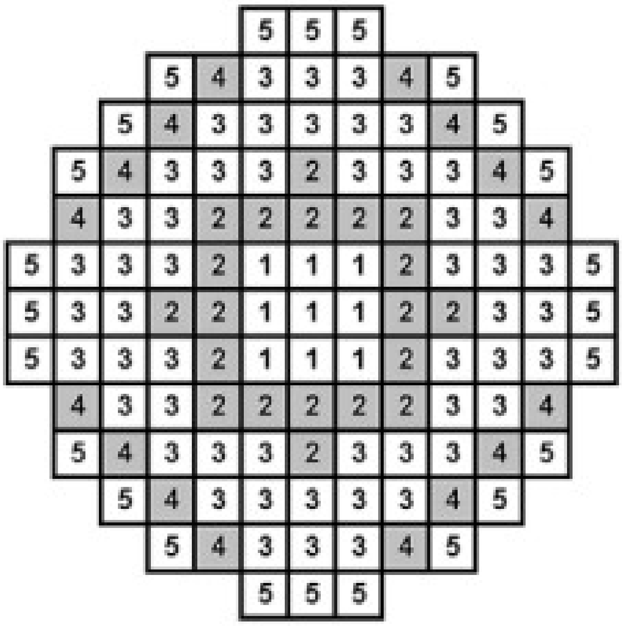

FIG. 4. SFAs distribution zones in SFP.

Such a ‘dense’ arrangement of SFAs corresponds to the cylindrical geometry embedded in the COR code package, and is more conservative in terms of lower heat losses from the SFAs to the volumes of containment and SFP.

According to the data obtained from SUNPP [5], the number of SFAs corresponds to the actual number of spent nuclear fuel in the SFP of power unit No.1 for 1998 to 2012.

The input energy release is the actual energy release of 222 filled SFA cells (out of a total of 244 cells) of the assembly compartment of the first unit of the South Ukraine NPP and equal to 0.988 MW [5].

In order to assess the dynamics of the decrease in the level of borated water in the SFP and the additional steam release and heating of the containment atmosphere, the model of the container compartment with racks and SFA Imitators is added to the simulation model of in terms thermal structures (HS). Energy input for container compartment is the actual energy release of 48

SFAs as the maximum possible number of cells SFAs (221 cells in total) of the first unit of the South Ukraine NPP that equal to 0.218 MW [5]. To consider the most unfavourable situation, SFAs with a shorter storage time are placed closer to the centre of the spent fuel.

The profile of energy release along the height of the core was adopted as similar for real unit at the end of refuelling interval in the model developed for RELAP5 / SCDAP [6], with the maximum shifted at the top. This additionally accelerates the heating and damage to the fuel while decreasing the water level in SFP.

4. SIMULATION OF SBO WITH FAILURE OF THE HEAT REMOVAL FROM THE SFP WITHOUT RECOVERY OF WATER FEEDING

The accident was calculated in order to obtain information on the dynamics of the depletion of the SFP, the time of heating and destruction of the fuel, the amount of hydrogen generated, etc.

Due to the complete de-energization of the power unit, the heat sink from the SFP is stopped. The supply of emergency power from diesel generators (DG) or from other sources is not considered.

The initial event leads to the heating of water in the SFP compartments. Due to the fact that the thermal power of the assembly compartment exceeds the capacity of the container compartment, the dynamics of heating and evaporation of the liquid in them have significant discrepancies. At the 46 300 second, the water of the assembly compartment boils and at 116 300 second — in the container compartment. Evaporation of water begins in the SFP compartments and, consequently, a decrease in their levels.

Due to the complete de-energization of the power unit, the beginning of exposure of the fuel section of the cassette compartment begins much earlier — 214 300 s, container — 851 900 s. The complete exposure of the fuel column of the SFA located in the assembly compartment occurs at 443 600 s, which is accompanied by a sharp increase in the temperature of the cladding of the fuel rods. From the 509 800 second, the destruction of the SFAs of the assembly compartment begins.

The mass of 271.5 kg of Hydrogen generates in the assembly compartment at period from 354 200 to 649 000 second. The value of the mass of hydrogen generated in the assembly and container compartments is determined from equations:

$$MH_{2cont} = MH_{2assemb} \times NTBC_{cont} / NTBC_{assemb} = 271.5 \times 48/222 = 58.7 \text{ kg} \quad (1)$$

$$MH_{2total} = MH_{2assemb} + MH_{2cont} = 271.5 + 58.7 = 330.2 \text{ kg} \quad (2)$$

where:
$NTBC_{cont}$ - the number of fuel assemblies located in the container compartment;
NTBCcont = 48 pcs;
$NTBC_{assemb}$ - the number of fuel assemblies located in the assembly compartment;
$NTBC_{assemb}$= 222 pcs;
MH_{2total} - mass of hydrogen generated in both compartments (kg);
$MH_{2assemb}$ - mass of hydrogen generated in the assembly compartment (kg) (this parameter is calculated by the MELCOR);
MH_{2cont} - mass of hydrogen generated in the container compartment (kg).

The calculation was stopped after 1 155 000 seconds from the moment of the beginning of initial event due to a failure of the bottom (lining) of the assembly compartment.

Table 1 presents the chronology of events of the source event under consideration. The main results of the emergency transient calculation in graphical form are shown in Figs. 5- 8.

TABLE 1. SBO WITH VIOLATION OF THE HEAT SINK FROM SFP WITHOUT RESTORING WATER FEEDING

Time (s)	Event	Description
0	SBO, non-start of diesel generators, shutdown of SFP cooling pumps	Initial event
46 300 (116 300)	Beginning of the boiling of liquid in SFP	The temperature of water in the SFP is 100 °C
214 300 (851 900)	Beginning of exposure of the active part of the SFA	Water level below 27.06 m
354 200	The beginning of the evolution of hydrogen	Beginning of the steam zirconium reaction
443 600	Complete exposure of the active part of the SFA of the assembly compartment	Water level below the active part of the SFA, elevation 23.47 m
509 800	The beginning of the destruction of the cladding of the fuel rods of the assembly compartment	The destruction of the SFA begins with the central radial segment
649 000	Completion of hydrogen generation	The mass of hydrogen generated in the assembly compartment is 271.5 kg
1 155 000	End of calculation	Failure of the bottom of the container compartment of SFP

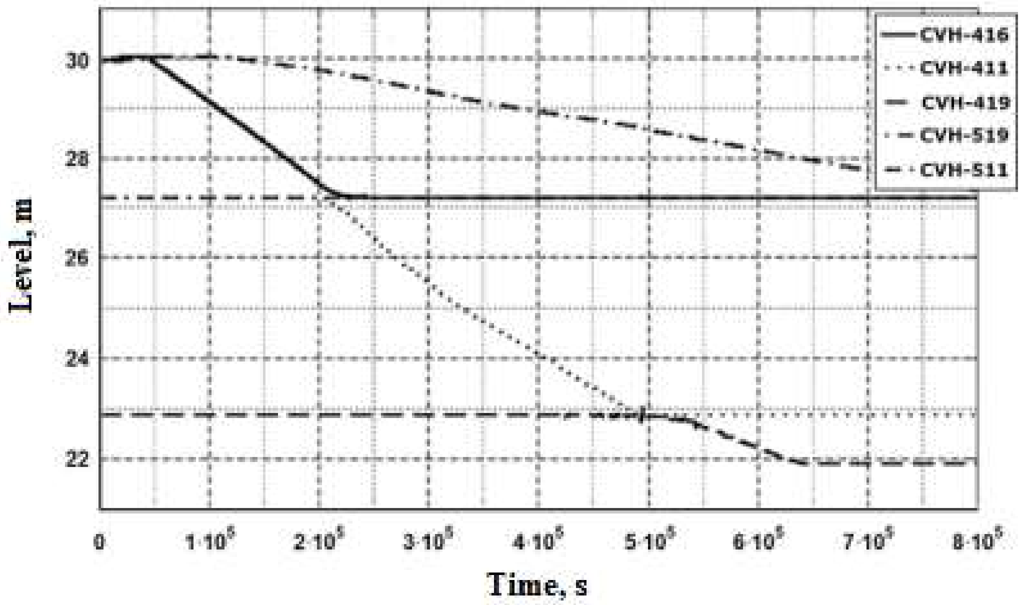

FIG. 5. Water levels in the simulated volumes of SFP: CVH416 - water level in the control volume of CV416; CVH411 - water level in the control volume of CV411; CVH419 - water level in the control volume of CV419; CVH516 - water level in the control volume of CV516; CVH511 - water level in control volume CV511.

The obtained results of computational modelling indicate the presence of a significant margin of time for the implementation of measures of stopping or mitigation of a severe accident in the spent fuel storage pool. To avoid damage to the spent fuel assemblies and the racks of SFP under severe accident conditions, it is advisable to consider options for implementing strategies with SFP replenishment at different stages of the accident, which will allow cooling the fuel mass when heat sink is lost.

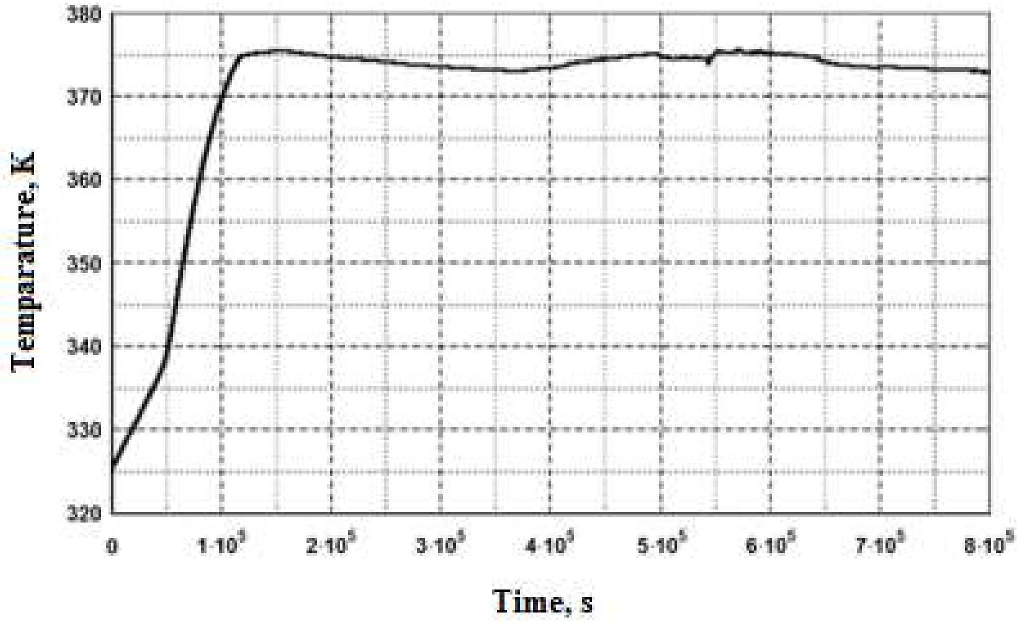

FIG. 6. Temperature of fuel rod shells.

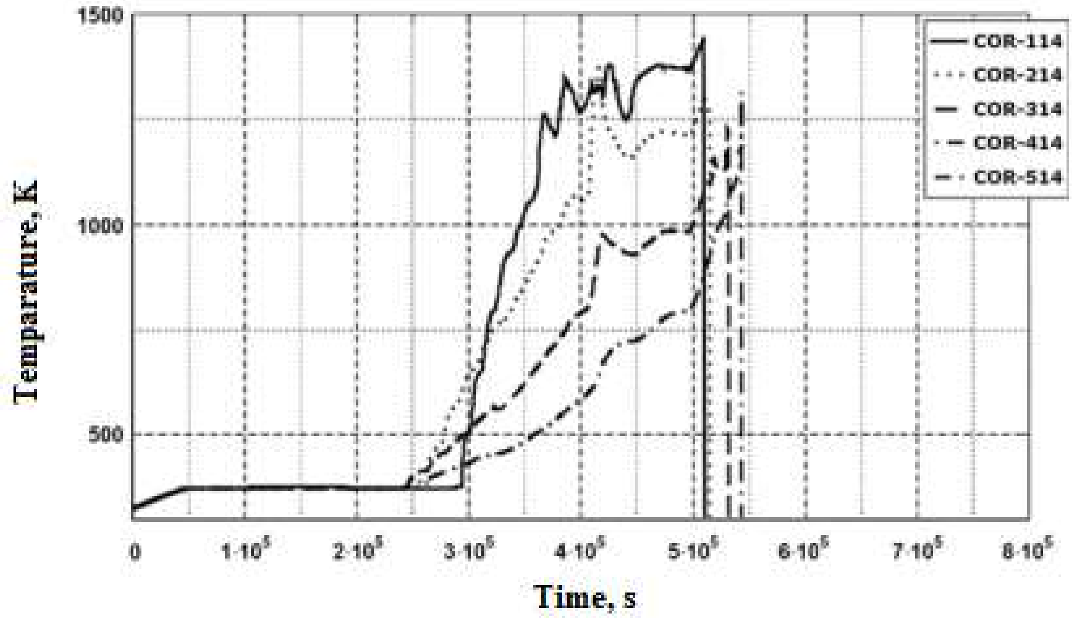

FIG. 7. Temperature of fuel rod shells over radial zones.

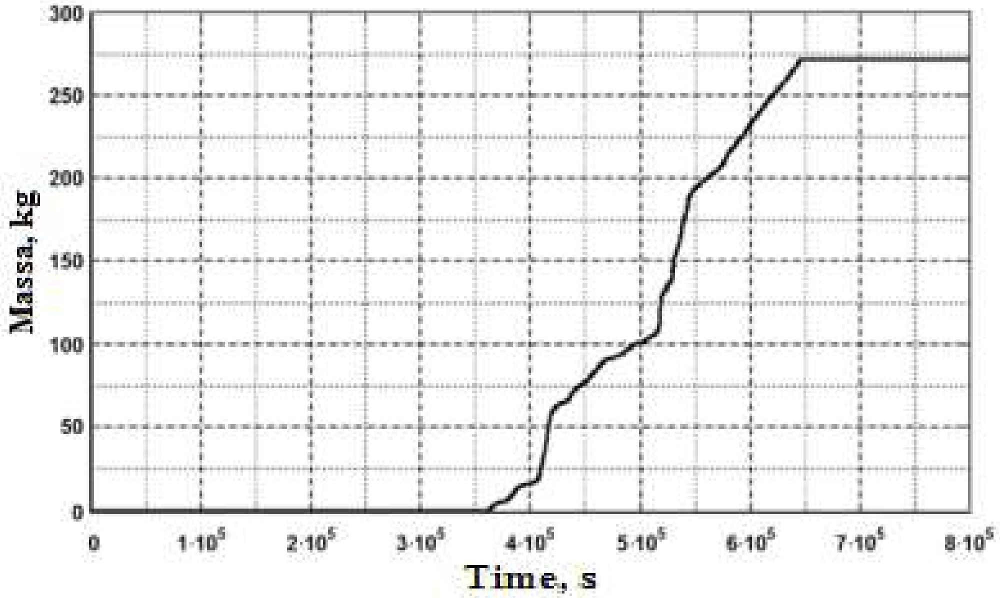

FIG. 8. Mass of generated hydrogen in SFP.

CONCLUSIONS

The calculations were performed using a developed realistic model of the spent fuel storage pool of the first unit of the South Ukrainian NPP for MELCOR 1.8.5. A basic option is analyzed with a complete blackout of the power unit without the intervention of the operational personnel of the station and, as consequence of the termination of heat removal from the spent fuel storage pool.

During the development of the model, it was assumed that spent fuel assemblies are of varying degrees of burnout and have different date of unloading in accordance with current actual data for power unit No.1 of the South Ukraine NPP.

The results obtained indicate the presence of a sufficient margin of time from the moment that the IS has been considered to take measures to prevent or stop the development of a severe accident in the spent fuel pool, namely, the operation personnel have a time of at least four days to prevent damage to the fuel in the storage pool or at least six days to prevent damage of lining of the storage pool and the interaction of the melt with concrete.

REFERENCES

[1] International Fact Finding Expert Mission of the Fukushima Daichi NPP Accident Following the Great East Japan Earthquake and Tsunami. Mission Report. Fukushima Daichi NPP and Tokai Daini NPP, Japan 24 May 2 June 2011, IAEA. - 2011.
[2] ENERGOATOM, South Ukrainian NPP Power Unit № 1. Unit vulnerability analysis in severe accidents, Final report.. EP42010.500.OD.1., SUNPP, Yuzhnoukrainsk (2011)
[3] ENERGOATOM Technological systems of SFP of unit № 1 of the South Ukraine NPP. User's manual. IE.1.0001.0088, SUNPP, Yuzhnoukrainsk (2009).

[4] ENERGOATOM, Zaporizhzhya NPP Security Analysis Report, Analysis of beyond design basis accidents, Description of the computational model of the core SFP for the MELCOR code. EP372006.420. OD.2, ZNPP, Enerhodar (2008).
[5] ENERGOATOM South Ukrainian NPP Power Unit № 1, The final cartogram of the SFP of unit № 1 of the South Ukraine NPP. 302.1.28.BV. 99.12.YU, SUNPP, Yuzhnoukrainsk.
[6] ENERGOATOM South Ukrainian NPP Power Unit. Development and validation of the RELAP /SCDAPSIM/MOD3.4 model for severe accident analysis, SUNPP, Yuzhnoukrainsk (2011).

ADDITIONAL CONTRIBUTIONS

The following additional contributions were made at the Technical Meeting:

ANALYSES OF SEVERE ACCIDENTS IN SFPS IN KOZLODUY NPPM

K. RASHKOV
Kozloduy NPP PLC, Units 5 and 6
Kozloduy, Bulgaria

MODELLING IN SUPPORT OF INTERIM/LONG TERM POND STORAGE OF SPENT FUEL AT SELLAFIELD

D. MORRIS
Spent Fuel Management, Sellafield Ltd.
Sellafield, United Kingdom

BURN-UP CREDIT IN CRITICALITY SAFETY OF PWR SPENT FUEL

R. F. MAHMOUD
Reactors Department, Egypt Second Research Reactor (ETRR-2), Calculation Group
Egyptian Atomic Energy Authority (EAEA)
Egypt

LIST OF PARTICIPANTS

ARMENIA

Hovhannisyan, A.	Armenian Scientific Research Institute for NPP Operation - “ARMATOM” CJSC 50/12 Admiral Isakov Avenue 0027 Yerevan, Armenia

BELGIUM

Thomas, R.	Tractebel ENGIE 6 rue Albert de Latour, 1030 Schaerbeek, Belgium

BRAZIL

Nunes Araujo, N.	Amazonia Azul Technologias de Defesa S.A. (AMAZUL) 1847 Corifeu de Azevedo Marques Ave. 05581-001 Sao Paulo, Brazil

BULGARIA

Rashkov, K.	Kozloduy NPP Plc 3321 Kozloduy, Bulgaria

CHINA

Huang, G.	Shanghai Nuclear Engineering Research and Design Institute (SNERDI) No. 169, Tianlin Road, Xuhui District Shanghai, China

EGYPT

Abou Zekry, M. A.	Nuclear Power Plants Authority (NPPA) P.O. Box 108, 4 El-Nasr Avenue, Nasr City Cairo, Egypt
Aboualou, R.	Egyptian Atomic Energy Authority Reactors Department, Nuclear Research Center 3 Ahmed El-Zomor St., El-Zohoor District Nasr City, Cairo, Egypt

FRANCE

Tregoures, N.	IRSN/PSN-RES/SEMIA/LIMAR Bât 700, Cadarache – BP 3 13115 St Paul Lez Durance Cedex, France

GERMANY

Braun, M. — Framatome GmbH
Paul-Gossen-Str. 100
91052 Erlangen, Germany

Fuchs, T. — Framatome GmbH
Paul-Gossen-Str. 100
91052 Erlangen, Germany

Gauter, K. — Framatome GmbH
Paul-Gossen-Str. 100
91052 Erlangen, Germany

Hollands, T. — Reactor Safety Research Division
Forschungszentrum, Boltzmannstr. 14
85748 Garching, Germany

HUNGARY

Lente, B. — Hungarian Atomic Energy Authority Fenyes Adolf u. 4
P.O. Box 676, 1036 Budapest, Hungary

Techy, Z. — NUBIKI
Konkoly-Thege Miklós u. 29-33
H-1121 Budapest, Hungary

INDIA

Padmanabhan, K. K. — Nuclear Power Corporation of India Ltd.
E-3, Nabhikiya Urja Bhavan
Anushaktinagar, Mumbai, India

JORDAN

Al Momani, B. G. — Energy and Minerals Regulatory Commission
Bayader Wadi Alsir - Next to Ministry of Information and Communication
P.O. Box 1865, 11821 Amman, Jordan

KOREA, REPUBLIC OF

Jung, J. Y. — Department of Severe Accident Research; Korea Atomic Energy Research Institute (KAERI)
P.O. Box 105, Yu-Song
Daejeon, Republic of Korea

Song, Y. — Korea Atomic Energy Research Institute (KAERI)
P.O. Box 105, 1045 Daedeok-daero, Yuseong-gu
Yusung
Daejeon, Republic of Korea

LITHUANIA

Kaliatka, T. — Lithuaian Energy Insitute (LEI)
Breslaujos 3
44403 Kaunas, Lithuania

PAKISTAN

Jaffer, S. K. — Pakistan Atomic Energy Commission (PAEC)
P.O. Box 3416, Islamabad, Pakistan

POLAND

Cwiek, K. — Radioactive Waste Management Plant (ZUOP)
Ul. Andrzeja Soltana 7
05-400 Otwock-Swierk, Poland

ROMANIA

Constantin, M. — Institute for Nuclear Research - Pitesti; Romanian Authority for Nuclear Activities (RAAN)
P.O. Box 78, Campului Street No. 1
115400 Mioveni, Romania

Zalog, C. — Societatea Nationala "Nuclearelectrica" SA
2 Medgidiei Street, PO Box 42
905200 Cernavoda, Romania

RUSSIAN FEDERATION

Dolganov, K. — Nuclear Safety Institute of Russian Academy of Sciences (IBRAE)
Bolshaya Tulskaya str. 52
Moscow, Russian Federation

Karyakin, M. — Scientific and Engineering Centre for Nuclear and Radiation Safety (SEC NRS)
Malaya Krasnoselskaya st. 2/8 bld. 5
107140 Moscow, Russian Federation

Kurskiy, I. — Mining and Chemical Combine (GKhK)
Krasnoyarsk Krai
Zheleznogorsk, Russian Federation

Tomashchik, D. — Nuclear Safety Institute of Russian Academy of Sciences (IBRAE)
Bolshaya Tulskaya str. 52
Moscow, Russian Federation

Zvonarev, Y. Nuclear Safety Institute; National Research Centre "Kurchatov Institute"
Kurchatov Square 1
123182 Moscow, Russian Federation

SPAIN

Lopez, C. Centro de Investigaciones Energeticas, Medioambientales y Tecnologicas (CIEMAT)
Av. Complutense 40
28040 Madrid, Spain

SWEDEN

Chen, Y. Swedish Royal Institute of Technology (KTH)
Roslagstullsbacken 21
SE-106 91 Stockholm, Sweden

SWITZERLAND

Jäckel, B. Paul Scherrer Institut
5232 Villigen, Switzerland

THAILAND

Vechgama, W. Thailand Institute of Nuclear Technology
16, Vibhavadi Rangsit Road, Ladeaw, Jatujak
Bangkok, Thailand

UKRAINE

Balashevskyi, O. Separated Subdivision 'Scientific and Technical Cener' of SE NNEGC 'Energoatom'
63a, Khmelnytskogo str.
01054 Kyiv, Ukraine

UNITED KINGDOM

Morris, D. Sellafield Ltd.
GFN B582, Cumbria
Seascale
CA20 1PG Sellafield, United Kingdom

IAEA

Alzahrani, Y. Nuclear Power Technology Development Section, Division of Nuclear Power, Department of Nuclear Energy

Jevremovic, T. Nuclear Power Technology Development Section, Division of Nuclear Power, Department of Nuclear Energy

Krause, M.	Nuclear Power Technology Development Section, Division of Nuclear Power, Department of Nuclear Energy
McManniman, L.	Section of Nuclear Fuel Cycle and Materials, Division of Nuclear Fuel Cycle and Waste Technology, Department of Nuclear Energy
Miassoedov, A.	Nuclear Power Technology Development Section, Division of Nuclear Power, Department of Nuclear Energy
Saenz, B.	Nuclear Power Technology Development Section, Division of Nuclear Power, Department of Nuclear Energy
Salem, A.	Nuclear Power Technology Development Section, Division of Nuclear Power, Department of Nuclear Energy

IAEA
International Atomic Energy Agency

No. 26

ORDERING LOCALLY

IAEA priced publications may be purchased from the sources listed below or from major local booksellers.

Orders for unpriced publications should be made directly to the IAEA. The contact details are given at the end of this list.

NORTH AMERICA

Bernan / Rowman & Littlefield

15250 NBN Way, Blue Ridge Summit, PA 17214, USA
Telephone: +1 800 462 6420 • Fax: +1 800 338 4550
Email: orders@rowman.com • Web site: www.rowman.com/bernan

REST OF WORLD

Please contact your preferred local supplier, or our lead distributor:

Eurospan Group

Gray's Inn House
127 Clerkenwell Road
London EC1R 5DB
United Kingdom

Trade orders and enquiries:

Telephone: +44 (0)176 760 4972 • Fax: +44 (0)176 760 1640
Email: eurospan@turpin-distribution.com

Individual orders:

www.eurospanbookstore.com/iaea

For further information:

Telephone: +44 (0)207 240 0856 • Fax: +44 (0)207 379 0609
Email: info@eurospangroup.com • Web site: www.eurospangroup.com

Orders for both priced and unpriced publications may be addressed directly to:

Marketing and Sales Unit
International Atomic Energy Agency
Vienna International Centre, PO Box 100, 1400 Vienna, Austria
Telephone: +43 1 2600 22529 or 22530 • Fax: +43 1 26007 22529
Email: sales.publications@iaea.org • Web site: www.iaea.org/publications

21-00312E

International Atomic Energy Agency
Vienna